UMONS
Université de Mons

Faculté Polytechnique

Metabolic Flux Analysis of CHO cell cultures

Francisca Zamorano Riveros

Biochemical Engineer
(Pontificia Universidad de Valparaíso)

Graduate Environmental Engineer
(Universidad de Santiago de Compostela)

Ph.D. Thesis

submitted in candidacy to the doctorate degree in engineering science.

University of Mons

April 19th, 2012.

Jury members

Prof. Dr. Ir. **A.-L. Hantson**	(Université de Mons)
Prof. Dr. **M. Pirlot**	(Université de Mons)
Prof. Dr. Ir. **Ph. Bogaerts**	(Université Libre de Bruxelles)
Prof. Dr. Ir. **M. Jolicoeur**	(École Polytechnique de Montréal, Canada)
Prof. Dr. **A. Alonso**	(Istituto Investigaciones Marinas de Vigo, España)
Prof. Dr. Ir. **G. Bastin**	(Université Catholique de Louvain-la-Neuve) – *Thesis Co-advisor*
Prof. Dr. Ir. **A. Vande Wouwer**	(Université de Mons) – *Thesis Advisor*

POLYTECH MONS

2011-2012

ACADÉMIE UNIVERSITAIRE WALLONIE-BRUXELLES

Metabolic Flux Analysis of CHO cell cultures

Francisca Zamorano Riveros,

THESIS
submitted at the
UNIVERSITY OF MONS

Acknowledgments

"Until one is committed, there is hesitancy, the chance to draw back, always in-effectiveness. Concerning all acts of initiative, there is one elementary truth the ignorance of which kills countless ideas and splendid plans: the moment one definitely commits oneself, then Providence moves too. All sorts of things occur to help one that would never otherwise have occurred. A whole stream of events issues from the decision, raising in one's favor all manner of unforeseen incidents and meetings and material assistance which no man could have dreamed would come his way. Whatever you can do or dream you can do, begin it. Boldness has genius, power, and magic in it. Begin it now."

<div align="right">Goethe</div>

The realization of this thesis was possible thanks to the IAP (Interuniversity Attraction Poles) and FSR (Fonds Spécial de Recherche) program support, and the confidence and support of Professors Alain Vande Wouwer and Georges Bastin. I would like to start by giving my deepest acknowledgment to both of them without whom none of this would have been possible.

I would like to thank all the jury members for accepting to be part of this committee and taking the time to read this manuscript.

I owe my deepest recognition to Professor Georges Bastin, a person of an outstanding brightness and a very particular sense of humour. Thanks for all the interesting discussions we had, your always insightful comments, your availability despite your busy agenda and your patience towards my "non-mathematical" background.

Next, I wish to thank my promoter, Alain, because he was ready and willing to give me the opportunity I was looking for back in Chili. Even though, our relationship was not always "smooth", I owe you gratitude and recognition for you are a person who sets his objectives and commit to them. In a personal level, I admire someone who looks forward to have fun and live life fully wherever he is. Thanks for all our discussions, your support and patience.

I cannot forget to thank Professor Anne-Lise Hantson, who ever since I came to Mons had always proved very kind towards me. She has been always available to offer me her help and support.

I must also thanks Raphaël Jungers whose invaluable help came just in the right moment. I deeply admire his intelligence and commitment towards everything he sets out to do.

Suite aux remerciements à mes promoteurs et aux membres du jury, je tiens à remercier tous les membres (anciens, permanents et sporadiques) du Service d'Automatique: Mr Remy, Cristine, Alain, Renato, Bob, Laurent, Guillaume, Véronique, Anne-Catherine, William, Vincent, Johan, Ixbalank, Cristina, Edmundo, Carlos, Inês, Pedro, Lino, Clarisse, Andrés, Paul, Mihaela, Micaela, Gilherme et Lamia. Je voudrais remercier spécialment, à Monsieur Remy pour m'avoir accueilli au sein de son departement, pour sa gentillesse et pour l'intérêt qu'il a toujours demontré vers la culture de mon pays, de la cordillère des Andes et pour les condors! Merci à tous pour votre accueil, et pour la bonne ambiance qui a toujours régné dans le service. Merci aussi de m'avoir aidé à apprendre le français, à répondre à toutes mes questions relatives à l'administration belge et aux multiplicités des erreurs dans les factures d'eau, d'électricité, d'internet, etc. Merci!

Merci aussi à tous les gens du Service de Chimie et Biochimie apliquées pour leur gentillesse et accueil. Merci spécialement à Joëlle et David avec qui j'ai travaillé coude à coude pour arriver à démarrer notre bioréacteur. Vous avez donné le coup de booste qu'il fallait! Merci à vous deux pour votre énorme aide et enthousiasme!

Infinitas gracias a Carlos, porque nunca tuviste problemas en concederme un par de minutos (e incluso horas!) para explicarme, enseñarme y ayudarme a resolver mis altercados con Matlab y LaTeX.

Gracias a mis amigos. Gracias a todos por su alegría, su apoyo y compañía.

Gracias a mis papás y mi hermana. Gracias a ustedes que me enseñaron a ir siempre hacia adelante y terminar lo que se comienza.

Gracias a mi abuelita. Porque siempre creíste en mis sueños con aún más fuerza que yo. Siempre estás conmigo en mi corazón.

Last but not the least, je te remercie à toi mon amour, mon *petits yeux* pour toute ta patience, ton soutien, ton amour inconditionnel et surtout pour ta bonne humeur. Sans toi je ne serais pas ici aujourd'hui et je ne serais pas la personne que je suis maintenant. Tu as remplis ma vie de bonheur. Je t'aime infiniment!

Abstract

The focus of this thesis is on the metabolic flux analysis of growing CHO-320 cells. A detailed metabolic network is established with the main purpose of embracing all the significant pathways describing the metabolism of CHO cells. The purpose is to investigate the efficiency of the flux analysis when it is based on a relatively small set of extracellular measurements, a set of common experimental data which can be easily achieved in most laboratories. In this case the flux analysis problem leads to a generally underdetermined mass balance system, as data are not sufficient to uniquely define the metabolic fluxes. The main contribution of this thesis work is to show that, provided the system of mass balance equations is well-posed, although it is underdetermined, very narrow intervals may be found for most fluxes. The importance of checking the well-posedness of the problem is emphasized and the influence of the number of available measurements on the accuracy of the metabolic flux intervals is systematically investigated. In all cases the computed flux intervals are bounded and a single well defined value is obtained for the formation rates of the cellular macromolecules (proteins, DNA, RNA, lipids) that are not measured. The potential gain of a simple theoretical assumption regarding the metabolism of Threonine is also discussed and compared with an optimal solution calculated by maximizing the biomass formation rate. Alternative network structures obtained by inverting the direction of reversible reactions are also considered. In addition, the results of the metabolic flux analysis are exploited to estimate the total energy production resulting from the metabolism of growing CHO-320 cells.

The effort is then directed to obtain dynamical models from metabolic networks. In a batch culture at least three different life phases can be distinguished: exponential growth, transition and death phases. For each one of these culture phases a detailed metabolic network is built so as to represent the cellular metabolism at each stage. A new approach is used for model reduction from detailed networks. This procedure allows obtaining a set of macroscopic reactions for each life phase which can be further translated into a dynamical model. For the corresponding culture phase, the models reproduce quite well the experimental data. Additionally, a dynamic model for the whole culture is attempted following a multiple model approach.

At the experimental level, part of this thesis work has been dedicated to

the set up of an animal culture cell laboratory and the realization of several CHO cell cultures. Indeed, most of the results presented in this thesis are supported by an existing database provided by Prof. Yves-Jacques Schneider (UCL) and it is crucial to have a more extensive database to verify the validity and applicability of the methods use in this thesis in the framework of different databases or even different culture modalities.

Finally, another important asset of this work is the incorporation of a chapter exclusively devoted to detail all MFA tools used in the course of this thesis and developing a model reduction Matlab toolbox. The objective of this chapter is to provide the reader with all the necessary tools to reproduce or implement the methodologies applied in this thesis.

Notations

$Acetoac$	Acetoacetate	IMP	Inosine monophosphate
$AcetoacCoA$	AcetoacetylCoA	Leu	Leucine
$AcCoA$	Acetyl Coenzyme A	Lys	Lysine
Ala	Alanine	Mal	Malate
Arg	Arginine	Met	Methionine
$ArgSucc$	Argininosuccinate	MFA	Metabolic Flux Analysis
Asn	Asparagine	NH_4^+	Ammonia
Asp	Aspartate	Orn	Ornitine
CHO	Chinese Hamster Ovary	$Orot$	Orotate
Cho	Choline	Phe	Phenylalanine
Cit	Citrate	$PhosphC$	Phosphatidylcholine
Cln	Citruline	$PhosphE$	Phosphatidylethanolamine
CTP	Cytidine triphosphate	$PhosphS$	Phosphatidylserine
$DHAP$	Dihydroxyacetone phosphate	PPP	Pentose Phosphate Pathway
$dATP$	Deoxyadenosine triphosphate	Pro	Proline
$dCTP$	Deoxycytidine triphosphate	$PropCoA$	Propionyl Coenzyme A
$dGTP$	Deoxyguanosine triphosphate	$PRPP$	$Phosphoribosyl-pyrophosphate$
$dTTP$	Deoxythymidine triphosphate	Pyr	Pyruvate
$E4P$	$Erythrose\ 4-phosphate$	Ser	Ser
$EFMs$	Elementary Flux Modes	$Sphm$	Sphingomyelin
$Ethn$	Ethanolamine	$Succ$	Succinate
$F6P$	$Fructose\ 6-phosphate$	$SucCoA$	Succinate Coenzyme A
Fum	Fumarate	TCA	Tricarboxylic acid
$G6P$	$Glucose\ 6-phosphate$	Thr	Threonine
$GA3P$	$Glyceraldehyde\ 3-phosphate$	Trp	Tryptophan
Gln	Glutamine	Tyr	Tyrosine
Glu	Glutamate	$UPLC$	Ultra Peformance Liquid
$Glu\gamma sa$	$Glutamate\gamma-semialdehyde$		Chromatography
Gly	Glycine	UTP	Uridinetriphosphate
GTP	Guanosine triphosphate	Val	Valine
$Glyc3P$	$Glycerol\ 3-phosphate$	$X5P$	$Xylulose\ 5-phosphate$
His	Histidine	$3PG$	$3-Phosphoglycerate$
$HPLC$	High Pressure Liquid	αKAd	$\alpha-ketoadipate$
	Chromatography	$\alpha KBut$	$\alpha-ketobutyrate$
Ile	Fumarate	αKG	$\alpha-Ketoglutarate$

Contents

List of Figures

List of Tables

Preface

Context and Motivation

Metabolic Flux Analysis of animal cells has been a subject of scientific interest for almost two decades. It has given rise to a large number of publications and caught the attention of many research groups. It is a very powerful methodology in metabolic engineering for the quantification of the pathway fluxes from limited experimental data. On the basis of the metabolic network, the flux distributions are found by applying steady-state mass balances around the internal balanced metabolites. This generally results in an underdetermined set of linear equations because the number of mass balances (or internal metabolites) is smaller than the number of unknown fluxes. To solve such a system either some fluxes must be determined experimentally or extra theoretical constraints must be added. In the reviewed literature, the main focus is on exactly determined or overdetermined systems. Such systems are established by defining a metabolic network with a restricted number of reactions and measuring a number of experimental data larger or equal to the degree of indetermination of the system. To collect a sufficient number of experimental data, different analytical techniques might be used, which allow the quantification of complex metabolic species and/or the determination of some internal flux rates. In this thesis work, the underdetermined case has been assessed. A detailed metabolic network involving 100 biochemical reactions has been built to represent the metabolism of growing CHO-320 cells. A standard set of 19 measurements of exo-cellular components, that can be easily achieved in most laboratories, is available. This data base comes from the Biochemistry Laboratory of the Catholic University of Louvain and have been kindly provided by Professor Yves-Jacques Schneider.

The metabolic flux analysis is then performed on an underdetermined system. We do not consider any theoretical constraints or assumptions about the metabolism. Our aim is to find out in which way the metabolic flux analysis of underdetermined system may provide useful information. Even though not all metabolic fluxes can be uniquely determined, the computation of bounded intervals allows to access the interdependence between bioreactions and the influence of the availability of specific measurements.

Although the available data set has proved extremely useful, the reduced number of measured species limits our analysis. From this perspective, it is of major interest to have a more extensive database for metabolic flux analysis and even modelling purposes. For this reason, we have participated in the ambitious project of setting up an animal cell culture laboratory so as to produce our own experimental data.

In addition, a new approach for model reduction has been studied which allows the translation of a detailed metabolic network into a set of macroscopic bioreactions and in turn into a dynamical model. This approach is based on the concept of elementary flux modes, which has been already used for dynamical model deduction. The novel aspect is that for detailed metabolic networks the calculation of these elementary modes is restricted (or even impossible) due to the combinatorial explosion (the number of elementary vectors grows exponentially with the size of the metabolic network). The theoretical foundation of the method is based on the fact that not all elementary vectors need to be calculated. The elementary flux vectors are the edges of the cone of solutions of the internal (around each intracellular metabolite) mass-balance system of equations. Thus, a particular solution for this system could be described by a linear combination of these basis vectors. This decomposition is not unique and the solution can be described by only a few of these basis vectors. In this way, the method allows the calculation of a reduced set of elementary flux modes from which a set of macroscopic reactions can be obtained for modelling purposes.

Outline

In what follows, the structure of the thesis is presented: Chapter 1 provides an overview on the state of the art around metabolic flux analysis. A brief description of this concept and a review of the main contributions in the field are given. Chapter 2 describes how a detailed metabolic network of CHO cells has been built, detailing the metabolic pathways considered. Chapter 3 introduces Metabolic Flux Analysis and the methods for network analysis. Firstly, Section 3.1 introduces the concept of metabolic networks and how it can be mathematically represented. The verifications needed before starting a flux analysis are also reviewed. Afterwards, Section 3.2 introduces the principles of metabolic flux analysis itself. Chapter 4 is devoted to the application of the flux analysis methodologies to a set of experimental data. In Section 4.1 the system is first checked for well-posedness and then the analysis is performed considering an underdetermined system. In addition, the influence of experimental errors and alternative network structures is assessed. The results of the metabolic flux analysis are exploited to estimate the total energy production resulting from the metabolism of growing CHO cells. The metabolic flux analysis is extended in Section 4.2

to a different set of experimental data and to the next two phases of the cell life: transition and death. Chapter 5 presents the framework for model reduction. Section 5.3 explains how a detailed metabolic network can be translated into a small set of macroscopic bioreactions. Section 5.4 presents the three models obtained for the different phases of CHO cell's life, and afterwards introduces the design of a global model for the entire process. Finally, Section 5.2 assesses the construction of a dynamical model for the whole cellular culture. In Chapter 6 the tools used for the different analysis performed in this thesis are presented. The reader who is interested in the calculation procedures is referred to this chapter. In Section 6.1 a detailed presentation of the analytical tools used for metabolic flux analysis is done. In Section 6.2 a toolbox for model reduction integrating the methodology proposed by [20] is presented. Chapter 7 introduces the overall setup of an animal cell culture laboratory and the subsequent development of culture experiences. Section 7.1 presents the laboratory equipment, cell lines and analytical methods used in the course of a series of cell culture experiences. In Section 7.2 the set of experimental data obtained from the cellular cultures experiences carried out in the laboratory are presented.

Finally, chapter 8 draws the main conclusions and perspectives of this work.

List of Publications

Journal Papers

Francisca Zamorano, Alain Vande Wouwer, Georges Bastin. **A detailed metabolic flux analysis of an underdetermined network of CHO cells**. *Journal of Biotechnology*, Volume 150, Issue 4, December 2010, Pages 497-508.

Raphael M. Jungers, Francisca Zamorano, Vincent D. Blondel, Alain Vande Wouwer, Georges Bastin. **Fast Computation of Minimal Elementary Decompositions of Metabolic Flux Vectors**. *Automatica*, Volume 47, 2011, Pages 1255-1259.

Francisca Zamorano, Raphael M. Jungers, Alain Vande Wouwer, Georges Bastin. **Modelling of CHO cell cultures using minimal sets of EFMs**. Paper submitted to *Journal of Biotechnology.*

Proceedings

Francisca Zamorano, Alain Vande Wouwer, Georges Bastin. **Metabolic Flux Analysis of CHO-320 Cells: Underdetermined Network and**

Effect of Measurement Errors. *11th IFAC Symposium on Computer Applications in Biotechnology (CAB 2010)*, Leuven, Belgium, July 2010.

F.Zamorano, A. Vande Wouwer, A.L. Hantson, G. Bastin. **Metabolic Flux Interval Analysis of CHO cells**. *MATHMOD 2009 - 6th Vienna International Conference on Mathematical Modelling*, Vienna, Austria, February 2009.

R. Jungers, F.Zamorano, V.D. Blondel, A. Vande Wouwer, G. Bastin. **A Fast Algorithm for computing a minimal decomposition of a Metabolic Flux vector in terms of of elementary flux vectors**. *MATHMOD 2009 - 6th Vienna International Conference on Mathematical Modelling*, Vienna, Austria, February 2009.

Conferences with Abstracts

Francisca Zamorano, Alain Vande Wouwer, Georges Bastin. **Convex Analysis Tools Applied to Underdetermined Reaction Networks**. *27th Benelux Meeting on Systems and Control*, Heeze, The Nederlands, 2008.

Francisca Zamorano, Alain Vande Wouwer, Georges Bastin. **Metabolic Flux Interval Analysis of CHO Cells**. *28th Benelux Meeting on Systems and Control*, Spa, Belgium, 2009.

Francisca Zamorano, Alain Vande Wouwer, Georges Bastin. **Metabolic Flux Analysis of an Underdetermined Network of CHO Cells considering Measurement Errors**. *29th Benelux Meeting on Systems and Control*, Heeze, The Nederlands, 2010.

Francisca Zamorano, Raphaîl Jungers, Georges Bastin. **Multiple Modelling of CHO cell cultures through the computation of minimal sets of EFMs**. *11thInternational Chemical and Biological Engineering Conference*, Lisbon, Portugal, September 5-7, 2011.

Chapter 1

Introduction

Cellular metabolism comprises hundreds of biochemical reactions by means of which the cell is able to metabolize substrates and energy to transform them into metabolic energy and cellular macromolecules. As outcome, cell growth is achieved thanks to the coordinated action of these sets of reactions, usually called pathways. Through these sequences of biochemical reactions, the conversion of a set of input metabolites (substrates) into a set of output metabolites (products) is achieved.

In the biotechnological industry, microorganisms are widely exploited for the synthesis of a large variety of products. However the cellular metabolism is not always in agreement with a production process. Nutrients are only partially used for growth and product synthesis, and partially for satisfying the cell energy requirements. Besides, a significant portion of the substrate can be transformed into waste products, whose accumulation can lead to inhibitory effects. It was with the desire of improving the productivity and properties of cultures of microorganisms, that the manipulation of metabolic pathways began and it is nowadays, an old concept already. Moreover, with the development of DNA recombination techniques, genetic engineering introduced a new dimension to pathway manipulation allowing a precise handling of specific enzymatic reactions.

Globally, the study of metabolic pathways is concerned with the elucidation of the control architecture of a metabolic network and the identification of the target reaction(s) for modification in order to achieve a certain objective. The latter is one of the original aspects of metabolic engineering as it focuses on integrated metabolic pathways rather than individual reactions. It examines complete bioreaction networks in a way of having a better perspective of the whole cellular metabolism, putting emphasis on the analysis of metabolic fluxes and their control under in vivo conditions. The combination of analytical methods to quantify fluxes and their control with molecular biological techniques to implement suggested genetic modifications is the essence of metabolic engineering [48].

Within these metabolic pathways, individual reactions take place, and the rate at which each particular reaction occurs is called metabolic flux. Rigorously, a metabolic flux can be defined as the rate at which a certain substrate or metabolite is processed through a metabolic pathway. How these fluxes are distributed within the metabolic network determines the physiology of the cell (and thus, it determines the efficiency of a hypothetical product process). Therefore, metabolic fluxes become the most critical parameters of a metabolic pathway.

Through metabolic fluxes, one can define the metabolic state of a cell and its physiology under a given set of environmental conditions. Several environmental conditions can lead to changes in cell growth, metabolism, and product formation. The examination of metabolic fluxes under different environmental conditions allows a better understanding of the metabolism of cells in cultures, which is fundamental for the design of bioreactors, media formulations and control strategies [57].

Intracellular fluxes can be determined by isotopic-tracer experiments, which allows either determining unidentifiable fluxes (due to linear dependencies), or corroborating estimates of certain metabolic fluxes. This technique for measuring intracellular fluxes is made possible by the use of labeled substrates combined with the measurement of the labeling state of intracellular metabolites, either by *in vivo* Nuclear Magnetic Resonance (NMR), or gas chromatography/mass spectrometry (GC-MS). The additional information acquired by metabolite labeling can be used to obtain more reliable estimates of fluxes, and a better analysis of the pathway structure. Though this direct flux measurement can be useful, it presents some drawbacks which make it not practical for large-scale processes. Besides it is limited to the observability of intracellular fluxes and certainly, it is laborious and requires expensive equipment.

The determination and study of metabolic fluxes *in vivo* is called metabolic flux analysis (MFA) and it has been widely used for the quantification of the intracellular fluxes in the central metabolism of bacteria, yeast, filamentous fungi and animal cells [14]. In MFA, by assuming that the internal metabolites are in quasi-steady state and by applying mass balances around the nodes of the metabolic network, a system of linear equations for the metabolic fluxes of the different branches of the network can be derived. These intracellular fluxes can be estimated from a set of additional constraints or measurements (generally, extracellular measurements) applying linear algebra or linear optimization, depending on the properties of the mass balance system of equations. Linear algebra can be used when the available extracellular measurements are sufficient to exactly determine the solution of the system, i.e., the flux distribution of intracellular reactions, or when the set of available data is large enough to allow one to compute a least-square solution. Linear optimization is generally applied defining a proper objective function in order to obtain a particular solution out of a

set of possible solutions [48].

Usually, when applied to large metabolic networks, MFA may not be sufficient to uniquely determine all fluxes, as the number of unknown fluxes may exceed greatly the number of linear mass balance equations [34, 11]. A fundamental problem encountered in complex metabolic networks is that they contain several cyclic and/or parallel pathways which are linearly dependent, resulting in an underdetermined system. As a way to tackle this problem, the measurement of intracellular fluxes could be used as additional data to complete the mass balance equation system to estimate the entire metabolic flux map [40, 41], it is however a fairly laborious and expensive method.

MFA of animal cells has been a subject of scientific interest for almost two decades and has given rise to a large number of publications. Some significant papers concerned with MFA of animal cells (Hybridoma, CHO, MDCK and HEK) are briefly reviewed in Table 1.1.

Generally, the study of MFA in the literature has been assessed for cases where the set of mass balance equations is either determined or overdetermined. For instance, when studying the metabolism of mammalian cells, Xie and Wang [54] instead of seeking additional data by measuring intracellular fluxes, reduce the number of reactions in the metabolic network by grouping serial reactions into single overall reactions and separating overlapped pathways into independent reactions. This way, with a simplified network and together with the measurements of substrate (glucose), products (ammonia, lactate and antibody), amino acids and the cell composition, it is sufficient for the stoichiometric mass balance model to become determined and to obtain an estimation of the complete metabolic flux map. Nadeau et al. [32] used MFA to compare different culture conditions at low glutamine concentrations with the aim of improving Human 293 cell growth. To this purpose, the authors consider a relatively simple metabolic network with 34 fluxes which together with 35 available measurements make possible the estimation and comparison of the flux distribution of 4 different culture conditions. In Henry et al. [16], the authors also used MFA to compare 6 different perfusion cultures for the production of adenoviral vectors from HEK-293 cells. They identify the best conditions to perform the infection of the cells by analyzing their metabolic state considering a metabolic network of similar dimensions to the one of Nadeau et al. [32].

Otherwise, Zupke and Stephanopoulos [57] used the ^{13}C NMR technique in order to validate the flux estimates with stoichiometric mass balances from a hybridoma cell line. They found good agreement between the estimated and measured fluxes. The authors simplify the metabolic network by lumping certain metabolic intermediates present in chains of reactions, as it was done in the work of Xie and Wang [54]. Thus, a stoichiometric material balance is performed for 20 biochemical reactions having a larger

number of measurements than the minimum required. The redundancy of the additional intracellular flux measurements performed with isotope labeling is used to reduce experimental error and to check the consistency of the measurements and the assumed biochemistry.

Recently, Provost and Bastin [36] developed a metabolic model for CHO cell cultures based on the elementary flux modes approach considering a simple metabolic network of 24 reactions. In their work, an original aspect is the application of positive linear algebra or convex analysis to obtain only the admissible positive solutions. Naturally, as the objective is to obtain only positive metabolic fluxes, the flux direction of the biochemical reactions describing the metabolism of the cell is fixed a priori in agreement with the metabolic state of the cells and assumed irreversible.

The present work focuses on the MFA of CHO-320 cells based on a detailed metabolic network comprising 100 reactions, built with the main purpose of embracing all the significant pathways describing the metabolism of these cells. As stated above, in general, when only external measurements are used, this type of complex network leads to an underdetermined system because the external measurements are not sufficient to provide all the information needed to obtain a unique solution. Thus, we focus our attention on the flux analysis of an underdetermined system considering a standard set of measurements of exo-cellular components which can be easily achieved in most laboratories.

To tackle our detailed metabolic network and analyze the set of admissible solutions, we use the approach developed in Provost and Bastin [37, 38] which allows the determination of intervals for the metabolic fluxes. In this study, we are interested in determining the non-negative set of solutions, i.e., non-negative flux distributions only. Convex analysis provides a way to calculate and characterize the solution set of a non-negative linear system. The set of basis vectors of the solution set is computed with the toolbox META-TOOL [35], a well validated, freely available and compatible with Matlab tool. Using this computational approach, we investigate the influence of the set of available extracellular measurements on the size of the metabolic flux intervals.

Noteworthy, [28] also proposes a method that allows the computation of the ranges of possible values for each non-calculable flux, resulting in a region so called $Flux - Spectrum$ (see Table 1.1). However, in contrast with the approach presented by Provost (and used herein), these ranges are obtained by solving a set of min-max linear programming problems, leading to a solution set larger than the space of admissible solutions. The calculation of the flux distributions space using the methodology described herein is far simpler than the one used in the work of [28].

Our main contribution is to show that, if the system of mass balance equations is *well-posed*, although it is underdetermined, very narrow intervals may be found for most fluxes using extracellular measurements only.

In particular, a single well defined value is obtained for the formation rates of the cellular macromolecules (proteins, DNA, RNA, lipids) that are not measured. Before beginning the metabolic flux analysis, it is of upmost importance to check for the well-posedness of the mass balance system, as the absence of measurements at some extreme points of the network may imply unbounded range of fluxes along certain elementary routes.

We also investigate the potential gain of a simple natural assumption regarding the Threonine (Thr) metabolism and we compare this result with the optimal solution calculated by maximizing the overall biomass production rate. From the available data, Threonine is the amino acid with the lowest ratio between its uptake rate and its stoichiometric coefficient for protein synthesis. Thus, assuming that Threonine is exclusively used for protein formation, the protein production rate is maximized. The MFA results that we get under this assumption shows that we have not only a maximization of the protein production but also a maximization of the overall biomass production (involving nucleotides and lipids). Thus, in our application to CHO cells, MFA under the constraint of no-Threonine catabolism appears to be equivalent to MFA under the constraint of biomass maximization. As it has been reported in the literature (see e.g.[7]), when MFA is applied to exponentially growing cells, it is reasonable to assume that the cellular system maximizes its resources to make biomass.

The validity of the chosen network structure is then analyzed by considering alternative network configurations, i.e., the direction of certain fluxes is systematically varied in order to test the feasibility of the chosen structure. Finally, the results obtained from the MFA are exploited to estimate the total energy production resulting from the metabolism of growing CHO-320 cells.

Thanks to the novel contribution of Raphaël Jungers [20] where he proposes a methodology for reducing complex metabolic networks to a small set of bioreactions, we were able to develop dynamical models for the different culture phases and for the entire culture. This approach is based on the concept of elementary flux modes (EFMs) so as a way to represent the complete metabolic network as a series of elementary reactions. The novelty is on the calculation method of these EFMs for it is based on the idea that not all EFMs need to be determined. This is particularly practical for detailed metabolic networks like the one herein considered.

Naturally, it is interesting to look for the applicability of the methods use in this thesis in the framework of different culture modalities, like fed-batch, continuous and perfusion. The validity of the pseudo steady state hypothesis would of course depend on the conditions in which the cell culture is carried out. Normally, the applicability of the MFA and model reduction procedures should be straightforward, except for the determination of the specific growth rate and the uptake and excretion rates of the extracellular species. This topic would be assessed in more detailed further in this thesis.

Throughout this thesis I have realized how important (and practical) it is to pick up the threads of a former work having a solid base where to start from. It is clear that a great deal of information lies on thesis, articles and books. But, when one wishes to reproduce someone else's results it would be of great help to have a clear picture of how the determination procedure was done. From here arises the interest of detailing all MFA tools used in the course of this thesis and developing a model reduction toolbox. The reader who is interested in deepening the mathematical aspect is referred to Chapter 6.

It clearly make sense to test the methodologies used in the framework of this thesis in a wider context. Not only using different culture modalities but also considering different environmental conditions, different sets of extracellular measurements, and even different cell lines. On this basis, we have decided to accept the challenge of creating our own animal cell culture laboratory. In this way, being able to design our own experiments, we would have "customized" data bases specially conceived to serve our goals.

Table 1.1: Overview of MFA publications

Method	n^o of reactions	Main achievements	Reference
MFA + labelling experiments	18 - 44	A mathematical algorithm for identifying the fluxes which should be selected for experimental measurements, based on the criterion that the calculated fluxes should have low sensitivity to experimental error in the measured fluxes. The algorithm is applied to two biological systems: *E.coli* and **Hybridoma** cells.	[40, 41]
MFA	-	Classification of metabolic systems and the conversion rates. The set of calculable flux rates is determined based on the singular value decomposition method.	[51]
MFA + labelling experiments	20	Stoichiometric balance is applied to estimate intracellular fluxes and to study energy metabolism of **Hybridoma** cells. Flux estimates are validated with labelling experiments, with a good agreement.	[57]
MFA	34	Material balance is applied to an **Hybridoma** cell stoichiometric reaction network. The role of essential and non-essential amino acids together with the metabolism of glucose and lactate are assessed. The second part of this study deals with the energetic metabolism to determine the stoichiometric ATP production rates.	[54, 55]
MFA + theoretical constraints	22	MFA is applied to investigate the metabolism of **Hybridoma** cells under different culture conditions or stress scenarios. The results provide a good insight on the cell metabolism and how they may react in a given stress situation.	[8, 10]
MFA	34	MFA is used to compare different culture conditions at low glutamine concentrations to improve cellular growth of **HEK-293** cells. A relatively simple metabolic network which, together with the available measurements give place to an overdetermined system.	[32]
MFA	41	The authors present a method based on the null-space of the stoichiometric matrix of the reactions with unknown rates to find out which reaction rates are feasible to be uniquely determined and to calculate them. An example on purple nonsulfur **bacteria** is given.	[26, 27]
MFA	24	Study of a metabolic model of **CHO** cell cultures based on a simple metabolic network. Convex analysis is employed to obtain only the admissible positive set of solutions of an underdetermined system.	[36, 37, 38, 39]
MFA	40	MFA is used to determine the best conditions to perform the infection of adenovirus in **HEK-293** cells by analyzing their metabolic state by means of MFA.	[16]
MFA + labelling experiments	26	Techniques for determining accurate flux intervals are introduced, based on flux sensitivities with respect to isotope measurements and measurement errors. These tools are applied to glucose metabolism in **human**.	[3]
MFA	24	MFA is used to further investigate the metabolism of lactate in **CHO** cells cultured in a medium containing glucose-galactose as carbon source.	[2]
MFA + linear optimization	22	An interval representation of fluxes is introduce to overcome uncertain or partially unknown fluxes. A method is proposed to compute the ranges of possible values for each non-calculable flux, resulting in a flux region called flux-spectrum. This method is applied in a **CHO** cell metabolic network.	[28]
MFA + theoretical constraints	112	MFA is used to evaluate the metabolism of **MDCK** cells cultivated in glutamine-containing and glutamine-free medium. By applying certain assumptions regarding extracellular measurements and the inactivity of intracellular fluxes, the authors get to resolve the underdetermination of the network.	[46, 52]

Chapter 2

Metabolic Network of CHO-320 cells

To formulate the stoichiometry of metabolic pathways is the basis for the quantitative treatment of cellular metabolism. In this chapter we intend to present a review of cellular metabolism, particularly the metabolism of the Chinese Hamster Ovary (CHO) cell line, and how such a metabolism can be mathematically represented in a metabolic network.

2.1 Chinese Hamster Ovary Cell Line

Chinese hamsters (*Cricetulus griseus*, see Fig. 2.1) are native to the deserts of northern China and Mongolia. The use of these rodents in research dates back to 1919 where they were used in place of mice for typing pnumococci. In the early 1920's, they gained reputation as valuable tools in epidemiological research, because they were known as carriers of a deadly parasite causing black fever. Chinese hamster became noteworthy for the cell lines that were derived from its tissues. Having a very low chromosome number (2n=22) for a mammal, the Chinese hamster is an ideal model for radiation cytogenetics and tissue culture [19]. In 1957, Dr. Theodore. T. Puck isolated an ovary from a female Chinese hamster and established the cells in culture plates, deriving the original Chinese hamster ovary (CHO) cell line.

The CHO cell line was one of the first mammalian cell lines successfully utilized in the production of therapeutically valuable proteins. The production of recombinant human proteins in mammalian cells is of great importance in the biotechnology industry since they are employed for human therapeutic purposes. They are able to perform the post-translational modifications, as glycosylation, required for the perfect functionality of the protein. Additionally, CHO cells are capable of secreting the recombinant proteins to the extracellular media, avoiding a cellular disruption process,

Figure 2.1: Chinese Hamster

otherwise necessary, to recover the product.

Chinese Hamster Ovary cells are used to produce about 70 percent of all pharmaceutically important recombinant proteins. CHO cells are considered especially significant for facilitating drug discovery and to increase production efficiencies of medicines for fighting certain cancers, controlling bleeding disorders, and boosting blood cell production.

Particularly, CHO-320 is a cell line derived from a mutant of the CHO-K1 cell (Figure 2.2), transfected with human interferon-γ gene (INF-γ), in order to synthesize and secrete this protein. CHO-K1 was first isolated by Puck and Kao in 1968 [23].
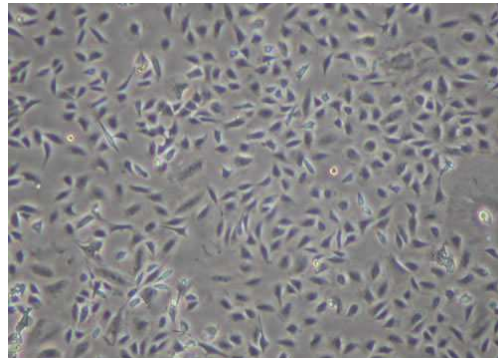
Figure 2.2: Adherent CHO-K1 cells through a phase contrast microscope

2.2 Mathematical Representation of CHO cell metabolism

The metabolism of CHO cells considered in this work is represented by the set of $n = 100$ biochemical reactions listed in Table 2.1. The metabolic

network involves the pathways schematically represented in Fig. 2.3, which will be explained in details in the following. It has to be stressed that this metabolic network corresponds to a metabolism of growing cells. Therefore, a single flux direction is assigned to reversible reactions according to this phase of the cell life. The choice of the direction of the net flux for some possibly reversible reactions will be assessed further on in Subsection 4.1.5.
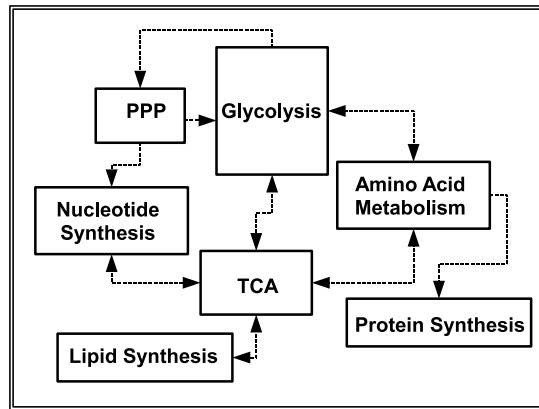
Figure 2.3: Schematic Representation of the CHO-320 cell Metabolic Network

The metabolic network includes:

- Glycolysis;

- Pentose Phosphate Pathway (PPP);

- Tricarboxylic Acid Cycle (TCA);

- the Amino Acid metabolism and Protein Synthesis;

- the Urea Cycle

- the Nucleic Acid Synthesis;

- the Membrane Lipid Synthesis.

- Biomass Formation

Table 2.1: Metabolic Reactions for the metabolism of CHO-320 cells

Flux	Reaction
	Glycolysis
v_1	$\textbf{Glucose}^a + ATP \rightarrow G6P + ADP$
v_2	$G6P \rightleftharpoons {}^b F6P$
v_3	$F6P + ATP \rightarrow DHAP + G3P + ADP$
v_4	$DHAP \rightleftharpoons G3P$
v_5	$G3P + NAD^+ + ADP \rightleftharpoons 3PG + NADH + ATP$
v_6	$3PG + ADP \rightarrow Pyr + ATP$
	Tricarboxylic Acid Cycle
v_7	$Pyr + NAD^+ + CoASH \rightarrow AcCoA + CO_2 + NADH$
v_8	$AcCoA + Oxal + H_2O \rightarrow Cit + CoASH$
v_9	$Cit + NAD(P)^+ \rightarrow \alpha KG + CO_2 + NAD(P)H$
v_{10}	$\alpha KG + CoASH + NAD^+ \rightarrow SucCoA + CO_2 + NADH$
v_{11}	$SucCoA + GDP + P_i \rightleftharpoons Succ + GTP + CoASH$
v_{12}	$Succ + FAD \rightleftharpoons Fum + FADH_2$
v_{13}	$Fum \rightleftharpoons Mal$
v_{14}	$Mal + NAD^+ \rightleftharpoons Oxal + NADH$
	Pyruvate Fates
v_{15}	$Pyr + NADH \rightleftharpoons \textbf{Lactate}^a + NAD^+$
v_{16}	$Pyr + Glu \rightleftharpoons Ala + \alpha KG$
	Pentose Phosphate Pathway
v_{17}	$G6P + 2NADP^+ + H_2O \rightarrow Rbl5P + 2NADPH + CO_2$
v_{18}	$Rbl5P \rightleftharpoons R5P$
v_{19}	$Rbl5P \rightleftharpoons X5P$
v_{20}	$X5P + R5P \rightleftharpoons F6P + E4P$
v_{21}	$X5P + E4P \rightleftharpoons G3P + F6P$
	Anaplerotic Reaction
v_{22}	$Mal + NAD(P)^+ \rightleftharpoons Pyr + HCO_3^- + NAD(P)H$
	Amino Acid Metabolism
v_{23}	$Glu + NAD(P)^+ \rightleftharpoons \alpha KG + NH_4^+ + NAD(P)H$
v_{24}	$Oxal + Glu \rightleftharpoons Asp + \alpha KG$
v_{25}	$Gln \rightarrow Glu + NH_4^+$
v_{26}	$Thr + NAD^+ + CoASH \rightarrow Gly + NADH + AcCoA$
v_{27}	$Ser \rightleftharpoons Gly$
v_{28}	$3PG + Glu + NAD^+ \rightarrow Ser + \alpha KG + NADH$
v_{29}	$Gly + NAD^+ \rightarrow CO_2 + NH_4^+ + NADH$
v_{30}	$Ser \rightarrow Pyr + NH_4^+$
v_{31}	$Thr \rightarrow \alpha Kb + NH_4^+$
v_{32}	$\alpha Kb + CoASH + NAD^+ \rightarrow PropCoA + NADH + CO_2$
v_{33}	$PropCoA + HCO_3^- + ATP \rightarrow SucCoA + ADP + P_i$
v_{34}	$Trp \rightarrow Ala + 2CO_2 + \alpha Ka$
v_{35}	$Lys + 2\alpha KG + 3NAD(P)^+ + FAD^+ \rightarrow \alpha Ka + 2Glu + 3NADPH + FADH_2$
v_{36}	$\alpha Ka + CoASH + 2NAD^+ \rightarrow AcetoAcCoA + 2NADH + 2CO_2$
v_{37}	$AcetoAcCoA + CoASH \rightarrow 2AcCoA$
v_{38}	$Val + \alpha KG + CoASH + 3NAD^+ + FAD^+ \rightarrow PropCoA + Glu + 2CO_2 + 3NADH + FADH_2$
v_{39}	$Ile + \alpha KG + 2CoASH + 2NAD^+ + FAD^+ \rightarrow AcCoA + PropCoA + Glu + CO_2 + 2NADH + FADH_2$
v_{40}	$Leu + \alpha KG + CoASH + NAD^+ + HCO_3^- + ATP + FAD^+ \rightarrow AcCoA + AcetoAc + Glu + CO_2 + NADH + ADP + FADH_2$
v_{41}	$AcetoAc + SucCoA \rightarrow AcetoAcCoA + Succ$
v_{42}	$Phe + NADH \rightarrow Tyr + NAD^+$
v_{43}	$Tyr + \alpha KG \rightarrow Fum + AcetoAc + Glu + CO_2$
v_{44}	$Met + Ser + ATP \rightarrow Cys + \alpha Kb + NH_4^+ + AMP$
v_{45}	$Cys \rightarrow Pyr + NH_4^+$
v_{46}	$Asn \rightleftharpoons Asp + NH_4^+$
v_{47}	$Arg \rightarrow Orn + Urea$
v_{48}	$Orn + \alpha KG \rightleftharpoons Glu\gamma SA + Glu$

a

Extracellular measured species

b

Chosen net direction for reversible reaction

Flux	Reaction
v_{49}	$Pro \rightarrow Glu\gamma SA$
v_{50}	$Glu\gamma SA + NAD(P)^+ \rightarrow Glu + NAD(P)H$
v_{51}	$His \rightarrow Glu + NH_4^+$

Urea Cycle

v_{52}	$Orn + CarbP \rightarrow Cln$
v_{53}	$Cln + Asp + ATP \rightarrow ArgSucc + AMP$
v_{54}	$ArgSucc \rightarrow Arg + Fum$

Protein Synthesis

v_{55}	$0.023His + 0.053Ile + 0.091Leu + 0.059Lys + 0.023Met + 0.039Phe + 0.059Thr + 0.014Trp + 0.066Val + 0.051Arg$ $+0.072Gly + 0.052Pro + 0.032Tyr + 0.078Ala + 0.043Asn + 0.053Asp + 0.019Cys + 0.042Gln + 0.063Glu + 0.068Ser + ATP$ $+3GTP \rightarrow Protein + AMP + Pp_i + 3GDP + 3P_i$

Nucleotide Synthesis

v_{56}	$R5P + ATP \rightarrow PRPP + AMP$
v_{57}	$PRPP + 2Gln + Gly + Asp + 4ATP + CO_2 \rightarrow IMP + 2Glu + Fum + 4ADP + 2H_2O$
v_{58}	$IMP + Asp + 2ATP + GTP \rightarrow ATP_{RN} + Fum + 2ADP + GDP$
v_{59}	$IMP + Gln + 3ATP + NAD^+ + 2H_2O \rightarrow GTP_{RN} + Glu + 2ADP + AMP + NADH$
v_{60}	$HCO_3^- + NH_4^+ + Asp + 2ATP + NAD^+ \rightarrow Orotate + ADP + NADH$
v_{61}	$Orotate + PRPP + ATP \rightarrow UTP_{RN} + CO_2 + 2ADP$
v_{62}	$UTP_{RN} + Gln + ATP \rightarrow CTP_{RN} + Glu + ADP$
v_{63}	$0.285(ATP_{RN} + UTP_{RN}) + 0.215(GTP_{RN} + CTP_{RN}) \rightarrow RNA$
v_{64}	$ATP_{RN} \rightarrow dATP$
v_{65}	$GTP_{RN} \rightarrow dGTP$
v_{66}	$CTP_{RN} \rightarrow dCTP$
v_{67}	$UTP_{RN} \rightarrow dTTP$
v_{68}	$0.285(dATP + dTTP) + 0.215(dGTP + dCTP) \rightarrow DNA$

Lipid Synthesis

v_{69}	$DHAP + NADH \rightarrow Glyc3P + NAD^+$
v_{70}	$Choline + 18AcCoA + Glyc3P + 23ATP + 33NADH \rightarrow PC + 17ADP + 6AMP + 33NAD^+$
v_{71}	$Ethanolamine + 18AcCoA + Glyc3P + 23ATP + 33NADH \rightarrow PE + 17ADP + 6AMP + 33NAD^+$
v_{72}	$PE + Ser \rightarrow PS + Ethanolamine$
v_{73}	$16AcCoA + Ser + Choline + 16ATP + 29NADPH \rightarrow SM + 2CO_2 + 14ADP + 2AMP + 29NADP^+$
v_{74}	$18AcCoA + 18ATP + 14NADPH \rightarrow Cholesterol + 6CO_2 + 18ADP + 14NADP^+$
v_{75}	$0.5PC + 0.2PE + 0.075PS + 0.075SM + 0.15Cholesterol \rightarrow MembraneLipid$

Biomass Formation

v_{76}	$0.9226Protein + 0.013RNA + 0.0052DNA + 0.0297MembraneLipid \rightarrow Biomass$

Transport Reactions

v_{77}	$\mathbf{Asp_{ext}}^a \rightarrow Asp$
v_{78}	$Cys_{ext} \rightarrow Cys$
v_{79}	$Gly \rightarrow \mathbf{Gly_{ext}}^a$
v_{80}	$\mathbf{Ser_{ext}}^a \rightarrow Ser$
v_{81}	$Glu \rightarrow \mathbf{Glu_{ext}}^a$
v_{82}	$\mathbf{Tyr_{ext}}^a \rightarrow Tyr$
v_{83}	$Ala \rightarrow \mathbf{Ala_{ext}}^a$
v_{84}	$\mathbf{Arg_{ext}}^a \rightarrow Arg$
v_{85}	$\mathbf{Asn_{ext}}^a \rightarrow Asn$
v_{86}	$\mathbf{Gln_{ext}}^a \rightarrow Gln$
v_{87}	$His_{ext} \rightarrow His$
v_{88}	$\mathbf{Ile_{ext}}^a \rightarrow Ile$
v_{89}	$\mathbf{Leu_{ext}}^a \rightarrow Leu$
v_{90}	$\mathbf{Lys_{ext}}^a \rightarrow Lys$
v_{91}	$\mathbf{Met_{ext}}^a \rightarrow Met$
v_{92}	$\mathbf{Phe_{ext}}^a \rightarrow Phe$
v_{93}	$Pro_{ext} \rightarrow Pro$
v_{94}	$\mathbf{Thr_{ext}}^a \rightarrow Thr$
v_{95}	$Trp_{ext} \rightarrow Trp$
v_{96}	$\mathbf{Val_{ext}}^a \rightarrow Val$
v_{97}	$Ethanolamine_{ext} \rightarrow Ethanolamine$
v_{98}	$Choline_{ext} \rightarrow Choline$
v_{99}	$NH_4^+ \rightarrow \mathbf{NH_{4,ext}^+}^a$
v_{100}	$CO_2 \rightarrow CO_{2,ext}$

Continued from previous page

2.2.1   Central Metabolism

Numerous works deal with MFA of animal cells, like Hybridoma [8, 10, 40, 41, 54, 55, 57], HEK-293 [16, 32], MDCK [46, 52] and CHO cells [2, 28, 36, 37, 38, 39]. The metabolic networks described in all these studies consider the main catabolic and anabolic pathways occurring within the cell with a relatively limited level of complexity. The central metabolism considered in these studies is quite similar, with the exception of a few reactions which are specific to each type of mammalian cell.
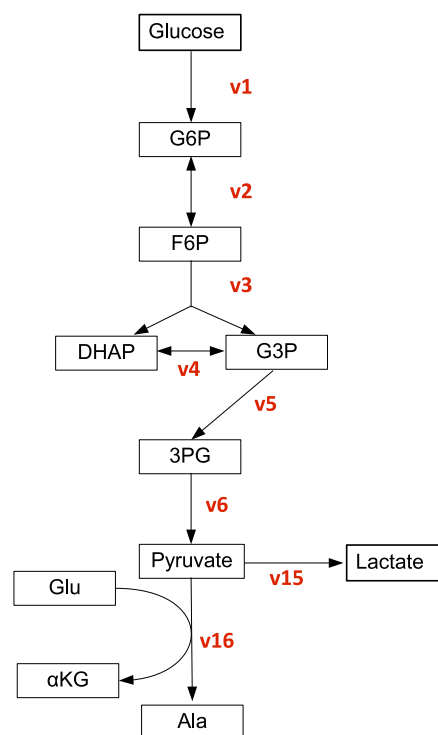
Figure 2.4: Glycolysis

In the present work, the considered central metabolism for CHO-320 cells is shown in Figures 2.4, 2.5 and 2.6. It comprises Glycolysis, PPP and TCA cycle, which is the usual metabolism used for strictly aerobic eukaryotic organisms [2, 9, 10, 34, 36, 53].

Glycolysis comprises a series of reactions through which the breakdown
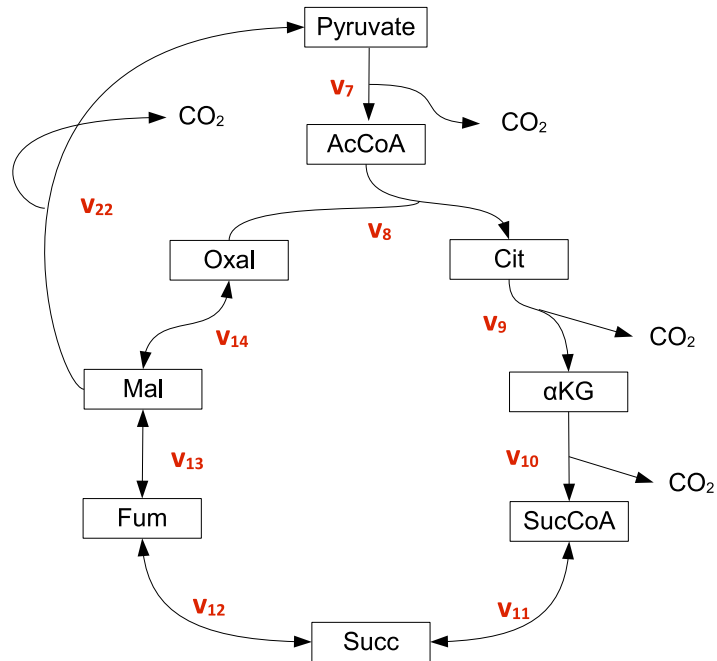
Figure 2.5: Tricarboxylic Acid Cycle

of glucose takes place, generating two molecules of pyruvate and releasing the energy contained in the molecule of glucose in the form of ATP and $NADH$. In mammalian cells, the pyruvate obtained from glycolysis can be further metabolized either entering the TCA to be oxidized to CO_2, or via lactic acid fermentation to be reduced to lactate, or participating in the synthesis of Alanine. The PPP is the pathway used by the cells to synthesize the precursors of nucleic acids (DNA and RNA) and reducing power in the form of $NADPH$. The PPP comprises two main phases: an oxidative phase, where Glucose 6-Phosphate is oxidized to Ribose 5-Phosphate (precursor of nucleotides) producing $NADPH$, and a non-oxidative phase where the Ribose 5-Phosphate is recycled into Glucose 6-Phosphate in the case where more $NADPH$ is needed by the cell. The TCA cycle is where all the living cells obtain energy by means of the cellular respiration. It is the second step in the breakdown of glucose into CO_2 and H_2O in order to release all the remaining energy. In addition, several intermediates of the TCA cycle serve as precursors for a wide variety of metabolic products. As intermediates of the TCA cycle are removed to serve as biosynthetic precursors, they are replenished by anaplerotic reactions. Normally, the draw off and the replenish reactions are in dynamic balance, thus concentrations of TCA cycle

intermediates remain almost constant. Among the most common anaplerotic reactions, the reversible reaction catalyzed by malic enzyme (reaction $v22$ in Table 2.1) is widely distributed in eukaryotes and prokaryotes.
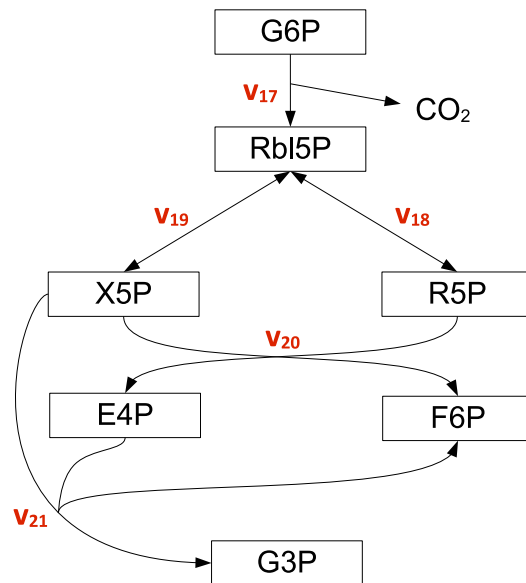
Figure 2.6: Pentose Phosphate Pathway

Although metabolism embraces hundreds of different enzyme-catalyzed reactions, the central metabolic pathways (present in all organisms), are limited in number and remarkably similar in all forms of life. Even if it is possible to find slight differences between different cell kinds, they are hardly noticeable among mammalian cells, with the exception of course, of genetically manipulated cell lines.

The main carbon and energy sources for mammalian cells in culture are glucose and glutamine, the latter also serving as the primary nitrogen source. There are additional requirements for other nutrients, but their contribution to energy metabolism is small compared to the demand for the main substrates. Major products of glucose and glutamine metabolism are biomass, secreted protein, energy in the form of ATP, reducing power for biosynthesis, carbon dioxide, and the waste products lactate and ammonia [57].

2.2.2 Amino Acid Metabolism and Protein Synthesis

In mammalian cells, essential amino acids cannot be synthesized and must therefore be provided in the culture medium. Accordingly, only catabolic pathways are considered for essential amino acids. In contrast, for non-essential amino acids, both anabolic and catabolic pathways are taken into account.

Considering that the pathways of amino acid metabolism are quite similar in most organisms, all catabolic and biosynthetic reactions of amino acids have been taken from references [24] and [33]. The routes of amino acid degradation converge to the central catabolic pathways, where their carbon skeleton find the way to the TCA cycle, and their amino group is shunted into other routes. The catabolic pathways of all 20 amino acids converge to form only five products, all of which enter the TCA cycle: Acetyl-CoA, Oxaloacetate, Fumarate, Succinyl-CoA and α-ketoglutarate. The series of reactions considered to represent the amino acid metabolism of CHO-320 cell are listed in Table 2.1 and are also showed in figure 2.7.

It has been reported in [8] that mammalian tissue is ureotelic, meaning that the excess NH_3 is converted into urea and then excreted. Accordingly, small amounts of urea can be detected during CHO-320 cell cultures. Hence, the Urea Cycle has been included in the network (see reactions $v52$, 53 and $v54$ in Table 2.1). Additionally, this cell line has the particularity of being auxotrophic with respect to Proline (Pro), and thus cannot synthesize it and relies on its external supply for growth [22]. Therefore, only the catabolic phase of the metabolism of Pro is taken into account.

Since proteins are built to play a specific role, and sometimes, their composition and structure depend on the organisms that produce them, their composition and dimensions can vary widely. Therefore, it is not possible to establish a standard protein composition, given that the stoichiometric coefficients should be evaluated for each organism and each type of protein. Reaction v_{55} in Table 2.1 describes the synthesis of proteins. It is taken from [36], where an average composition of proteins for eukaryotic cells is presented and used to simulate the protein synthesis of CHO-320.

In table 2.2 the different contributions of amino acids to protein synthesis are presented.

2.2.3 Nucleotide Metabolism

For nucleotide synthesis, and in turn DNA and RNA synthesis, we consider only the *de novo* pathways (i.e., they are synthesized from their main precursor $Ribose\ 5-Phosphate$, final product of the PPP). As this study does not consider degradation of nucleic acids, the routes synthesizing nucleotides from the recycling of free monomers released from nucleic acid breakdown

Table 2.2: Average Stoichiometric Composition for Protein Synthesis

Amino acids	Percentage of occurrence in Proteins
Alanine	7.8
Arginine	5.1
Histidine	2.3
Asparagine	4.3
Cysteine	1.9
Isoleucine	5.3
Aspartate	5.3
Glutamine	4.2
Leucine	9.1
Glutamate	6.3
Glycine	7.2
Lysine	5.9
Serine	6.8
Proline	5.2
Methionine	2.3
Tyrosine	3.2
Phenylalanine	3.9
Threonine	5.9
Tryptophan	1.4
Valine	6.6

are not taken into account. The reactions for the nucleotide metabolism are listed in Table 2.1 and depicted in Fig. 2.8.

Nucleotides are the base molecules of DNA and RNA structures. Thus, in order to simulate nucleic acid synthesis as two simplified reactions (in a similar way as for proteins), average percentages of nucleotide composition have been considered. In [45, 49, 50] an average composition of nucleic acids is given, at different guanine-cytosine base concentrations for several cell types. On this basis, two overall reactions for both RNA and DNA synthesis, can be established (see reactions v_{69} and v_{75} in Table 2.1).

The subindex "$_{RN}$" used in these sets of reactions stands for Ribonucleotides, and is used to differentiate nucleotides as biomass constituents (making up RNA) from nucleotides as energetic molecules (Section 4.1.6).

2.2.4 Lipid Metabolism

Among all different kinds of lipids, we only consider those which play a structural role as components of cellular membranes: Glycerophospholipids as phosphatidylcholine (PC), phosphatidylethanolamine (PE) and phosphatidylserine (PS); Sphingolipids as shpingomyelin (SM); and Sterols as cholesterol.

At this stage of the metabolism, we have significantly simplified the synthesis routes of membrane lipids, so as to be able to analyze the metabolic fluxes. The existence of a large number of reactions set in parallel introduces linear dependencies in the metabolic network preventing the analysis of the whole flux distribution.

The metabolism of lipids (reactions v_{69} to v_{75}) accounted in this study, assumes that the cellular membrane contains particular percentages of PC, PE, PS, SM and cholesterol which are established on the basis of references [17] and [33], where usual percentages of membrane phospholipids are specified. The reactions for the lipid metabolism are listed in Table 2.1 and depicted in Fig. 2.9.

2.2.5 Biomass Synthesis

The reaction synthesis representing the flux for biomass growth is defined in terms of the biomass composition on the precursors required by the cell for its formation: Proteins, Nucleic Acids and Membrane Lipids. The metabolic reaction v_{76} describing the biomass production of CHO-320 cells (see Table 2.1) is based on the cellular composition of a recombinant t-PA producing cell line (CHO TF 70TR) used in [2]. The cellular composition of these CHO cells is stated as follows: 92.26% of proteins, 1.3% of RNA, 0.52% of DNA and 2.97% of Lipids.
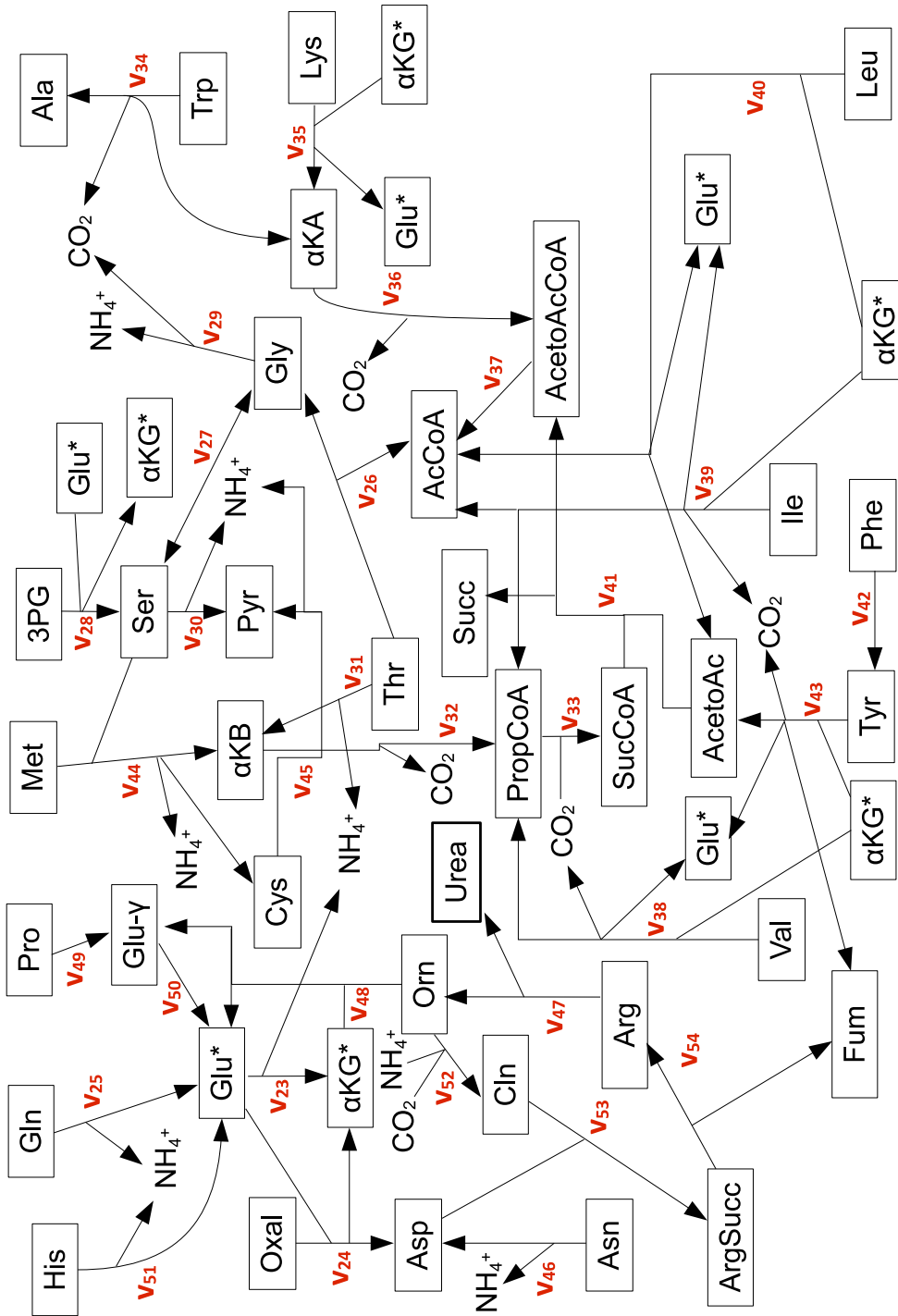
Figure 2.7: Amino Acid Metabolism
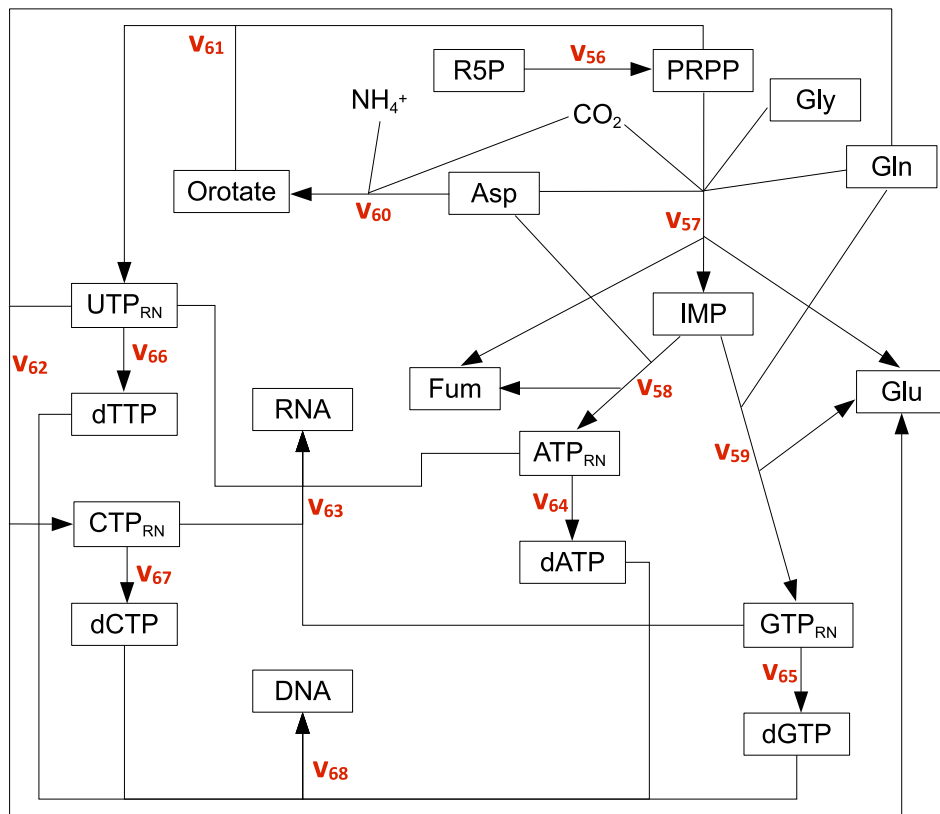
Figure 2.8: Schematic Representation of Nucleotide Metabolism
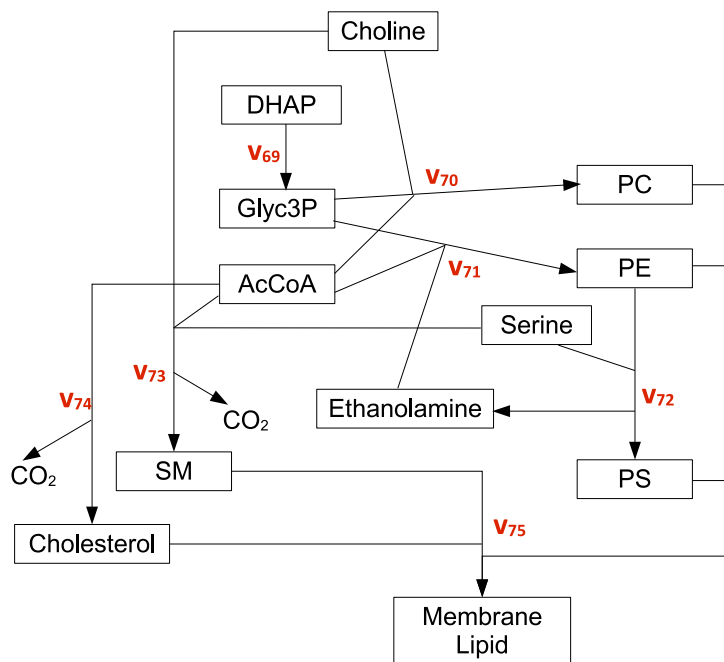
Figure 2.9: Schematic Representation of Lipid Metabolism

Chapter 3

Analysis of Metabolic Networks

This chapter is devoted to the metabolic flux analysis of CHO-320 cells performed for a detailed metabolic network involving 100 reactions. This metabolic network embraces the most significant pathways describing the metabolism of CHO cells. The purpose is to investigate the efficiency of the flux analysis when it is based on a relatively small set of extracellular measurements that can be easily achieved in most laboratories. In this case the flux analysis problem leads to an underdetermined mass balance system, as data are not sufficient to uniquely define the metabolic fluxes. Here, the main outcome is to show that, provided the system of mass balance equations is proved to be well-posed, although it is underdetermined, very narrow intervals may be found for most fluxes. The importance of checking the well-posedness of the problem is assessed and emphasized and the influence of the number of available measurements on the accuracy of the metabolic flux intervals is systematically investigated. In all cases the computed flux intervals are bounded and a single well defined value is obtained for the formation rates of the cellular macromolecules (proteins, DNA, RNA, lipids) that are not measured. The potential gain of a simple theoretical assumption regarding the metabolism of Threonine is also discussed and compared with an optimal solution calculated by maximizing the biomass formation rate. Alternative network structures obtained by inverting the direction of reversible reactions are also considered. Finally, the results of the metabolic flux analysis are exploited to estimate the total energy production resulting from the metabolism of growing CHO-320 cells. In addition, the influence of the measurement errors on the numerical results is explored using Monte Carlo techniques.

Firstly, the main concepts and the methods used for building metabolic networks are introduced. Additionally, a calculability analysis of the metabolic network and a check of the well-posedness of the mass balance system are

performed before tackling the MFA problem itself.

3.1 Network Construction/Definition

3.1.1 Stoichiometry and Reaction Rates

Stoichiometry

The overall result of the cellular reactions is the conversion of substrates into products and free energy. This conversion takes place through a large number of metabolites, including precursors and building blocks of macromolecules, and by specifying the stoichiometry of these reactions it is possible to analyze them. To do this in a rigorous way, it is important to make a distinction between the different metabolites interacting within the cellular metabolism.

- A substrate is a compound present in the medium that can be metabolized by the cell as a carbon, nitrogen or energy source.

- A product is a compound generated as result of the cell metabolism that is excreted to the extracellular medium. It may be either a primary metabolite (directly involved in normal growth, as lactate or carbon dioxide), or a secondary metabolite (resultant of more specific functions) or a recombinant protein.

- Biomass Constituents are pools of macromolecules that constitute the cell, like RNA, DNA, lipids, proteins, etc.

- Intracellular metabolites are all other compounds within the cell that are intermediates in the different cellular pathways.

It must be stressed that intracellular metabolites have a very rapid turnover of their pool compared with macromolecules, and a pseudo-steady state assumption is generally applicable to them [48]. Nevertheless, in some cases it is not clear whether a compound is to be considered as an intracellular metabolite or as a metabolic product. In Saccharomyces cerevisiae, for example, Pyruvate may accumulate and be excreted at high glycolytic fluxes. Clearly, Pyruvate is an intracellular intermediate, but since it can be excreted it can also be considered as a metabolic product. Therefore, any compounds that can be measured in the extracellular medium must be considered as either a substrate or a metabolic product. To set the stoichiometry of a metabolic model in view of the above classification, we must define the stoichiometric coefficients for substrates (α), products (β) and intracellular metabolites (g). Generally, the stoichiometric coefficients for substrates are negative and those for products are positive, whereas the stoichiometric coefficients for the intermediates may be either positive or negative. Biomass

compounds should be designated independently to differentiate them from intracellular metabolites or metabolic products. To formulate a general stoichiometry for a cellular reaction, we consider a system where n substrates are transformed to m products and q biomass constituents. There are J reactions taking place in which k intracellular metabolites participate as intermediates. One stoichiometric coefficient is introduced in each reaction for each compound (substrates, products, intermediates and biomass constituents), many of them being zero since not all the compounds participate in all the reactions. Designating the substrates by S_i, the metabolic products by P_i, the biomass constituents $X_{macro,i}$ and the intracellular metabolites by $X_{met,i}$, the stoichiometry for the jth reaction can be expressed as

$$\sum_{i=1}^{n} \alpha_{ji} S_i + \sum_{i=1}^{m} \beta_{ji} P_i + \sum_{i=1}^{q} \gamma_{ji} X_{macro,i} + \sum_{i=1}^{k} g_{ji} X_{met,i} = 0; \qquad (3.1)$$

where α_{ji}, β_{ji}, γ_{ji} and g_{ji}, are the stoichiometric coefficients for the ith substrate, product, biomass component and intracellular metabolite, respectively in the jth reaction. In a metabolic model there is an equation like (3.1) for each of the J reactions, therefore it is convenient to write the stoichiometry of the whole system in a compact form using matrix notation as

$$\mathrm{A}S + \mathrm{B}P + \Gamma X_{macro} + G X_{met} = 0 \qquad (3.2)$$

where A, B, Γ and G are the matrices containing the stoichiometric coefficients of the substrates, products, biomass constituents and pathways intermediates, respectively. Stoichiometric matrix columns collect the stoichiometric coefficients for a particular compound in all J reactions. In these matrices, rows represent reactions and columns represent metabolites. The matrix formulation facilitates much of the subsequent analysis since general matrix operations can be used, and it also helps to get an easy overview of the metabolic model by looking at the coefficients in the ith column (related to the ith compound) in the appropriate matrix.

Example   To illustrate this, we take the example of glycolysis (Figure 2.4) to represent the stoichiometry of the system following the formalism of equations (3.1) and (3.2). Obviously, the metabolism of CHO cells is more complicated and the formulation of the general stoichiometric of such a metabolism implies the participation of a larger number of compounds, nevertheless, taking only one part of the entire network is enough for a descriptive example.

To set up a simple metabolic model for glycolysis we describe the overall reactions considering only metabolites at branch points. This is a consequence of pseudo-steady state assumptions for all internal metabolites, assumption that we shall discuss hereafter. In this model there are two substrates: glucose and glutamate (glu), three products: lactate, alanine (ala) and α-ketoglutarate (aKG), six intracellular metabolites and no biomass constituents. In order to minimize undue complexity, one may lump certain intracellular metabolites into an overall reaction, as reactions v_1 and v_2 (simple transformation of one metabolite into another), resulting in the following stoichiometry:

$$- glucose - ATP + F6P = 0 \tag{3.3a}$$
$$- F6P - ATP + DHAP + G3P = 0 \tag{3.3b}$$
$$- DHAP + G3P = 0 \tag{3.3c}$$
$$- G3P + 3PG + ATP + NADH = 0 \tag{3.3d}$$
$$- 3PG + Pyr + ATP = 0 \tag{3.3e}$$
$$- Pyr - NADH + lactate = 0 \tag{3.3f}$$
$$- Pyr - glu + ala + \alpha KG = 0 \tag{3.3g}$$

The preceding equations can be written in matrix form as in equation (3.2), where the distinction between substrates, products and intermediates become clear.

$$
\begin{pmatrix}
-1 & 0 \\
0 & 0 \\
0 & 0 \\
0 & 0 \\
0 & 0 \\
0 & 0 \\
0 & -1
\end{pmatrix}
\cdot
\begin{pmatrix}
S_{glucose} \\
S_{glu}
\end{pmatrix}
+
\begin{pmatrix}
0 & 0 & 0 \\
0 & 0 & 0 \\
0 & 0 & 0 \\
0 & 0 & 0 \\
0 & 0 & 0 \\
1 & 0 & 0 \\
0 & 1 & 1
\end{pmatrix}
\cdot
\begin{pmatrix}
P_{lactate} \\
P_{Ala} \\
P_{\alpha KG}
\end{pmatrix}
$$

$$
+
\begin{pmatrix}
1 & 0 & 0 & 0 & 0 & -1 & 0 \\
-1 & 1 & 1 & 0 & 0 & -1 & 0 \\
0 & -1 & 1 & 0 & 0 & 0 & 0 \\
0 & 0 & -1 & 1 & 0 & 1 & 1 \\
0 & 0 & 0 & -1 & 1 & 1 & 0 \\
0 & 0 & 0 & 0 & -1 & 0 & -1 \\
0 & 0 & 0 & 0 & -1 & 0 & 0
\end{pmatrix}
\cdot
\begin{pmatrix}
X_{F6P} \\
X_{DHAP} \\
X_{G3P} \\
X_{3PG} \\
X_{Pyr} \\
X_{ATP} \\
X_{NADH}
\end{pmatrix}
= 0 \quad (3.4)
$$

This last equation provides an overview of the reactions involved in the model. For example, by looking at the sixth column of the last stoichiometric matrix (that of intracellular metabolites named G) it is possible to see that ATP is consumed in reactions (3.3a) and (3.3b) and then produced in reactions (3.3d) and (3.3e). When measuring or estimating the metabolic fluxes of these reactions, one can obtain an estimative of the total rate of ATP synthesis. As it will be discuss hereafter, the energetic cofactors as ATP and $NAD(P)H$ are indeed intracellular metabolites, but the pseudo-steady state assumption cannot be applied to them.

Reaction Rates

Once the stoichiometry is specified for all the intracellular fluxes, the following step is to calculate the rates at which the reactions are taking place. Normally, the rate of a chemical reaction is the velocity ν, determining that a compound with a stoichiometric coefficient β is formed at a rate $\beta\nu$. In each reaction, it is typical to set one of the stoichiometric coefficient to ± 1, through which the reaction rate is expressed as the consumption or production rate of this compound in a particular reaction. For example, for the reaction represented by equation (3.3a), the reaction rate could be expressed in terms of moles of *glucose* consumed per hour, or moles of $F6P$ produced per hour. Additionally, It is common for cellular reactions to employ the biomass or cellular density as reference to define the specific rates as for example $[mol/gDW\dot{h}]$ or $[mol/cell\dot{h}]$.

The reaction rates of all J reactions considered in the previous subsection, can be collected in a vector v, in a way that $\beta_{ji}\nu_j$ denotes the specific rate of formation of the ith metabolic product in the jth reaction. As reaction rates of substrates are negative, the specific consumption rate of the ith substrate in the jth reaction is expressed as $-\alpha_{ji}\nu_j$. In order to calculate the overall consumption or production of a compound, the contributions of all reactions must be added. Therefore, it is possible to write the net specific uptake rate for the ith substrate as the sum of its consumption rates in all J reactions:

$$r_{s,i} = -\sum_{j=1}^{J} \alpha_{ji}\nu_j \tag{3.5}$$

and similarly, the net specific production rate of the ith metabolic product:

$$r_{p,i} = \sum_{j=1}^{J} \beta_{ji}\nu_j \tag{3.6}$$

The preceding equations denote the specific uptake rates of substrates and the specific production rates of products, which represent, in fact, what can be directly measured from the medium. In a similar way, the rates for the intracellular metabolites and the biomass constituents can be written as:

$$r_{met,i} = \sum_{j=1}^{J} g_{ji}\nu_j \tag{3.7}$$

and similarly, the net specific production rate of the ith metabolic product:

$$r_{macro,i} = \sum_{j=1}^{J} \gamma_{ji}\nu_j \tag{3.8}$$

These rates can be quantified from measurements of intracellular components, nevertheless, they are not as easy to determine experimentally as the specific uptake and production rates. One compound can be formed in one reaction and be consumed in another, thus, the specific rates are the net result of consumption and production of that compound in all J intracellular reactions (which could involve a large number of measurements and some of them might be not feasible).

If the specific rate of the ith intracellular metabolite is zero, the rates of formation exactly balance the rates of consumption, which is the foundation of metabolic flux analysis, discussed in details hereafter.

Equations (3.5), (3.6), (3.7) and (3.8) can be formulated in matrix notation as:

$$r_s = -\mathrm{A}^T v \tag{3.9}$$

$$r_p = \mathrm{B}^T v \tag{3.10}$$

$$r_{met} = \mathrm{G}^T v \tag{3.11}$$

$$r_{macro} = \Gamma^T v \tag{3.12}$$

3.1.2   Network Consistency - Elementary Mass Conservation

A fundamental issue when assembling independent metabolic pathways together to form a more detailed metabolic network, is to check whether the mass conservation principle is fulfilled.

To ensure that mass conservation is verified by the network (and thus, the validity of all results and conclusions obtained form its analysis), a simple test can be established by defining a 'total mass' variable z. In fact, z can be defined in various ways depending on which type of mass indicator we wish to consider, and to this purpose, (positive) conversion factors will be included in a vector a . For example, z may be defined as the number of total carbon atoms involved in the metabolic reactions, and then a would contain the information about the number of carbon atoms in each metabolite. The same may be done by defining z as the number of total nitrogen atoms.

To formulate this mathematically, consider the dynamical reaction system:

$$\frac{dx}{dt} = M \cdot r(x) \tag{3.13}$$

where x denotes the vector of concentrations of all, internal and extra-cellular, metabolites, M is the Stoichiometric matrix, and $r(x)$ represents the reaction rates vector. A non-negative vector a is introduced such that:

$$z = a^T \cdot x \tag{3.14}$$

Differentiating z with respect to time, we get:

$$\frac{dz}{dt} = a^T \cdot \frac{dx}{dt} = a^T \cdot M \cdot r(x) \tag{3.15}$$

If mass conservation applies (which should always be the case), then z must be constant, and consequently, its time derivate should be zero, so that

$$a^T \cdot M \cdot r(x) = 0, \quad \forall r(x) \tag{3.16}$$

This must be true independently of $r(x)$, hence,

$$a^T \cdot M = 0 \tag{3.17}$$

If vector a indeed exists, we can demonstrate that no mass violation occurs when building the reaction network.

In this study, a has been defined as either of two column vectors relative to the most relevant atoms taking part in the cellular metabolism, i.e., carbon and nitrogen atoms. For both cases vector a is always proved to exist, and thus no mass violation has occur during the construction of the metabolic network. For the mass balance of biomass and macromolecules (Proteins, Nucleic Acids and Lipids), as they are widely different in their structure and composition, an average 'atomic composition' as been considered in agreement with the monomerical composition used to state their biosynthetic reactions. With this we are able to verify the mass balance conservation principle through the whole metabolic network.

3.2 Metabolic Flux Analysis

Metabolic Flux Analysis is a methodology in metabolic engineering for the quantification of pathway fluxes when extracellular measurements are the only available data. By building a proper metabolic network for the intracellular reactions and applying steady state mass balances around the internal metabolites, an admissible flux distribution can be found. A set of extracellular measurements, typically uptake rates of substrates and excretion rates of metabolic products, is used as input to the calculations. The result of calculating the metabolic fluxes is a metabolic flux map showing a diagram of the biochemical reactions along with an estimate of the steady state rate for each metabolic flux. This estimate is obtained as a flux distribution vector, where its entries are the rates at which each reactions take place.

This flux maps contain useful information about the contribution of certain pathways to the overall metabolic processes, i.e., to the substrates consumption and products formation. However, the real importance of obtaining this metabolic flux maps lies in the differences between the flux estimates that are observed when comparing flux maps obtained in different strains or under different culture conditions. It is through these comparisons that the relevance of environmental (or genetic) changes can be analyzed.

A particular aspect of MFA is that depending on the information provided by the extracellular measurements and on the properties of the stoichiometric matrix N, the determination of the intracellular metabolic fluxes may be based either on an exactly determined metabolite balance equation system or on a overdetermined or underdetermined system. If the degrees of freedom of the mas balance system (i.e., the number of unknown fluxes minus the number of independent linear equations in matrix N) equals the number of extracellular measurements ($\dim(v_m)$), then the system is exactly determined and a unique solution exists. Otherwise, if the degrees of freedom are less than the number of extracellular measurements, the extra information provided by the available data can be used to calculate an

approximate solution by the least-square method. In an overdetermined system the redundancies can be exploited to calculate not only better estimates for the non-measured fluxes but also better estimates for the measured fluxes. On the contrary, if the number of measurements is smaller than the number of degrees of freedom, the system is underdetermined, and an infinity of solutions exist. In this case, a possible way is to formulate theoretical assumptions in order to further constrain the solution space, as the reactions irreversibility applied in the present analysis. For instance, in [8] and [10], the authors force a change in the metabolism by manipulating the environmental conditions, imposing hypoxia or high concentrations of ammonia. Another possibility is to use linear programming by specifying a suitable objective function, such as "maximizing the specific growth rate of the cells", so that optimal solutions can be calculated. With this approach it is possible to obtain a unique solution for the flux distribution by optimizing the objective function subject to the constraints of the metabolite balances.

3.2.1 Principle

The metabolism of CHO cells considered in this analysis is described by the set of $n = 100$ biochemical reactions listed in Table 2.1. The metabolic network $\mathbf{N}$ involves different metabolites and biochemical species, which are divided in two major groups:

1) The group of $m = 72$ internal balanced metabolites.

2) The group of unbalanced species which is further divided in two subgroups:

    a) The intracellular energetic cofactors .
    b) The 26 extracellular metabolites present in the culture medium which are either nutrients or products of excretion.

Each admissible flux distribution is represented by a vector $v = (v_1, v_2, \ldots, v_m)^T$ whose entries are the rates (or fluxes) at which the reactions proceed. The steady-state balance around the internal metabolites is expressed by the algebraic problem

$$\mathbf{Nv} = \mathbf{0} \qquad \mathbf{v} \geqslant \mathbf{0} \tag{3.18}$$

where the $m \times n$ matrix $\mathbf{N}$ is the stoichiometric matrix deduced from the metabolic network (m is the number of internal balanced metabolites and n the number of fluxes). In our case, the stoichiometric matrix $\mathbf{N}$ has dimensions 72×100. It is a rather sparse matrix. A schematic representation showing the locations of the non-zero entries is given in Fig. 3.1 while the complete stoichiometric matrix $\mathbf{N}$ is presented in Appendix A.
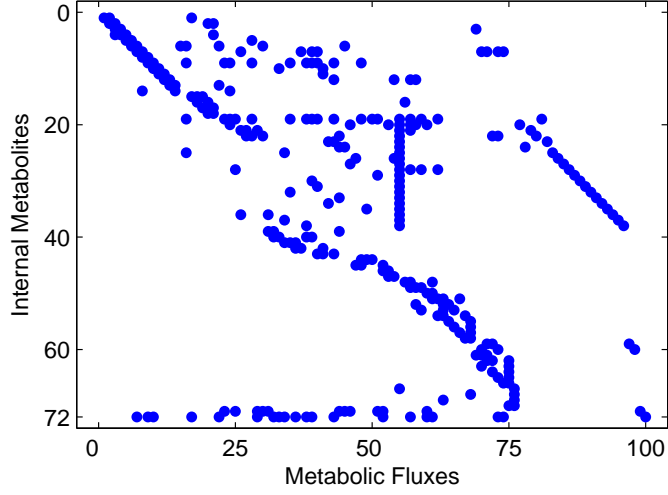
Figure 3.1: Cartographic representation of Matrix N.

An admissible flux distribution $\mathbf{v}$ must satisfy the steady state balance equation (3.18) and be compatible with the experimental measurements. The specific uptake and excretion rates of the measured external species are collected in a vector $\mathbf{v}_m$ and are by definition linear combinations of the unknown fluxes v_i. This is expressed as

$$\mathbf{v}_m = \mathbf{N}_m \mathbf{v} \tag{3.19}$$

where $\mathbf{N}_m$ is a $p \times n$ full-rank matrix with p the number of available measurements.

The aim of MFA is to compute the set of admissible flux distributions $\mathbf{v}$, i.e., the set of non-negative vectors $\mathbf{v}$ that satisfy the system (3.18)-(3.19).

$$\begin{pmatrix} \mathbf{N} & \mathbf{0} \\ \mathbf{N}_m & -v_m \end{pmatrix} \cdot \begin{pmatrix} \mathbf{v} \\ \mathbf{1} \end{pmatrix} = 0 \tag{3.20}$$

In general, this system is underdetermined, as a metabolic network happens to be composed of less nodes (internal metabolites) than connections (reactions), and usually, the number of external measurements is not sufficient to provide the missing information, i.e., the missing linear equations. Therefore, the solution of the system is not unique but admits a set of admissible non-negative flux distributions.

It is worth noting that the flux distribution vector $\mathbf{v}$ has been defined as a non-negative vector, since the flux direction has been fixed depending on the metabolic phase under consideration (the exponential growth phase in this case). The flux distribution vector is fixed as positive because for all

the irreversible reactions in the network, we necessarily look for positive flux rates. Moreover, we must correctly choose the net direction of all reversible reactions if we wish to obtain a set of solutions. Many metabolic reactions are reversible, but they have a predominant direction depending on the metabolic conditions. Therefore, each of them could be seen as a net reaction with a fixed direction.

Geometrically, the set of positive solutions of equation (3.18) generates a convex polyhedron cone S which is the intersection between the positive half-space and the complete set of solutions of equation (3.18) (the Kernel of $\mathbf{N}$). If we further constrain this solution space with the equations provided by the extracellular measurements, the system (3.20) generates a convex polytope $\mathcal{F}$ in the positive orthant containing all admissible flux distributions $\mathbf{v}$ (in agreement with the experimental data). These two sets of solutions are depicted in Figure 3.2.1.
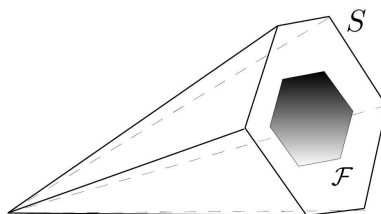
Figure 3.2: Convex polyhedron cones S and F.

The problem is said to be *well posed* if the solution set is not empty and if all the solutions are bounded. Otherwise, the system is said to be *ill posed*. When the problem is well posed, the solution set of system (3.20) generates polytope $\mathcal{F}$ and each admissible flux distribution $\mathbf{v}$ can be expressed as a convex combination of a set of non-negative basis vectors $\mathbf{f}_i$. These vectors $\mathbf{f}_i$ are the vertices of this polytope and form therefore a unique convex basis of the solution space. In other words, the solution set of the MFA problem is the set of admissible flux vectors defined as

$$\mathbf{v} = \sum_i \alpha_i \mathbf{f}_i, \ \ \alpha_i \geqslant 0, \ \ \sum_i \alpha_i = 1. \tag{3.21}$$

The basis vectors $\mathbf{f}_i$ are obtained by applying the software METATOOL [35, 44] to the matrix

$$\begin{pmatrix} \mathbf{N} & \mathbf{0} \\ \mathbf{N}_m & -\mathbf{v}_m \end{pmatrix}.$$

Every basis vector of polytope $\mathcal{F}$ provides a particular solution $\mathbf{v}$ because of equation 3.21. Thus, in a straightforward way, the basis vectors $\mathbf{f}_i$ can provide a range of possible values for each metabolic flux. From these flux ranges a flux interval can be defined for every metabolic reaction.

$$v_j^{\min} \leqslant v_j \leqslant v_j^{\max}$$

with $v_j^{\min} \triangleq \min \left\{ f_{ij},\ i = 1, \ldots, m \right\}$, $v_j^{\max} \triangleq \max \left\{ f_{ij},\ i = 1, \ldots, m \right\}$

where f_{ij} denotes the j-th element of the basis vector $\mathbf{f}_i$.

For a more detailed explanation of the calculation procedure, the reader is referred to Chapter 6.2.

3.3 Calculability Analysis

In [27] a procedure for determining the fluxes that can be uniquely calculated in underdetermined networks is presented. The method, named Calculability/Observability analysis, is based on the calculation of the kernel or null space of the stoichiometric matrix. The starting point is the same system of equations as in MFA.

$$\mathbf{N}\mathbf{v} = \mathbf{0} \tag{3.22}$$

where $\mathbf{N}$ is the $m \times n$ stoichiometric matrix and $\mathbf{v}$ the reaction rate vector.

3.3.1 Kernel of N

In linear algebra, the kernel or null space of a matrix $\mathbf{A}$ is the set of all vectors $\mathbf{x}$ for which $\mathbf{A}x = 0$. On this basis, the complete set of linearly independent solutions of equation 3.22 form the kernel of matrix $\mathbf{N}$. While metabolic flux analysis only considers the positive set of solutions (cone S), calculability analysis considers the entire set of solutions.

Let us call $\mathbf{K}$ the matrix whose columns span the kernel of $\mathbf{N}$. Matrix $\mathbf{K}$ gives rise to infinitely many solutions, because each independent solution (columns $\mathbf{k}_i$) can be linearly combined with each other.

The dimension of $\mathbf{K}$ depends on the dimension of matrix $\mathbf{N}$ and the degrees of freedom of the system $(n - \mathbf{r}ank(N))$. If the stoichiometric matrix $\mathbf{N}$ has full row rank $(\mathbf{r}ank(N) = m)$, it then follows that the dimension of $\mathbf{K}$ is $n \times (n - m)$.

Equation (3.22) is usually highly underdetermined. For instance, for our stoichiometric matrix $\mathbf{N}$ there are 28 degrees of freedom, as $n = 100$ and $\mathbf{r}ank(N) = m = 72$. Then, matrix $\mathbf{K}$ has a dimension of 100×28.

3.3.2 Partitioning of v and N

The reaction rate vector $\mathbf{v}$ can be partitioned into two vectors: one containing the measured or known reaction rates and another containing the unmeasured or unknown reaction rates. The known part of the reaction rates is contained in vector $(\mathbf{v}_k)$ and the unknown part is included in vector $(\mathbf{v}_u)$. In the same way, matrix $\mathbf{N}$ can be partitioned into $\mathbf{N}_k$ and $\mathbf{N}_u$:

$$\mathbf{v} = \begin{pmatrix} \mathbf{v}_k \\ \mathbf{v}_u \end{pmatrix}$$

$$\mathbf{N} = \begin{pmatrix} \mathbf{N}_k & \mathbf{N}_u \end{pmatrix}$$

Thus, equation (3.22) is rewritten in the following form:

$$0 = \mathbf{N}\mathbf{v} = \mathbf{N}_k\mathbf{v}_k + \mathbf{N}_u\mathbf{v}_u \Leftrightarrow \mathbf{N}_u\mathbf{v}_u = -\mathbf{N}_k\mathbf{v}_k \qquad (3.23)$$

3.3.3 Calculable Fluxes

If the system is exactly determined, $\mathbf{N}_u$ is a $m \times m$ full-rank matrix ($\mathbf{rank}(N_u)$ = m = number of unknown fluxes $(\mathbf{v}_u)$) and $\mathbf{v}_u = $ -$\mathbf{N}_u^{-1}\mathbf{N}_k\mathbf{v}_k$. In a more general case, when $\mathbf{N}_u$ is a non invertible matrix, solutions of equation (3.23) can be computed using the Moore-Penrose pseudo-inverse.

$$\mathbf{v}_{u,s} = -\mathbf{N}_u^{\#}\mathbf{N}_k\mathbf{v}_k + \mathbf{K}_u\mathbf{a} = \mathbf{v}_{u,part} + \mathbf{K}_u\mathbf{a} \qquad (3.24)$$

where $\mathbf{v}_{u,part}$ is a particular solution and $\mathbf{K}_u$ is the kernel of $\mathbf{N}_u$. $\mathbf{a}$ is an arbitrary vector with $(dim(\mathbf{v}_u) - rank(\mathbf{N}_u))$ elements, which reflects the indeterminacy of $\mathbf{v}_{u,s}$. It can be verified that for an arbitrary vector $\mathbf{a}$ the resulting vector $\mathbf{v}_{u,part}$ is a solution of equation ((3.23).

$$\mathbf{N}_u\mathbf{v}_{u,s} = \mathbf{N}_u\mathbf{v}_{u,part} + \mathbf{N}_u\mathbf{K}_u\mathbf{a} = \mathbf{N}_u\mathbf{v}_{u,part} \qquad (3.25)$$

since $\mathbf{N}_u\mathbf{K}_u$ is equal to zero.

Therefore, independently of vector $\mathbf{a}$, if there exist calculable fluxes for the system considered, all different solutions $\mathbf{v}_{u,s}$ will give exactly the same value for those calculable fluxes. In other words, if the ith metabolic flux can be uniquely determined, then all the solutions obtained as $\mathbf{v}_{u,s}$ will have the same value at the ith position. A concrete example of calculable flux determination is given in Chapter 6.1, Section 6.1.1.

Chapter 4

Application of MFA

4.1 Metabolic Flux Analysis results

We perform a flux analysis for CHO cells on the basis of the underlying metabolic network presented in Table 2.1. Thus, the metabolic matrix N (see Appendix A) representing the intracellular mass balances at quasi steady-state, includes 100 bioreactions and 72 internal metabolites.

The first purpose is to characterize the feasible set of solutions by using only extracellular measurements and as few additional constraints as possible. Depending on the number and type of available extracellular measurements, the system can be well- or ill-posed. If the system is well-posed, the number of basis vectors $\mathbf{f}_i$ and the size of the flux intervals will depend on the extracellular measurements that are considered. Some measurements are critical for the determination of the flux intervals, whereas other measurements are less influential.

4.1.1 Experimental data base

The experimental data come from CHO-320 cell cultures used in [36, 38]. The experiments were performed by the Biochemistry Laboratory, Catholic University of Louvain and have been kindly provided by Professor Y.J. Schneider. These experimental data correspond to measurements collected from the exponential growth phase of three different batch cultures of a CHO-320 cell line, carried out in a serum-free medium supplemented with rice protein hydrolysate and glutamine. In Figures 4.1 and 4.2 the experimental measurements corresponding to the exponential growth phase are denoted by blues asterisks. Cultures were settled in a working volume of 25 mL in shake-flasks and incubated at 100 rpm in a CO_2 incubator at 37° C in an atmosphere of 5% CO_2 in air. The cultures were inoculated to reach an initial concentration of 0.3×10^9 cells/L. Cultures were kept for 190 hours, with an exponential growth phase of 80 hours approximately. These

experiments have been designed to have initial concentrations of 16 mM of glucose and 6 mM of glutamine.
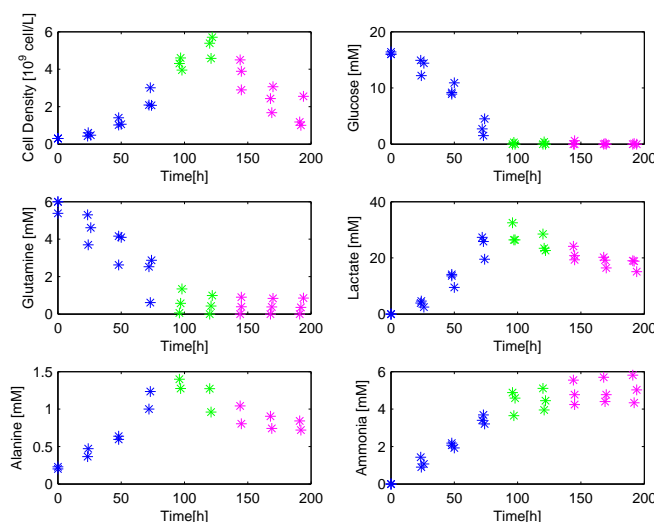
Figure 4.1: Time evolution of biomass, main substrates and products.

This data set contains the time evolution of the extracellular concentrations of the main substrates: Glucose and Glutamine, the main metabolism excretion products: Lactate, Alanine and Ammonia, and the concentration of 14 additional amino acids, along with the evolution of the biomass inside the bioreactor during the growth phase. It should be noticed that among the 14 additional amino acids measured, Glycine (Gly) and Glutamate (Glu) appear to be produced. The specific uptake and excretion rates are obtained by linear regression of substrates and products during the growth phase. The estimated rates are given in Table 4.1 and will serve as the data for our MFA.

For a more detailed calculation procedure, the reader is referred to Chapter 6.1.

4.1.2 Check for well-posedness

Before any flux analysis, the system should be checked for well-posedness for it might occur that certain paths in the network link non-measured inputs to non-measured outputs giving rise to an unbounded set of solutions for the reaction rates in these routes. In system (3.20)
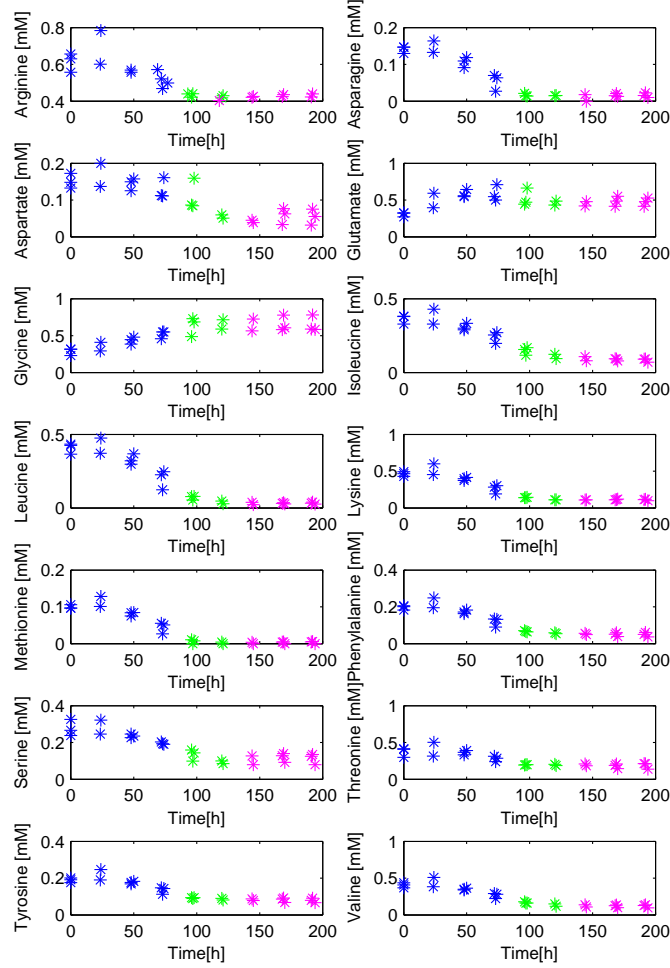
Figure 4.2: Time evolution of amino acids.

$$\begin{pmatrix} \mathbf{N} & \mathbf{0} \\ \mathbf{N}_m & -v_m \end{pmatrix} \cdot \begin{pmatrix} \mathbf{v} \\ \mathbf{1} \end{pmatrix} = 0$$

the matrix $\mathbf{N}_m$ is defined for the set of external measurements given in the previous Subsection 4.1.1, consisting in 19 measurement data. The resulting set of basis vectors, obtained from the calculation with METATOOL, shows the presence of 3 columns formed entirely by zero elements. This occurs because there exist 3 elementary paths linking non-measured substrates

Table 4.1: Extracellular Measurements in mmol $h^{-1}10^9 cell-1$

Substrates	Specific Uptake Rates	Products	Specific Excretion Rates
Glucose	-0.1871	Lactate	0.3445
Glutamine	$-5.0246e^{-2}$	NH_4^+	$4.5712e^{-2}$
Arginine	$-2.1417e^{-3}$	Glycine	$2.2295e^{-3}$
Asparagine	$-1.1278e^{-3}$	Alanine	$8.8100e^{-3}$
Aspartate	$-3.1785e^{-4}$	Glutamate	$9.5475e^{-4}$
Isoleucine	$-1.5278e^{-3}$		
Leucine	$-2.6013e^{-3}$		
Lysine	$-2.1245e^{-3}$		
Methionine	$-7.2375e^{-4}$		
Phenylalanine	$-9.9808e^{-4}$		
Serine	$-9.2342e^{-4}$		
Threonine	$-1.1842e^{-3}$		
Tyrosine	$-7.6104e^{-4}$		
Valine	$-1.9561e^{-3}$		

to non-measured products, meaning that the reaction rates participating in these routes are all unbounded.

A way to recognize which are those unbounded paths is to analyze the set of elementary flux modes of the reaction network. The elementary flux modes are the simplest metabolic pathways linking substrates to products. Hence, if the substrates and final products participating in one particular elementary flux mode are not measured, then this pathway is unbounded. For a more rigorous definition, the reader is referred to Chapter 5, Subsection 5.2.2, where the concept of elementary flux modes is introduced.

Unfortunately, the calculation of the elementary flux modes is not always possible for as the number of elementary modes grows exponentially with the level of complexity of the network. Nonetheless, we were able to identify, among a huge number of elementary flux modes, those unbounded paths where no measurements of extracellular species were available. The global reactions of these paths are:

$$Cysteine_{ext} + Proline_{ext} \rightarrow Urea + 7\,CO_{2\,ext}$$
$$2\,Proline \rightarrow Urea + 9\,CO_{2\,ext}$$
$$2\,Histidine \rightarrow Urea + 10\,CO_{2\,ext}$$

It becomes clear then, that we should have at least one measured specie for each unbounded reaction if we want the system to be well-posed. It happens here, that there are two species that participate in all three reactions: Urea and CO_2, meaning that by measuring one of these two species the solution system will become well posed. Additionally, this is correlated with the number of columns of zero elements found in the matrix of basis vectors. For instance, when urea or CO_2 are considered among the experimental measurements as a twentieth measurement, all columns of

zero element disappear. If cysteine or histidine are to be considered instead, two null columns endure, meaning that only one metabolic route would be bounded. Similarly, by considering proline as a twentieth measurement, we find that only one null column remains and so, the two routes were proline takes part would be bounded.

Therefore, in order to have a well-posed system the set of actual measurements should be complemented with one extra measurement, either CO_2 or urea. We decided to consider CO_2 as our twentieth measurement and an estimative value was took from [29] Fig.4(b) where a value of $0.68[mmol 10^{-9} cell^{-1} h^{-1}]$ is given for the CO_2 excretion rate of CHO cell cultures. Although, we could have used an estimative rate for urea, as we believe it may be easily measurable, we could not find any references for this measurement in the literature.

4.1.3   MFA of the Underdetermined System

Once the system has been checked for well-posedness, the size of the intracellular flux intervals is analyzed in this section under different assumptions that are successively considered. For this purpose, the 20 experimental measurements (19 real and 1 estimated) are first used to compute the flux intervals of system (3.20). Although most of the obtained intervals are already fairly narrow, it results from this first run that the intervals are unsatisfactory for the cellular macromolecules. Therefore, in a second case study, the system is further constrained with the theoretical assumption of no catabolism of Threonine (Thr), i.e. that Threonine is exclusively used for protein synthesis. With this single additional constraint, we get satisfactory results for the flux analysis with, in particular, a single well defined value for the formation rates of the cellular macromolecules (proteins, DNA, RNA, lipids). We also show that this result is optimal for the criterion of maximizing the biomass production rate.

The second purpose is to assess the impact of the missing extracellular measurements on the quality of the flux analysis. Thus further on, the set of actual measurements is complemented with "pseudo-measurements" for the missing data (Table 4.2). Firstly, two additional estimated measurements are added, the measurements of Cysteine (Cys) and Proline (Pro) and afterwards, the assumption of no Thr catabolism is relaxed and the case in which we are able to measure a large number of extracellular species (i.e., the input-output fluxes) defined by the metabolic network is also assessed. The results show that, with a larger set of extracellular data, the flux analysis can be significantly improved with most estimated intervals (53 out of 74) reduced to a single value and without any additional theoretical constraint being needed.

If calculability is first evaluated for a system considering the 19 extracellular measurements presented in Section 4.1.1, there are no calculable fluxes. We know that the system considering only 19 measurement is ill-posed, thus the fact that no uniquely determined fluxes are found is consistent. Nonetheless, for a system considering 20 measurements (including CO_2) the calculability analysis shows no calculable fluxes as well. Once the system is further constrained considering the assumption of no Threonine catabolism, the calculability analysis finds 37 uniquely determined metabolic fluxes. The calculability analysis performed on the system complemented with additional measurements of Cysteine and Proline (i.e., 22 measurements) shows no calculable fluxes. When the assumption of no catabolism of

Threonine is added the calculability analysis shows that 40 metabolic fluxes can be exactly determined. For the case where the assumption of no catabolism of Thr is relaxed and the set of measurements is complemented with the measurements of Histidine, Tryptophan, Urea and Ethanolamine, the calculability analysis finds 53 uniquely determined fluxes. Exactly the same result obtained through the MFA.

Intervals obtained with the initial set of experimental measurements (p=20)

We first perform the MFA with the experimental data of Table 4.1 plus the CO_2 measurement. The obtained intervals are presented (delimited by circles) in Fig. 4.3 for biomass and its main macromolecules, Fig. 4.4 for the central metabolism (Glycolysis, TCA and PPP), Fig. 4.5 for amino acids, Fig. 4.6 for nucleotides and Fig. 4.7 for lipids. From these results the two main conclusions are:
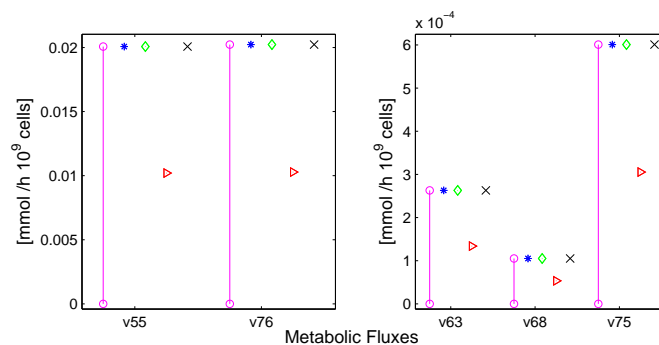
Figure 4.3: Flux Distribution Intervals for biomass synthesis.

1. The MFA problem is well-posed and produces bounded non-negative intervals for all metabolic fluxes. Many of the flux intervals are fairly narrow.

2. The calculability analysis gives no calculable fluxes for this system. The same result is obtained via MFA, where all metabolic fluxes remain as intervals.

3. Some intervals include zero as a feasible solution. It is the case in particular for reactions v_{55}, v_{63}, v_{68}, v_{75} and v_{76} (see Fig. 4.3), which correspond to the formation of the cellular macromolecules (proteins, RNA, DNA, lipids and biomass).

Even though a zero flux is mathematically feasible, it is clear from a biological viewpoint that it is not a valid possibility during the cell growth and it would be desirable to have smaller and more realistic intervals for these species.

In the next subsection, we shall see that this issue is efficiently addressed by introducing a very mild assumption regarding the consumption of Threonine.
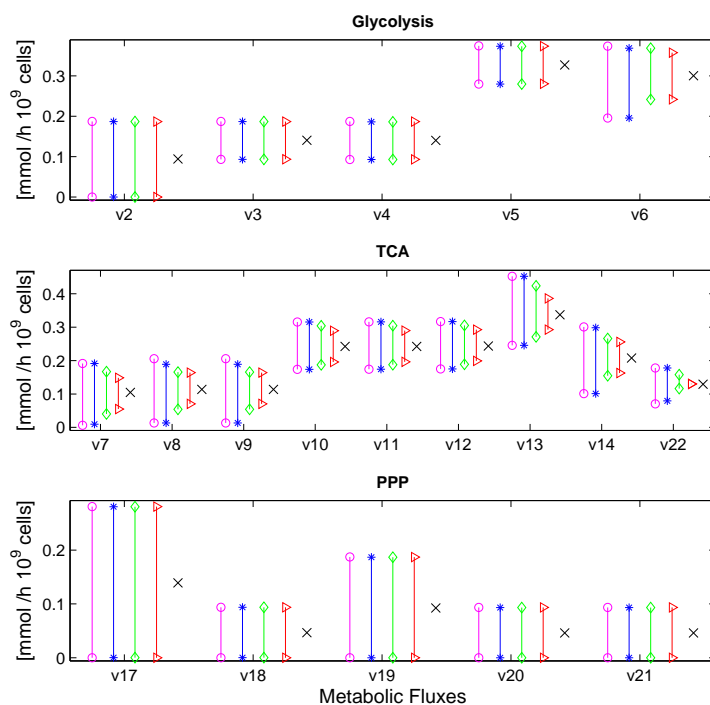
Figure 4.4: Flux Distribution Intervals for the central metabolism.

Intervals obtained with the initial set of measurements under the assumption of no Threonine catabolism

As an additional modelling assumption, we now assume that Threonine is exclusively used for protein formation in reaction v_{55}. This assumption implies that Threonine is not used for catabolic purposes and that fluxes v_{26} and v_{31} (Table 2.1) are set to zero. There are two main reasons that make this a well motivated assumption:

1. The maximum possible production rate of proteins is given by the essential amino acid with the lowest ratio between its uptake rate and its stoichiometric coefficient for protein synthesis. Among all essential amino acids, Threonine is precisely the amino acid with this lower ratio (i.e., Threonine is the most limiting amino acid).

2. The intervals for v_{26} and v_{31} in the previous results include effectively zero as a possible solution and are very small in comparison to the other amino-acid intervals that also include zero (v_{16}, v_{23}, v_{27}, v_{30}, v_{34}, v_{45}, v_{49}, v_{51}).

The flux intervals obtained in this case are delimited by stars in all figures. The following conclusions can be drawn:

1. The flux intervals of the central metabolism as well as those of metabolic
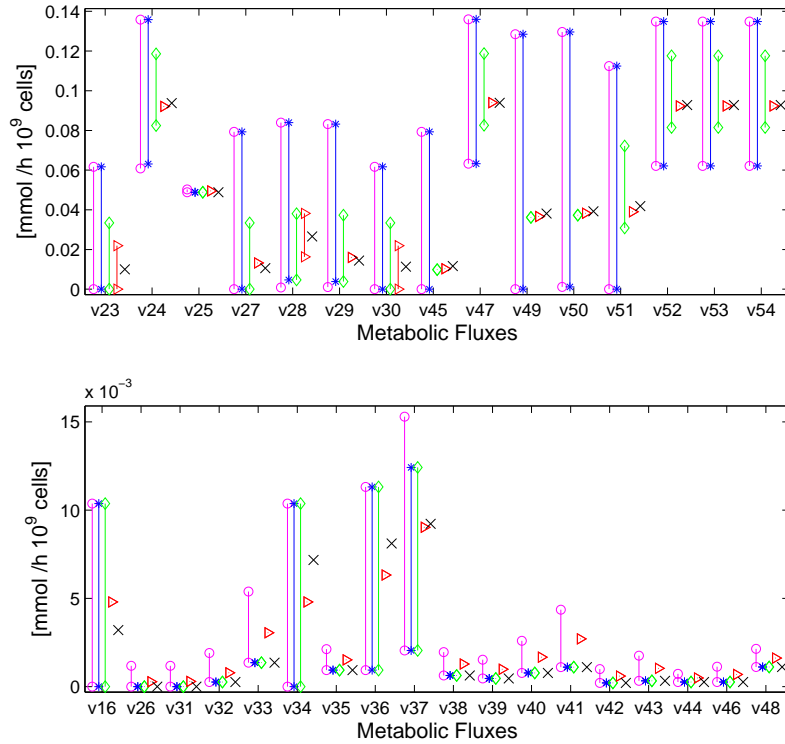
Figure 4.5: Flux Distribution Intervals for the amino acid metabolism.

reactions directly connected to it, are not significantly modified (see Fig. 4.4 and 4.5).

2. For the production of the cellular macromolecules (proteins, RNA, DNA and lipids) the intervals are now reduced to a single plausible value (see Fig. 4.3). In other words, with the initial set of data and the additional assumption that Threonine is an essential amino acid exclusively used for protein formation, the MFA (although globally underdetermined) allows to predict uniquely the specific production rates of these macromolecules which are not directly measured. Additionally, the flux intervals obtained for the pathways of nucleotides and lipids are reduced to a single value as well (see Fig.4.6 and Fig.4.7). In total there are 37 metabolic fluxes for which a single value is determined, same result as the one obtained through the calculability analysis.

3. As expected, the protein production rate v_{55} is maximized (This was precisely the goal of choosing the "no Threonine catabolism" constraint). But it is worth to notice that the formation rates of all other macromolecules (v_{63} for RNA, v_{68} for DNA, v_{75} for lipids) as well as the total biomass production rate v_{76} are also maximized. Above, our purpose has been to investigate

the issue of reducing the range of feasible flux distributions by using exper-
imental data combined with one additional linear theoretical constraint. A
second well-known approach to reduce the range of solutions is to use Linear
Programming. In this approach, the goal is to compute solutions that op-
timize some behavioral optimization objective. The most typical examples
of considered optimization objectives are maximization of cell growth rate,
maximization of ATP synthesis or minimization of substrate utilization (see
for instance [1] and the references therein). Here we see that our results
give the flux distribution that maximizes the biomass production rate (or,
in other words, that the cell maximizes its resources for growth and duplica-
tion) under the constraint of the set of data from Table 4.1. This is a nice
example of a situation were the two approaches for reducing the range of
flux distributions are completely equivalent : either to add theoretical linear
constraints or to select an optimization criterion. As a matter of comparison
we give also the solution obtained with the Matlab optimization function
`fmincon`. Obviously, this is only one arbitrary solution in the set of all
possible optimal solutions. The optimal fluxes are exactly identical to the
fluxes for which there was a single well defined value in the previous solution
(including obviously the biomass production rate v_{76}). For the other reac-
tions, it is interesting to notice that the optimal fluxes are located almost at
the center of the concerned intervals. The optimization code is described in
Section 6.1, Chapter .
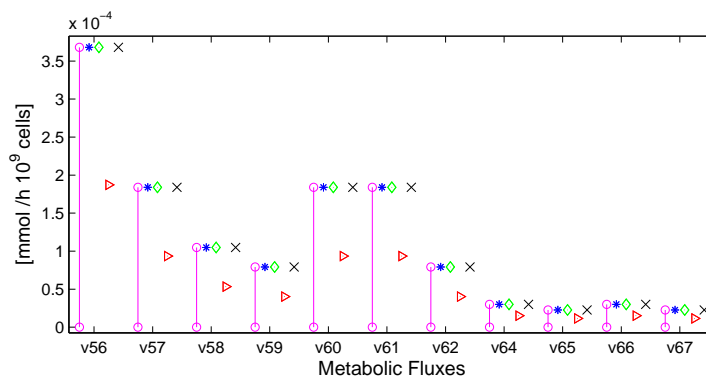
Figure 4.6: Flux Distribution Intervals for the nucleotide metabolism.

Intervals obtained with no Thr catabolism and a larger set of measurements (p=22)

From the previous results, it is clear that a part of the uncertainty is linked to
the fact that measurements of some nutrients in the culture medium are missing.
Hence, in order to further constrain the system, in addition to the assumption re-
garding Thr, we assume that additional measurements of Cys and Pro are available.
To estimate the uptake/excretion rate of these two (and a few more significant) ex-
tracellular species in the culture medium, we have taken as plausible rates the
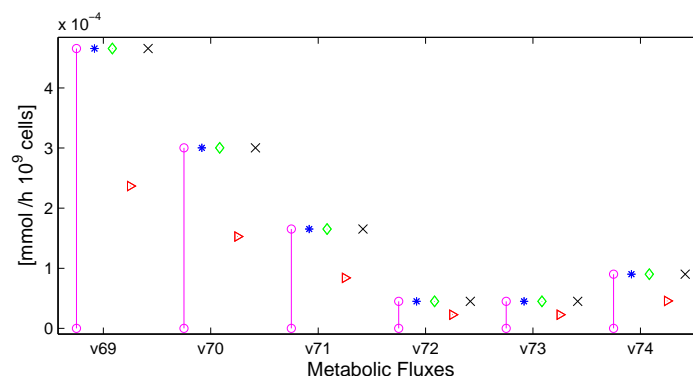
Figure 4.7: Flux Distribution Intervals for the lipid metabolism.

central (average) values given by the flux intervals computed in Section 4.1.3. The estimated rates of Cys and Pro are presented in Table 4.2.

The intervals for this set of measurements are delimited by diamonds. The MFA results show that:

1. Again, the flux intervals of the central metabolism are not modified. For some of the reactions connected to the central pathways the intervals become narrower than in the two previous cases. The intervals are also narrower for the amino acid metabolism where certain intervals are even reduced to a single value.

2. In total, there are 40 metabolic fluxes for which a unique value is found. This result verifies the number of calculable fluxes determined by the calculability analysis.

3. Zero is excluded from the solution set of a few more reactions, but not completely.

We see here that in spite of the addition of further constraints the size of the flux intervals of the central metabolism is not reduce. This is explained by the fact that Glycolysis and PPP are set in parallel, and thus are not distinguishable from extracellular measurements only. The assimilation of $G6P$ could occur in the Glycolysis or in the PPP indistinctly, and thus their flux intervals are in counterbalance.

Intervals that could be obtained with an even larger set of extracellular measurements (p=26) but no assumption

We now consider that a larger set of measurements is available and we relax the assumption of no Thr catabolism so as to assess the impact on the size of the flux intervals and on the quality of the flux analysis. For this purpose, the previous set of measurements is complemented with four additional "pseudo-measurements" for Histidine, Tryptophan, Urea and ethanolamine (see Table 4.2). All these species could possibly be measured in the culture medium in more extensive experimental studies. These pseudo-measurements are just arbitrarily taken from an admissible flux distribution located in the middle of the solution polytope obtained in Subsection 4.1.3 as described above (see Subsection 4.1.3)

Table 4.2: Estimated rates in mmol $h^{-1}10^9 cell-1$

Extracellular Specie	Specific Rate
Cysteine	$-9,98e^{-3}$
Proline	$-3.718e^{-2}$
Histidine	$-3.923e^{-2}$
Tryptophan	$-4.946e^{-3}$
Urea	$9.399e^{-2}$
Ethanolamine	$-6.1086e^{-5}$

In this case the MFA is again well-posed and we have the following conclusions:

1. In this case, the solution gives a biomass formation rate which is smaller than the maximum value of the previous Section 4.1.3. The reason is that, with the chosen additional pseudo-measurements, the unmeasured amino acids become slightly limiting. Obviously, it is natural that the solution depends on the selection of the pseudo-measurements but this is not critical with respect to our purpose here. Indeed, the key point is that, with a complete set of measurements, the flux intervals are now almost completely reduced to a single value. As predicted by the calculability analysis, 53 out of 74 metabolic fluxes are exactly determined. In fact most fluxes are exactly determined while others remains as very small intervals with a length which is less than 10% of the maximum value. In the amino acid metabolism, only 3 metabolic fluxes remain as intervals (being drastically reduced) while the others are set to a unique value. The same holds for the reactions of the nucleotide and lipid pathways, where the metabolic fluxes are now totally determined.

2. Regarding the flux intervals that include zero among the solutions, the number is notably reduced to 6 reactions out of 44 at the beginning. These reactions are:

   - v_7: Pyr + NAD^+ → AcCoA + CO_2 + NADH
   - v_{19}: Rbl5P $\longleftrightarrow$ X5P
   - v_{20}: X5P + R5P $\longleftrightarrow$ F6P + E4P
   - v_{21}: X5P + E4P $\longleftrightarrow$ G3P + F6P
   - v_{23}: Glu + $NAD(P)^+$ $\longleftrightarrow$ αKG + NH_4^+ + NAD(P)H
   - v_{30}: Ser → Pyr + NH_4^+

   The presence of zero within the flux intervals does not necessarily mean that these reactions could occur in the reverse direction. This

Table 4.3: Number of basis vectors defining the space of solutions

Case Study	f_i
Initial set of measurements	144
Initial set of measurements + no Thr catabolism	32
Additional measurements of Cys and Pro + no Thr catabolism	12
Additional measurements of Cys, Pro, His, Trp, Urea and Ethanolamine	4

condition can also be explained by the fact that certain reactions are in counterbalance. Similarly as it occurs for the central metabolism, some reactions occur in parallel in certain paths synthesizing the same intermediary metabolite(s) and cannot therefore be completely distinguished from the available data.

An interesting issue concerns the number of basis vectors computed for each one of the analyzed systems. The number of basis vectors calculated decreases considerably with each additional constraint applied. For instance, from 114 basis vectors obtained for the initial mass balance system analyzed (Subsection 4.1.3) by applying the simple theoretical assumption of no catabolism of Threonine, the number of basis vectors is notably reduced to 32 vectors. In the last case analyzed (Subsection 4.1.3) with the largest set of measurements, the set of solutions is defined by only 4 basis vectors, meaning that the space of solution is now quite restricted. The number of basis vectors calculated for each case study are presented in Table 4.3.

The results obtained through MFA had proved to be in agreement with the ones obtained with the calculability analysis. Actually, in a few easy steps, the calculability check makes possible to find out *a priori* which fluxes may be uniquely calculated. Nonetheless, this systematic procedure does not inform about the well or ill-posedness of the mass balance system, since when the system is ill-posed (considering 19 measurements) it only tells that no fluxes are to be uniquely determined.

In addition, this ill-posed system is analyzed with *CellNetAnalyzer* ([25]), a Matlab toolbox created by the research group of Steffen Klamt. This toolbox proposes several analytical functions. A feasibility analysis checks whether there is at least one (feasible) flux distribution in the network under the constraints imposed. When the feasibility check is done on the metabolic network considering only the 19 experimental data, the system is classified as feasible and even a possible solution is proposed. The reader is reminded that, in Section 4.1.2, this system was proved to be ill-posed. The proposed solution given by this feasibility analysis has no metabolic meaning and thus, is not "metabolically feasible". Even though, this result leads us already to suspect that the system might be ill-posed, a second analysis can be done to

prove this last statement. *CellNetAnalyzer* includes a flux variability analysis, which checks the feasible upper and lower boundaries of each reaction rate. When this flux variability analysis is performed, the result tells us that either the scenario analyzed is overly stringent and no feasible solution exists or that the system is unbounded. As the first argument has already been excluded, the only possibility is that the system is unbounded. Hence, this procedure leads us to the same conclusion as in Subsection 4.1.2.

4.1.4   Experimental Error Analysis

As an extension, the influence of the measurement accuracy on the numerical results is explored using Monte Carlo techniques. Herein, random errors following a normal distribution with zero mean and 5 or 10% of relative standard deviation, respectively, are considered and the solution of the steady-state mass balance equations ((3.18)-(3.19)) under positivity constraints is evaluated for a large number of occurrences of the measurement noise (e.g. ten thousands of runs). For a 5% measurement error the Monte Carlo study always results in a well-posed system and a distribution of errors can be inferred for the upper and lower limits of the flux intervals (an average value and confidence intervals can be evaluated).
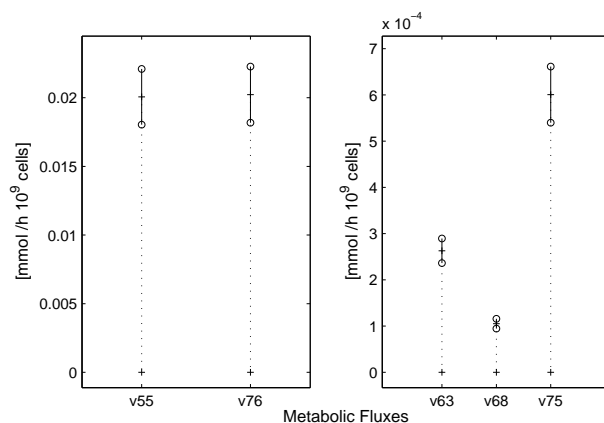
Figure 4.8: Flux Distribution Intervals for biomass synthesis.

As an illustration, the flux intervals are depicted in Fig. 4.8 for macromolecules and biomass synthesis, Fig. 4.9 for the central metabolism, Fig. 4.10 for ammino acids, Fig. 4.11 for nucleotides and Fig. 4.12 for lipids. 95% confidence intervals are built for the upper and lower bounds, assuming a normal error distribution.
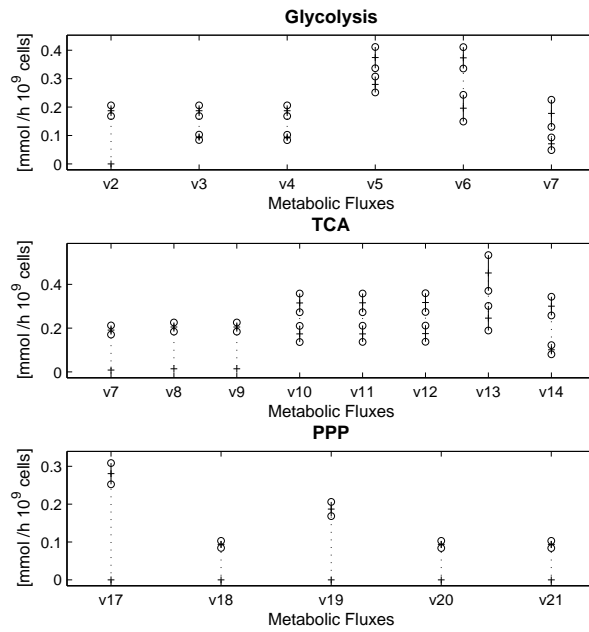
Figure 4.9: Flux Distribution Intervals for the TCA cycle.
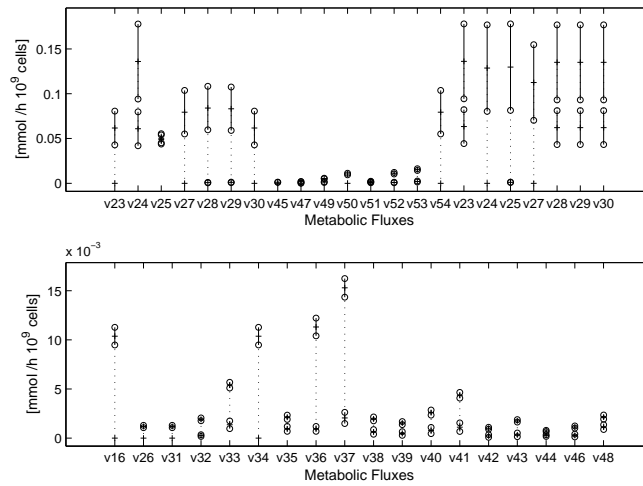
Figure 4.10: Flux Distribution Intervals for the amino acid metabolism.

A distribution of errors is inferred for the upper and lower limits of the flux intervals. The results show that the measurement errors affect the upper limit in a rather linear way, i.e. the distribution of errors on the upper
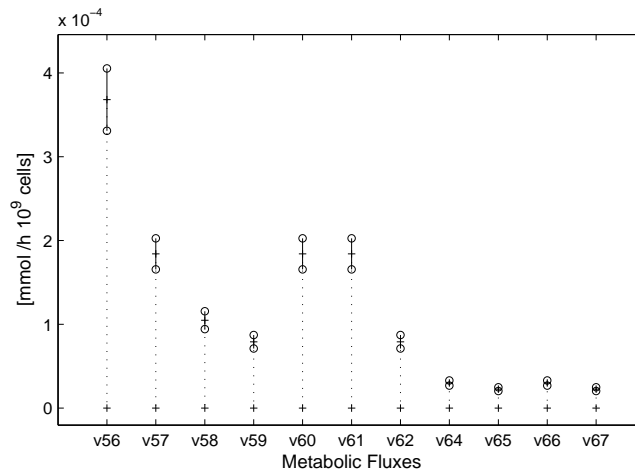
Figure 4.11: Flux Distribution Intervals for the nucleotide metabolism.
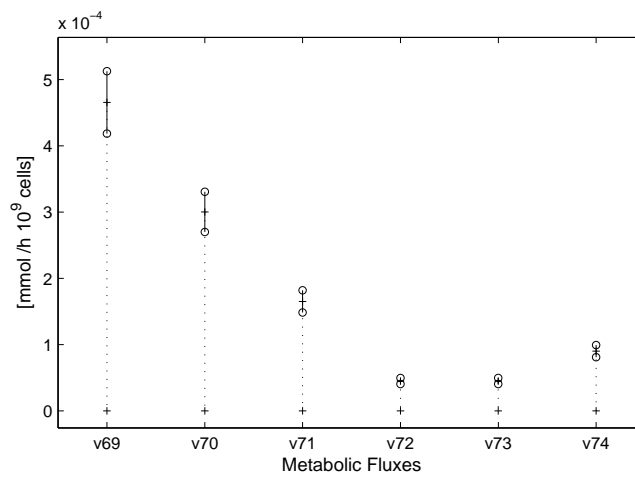
Figure 4.12: Flux Distribution Intervals for the lipid metabolism.

bounds is assimilable to a normal distribution with standard deviation in the same proportion as the introduced error. In contrast, some of the lower bounds are affected in a nonlinear way (due to the positivity constraints) and the distribution of errors is then no longer assimilable to a normal one. The distributions of errors inferred for the upper and lower bounds in the case of 5% error measurements are presented in Appendix B.

On the other hand, considering a 10% of error on the experimental measurements can lead to ill-posed systems. For 42 out of ten thousand runs the system do not have a solution, meaning that experimental data with a 10% error will still generate a well-posed system in the 99,58% of the cases.

4.1.5   Testing the direction of possibly reversible reactions

From the previous section, it appears that some computed flux intervals include zero as a feasible solution, implying that the corresponding reactions could possibly operate in the reverse direction. In this section, we analyze this issue from a metabolic structure viewpoint.

The network describing the metabolism of CHO-320 cells involves both irreversible and reversible reactions. Up to now we have considered that the net steady-state direction during the exponential growth is known beforehand and can therefore be imposed in the statement of the MFA problem. For instance, the reversible reactions of Glycolysis and PPP should run in the direction which allows glucose assimilation and nucleic acid synthesis, respectively, to actually achieve cellular growth.

Nevertheless, there are some reversible reactions whose net direction cannot be guessed in advance only on the basis of the qualitative metabolic behaviour of the cells. It is the case for the four reactions in Fig. 4.13, which can run in both directions depending on the need for some metabolites in particular reactions or pathways.
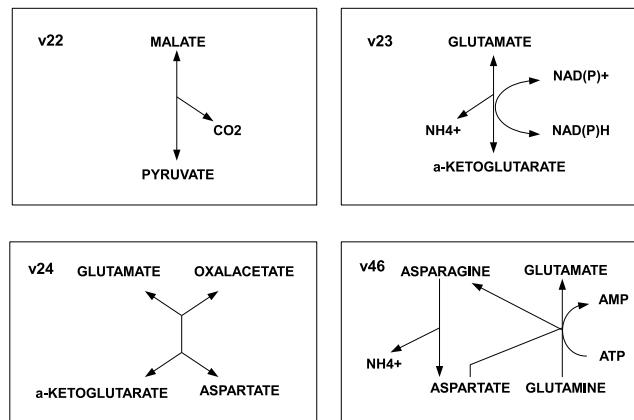
Figure 4.13: Reversible reactions considered in the analysis

The MFA presented in the previous subsections has been made for a particular choice on the net direction of these four reversible reactions (as they appear in Table 2.1). Nevertheless, other network configurations might be obtained by alternating the net direction of reactions v_{22}, v_{23}, v_{24} and v_{46}. Hence, we shall test whether a solution set to the flux analysis exists (i.e., if the system is *well posed*) when these reactions are reversed. It must be stressed that this analysis is performed using only the initial data set in Table 4.1.

Among the 16 possible network structures that can be obtained by chang-

ing the direction of the above-mentioned reactions, only two of them have a non-empty solution set, i.e., only two network configurations give rise to a *well posed* problem, admitting a solution which satisfies the constraints imposed by the extracellular measurements. One of them is obviously the configuration considered to calculate the solution set of the previous subsections. The second admissible configuration is characterized by the following four reactions:

$$v_{22} : Malate \rightarrow Pyruvate + CO_2$$
$$v_{23\,rev} : \alpha KG + NH_4^+ + NAD(P)H \rightarrow Glu + NAD(P)^+$$
$$v_{24} : Oxaloacetate + Glu \rightarrow Asp + \alpha KG$$
$$v_{46} : Asn \rightarrow Asp + NH_4^+$$
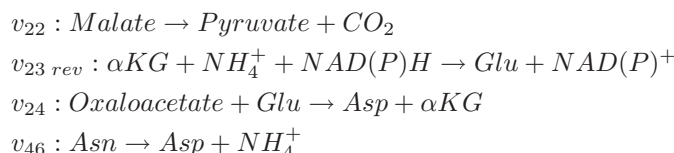
This flux distribution implies the occurrence of reaction v_{23} in the reverse direction, from α-ketoglutarate to glutamate, which has generally been reported to be feasible in cultures under high ammonia concentrations. Normally, this reaction produces α-ketoglutarate from glutamate, as a second step of the metabolic pathways for glutamine degradation [42]. Also in other kind of mammalian cells, specifically Hybridoma cell cultures, it has been demonstrated that under ammonia-stress conditions, the reaction catalyzed by glutamate dehydrogenase (reaction v_{23}) goes in the reverse direction, while control cells transform glutamate in α-ketoglutarate and ammonia [9]. In our CHO cell culture, ammonia is constantly produced and accumulated, but its concentration during the growth phase is probably not sufficient to stimulate the shift of direction in v_{23}, even if it is mathematically possible. In [9] the ammonia-stress condition is given by 10 mM of ammonia, while, in our culture at the end of the growth phase the concentration only reaches 5 mM.

In summary, it is seen that by systematically considering all the possible configurations, the network structure allows only two feasible distributions in agreement with the experimental observations. Otherwise, an *ill posed* problem emerges, for which no solution exists. We believe that we can interpret the results of this analysis as a strong evidence of the consistency of the chosen metabolic network and the results obtained in Section 4.

4.1.6   Balance of energetic co-factors

As it is clearly documented in the literature [8, 11, 16, 48, 53, 55], energetic cofactors ATP, $NAD(P)H$ and $FADH_2$ cannot be considered as internal balanced metabolites. The reason is that an important basic function of the metabolism is also to provide energy for mechanisms not represented by the network, like for instance the turnover of macromolecules and other so-called futile cycles.

Here, we use the optimal solution obtained in Subsection 4.1.3 to estimate the energy production.

Assuming that 1 mol of $NAD(P)H$ yields 3 mol of ATP in the respiratory chain (P/O), 1 mol of $FADH_2$ yields 2 mol of ATP, and 1 mol of GTP yields 1 mol of ATP [16, 42, 53], the equivalent ATP production rates given in Table 4.4 are obtained.

Table 4.4: Equivalent ATP production rate $[mmol/h \cdot 10^9 cell]$.

Energetic cofactor	Production		Consumption		ATP
	Production Rate	ATP equivalents	Consumption Rate	ATP equivalents	Net Production
$ATP \ / \ GTP$	0,8695	0,8695	0,7041	0,7041	0,1654
$NAD(P)H$	1,5001	4,5004	0,3631	1,0894	3,4110
$FADH_2$	0,2463	0,4926	–	–	0,4926
ATP_{TOTAL}					4,0691

As compared with the results found in the literature [16, 55], the net ATP production through our metabolic network for CHO cells appears to be far more important than the ATP production for Hybridoma cells.

However, the general qualitative trend is similar (but with a larger magnitude) to that observed in [55] for Hybridomas. For instance, NAD(P)H is the main source of energy, around 84% of the total ATP production. It also appears that the TCA cycle provides the major part of the energy, around 76%, a percentage close to that given in [55] where the TCA cycle provides 51-68% of the total ATP production for Hybridoma cells. Similar results were obtained in [16] also for Hybridomas.

4.2   Complementary Results

4.2.1   MFA for a different set of experimental data

The same metabolic network of CHO-320 cells introduced in Section 2.2 is now the basis of a new metabolic flux analysis, considering a different ratio between the initial concentration of the two main substrates: glucose and glutamine. A different data set from the one presented in Subsection 4.1.1 is used for this analysis, though the measured species remain the same. The specific uptake and excretion rates resulting from these other measurement data are presented in Table 4.5.

The culture conditions are basically the same as described in Subsection 4.1.1 but an initial concentration of glucose equal to 32 mM (2-fold increase) and of glutamine equal to 6 mM are considered. In Figures 4.14 and 4.15 the evolution of cell densities, main substrates and metabolic products of both

Table 4.5: Extracellular Measurements in mmol $h^{-1}10^9cell-1$

Substrates	Specific Uptake Rates	Products	Specific Excretion Rates
Glucose	$-1.355e^{-1}$	Lactate	$2.275e^{-1}$
Glutamine	$-5.023e^{-2}$	NH_4^+	$3.712e^{-2}$
Arginine	$-2.621e^{-3}$	Glycine	$2.609e^{-3}$
Asparagine	$-1.534e^{-3}$	Alanine	$1.055e^{-2}$
Aspartate	$-8.989e^{-4}$	Glutamate	$6.149e^{-3}$
Isoleucine	$-2.529e^{-3}$		
Leucine	$-3.920e^{-3}$		
Lysine	$-4.060e^{-3}$		
Methionine	$-1.091e^{-4}$		
Phenylalanine	$-1.662e^{-3}$		
Serine	$-1.267e^{-3}$		
Threonine	$-2.813e^{-3}$		
Tyrosine	$-1.380e^{-3}$		
Valine	$-3.177e^{-3}$		

cultures (at glucose 16 mM and glucose 32 mM) are shown. ($*$): Glucose 32 mM; ($\circ$): Glucose 16 mM.

From this figure one may see that even though the initial concentration of glucose is increased to 32 [mM], a slightly lower biomass concentration is achieved than that obtained for 16 [mM] of glucose initial concentration. It appears that increasing the initial concentration of glucose alone will not increase the production of biomass. The profiles of production/consumption of the main extracellular species remain quite similar for both culture conditions during the growth phase (first 80 h approximately). As the initial concentration of glucose alone is increased, it is quite likely that one or maybe more substrates are limiting the metabolism.

As seen in the previous analysis in Section 4.1 , the set of actual measurements should be complemented with one extra measurement, the excretion rate of CO_2, in order to have a well-posed system. Otherwise, the presence of three unbounded routes is once more verified. As the evolution of both culture seem similar, we consider the same estimative value of $0.68[mmol10^{-9}cell^{-1}h^{-1}]$ given for the CO_2 excretion rate.

The performed analysis is almost the same, with one or two differences as we shall see.
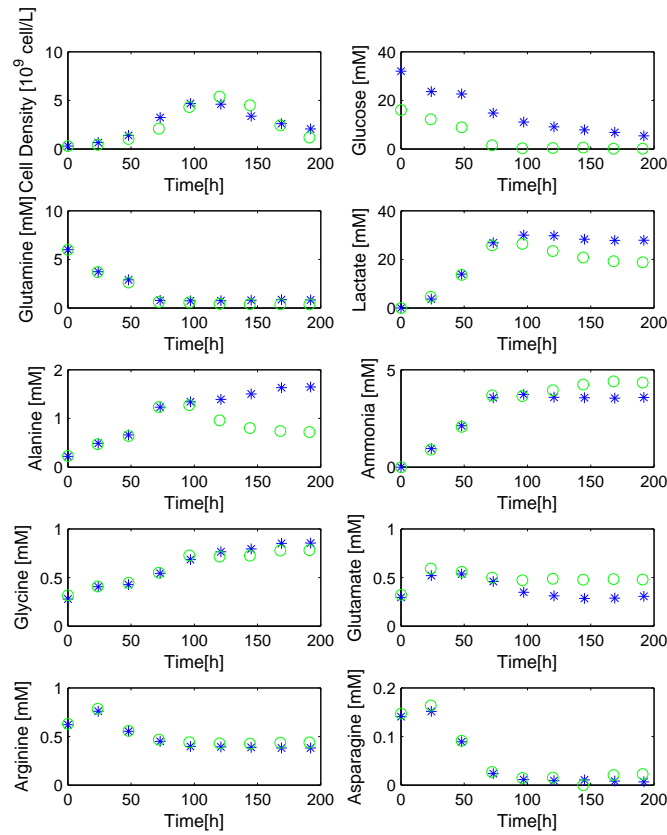
Figure 4.14: Time evolution of the biomass, substrates and products.

Intervals obtained with the initial set of experimental measurements

The metabolic flux analysis is first performed for the experimental data of Table 4.5 plus the CO_2 measurement. The obtained intervals are delimited by red circles in Figure 4.16 for biomass and its main macromolecules, Fig. 4.17 for the central metabolism, Fig. 4.18 for amino acids, Fig. 4.19 for nucleotides and Fig. 4.20 for lipids. For comparison purposes, the intervals obtained for a glucose initial concentration of 32 mM are presented in red, while depicted in black, the intervals obtained in the previous analysis for a glucose initial concentration of 16 mM.

This first analysis shows that the problem is well-posed, producing bounded non-negative intervals for all fluxes. It can be noticed that for several metabolic fluxes the range of specific rates reach lower values than in the
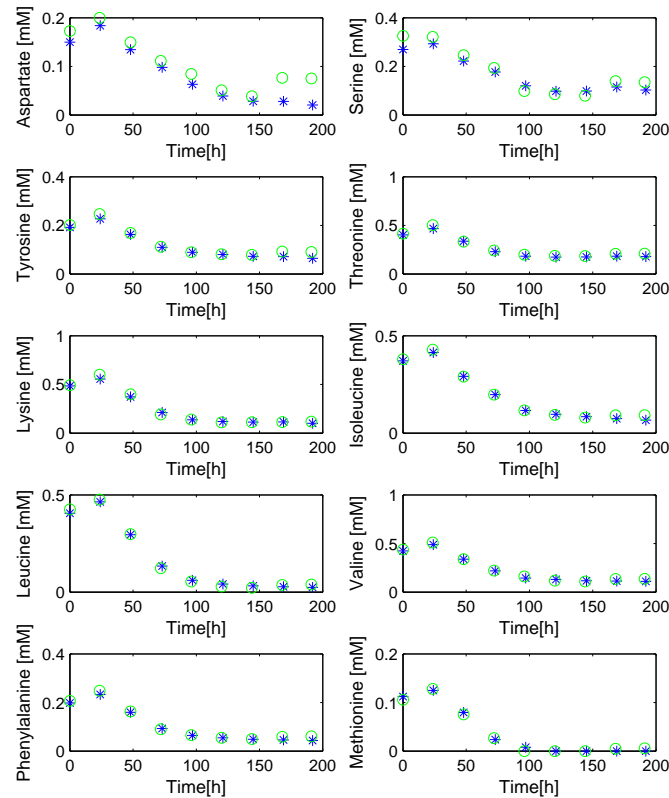
Figure 4.15: Time evolution of amino acids.

previous case analyzed in Section 4.1.3. This is particularly clear for the biomass production and the synthesis of its main macromolecules, whose specific production rates appear to be lower when increasing the initial concentration of glucose. It seems that the proportion in which the initial concentration of all or at least the main (and limiting) substrates are added will influence the metabolic fluxes within the cells.

Intervals obtained with the initial set of measurements under the assumption of no Methionine catabolism

Similarly as done is Subsection 4.1.3, an additional assumption is considered regarding the catabolism of a certain amino acid which is exclusively used for protein formation. Unlike the previous analysis, for the cellular culture carried out at 32 mM it appears that Threonine is no longer the (essential)
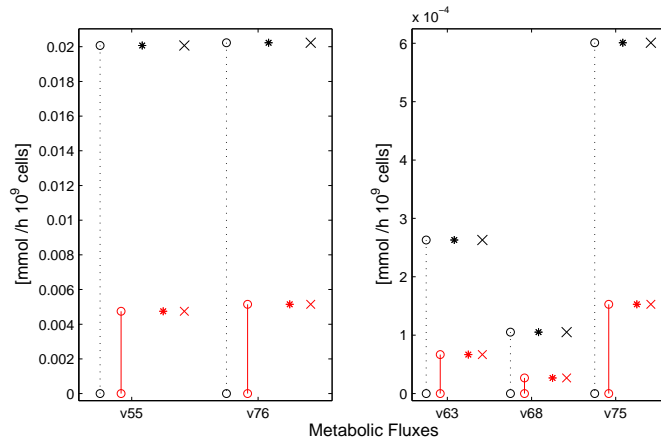
Figure 4.16: Flux Distribution Intervals for biomass synthesis.
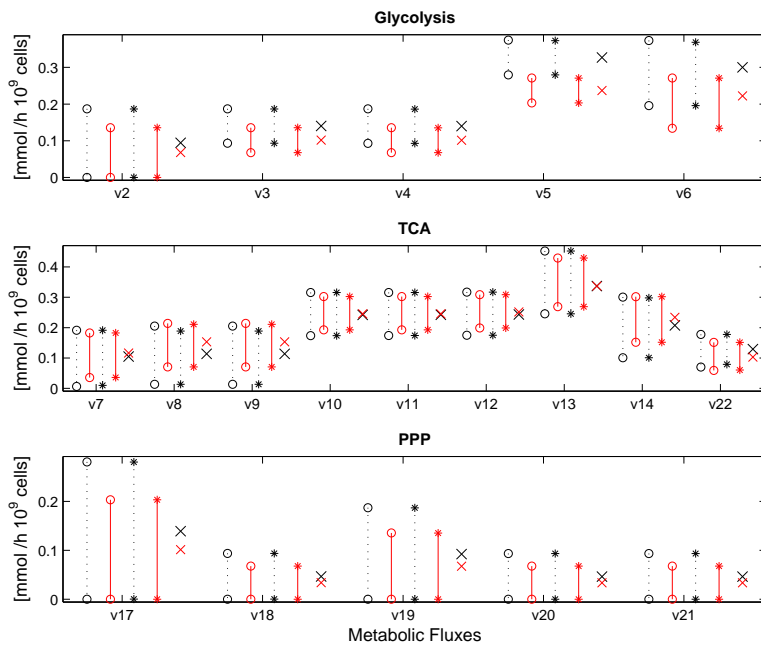
Figure 4.17: Flux Distribution Intervals for the central metabolism.

amino acid limiting the production of cellular proteins. The essential amino acid with the lowest ratio between its uptake rate and its stoichiometric coefficient for protein synthesis, and thus the amino acid determining the maximum production rate of protein, is now Methionine.
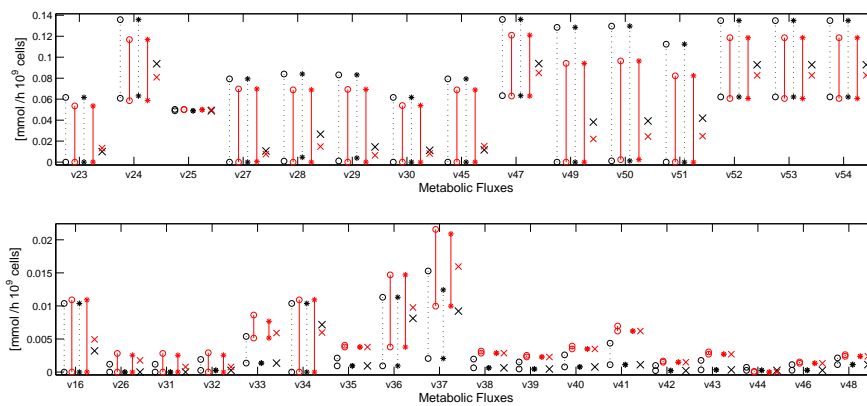
Figure 4.18: Flux Distribution Intervals for the amino acid metabolism.

Actually, in Figure 4.18 it can be noticed that the interval for v_{44} (the catabolic reaction of Methionine delimited by red circles) obtained previously includes zero as a possible solution and is the smallest in comparison to the rest of the amino acid fluxes including zero (v_{16}, v_{23}, v_{26}, v_{27}, v_{28}, v_{29}, v_{30}, v_{31}, v_{32}, v_{34}, v_{45}, v_{49}, v_{51}). Consequently, the flux analysis is performed by setting v_{44} equal to zero and the resulting flux intervals are shown delimited by red stars in all figures.
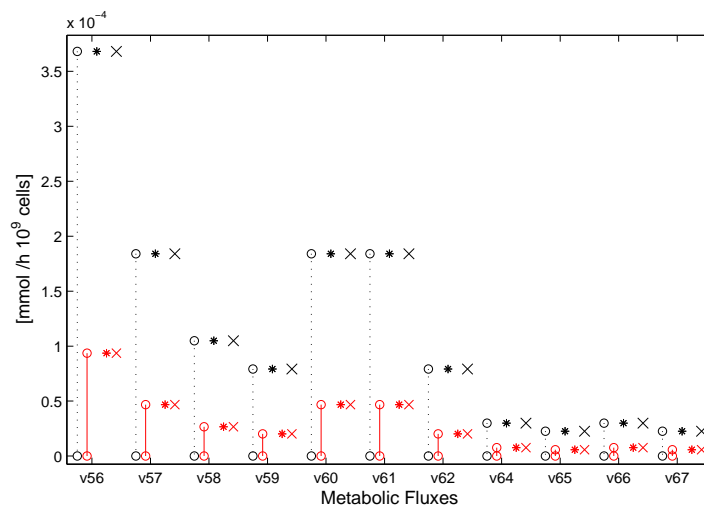
Figure 4.19: Flux Distribution Intervals for the nucleotide metabolism.

The flux intervals obtained for the central metabolism as well as certain fluxes of the amino acid pathways are not significantly modified (see Fig.

4.17 and 4.18). In an analogous way as considering the hypothesis of no Threonine catabolism in Subsection 4.1.3, the protein production rate is maximized (v_{55}), thus maximizing the biomass formation and the fluxes for the production of the other cellular macromolecules (see Fig. 4.16). The flux intervals obtained for the routes of nucleotides and lipids are reduced to a single value as well (see Fig. 4.19 and 4.20). In total, 34 metabolic fluxes out of 75 are uniquely determined and zero is excluded from the solution set of the metabolic fluxes directly involved with cellular growth.
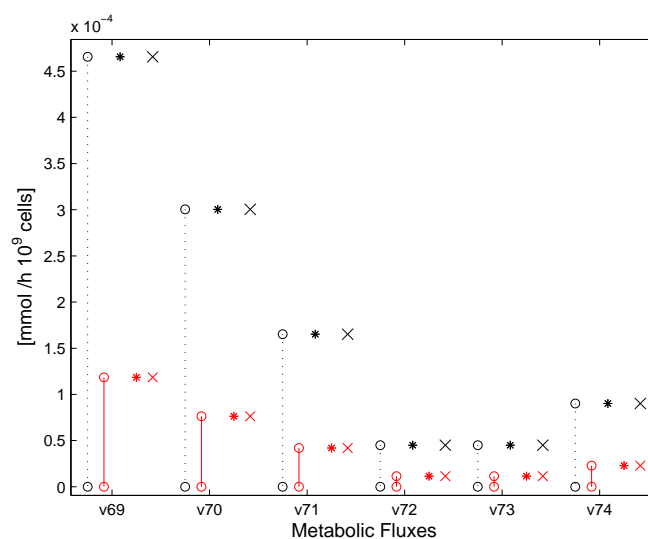
Figure 4.20: Flux Distribution Intervals for the lipid metabolism.

As a matter of comparison we also present the solution obtained by linear optimization with the maximization of the biomass production as selected criterion. The 34 fluxes for which there was a uniquely determined value when considering the assumption of no Methionine catabolism match exactly the optimal fluxes. This particular (arbitrary) solution is depicted by crosses in all figures.

As methionine is the limiting amino acid for the experiences carried out at a glucose initial concentration of 32 mM, the production rates of proteins and subsequently of biomass are determined by the consumption rate of this amino acid. If we look at Table 4.5 the specific consumption rate of methionine is -1.091e^{-4} [mmol $h^{-1}10^9 cell-1$], a much lower rate of that of threonine given in Table 4.1 (-1.1842e^{-3} [mmol $h^{-1}10^9 cell-1$]), the limiting amino acid for the experiences carried out at 16 mM of glucose initial concentration. This will then explain why the flux distribution that maximizes biomass production is lower at 32 [mM] than it is at 16 [mM], and thus why the flux intervals appear to be narrower, considering smaller

flux values at 32 [mM]. For certain amino acids, the flux intervals at 32 [mM] consider larger possible values for the fluxes, this is explained by more important consumption rates of the essential amino acids in these conditions than at 16 [mM] of initial glucose concentration (see Tables 4.1 and 4.5).

4.2.2 MFA for the next two phases of the culture

In this Section the same MFA methodology is applied to the next phases of a (batch) cellular culture: the transition and death phases. Since we would like to have an idea of how the metabolic state of the cell change through the whole culture, we perform a metabolic flux analysis so as to determine which range of flux distributions characterize these two phases. The measurements of the biomass formation and the time evolution of the main substrates and products for the entire cell life are presented in Figure 4.21. Growth, transition and death phases data are represented in blue, green and magenta, respectively.
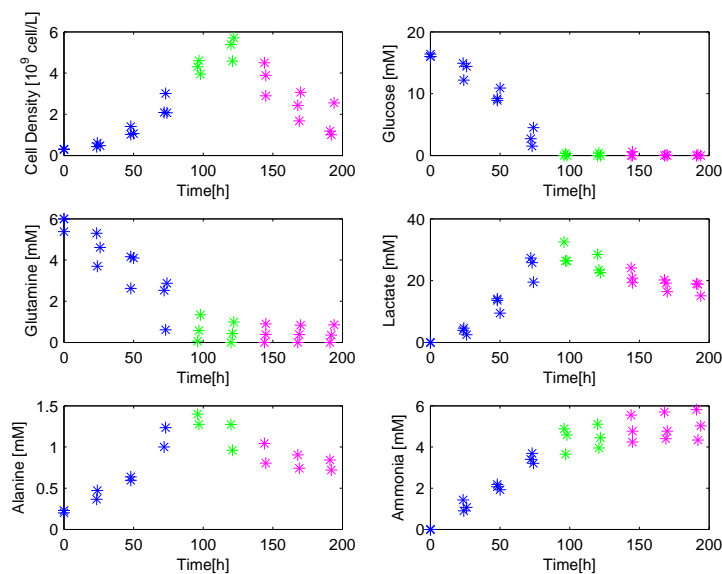
Figure 4.21: Biomass, substrate and product concentration profiles.

Transition Phase

The transition phase starts right after the depletion of glucose from the culture medium. Since the main carbon source is exhausted, the cells are not longer able to growth at their maximum rate. In the experiences presented in Figure 4.21, this occurs form about 80 to 120 hours. Some cells have started

dying while other cells continue to divide. In consequence, this phase of the cell life is characterized by a maintenance of the cell density in the culture.

The metabolism of the cells changes during this period, to adapt to the new environmental conditions where no more glucose is available. The cell regulates itself and starts consuming lactate and alanine instead of producing them in order to provide an alternative carbon and energy source for biosynthesis and growth. As a consequence, the metabolic network representing the metabolism of the cells during the transition phase needs to be adapted. The set of reactions are presented in Table 4.6. The metabolic regulation induces the change in the direction of the reactions of Glycolysis, which now run from lactate through pyruvate to glucose-6 phosphate ($G6P$) in a pathway known as Gluconeogenesis. This reverse pathways, by the synthesis of $G6P$, ensures the continuous production of nucleotides and in turn, of biomass. Thus, the pathways for the production of lipids and proteins are still active during this phase. Another change in the metabolism is that of glutamate. From Figure 4.21, it can be seen that during the transition phase the concentration level of glutamate diminishes implying that instead of being produced glutamate is now consumed.

The experimental data come from the same experiments used in [36, 38], which were presented in Subsection 4.1.1. The specific uptake and excretion rates are obtained by linear regression of substrates and products during the transition phase. The estimated rates are given in Table 4.7.
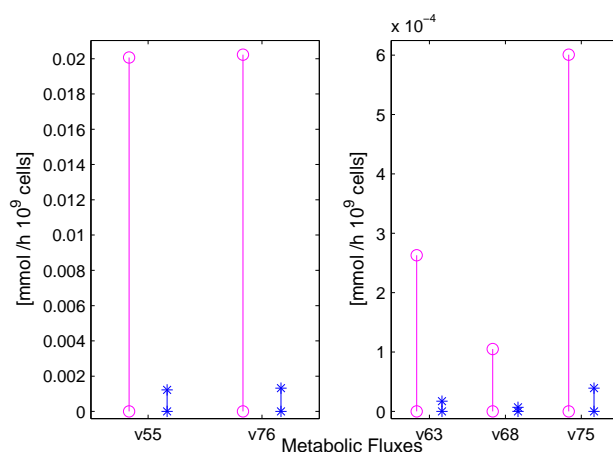
Figure 4.22: Flux Distribution Intervals for biomass synthesis.

For this new analysis, the data set has reduced to 18 measurements while the number of reactions remains the same. Hence, it is likely to encounter

Table 4.6: Metabolic Reactions for the transition phase

Flux	Reaction
	Gluconeogenesis
v_1	**Lactate**^{a} $+ NAD^+ \xrightleftharpoons{} {}^b Pyr + NADH$
v_2	$Pyr + HCO_3^- + ATP \rightarrow Oxal + ADP$
v_3	$Oxal + GTP \rightarrow 3PG + GDP + CO_2$
v_4	$3PG + NADH + ATP \xrightleftharpoons{} G3P + NAD^+ + ADP$
v_5	$G3P \xrightleftharpoons{} DHAP$
v_6	$DHAP + G3P \rightarrow F6P$
v_7	$F6P \xrightleftharpoons{} G6P$
	Tricarboxylic Acid Cycle
v_8	$Pyr + NAD^+ + CoASH \rightarrow AcCoA + CO_2 + NADH$
v_9	$AcCoA + Oxal + H_2O \rightarrow Cit + CoASH$
v_{10}	$Cit + NAD(P)^+ \rightarrow \alpha KG + CO_2 + NAD(P)H$
v_{11}	$\alpha KG + CoASH + NAD^+ \rightarrow SucCoA + CO_2 + NADH$
v_{12}	$SucCoA + GDP + P_i \xrightleftharpoons{} Succ + GTP + CoASH$
v_{13}	$Succ + FAD \xrightleftharpoons{} Fum + FADH_2$
v_{14}	$Fum \xrightleftharpoons{} Mal$
v_{15}	$Mal + NAD^+ \xrightleftharpoons{} Oxal + NADH$
	Pentose Phosphate Pathway
v_{16}	$G6P + 2NADP^+ + H_2O \rightarrow Rbl5P + 2NADPH + CO_2$
v_{17}	$Rbl5P \xrightleftharpoons{} R5P$
v_{18}	$Rbl5P \xrightleftharpoons{} X5P$
v_{19}	$X5P + R5P \xrightleftharpoons{} F6P + E4P$
v_{20}	$X5P + E4P \xrightleftharpoons{} G3P + F6P$
	Anaplerotic Reaction
v_{21}	$Mal + NAD(P)^+ \xrightleftharpoons{} Pyr + HCO_3^- + NAD(P)H$
	Amino Acid Metabolism
v_{22}	$Ala + \alpha KG \xrightleftharpoons{} Pyr + Glu$
v_{23}	$Glu + NAD(P)^+ \xrightleftharpoons{} \alpha KG + NH_4^+ + NAD(P)H$
v_{24}	$Oxal + Glu \xrightleftharpoons{} Asp + \alpha KG$
v_{25}	$Gln \rightarrow Glu + NH_4^+$
v_{26}	$Thr + NAD^+ + CoASH \rightarrow Gly + NADH + AcCoA$
v_{27}	$Ser \xrightleftharpoons{} Gly$
v_{28}	$3PG + Glu + NAD^+ \rightarrow Ser + \alpha KG + NADH$
v_{29}	$Gly + NAD^+ \rightarrow CO_2 + NH_4^+ + NADH$
v_{30}	$Ser \rightarrow Pyr + NH_4^+$
v_{31}	$Thr \rightarrow \alpha Kb + NH_4^+$
v_{32}	$\alpha Kb + CoASH + NAD^+ \rightarrow PropCoA + NADH + CO_2$
v_{33}	$PropCoA + HCO_3^- + ATP \rightarrow SucCoA + ADP + P_i$
v_{34}	$Trp \rightarrow Ala + 2CO_2 + \alpha Ka$
v_{35}	$Lys + 2\alpha KG + 3NAD(P)^+ + FAD^+ \rightarrow \alpha Ka + 2Glu + 3NADPH + FADH_2$
v_{36}	$\alpha Ka + CoASH + 2NAD^+ \rightarrow AcetoAcCoA + 2NADH + 2CO_2$
v_{37}	$AcetoAcCoA + CoASH \rightarrow 2AcCoA$
v_{38}	$Val + \alpha KG + CoASH + 3NAD^+ + FAD^+ \rightarrow PropCoA + Glu + 2CO_2 + 3NADH + FADH_2$
v_{39}	$Ile + \alpha KG + 2CoASH + 2NAD^+ + FAD^+ \rightarrow AcCoA + PropCoA + Glu + CO_2 + 2NADH + FADH_2$
v_{40}	$Leu + \alpha KG + CoASH + NAD^+ + HCO_3^- + ATP + FAD^+ \rightarrow AcCoA + AcetoAc + Glu + CO_2 + NADH + ADP + FADH_2$
v_{41}	$AcetoAc + SucCoA \rightarrow AcetoAcCoA + Succ$
v_{42}	$Phe + NADH \rightarrow Tyr + NAD^+$
v_{43}	$Tyr + \alpha KG \rightarrow Fum + AcetoAc + Glu + CO_2$
v_{44}	$Met + Ser + ATP \rightarrow Cys + \alpha Kb + NH_4^+ + AMP$
v_{45}	$Cys \rightarrow Pyr + NH_4^+$
v_{46}	$Asn \xrightleftharpoons{} Asp + NH_4^+$
v_{47}	$Arg \rightarrow Orn + Urea$
v_{48}	$Orn + \alpha KG \xrightleftharpoons{} Glu\gamma SA + Glu$

^{a} Extracellular measured species

^{b} Chosen net direction for reversible reaction

Flux	Reaction
v_{49}	$Pro \rightarrow Glu\gamma SA$
v_{50}	$Glu\gamma SA + NAD(P)^+ \rightarrow Glu + NAD(P)H$
v_{51}	$His \rightarrow Glu + NH_4^+$

Urea Cycle

v_{52}	$Orn + CarbP \rightarrow Cln$
v_{53}	$Cln + Asp + ATP \rightarrow ArgSucc + AMP$
v_{54}	$ArgSucc \rightarrow Arg + Fum$

Protein Synthesis

v_{55}	$0.023His + 0.053Ile + 0.091Leu + 0.059Lys + 0.023Met + 0.039Phe + 0.059Thr + 0.014Trp + 0.066Val + 0.051Arg$ $+0.072Gly + 0.052Pro + 0.032Tyr + 0.078Ala + 0.043Asn + 0.053Asp + 0.019Cys + 0.042Gln + 0.063Glu + 0.068Ser + ATP$ $+3GTP \rightarrow Protein + AMP + Pp_i + 3GDP + 3P_i$

Nucleotide Synthesis

v_{56}	$R5P + ATP \rightarrow PRPP + AMP$
v_{57}	$PRPP + 2Gln + Gly + Asp + 4ATP + CO_2 \rightarrow IMP + 2Glu + Fum + 4ADP + 2H_2O$
v_{58}	$IMP + Asp + 2ATP + GTP \rightarrow ATP_{RN} + Fum + 2ADP + GDP$
v_{59}	$IMP + Gln + 3ATP + NAD^+ + 2H_2O \rightarrow GTP_{RN} + Glu + 2ADP + AMP + NADH$
v_{60}	$HCO_3^- + NH_4^+ + Asp + 2ATP + NAD^+ \rightarrow Orotate + ADP + NADH$
v_{61}	$Orotate + PRPP + ATP \rightarrow UTP_{RN} + CO_2 + 2ADP$
v_{62}	$UTP_{RN} + Gln + ATP \rightarrow CTP_{RN} + Glu + ADP$
v_{63}	$0.285(ATP_{RN} + UTP_{RN}) + 0.215(GTP_{RN} + CTP_{RN}) \rightarrow RNA$
v_{64}	$ATP_{RN} \rightarrow dATP$
v_{65}	$GTP_{RN} \rightarrow dGTP$
v_{66}	$CTP_{RN} \rightarrow dCTP$
v_{67}	$UTP_{RN} \rightarrow dTTP$
v_{68}	$0.285(dATP + dTTP) + 0.215(dGTP + dCTP) \rightarrow DNA$

Lipid Synthesis

v_{69}	$DHAP + NADH \rightarrow Glyc3P + NAD^+$
v_{70}	$Choline + 18AcCoA + Glyc3P + 23ATP + 33NADH \rightarrow PC + 17ADP + 6AMP + 33NAD^+$
v_{71}	$Ethanolamine + 18AcCoA + Glyc3P + 23ATP + 33NADH \rightarrow PE + 17ADP + 6AMP + 33NAD^+$
v_{72}	$PE + Ser \rightarrow PS + Ethanolamine$
v_{73}	$16AcCoA + Ser + Choline + 16ATP + 29NADPH \rightarrow SM + 2CO_2 + 14ADP + 2AMP + 29NADP^+$
v_{74}	$18AcCoA + 18ATP + 14NADPH \rightarrow Cholesterol + 6CO_2 + 18ADP + 14NADP^+$
v_{75}	$0.5PC + 0.2PE + 0.075PS + 0.075SM + 0.15Cholesterol \rightarrow MembraneLipid$

Biomass Formation

v_{76}	$0.9226Protein + 0.013RNA + 0.0052DNA + 0.0297MembraneLipid \rightarrow Biomass$

Transport Reactions

v_{77}	$\mathbf{Asp_{ext}}^a \rightarrow Asp$
v_{78}	$Cys_{ext} \rightarrow Cys$
v_{79}	$Gly \rightarrow \mathbf{Gly_{ext}}^a$
v_{80}	$\mathbf{Ser_{ext}}^a \rightarrow Ser$
v_{81}	$\mathbf{Glu_{ext}}^a \rightarrow Glu$
v_{82}	$\mathbf{Tyr_{ext}}^a \rightarrow Tyr$
v_{83}	$\mathbf{Ala_{ext}}^a \rightarrow Ala$
v_{84}	$\mathbf{Arg_{ext}}^a \rightarrow Arg$
v_{85}	$\mathbf{Asn_{ext}}^a \rightarrow Asn$
v_{86}	$\mathbf{Gln_{ext}}^a \rightarrow Gln$
v_{87}	$His_{ext} \rightarrow His$
v_{88}	$\mathbf{Ile_{ext}}^a \rightarrow Ile$
v_{89}	$\mathbf{Leu_{ext}}^a \rightarrow Leu$
v_{90}	$\mathbf{Lys_{ext}}^a \rightarrow Lys$
v_{91}	$\mathbf{Met_{ext}}^a \rightarrow Met$
v_{92}	$\mathbf{Phe_{ext}}^a \rightarrow Phe$
v_{93}	$Pro_{ext} \rightarrow Pro$
v_{94}	$\mathbf{Thr_{ext}}^a \rightarrow Thr$
v_{95}	$Trp_{ext} \rightarrow Trp$
v_{96}	$\mathbf{Val_{ext}}^a \rightarrow Val$
v_{97}	$Ethanolamine_{ext} \rightarrow Ethanolamine$
v_{98}	$Choline_{ext} \rightarrow Choline$
v_{99}	$NH_4^+ \rightarrow \mathbf{NH_{4,ext}^+}^a$
v_{100}	$CO_2 \rightarrow CO_{2,ext}$

Continued from previous page

Table 4.7: Transition phase specific rates in mmol $h^{-1}10^9 cell - 1$

Substrates	Specific Uptake Rates	Products	Specific Excretion Rates
Lactate	$-3.4514e^{-2}$	Glycine	$9.0008e^{-4}$
Glutamine	$-1.0604e^{-3}$	NH_4^+	$9.0092e^{-4}$
Alanine	$-3.9000e^{-4}$		
Glutamate	$-7.6471e^{-4}$		
Arginine	$-6.2246e^{-5}$		
Asparagine	$-1.3583e^{-4}$		
Aspartate	$-5.6883e^{-4}$		
Isoleucine	$-5.4725e^{-4}$		
Leucine	$-5.1221e^{-4}$		
Lysine	$-6.6583e^{-4}$		
Methionine	$-9.2775e^{-5}$		
Phenylalanine	$-1.9647e^{-4}$		
Serine	$-5.7292e^{-4}$		
Threonine	$-1.5100e^{-4}$		
Tyrosine	$-1.4006e^{-4}$		
Valine	$-4.6367e^{-4}$		

problems of well-posedness. Indeed, when the space of solutions is calculated, several metabolic fluxes appear to be unbounded. In order to tackle this problem, again, an estimative value of 0.3 $[mmol10^{-9}cell^{-1}h^{-1}]$ for the excretion rate of CO_2 is taken from reference [29]. From this attempt, a set of solutions is calculated and the flux ranges for each metabolic reaction are established. So as to have a clear idea of the metabolic changes induced by the cells, the obtained intervals for the exponential growth phases are presented along side the intervals obtained for the transition phase. Flux notation corresponds to that given for the transition phase in Table 4.6. The flux intervals for the exponential and transition phases are presented in Fig. 4.22 for biomass and its main macromolecules, Fig. 4.23 for the central metabolism (Gluconeogenesis, TCA and PPP), Fig. 4.24 for amino acids, Fig. 4.25 for nucleotides and Fig. 4.26 for lipids. The flux intervals for the exponential and transition phases are respectively depicted in circles and stars in all figures.

From the range of flux rates given in Figure 4.22 for the production of biomass and its main macromolecules, it appears clearly that the levels of synthesis have diminished with respect to those obtained for the exponential growth phase. As it should be suspected from Fig. 4.21, which shows the evolution of the cell density throughout the whole culture, the biomass production is less important during the transition phase producing a stagnation of the cell density. Then, the resulting intervals for the transition
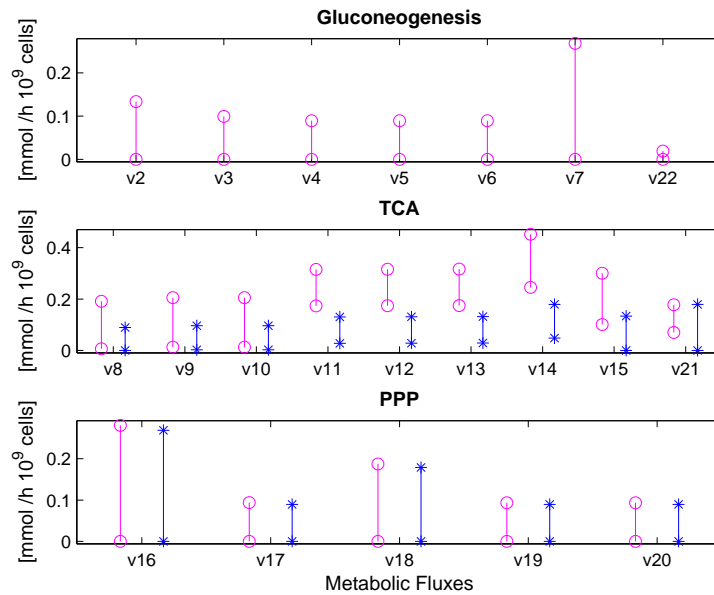
Figure 4.23: Flux Distribution Intervals for the central metabolism.

phase are in total agreement with this statement. Some cells are growing from Lactate and Alanine while others are dying, which results in a (global) low cell production.

As the carbon source follows now a different path, a way to compare the adaptation of the metabolism during the transition phase may be to look at the reaction leading pyruvate towards the TCA cycle (v_8) as well as the activity of the TCA cycle itself. Lactate and alanine, both produce pyruvate which is shuttled into the TCA cycle in order to allow the cell to generate energy. It appears that all the intervals of the metabolic fluxes participating in the TCA cycle have become smaller (See Fig.4.23). It is clearly seen then, that the activity of the transition phase has decreased significantly. Flux names for the TCA cycle and PPP in Figure 4.23 correspond to those for the transition phase (see Table 4.6).

The Pentose Phosphate Pathway does not change the range of values for the metabolic fluxes during the transition phase. We cannot trust the information provided by these results, since the PPP seems to behave here more like a simple cycle than actually playing a metabolic role. It is only recirculating $G6P$ at the same time it produces $R5P$, which is then withdrawn with a tiny flux shuttling it to nucleotide production. This is all due to the fact that the PPP cannot be clarified unless a measurement inside
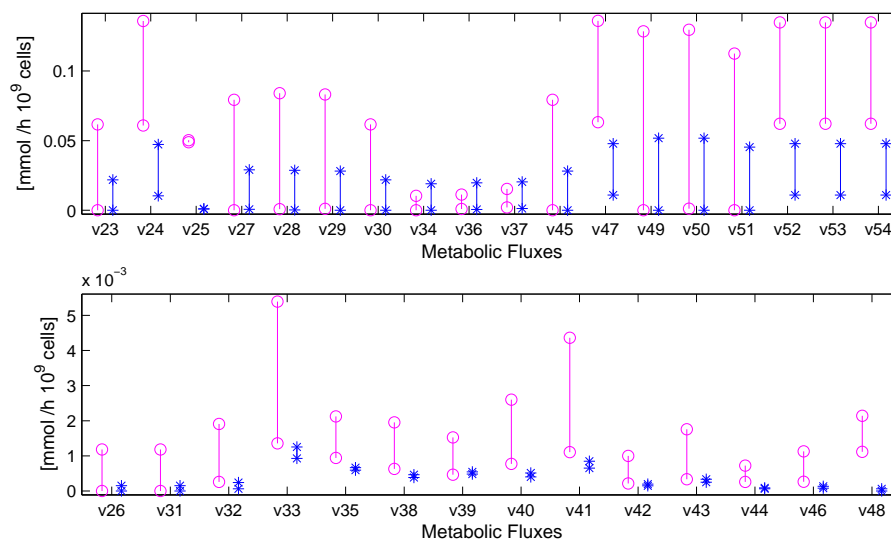
Figure 4.24: Flux Distribution Intervals for the amino acid metabolism.

the pathway is done.

From Figure 4.24, we can first notice a decrease in the catabolic fluxes of the amino acids, mainly for the essential amino acids. For instance, glutamine (v_{25}), threonine(v_{26} and v_{31}), lysine (v_{35}), valine (v_{38}), isoleucine (v_{39}), leucine (v_{40}), phenylalanine (v_{42}), methionine (v_{44}) and asparagine (v_{46}) have very small fluxes, which in turn affects the flux values of the rest of the amino acid reactions. Only reactions v_{34}, v_{36} and v_{37} seem not affected. Actually, these fluxes correspond to the catabolic reactions of Tryptophan, one of the unmeasured amino acids. Therefore, the intervals for its uptake and downstream fluxes might comprise a wide range of values depending on the network and the experimental data.

As seen from Figure 4.22,the synthesis of biomass has been reduced notably. Accordingly, the pathways for nucleotide and lipids synthesis have now very small fluxes in comparison to those intervals obtained for the exponential phase (see Fig.4.25 and Fig.4.26). In particular, reactions v_{56} and v_{69} which are the reactions leading $R5P$ towards the nucleotides synthesis and $DHAP$ towards the lipid synthesis have now greatly diminished. Their maximum flux value is now a 10% of that obtained for the exponential growth phase.

Death Phase

In this phase of the culture, as its name states, cell death takes place. Now, the biomass production stops completely and thus, cell density starts to
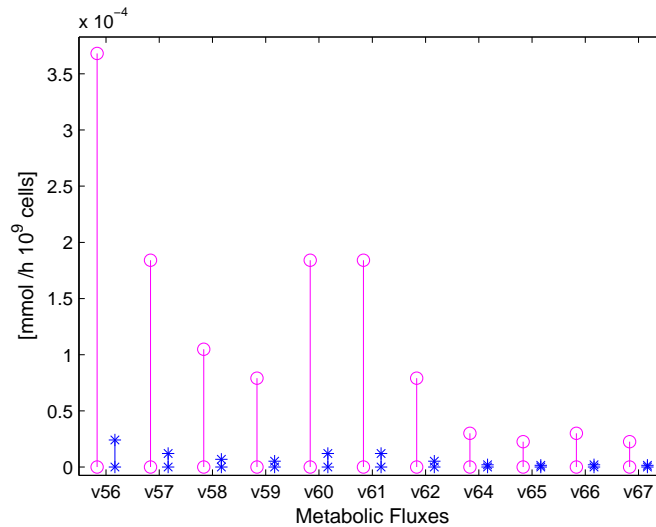
Figure 4.25: Flux Distribution Intervals for the nucleotide metabolism.

decay (see Fig.4.21 from 120 hours ahead). Several metabolic processes stop their activity as the metabolism turns towards energy production to keep the cells alive as long as possible. Therefore, lactate, glutamine and alanine are still consumed but mainly to fuel the TCA cycle. In addition, the pathways of pentose phosphates, nucleotides, proteins and lipids are discarded since the synthesis of macromolecules is no longer necessary.

Thus, as the metabolism of the cells is once more modified, the metabolic network representing this phase needs to be readjusted. The assimilation of lactate, glutamine and alanine continues just to allow the production of energy through the TCA cycle. Nonetheless, the consumption and production of the rest of the amino acids is fairly low. One may even notice that some of them have changed from being produced to being consumed, and vice versa. The pathways for nucleotide, protein, lipid and in turn, of biomass synthesis are no longer taken into account. These set of reactions are presented in Table 4.8.

The specific uptake and excretion rates for the death phase are obtained by linear regression of the experimental data from the experiments presented in Subsection 4.1.1. The estimated rates are given in Table 4.7.

Once more, as the metabolism has been completely rearranged, we cannot compare the activity of the metabolic pathways we had in the exponential or transition phases with the death phase. As the reader may suspect by looking at Table 4.9, the routes of several amino acids must now run differently so as to make possible the switch of an amino acid from being

Table 4.8: Metabolic Reactions for the death phase

Flux	Reaction

Gluconeogenesis

v_1 **Lactate**^{a} $+ NAD^+ \xrightarrow{\quad} {}^b Pyr + NADH$

v_2 $Pyr + HCO_3^- + ATP \rightarrow Oxal + ADP$

v_3 $Oxal + GTP \rightarrow 3PG + GDP + CO_2$

Tricarboxylic Acid Cycle

v_4 $Pyr + NAD^+ + CoASH \rightarrow AcCoA + CO_2 + NADH$

v_5 $AcCoA + Oxal + H_2O \rightarrow Cit + CoASH$

v_6 $Cit + NAD(P)^+ \rightarrow \alpha KG + CO_2 + NAD(P)H$

v_7 $\alpha KG + CoASH + NAD^+ \rightarrow SucCoA + CO_2 + NADH$

v_8 $SucCoA + GDP + P_i \xrightarrow{\quad} Succ + GTP + CoASH$

v_9 $Succ + FAD \xrightarrow{\quad} Fum + FADH_2$

v_{10} $Fum \xrightarrow{\quad} Mal$

v_{11} $Mal + NAD^+ \xrightarrow{\quad} Oxal + NADH$

Anaplerotic Reaction

v_{12} $Mal + NAD(P)^+ \xrightarrow{\quad} Pyr + HCO_3^- + NAD(P)H$

Amino Acid Metabolism

v_{13} $Ala + \alpha KG \xrightarrow{\quad} Pyr + Glu$

v_{14} $Glu + NAD(P)^+ \xrightarrow{\quad} \alpha KG + NH_4^+ + NAD(P)H$

v_{15} $Oxal + Glu \xrightarrow{\quad} Asp + \alpha KG$

v_{16} $Gln \rightarrow Glu + NH_4^+$

v_{17} $Thr + NAD^+ + CoASH \rightarrow Gly + NADH + AcCoA$

v_{18} $Gly \xrightarrow{\quad} Ser$

v_{19} $3PG + Glu + NAD^+ \rightarrow Ser + \alpha KG + NADH$

v_{20} $Gly + NAD^+ \rightarrow CO_2 + NH_4^+ + NADH$

v_{21} $Thr \rightarrow \alpha Kb + NH_4^+$

v_{22} $\alpha Kb + CoASH + NAD^+ \rightarrow PropCoA + NADH + CO_2$

v_{23} $PropCoA + HCO_3^- + ATP \rightarrow SucCoA + ADP + P_i$

v_{24} $Trp \rightarrow Ala + 2CO_2 + \alpha Ka$

v_{25} $Lys + 2\alpha KG + 3NAD(P)^+ + FAD^+ \rightarrow \alpha Ka + 2Glu + 3NADPH + FADH_2$

v_{26} $\alpha Ka + CoASH + 2NAD^+ \rightarrow AcetoAcCoA + 2NADH + 2CO_2$

v_{27} $AcetoAcCoA + CoASH \rightarrow 2AcCoA$

v_{28} $Val + \alpha KG + CoASH + 3NAD^+ + FAD^+ \rightarrow PropCoA + Glu + 2CO_2 + 3NADH + FADH_2$

v_{29} $Ile + \alpha KG + 2CoASH + 2NAD^+ + FAD^+ \rightarrow AcCoA + PropCoA + Glu + CO_2 + 2NADH + FADH_2$

v_{30} $Leu + \alpha KG + CoASH + NAD^+ + HCO_3^- + ATP + FAD^+ \rightarrow AcCoA + AcetoAc + Glu + CO_2 + NADH + ADP + FADH_2$

v_{31} $AcetoAc + SucCoA \rightarrow AcetoAcCoA + Succ$

v_{32} $Phe + NADH \rightarrow Tyr + NAD^+$

v_{33} $Tyr + \alpha KG \rightarrow Fum + AcetoAc + Glu + CO_2$

v_{34} $Cys \rightarrow Pyr + NH_4^+$

v_{35} $Asp + NH_4^+ \xrightarrow{\quad} Asn$

v_{36} $His \rightarrow Glu + NH_4^+$

v_{37} $Pro \rightarrow Glu\gamma SA$

v_{38} $Glu\gamma SA + NAD(P)^+ \rightarrow Glu + NAD(P)H$

v_{39} $Glu\gamma SA + Glu \xrightarrow{\quad} Orn + \alpha KG$

---

^{a} Extracellular measured species

^{b} Chosen net direction for reversible reaction

Flux	Reaction
	Urea Cycle
v_{40}	$Orn + HCO_3^- + NH_4^+ + 2ATP \rightarrow Cln + ADP$
v_{41}	$Cln + Asp + ATP \rightarrow ArgSucc + AMP$
v_{42}	$ArgSucc \rightarrow Arg + Fum$
v_{43}	$Arg \rightarrow Orn + Urea$
	Transport Reactions
v_{44}	$\mathbf{Asp_{ext}}^a \rightarrow Asp$
v_{45}	$Cys_{ext} \rightarrow Cys$
v_{46}	$\mathbf{Gly_{ext}}^a \rightarrow Gly$
v_{47}	$Ser \rightarrow \mathbf{Ser_{ext}}^a$
v_{48}	$\mathbf{Glu_{ext}}^a \rightarrow Glu$
v_{49}	$\mathbf{Tyr_{ext}}^a \rightarrow Tyr$
v_{50}	$\mathbf{Ala_{ext}}^a \rightarrow Ala$
v_{51}	$Arg \rightarrow \mathbf{Arg_{ext}}^a$
v_{52}	$Asn^a \rightarrow \mathbf{Asn_{ext}}$
v_{53}	$\mathbf{Gln_{ext}}^a \rightarrow Gln$
v_{54}	$His_{ext} \rightarrow His$
v_{55}	$\mathbf{Ile_{ext}}^a \rightarrow Ile$
v_{56}	$\mathbf{Leu_{ext}}^a \rightarrow Leu$
v_{57}	$\mathbf{Lys_{ext}}^a \rightarrow Lys$
v_{58}	$\mathbf{Phe_{ext}}^a \rightarrow Phe$
v_{59}	$Pro_{ext} \rightarrow Pro$
v_{60}	$\mathbf{Thr_{ext}}^a \rightarrow Thr$
v_{61}	$Trp_{ext} \rightarrow Trp$
v_{62}	$\mathbf{Val_{ext}}^a \rightarrow Val$
v_{63}	$NH_4^+ \rightarrow \mathbf{NH_{4,ext}^+}^a$
v_{64}	$CO_2 \rightarrow CO_{2,ext}$

Continued from Table 4.8

Table 4.9: Death phase specific rates in mmol $h^{-1}10^9 cell-1$

Substrates	Specific Uptake Rates	Products	Specific Excretion Rates
Lactate	$-3.6726e^{-2}$	Serine	$1.1874e^{-4}$
Glutamine	$-5.9150e^{-4}$	NH_4^+	$2.1066e^{-3}$
Alanine	$-1.8713e^{-3}$	Arginine	$3.0785e^{-5}$
Glutamate	$-3.2764e^{-4}$	Asparagine	$1.9790e^{-5}$
Aspartate	$-6.5967e^{-6}$		
Isoleucine	$-1.5392e^{-4}$		
Leucine	$-1.7591e^{-5}$		
Lysine	$-1.9790e^{-5}$		
Phenylalanine	$-4.8376e^{-5}$		
Threonine	$-9.2354e^{-5}$		
Tyrosine	$-7.4763e^{-5}$		
Valine	$-1.2534e^{-4}$		
Glycine	$-2.6607e^{-4}$		
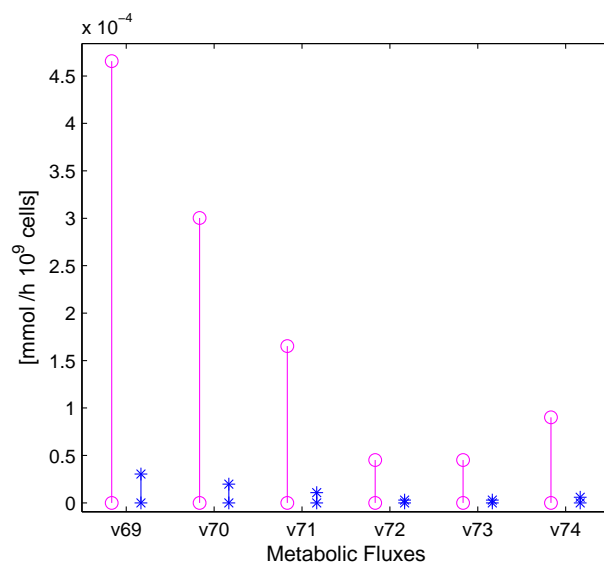
Figure 4.26: Flux Distribution Intervals for the lipid metabolism.

produced to be consumed during this phase, and vice versa. All this just to state that the activity of certain paths in the metabolism of amino acids can no longer be compared to the activity of the same paths during the earlier stages of the culture. Yet, a good way to compare the adaptation of the metabolism during the death phase remains the activity of the TCA cycle, which is one of the only remaining active pathways.

From Figure 4.27, it is clearly seen that the intervals of the metabolic fluxes participating in the TCA cycle have not only lower values, meaning that the activity of the TCA has decreased significantly, but they have also become quite small. Flux names correspond to those for the death phase.

In fact, as the metabolic network now comprises only 64 reactions, for 17 available measurements the MFA returns not only fairly narrow intervals but 20 uniquely determined values. As it might be already noticed, there is no need to include any supplementary measurement for the CO_2 production rate.

Again, for the reactions in the amino acid pathways, the fluxes have clearly diminished with respect to the earlier phases of the culture. In Figure 4.28 it is possible to see that flux v_{16}, fluxes from v_{24} to v_{33} and fluxes from v_{36} to v_{38} are fixed. Flux names in Figures 4.27 and 4.28 correspond to those for the death phase (see Table 4.8).

Once more, these results are in agreement with what we expected: a clear decrease of the metabolism activity. Again, the conclusion is that the metabolic network chosen to represent the death phase of the culture, as
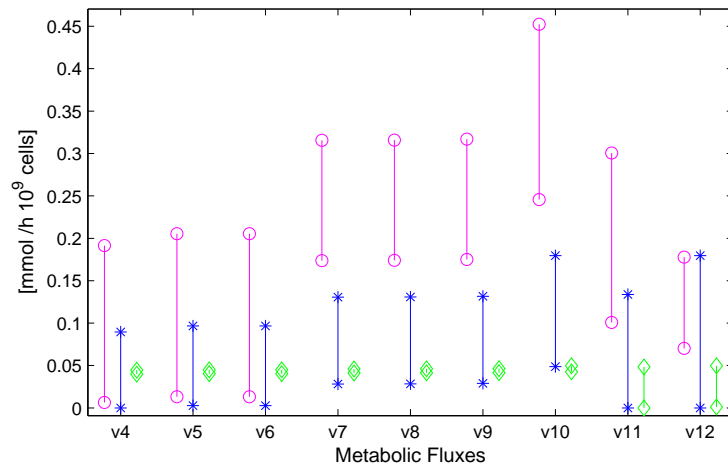
Figure 4.27: Flux Distribution Intervals for the central metabolism.

well as the procedure for the calculation of the flux intervals, are correct.
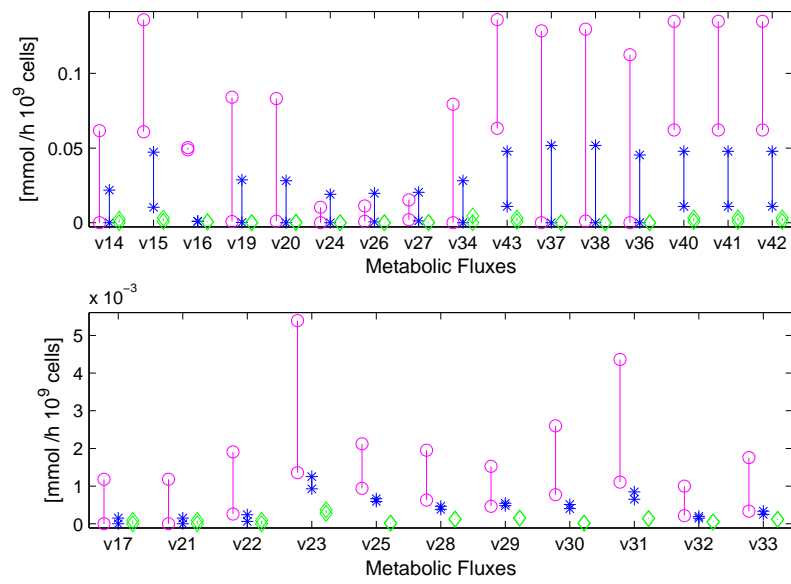
Figure 4.28: Flux Distribution Intervals for the amino acid metabolism.

Chapter 5

Model Reduction and Dynamic Modelling

In the previous sections, metabolic bioreaction networks were studied to analyze the metabolism of the different phases of the cell life. In the following, these metabolic networks will be crucial in the model reduction procedure aiming at the determination of dynamical models.

The concept of Elementary Flux Modes (EFMs) has been of central importance in a number of studies involving the analysis of metabolism. In [1] this concept is used to translate the metabolic networks of the different phases of CHO cell culture into macroscopic bioreactions linking extracellular substrates to products. However, a critical issue concerns the calculation of these elementary flux vectors, as their number combinatorially increases with the size of the metabolic network. In this study, a detailed metabolic network of CHO cells is considered, where the above-mentioned combinatorial explosion makes the computation of the elementary flux modes impossible. To alleviate this problem, a methodology proposed in [20] is used to compute a decomposition of admissible flux vectors in a minimal number of elementary flux modes without explicitly enumerating all of them. As a result, a set of macroscopic bioreactions linking the extracellular measured species is obtained at a very low computational expense. The procedure is repeated for the several cell life phases and a global model is built using a multi-model approach, which is able to successfully predict the evolution of experimental data.

5.1   Motivation

Macroscopic models of bioprocesses have been used in many applications, ranging from simulation to estimation, optimization and control [5]. These models represent the conversion of substrates into products by a few macroscopic reactions, without taking the intracellular reaction network into con-

sideration (black box representation).

These models can be derived using two main approaches. The first approach is essentially data-driven. Macroscopic models are derived solely from the experimental observation of the time evolution of a few extracellular components (substrates, products of interest, inhibiting compounds). Various techniques can be combined, including data analysis techniques such as principal component analysis to deduce the number of bioreactions and partial stoichiometry [6], and identification methods based on - whenever possible - decoupling techniques to estimate independently the stoichiometry and the kinetics (concept of C-identifiability) [12], [18]. In the second approach, the available prior knowledge about the metabolic network is exploited, and a macroscopic set of reactions is derived in agreement with the intracellular metabolism [15].

This is the second approach which is of interest in the present study, and particularly, the procedure devised in [38] where dynamic models are derived from the concept of Elementary Flux Modes (EFMs) for a metabolic network of CHO cells under balanced growth conditions. This latter assumption stipulates that the intracellular metabolites do not accumulate in the cell, or in other words, that the intracellular processes occur much faster than those happening outside the cell. In [1], this approach is further used to translate the metabolic networks of the different phases of the cell culture into macroscopic bioreactions linking extracellular substrates to products. However, a critical issue concerns the calculation of these elementary flux vectors, as their number combinatorially increases with the size of the metabolic network.

This latter point is one of the motivations behind this study, in which we consider a more detailed metabolic network of CHO cells developed by the authors in [56], where the above-mentioned combinatorial explosion makes the computation of the elementary flux modes impossible. To alleviate this problem, we apply a methodology to compute a decomposition of admissible flux vectors in a minimal number of elementary flux modes without explicitly enumerating all of them, as proposed by the authors in [20]. As a result, a set of macroscopic bioreactions linking the extracellular measured species is obtained at a very low computational cost. Further, the procedure is repeated for the different life cell phases (exponential growth, transition and death) to determine local dynamic models, which can then be assembled to form a global (piecewise) model for the entire culture. The multi-model approach has already been applied successfully to describe the behavior of complex bioprocesses in other areas of applications such as wastewater treatment [47], or the culture of micro-algae in photo-bioreactors [30].

This chapter is organized as follows. Section 5.2 introduces the general form of a dynamic model of batch cell cultures and the concept of Elementary Flux Modes (EFMs). The methodology for the computation of a minimal set of EFMs and the decomposition of an admissible flux distribu-

tion is presented in Section 5.3. A practical application of the methodology is presented in Section 5.4, where sets of macroscopic bioreactions are computed for each of the cell life phases of batch cultures of CHO-320 cells. Finally, Section 5.5 discusses the construction of a piecewise global dynamic model for the entire culture, based on the previous local models.

5.2 Cell Culture Modelling

5.2.1 Dynamics of a batch culture

In general, cell cultivation in a batch process can be divided in at least three phases, according to the physiological states of the cells.

- the first phase corresponds to the exponential growth, where the concentration of the carbon source and all other substrates are in excess and there is sufficient dissolved oxygen allowing a rapid proliferation of the biomass. Lactate, alanine and ammonia are produced because of the high level of glucose and glutamine.

- the second phase is known as transition, where the sugar concentration decreases below a critical level and the produced lactate and alanine start to be consumed instead. There is sufficient dissolved oxygen in the medium in order to allow the oxidative pathways metabolize lactate and alanine and keep the cellular division, however in a less effective way.

- the third state corresponds to cellular death, where programmed cell death takes place upon exposure to stress encountered in the bioreactor. There could be various causes for apoptosis: nutrient depletion, waste byproduct accumulation, hypoxia, mechanical agitation, etc ([4]).

For a cell culture carried out in batch mode in a stirred tank reactor, the dynamics of substrates and products are described by:

$$\begin{array}{rcl} \frac{dS}{dt} & = & -v_s X(t) \\ \frac{dP}{dt} & = & v_p X(t) \end{array} \tag{5.1}$$

where

- $X(t)$ is the biomass concentration,

- $S(t)$ is the vector of substrate concentrations,

- $P(t)$ is the vector of product concentrations,

- v_s is the vector of specific uptake rates,

- s_p is the vector of specific production rates.

As already stated in Section 3.2, v_s and v_p are linear combinations of some of the (intracellular) metabolic fluxes v. Thus, by defining appropriate matrices N_s and N_p (the stoichiometric matrices for the extracellular substrates and final products), respectively, this relation can be expressed as:

$$
\begin{aligned}
v_s(t) &= N_s v(t) \\
v_p(t) &= N_p v(t).
\end{aligned}
$$

(5.2)

5.2.2 Metabolic network and elementary flux modes

In the previous sections, we have seen that the intracellular metabolism of living cells can be represented by a metabolic network under the form of a hypergraph encoding a set of biochemical reactions. Each node representing a particular intracellular metabolite and the edges representing the metabolic reactions or fluxes.

According to the pseudo steady-state assumption of metabolic flux analysis (MFA), it is assumed that the fluxes are balanced at each internal node, i.e. intracellular metabolites do not accumulate in the cell. This means that the net sum of production and consumption fluxes, weighted by their stoichiometric coefficients, is zero for each internal metabolite of the network. As seen in Subsection 3.2.1, this steady-state balance around the internal metabolites is expressed by the algebraic relation:

$$
\mathbf{N}\mathbf{v} = \mathbf{0} \qquad \mathbf{v} \geqslant \mathbf{0}
$$

(5.3)

where $\mathbf{v} = (v_1, v_2, \ldots, v_n)^T$ is the n-dimensional column vector of fluxes and $\mathbf{N} = [n_{ij}]$ is the $m \times n$ stoichiometric matrix of the metabolic network (m is the number of internal metabolites and n is the number of fluxes). More precisely, a flux v_j denotes the rate of reaction j and a non-zero n_{ij} is the stoichiometric coefficient of the metabolite i in reaction j.

For a given metabolic network, the set S of possible flux distributions is the set of vectors $\mathbf{v}$ that satisfy the linear system 5.3. This set S is the pointed polyhedral cone resulting from the intersection of the kernel of $\mathbf{N}$ with the non-negative orthant (see Figure 3.2.1). This implies that there exists a set of elementary flux vectors $\mathbf{e}_i$, the extreme rays (or edges) of this polyhedral cone, such that any flux distribution $\mathbf{v}$ can be expressed as a non-negative linear combination of them:

$$
\mathbf{v} = w_1 \mathbf{e}_1 + w_2 \mathbf{e}_2 + \cdots + w_q \mathbf{e}_q \quad w_i \geqslant 0.
$$

(5.4)

The $n \times q$ non-negative matrix $\mathbf{E}$ with column vectors $\mathbf{e}_i$ obviously satisfies $\mathbf{N}\mathbf{E} = 0$ and Equation (5.4) can be written in matrix form as

$$
\mathbf{v} = \mathbf{E}\mathbf{w} \quad \text{with} \quad \mathbf{w} \triangleq (w_1, w_2, \ldots, w_q)^T.
$$

(5.5)

Thus, the elementary flux vectors are a way of representing the set of possible flux distributions. The dynamics of the concentration of each substrate and product in a batch reactor, where no exchange occurs with the outside environment, are written as follows:

$$\frac{d}{dt}\begin{pmatrix} S(t) \\ P(t) \end{pmatrix} = \begin{pmatrix} -N_s \\ N_p \end{pmatrix} vX \tag{5.6}$$

From 5.5 and 5.6, we obtain:

$$\frac{d}{dt}\begin{pmatrix} S(t) \\ P(t) \end{pmatrix} = \begin{pmatrix} -N_s \\ N_p \end{pmatrix} EwX \tag{5.7}$$

The product of stoichiometric matrices $\mathbf{N}_s$ and $\mathbf{N}_p$ times the elementary flux modes matrix $\mathbf{E}$ yields the stoichiometric matrix for a set of macroscopic reactions, linking the extracellular substrates to the final products. Let us consider that the reaction scheme of the process involves N macroscopic reactions and M extracellular species, either substrates or products, with K being the $M \times N$ matrix for the stoichiometric coefficients.

$$K = \begin{pmatrix} -N_s \\ N_p \end{pmatrix} E \tag{5.8}$$

Then, if the vector ξ is defined as:

$$\xi = \begin{pmatrix} S(t) \\ P(t) \end{pmatrix}, \tag{5.9}$$

The dynamic model defined by the macroscopic bioreactions may be written as:

$$\frac{d\xi}{dt} = K\mathbf{w}(t)X(t) = K\varphi(\xi, t) \tag{5.10}$$

where $\mathbf{w}(t)$ is the vector of the specific reaction rates w_i of the macroscopic bioreactions and φ is the vector of reaction rates.

5.3 Computation of the EFMs and of minimal flux decomposition

5.3.1 Problem statement

A well known issue related to the EFMs representation is that the number of such vectors grows exponentially with the size of the network. This means that for detailed metabolic networks, such as the one considered in the following of this study, the computation of matrix $\mathbf{E}$ becomes prohibitive.

In general, the decomposition of a flux distribution $\mathbf{v}$ in the convex basis of elementary flux vectors $\mathbf{e}_i$ does not necessitate the whole enumeration of the convex basis but requires only the knowledge of a few elementary vectors. Thus, the objective is to determine a minimal such decomposition. Nonetheless, when the vector $\mathbf{v}$ is the solution of an underdetermined metabolic flux analysis problem, the situation is more complex, though it may be possible to find a decomposition with even less elementary flux modes. Indeed, it is not known a priori which vector, among all admissible flux distributions, is the one that can be decomposed in the minimal number of elementary flux modes. The information needed for computing these elementary vectors can be obtained directly from the stoichiometric matrix $\mathbf{N}$ together with the extracellular measurements. Herein, this methodology is used to compute this decomposition without actually evaluating the whole convex basis, thanks to the convex programming techniques presented in [20].

5.3.2   Definition of some polytopes of interest

If we consider system 5.3 and take the constraints imposed by the extracellular measurements into account, it is possible to write

$$\begin{pmatrix} \mathbf{N} \\ \mathbf{N_m} \end{pmatrix} \mathbf{v} = \begin{pmatrix} \mathbf{0} \\ \mathbf{v}_m \end{pmatrix} \qquad \mathbf{v} \geqslant \mathbf{0}. \tag{5.11}$$

for a given metabolic network and a given set of measurements. The reader is reminded that $\mathbf{N_m}$ stands for the stoichiometric matrix of the extracellular species and $\mathbf{v_m}$ is the vector of measurements.

As demonstrated in [20, 36], any admissible flux distribution $\mathbf{v}$ can be expressed as a convex combination of n-m elementary flux vectors $\mathbf{e}_i$. n-m corresponds to the degrees of freedom of the system, if $\mathbf{N}$ and $\mathbf{N_m}$ are full rank matrices. Notice that the decomposition of $\mathbf{v}$ in the convex basis $\{\mathbf{e}_i\}$ is not unique.

Moreover, if the number of measurements p is smaller than n-m, then there is at least one vector $\mathbf{v}^*$ that can be expressed as a convex combination of only p elementary flux vectors. Hence, the objective is to determine such a decomposition in a minimal number of elementary flux vectors $\{\mathbf{e}_i\}$.

Using Equation (5.5), system 5.11 is equivalent to the system:

$$\begin{pmatrix} \mathbf{NE} \\ \mathbf{N_mE} \end{pmatrix} \mathbf{w} = \begin{pmatrix} \mathbf{0} \\ \mathbf{v}_m \end{pmatrix} \qquad \mathbf{w} \geqslant 0. \tag{5.12}$$

We observe that the first equation $\mathbf{NEw} = \mathbf{0}$ is trivially satisfied independently of $\mathbf{w}$ since by definition $\mathbf{NE} = 0$. Hence, system 5.12 may be reduced to the second equation:

$$\mathbf{N_mEw} = \mathbf{v}_m \qquad \mathbf{w} \geqslant \mathbf{0}. \tag{5.13}$$

or equivalently written

$$\begin{pmatrix} N_m E & -v_m \end{pmatrix} \begin{pmatrix} w \\ 1 \end{pmatrix} = 0. \tag{5.14}$$

In this form, it is clear that the set of admissible weighting vectors $\mathbf{w}$ that satisfy Equation (5.13) constitutes a convex polytope that will be denoted $\mathcal{H}$. Therefore, there exists a set of appropriate edge vectors $\mathbf{h}_i$ such that any arbitrary convex combination of the form:

$$\mathbf{w} = \sum_i \beta_i \mathbf{h}_i \quad \beta_i \geqslant 0 \quad \sum_i \beta_i = 1 \tag{5.15}$$

is necessarily an admissible $\mathbf{w}$ satisfying Equation (5.13). The convex basis vectors $\mathbf{h}_i$ have a critical property : the number of non-zero entries in these vectors is equal to the number of measurements p.

From a metabolic viewpoint, each vector $\mathbf{h}_i$ is a solution $\mathbf{w}$ of Equation (5.13). Vectors $\mathbf{Eh}_i$ correspond to *minimal flux distributions* $\mathbf{v}$:

$$\hat{\mathbf{v}}_\mathbf{i} = \mathbf{Eh}_i \quad \mathbf{v} \in \mathcal{F}. \tag{5.16}$$

Each minimal flux distribution $\hat{v}_i$ represent the simplest pathways that satisfy the pseudo-steady state assumption and the constraints imposed by the extracellular measurements. Equation (5.16) implies that a minimal flux distribution (in terms of EFMs) can be obtained by different combinations of EFMs and in turn, of metabolic pathways. This will be illustrated further in the chapter, when we will assess the calculation procedure of the minimal set of EFMs.

5.3.3 Decomposing v in a convex basis

As already stated, the number of distinct extreme rays or cone vertices that are generated when computing the cone S may become very large because it combinatorially increases with the size of the underlying metabolic network. It is also the case for the number of vectors h_i that are vertices of the polytope $\mathcal{H}$.

We apply here the method presented in [20] to decompose a flux distribution $\mathbf{v}$ in a minimal number ($p < n - m$) of elementary flux modes. To this end, we introduce yet another cone $\mathcal{K} \subset \mathbb{R}^p$. This cone is the projection of S by the matrix $\mathbf{N}_m : \mathcal{K} = \{\mathbf{y} = \mathbf{N_m v} : \mathbf{v} \geqslant \mathbf{0}, \mathbf{Nv} = \mathbf{0}\}$.

We know that the vector $\mathbf{v}_m$ is in $\mathcal{K}$ because of Equation (5.11). So, $\mathbf{v}_m$ can be expressed as a convex combination of p extreme rays y_i of cone $\mathcal{K}$ (because $\mathcal{K}$ has dimension p).

$$\mathbf{v}_m = \sum_i^p \alpha_i y_i \quad \alpha_i \geqslant 0 \quad \sum_i \alpha_i = 1 \tag{5.17}$$

Now, the extreme rays of $\mathcal{K}$ are the projections of extreme rays $\mathbf{e}_i$ of $\mathcal{S}$ under the matrix $\mathbf{N}_m$. This implies that the corresponding convex combination of the $\mathbf{e}_i$ gives us the required $\mathbf{v}$. In other words, if y_i is an extreme ray of the projected cone $\mathcal{K}$, then $\mathbf{e}_i$ is an extreme ray of cone S.

$$\mathbf{v_m} = \mathbf{N}_m\mathbf{v} \quad \Rightarrow \quad y_i = \mathbf{N}_m\mathbf{e}_i \tag{5.18}$$

As $\mathbf{v}_m$ has been decomposed in p extreme rays in 5.17, a decomposition in the extreme rays of cone S is also achieved

$$\mathbf{v}_m = \sum_1^p \alpha_i\mathbf{N}_m\mathbf{e}_i = \mathbf{N}_m \sum_1^p \alpha_i\mathbf{e}_i \tag{5.19}$$

and thus, $\mathbf{v}$ is decomposed in a minimal set of p elementary flux vectors.

$$\mathbf{v} = \sum_1^p \alpha_i\mathbf{e}_i \tag{5.20}$$

For more details on the algorithm and the theory behind it, the reader is referred to references [21] and [20].

5.4 Macroscopic bioreactions for cultures of CHO cells

In this section we apply the methodology described above to three detailed (and underdetermined) metabolic networks describing the metabolism of CHO-320 cells. Each network represents the metabolism of one of the life phases of a cell in a batch culture: exponential growth, transition and death. For each of these networks, a minimal set of elementary flux modes is computed by applying the procedure described in Section 5.3. The list of reactions describing the exponential growth phase was presented in Table 2.1, Section 2.2), and the ones corresponding to the transition and death phases, were presented in Tables 4.6 and 4.8, Subsection 4.2.2, respectively.

To apply this procedure we need to define stoichiometric matrices $\mathbf{N}$ and $\mathbf{N_m}$ and the vector of extracellular measurements $\mathbf{v_m}$ for each phase. The set of experimental data contains, respectively 19, 18 and 17 extracellular measurements for the exponential growth, transition and death phases. These vectors of experimental measurements $\mathbf{v_m}$ are listed in Table 5.1.

The dimension of the vector $\mathbf{v_m}$ will then determine the dimension of the matrix containing the minimal set of vectors $\mathbf{e}_i$ ($\mathbf{E}_{min}$). Each elementary vector defines a metabolic path linking extracellular substrates to final

Table 5.1: Specific uptake/excretion rates for the three life phases

Specie	Exponential Growth Phase	Transition Phase	Death Phase
Glucose	$-1.6383 \pm 0.244e^{-1}$	-	-
Glutamine	$-4.7922 \pm 1.107e^{-2}$	$-1.4582 \pm 7.678e^{-3}$	$-8.9527 \pm 62.97e^{-4}$
Arginine	$-1.7381 \pm 1.659e^{-3}$	$-8.9108 \pm 0.271e^{-5}$	$5.1413 \pm 16.66e^{-5}$
Asparagine	$-1.2354 \pm 0.203e^{-3}$	$-1.7873 \pm 3.316e^{-5}$	$6.0603 \pm 10.76e^{-5}$
Aspartate	$-2.7112 \pm 4.304e^{-4}$	$-4.6172 \pm 4.601e^{-4}$	$-7.4483 \pm 20.77e^{-5}$
Isoleucine	$-1.7422 \pm 0.521e^{-3}$	$-4.1392 \pm 2.982e^{-4}$	$-1.7901 \pm 2.393e^{-4}$
Leucine	$-2.9556 \pm 0.610e^{-3}$	$-3.1471 \pm 2.109e^{-4}$	$-1.1150 \pm 8.286e^{-5}$
Lysine	$-3.0675 \pm 0.839e^{-3}$	$-2.7181 \pm 1.628e^{-4}$	$-1.9790e^{-5}$
Methionine	$-8.1777 \pm 1.777e^{-4}$	$-6.6621 \pm 6.668e^{-5}$	-
Phenylalanine	$-1.1747 \pm 0.309e^{-3}$	$-1.0902 \pm 0.832e^{-4}$	$-4.6531 \pm 18.38e^{-5}$
Serine	$-1.0054 \pm 0.499e^{-3}$	$-4.4716 \pm 3.295e^{-4}$	$1.5091 \pm 4.229e^{-4}$
Threonine	$-1.5358 \pm 0.928e^{-3}$	$-1.2195 \pm 2.679e^{-4}$	$-1.2157 \pm 7.073e^{-4}$
Tyrosine	$-8.7011 \pm 3.171e^{-4}$	$-8.5351 \pm 7.158e^{-5}$	$-1.2778 \pm 2.528e^{-4}$
Valine	$-2.0238 \pm 0.664e^{-3}$	$-2.7412 \pm 2.827e^{-4}$	$-1.5805 \pm 4.369e^{-4}$
Lactate	$2.9880 \pm 0.599e^{-1}$	$-2.0169 \pm 4.971e^{-2}$	$-3.8359 \pm 3.793e^{-2}$
NH_4^+	$3.8858 \pm 0.954e^{-2}$	$1.4428 \pm 8.118e^{-3}$	$1.5064 \pm 10.11e^{-3}$
Glycine	$2.6166 \pm 0.847e^{-3}$	$4.6293 \pm 14.47e^{-4}$	$-5.3266 \pm 22.34e^{-4}$
Alanine	$1.0273 \pm 0.144e^{-2}$	$-1.1855 \pm 56.37e^{-4}$	$-2.1682 \pm 1.527e^{-3}$
Glutamate	$3.0143 \pm 1.942e^{-3}$	$-9.7355 \pm 8.015e^{-4}$	$-9.0875 \pm 11.29e^{-4}$

Table 5.2: Macroscopic Reactions for the exponential growth phase

EFM	Macroscopic Reaction
e_1	$Tyr \rightarrow Glu + 4\ CO_2$
e_2	$Glucose + 1.7\ Gln \rightarrow 1.7\ Lactate + 3.3\ NH_4^+ + 6\ CO_2$
e_3	$Gln \rightarrow Glu + NH_4^+$
e_4	$Ser \rightarrow Gly$
e_5	$Asn \rightarrow Lactate + Urea$
e_6	$3.3\ Glucose + 6.4\ Gln + Asn + 1.9\ Asp + 1.2\ Arg + 1.4\ Thr + 1.7\ Lys + 1.6\ Val + 1.3\ Ile + 6.5\ Leu + 1.7\ Phe + Met + 1.2\ Pro + 0.3\ Trp + 0.5\ His +\ 0.2\ Eth + 0.4\ cho \rightarrow 25.8\ Biomass + 2.9\ Ala + 5\ NH_4^+ + 13.1\ CO_2$
e_7	$15.2\ Glucose + 7.7\ Gln + 4.7\ Asn + 14.2\ Arg + 6.5\ Thr + 13.5\ Lys + 7.2\ Val + 5.8\ Ile + 10\ Leu + 7.8\ Phe + 4.6\ Met + 5.7\ Pro + 25.9\ Trp + 2.5\ His + 0.7\ Eth + 2\ Cho \rightarrow 118.6\ Biomass + 15.8\ Ala + 8.6\ Urea + NH_4^+ + 134.2\ CO_2$
e_8	$Glucose + 1.7\ Val \rightarrow 3.3\ Lactate + 1.7\ NH_4^+ + 4.3\ CO_2$
e_9	$2.1\ Glucose + 2.5\ Gln + Asn + 1.2\ Arg + 3.4\ Thr + 1.5\ Lys + 1.6\ Val + 4.2\ Ile + 5.1\ Leu + 1.7\ Phe + 1\ Met + 1.2\ Pro + 0.3\ Trp + 0.5\ His + 0.2\ Eth + 0.4\ Cho \rightarrow 25.8\ Biomass + NH_4^+ + 4.7\ CO_2$
e_{10}	$15.2\ Glucose + 7.7\ Gln + 4.7\ Asn + 9.4\ Arg + 6.5\ Thr + 6.5\ Lys + 7.2\ Val + 68.7\ Ile + 10\ Leu + 7.8\ Phe + 4.6\ Met + 5.7\ Pro + 1.5\ Trp + 2.5\ His + 0.7\ Eth + 2\ Cho \rightarrow 118.6\ Biomass + 19\ Lactate + 30.6\ Ala + 3.8\ Urea + NH_4^+ + 75.9\ CO_2$
e_{11}	$Gln \rightarrow Ala + NH_4^+ + 2\ CO_2$
e_{12}	$6.6\ Glucose + 2.4\ Gln + Asn + 1.2\ Arg + 1.4\ Thr + 8.1\ Lys + 1.5\ Val + 1.2\ Ile + 2.1\ Leu + 1.7\ Phe + 2.4\ Met + 1.2\ Pro + 0.3\ Trp + 0.5\ His + 0.1\ Eth + 0.4\ Cho \rightarrow 25.2\ Biomass + 4.3\ Gly + 3.9\ NH_4^+ + 21\ CO_2$
e_{13}	$Gln \rightarrow Lactate + Urea + CO_2$
e_{14}	$Glucose \rightarrow 1.7\ Lactate + CO_2$
e_{15}	$6.8\ Glucose + 1.7\ Gln + Asn + 6.2\ Arg + 1.4\ Thr + 1.4\ Lys + 1.6\ Val + 1.3\ Ile + 6.7\ Leu + 1.7\ Phe + Met + 1.2\ Pro + 0.3\ Trp + 0.5\ His + 0.2\ Eth + 0.4\ Cho \rightarrow 25.8\ Biomass + 7\ Lactate + 4.9\ Urea + 6\ NH_4^+ + 14.5\ CO_2$
e_{16}	$49.6\ Glucose + 7.7\ Gln + 4.7\ Asn + 22.7\ Arg + 6.5\ Thr + 37.9\ Lys + 7.2\ Val + 5.8\ Ile + 10\ Leu + 7.8\ Phe + 4.6\ Met + 5.7\ Pro + 1.5\ Trp + 2.5\ His + 0.7\ Eth + 2\ Cho \rightarrow 118.6\ Biomass + 57.3\ Gly + 17.1\ Urea + NH_4^+ + 136.9\ CO_2$
e_{17}	$1.2\ Glucose + Arg \rightarrow 3\ Lactate + Urea + 2\ NH_4^+ + 3.2\ CO_2$
e_{18}	$7.3\ Glucose + 3.5\ Gln + Asn + 1.2\ Arg + 1.4\ Thr + 8.1\ Lys + 1.5\ Val + 1.2\ Ile + 2.1\ Leu + 1.7\ Phe + Met + 1.2\ Pro + 0.3\ Trp + 0.5\ His + 0.1\ Eth + 0.4\ Cho \rightarrow 25.2\ Biomass + 4.9\ Lactate + 8.7\ NH_4^+ + 22.2\ CO_2$
e_{19}	$Glucose + 1.7\ Gln \rightarrow 3.3\ Lactate + 3.3\ NH_4^+ + 4.3\ CO_2$

Table 5.3: Reaction rates for the three sets of macroscopic reactions

Reaction Rate	Exponential Growth Phase	Transition Phase	Death Phase
w_1	$7.6104e^{-4}$	$1.4006e^{-4}$	$1.9790e^{-5}$
w_2	$3.3737e^{-3}$	$3.8043e^{-4}$	$1.9790e^{-5}$
w_3	$1.9371e^{-4}$	$4.1514e^{-5}$	$5.8637e^{-6}$
w_4	$9.2342e^{-4}$	$5.7292e^{-4}$	$2.0670e^{-4}$
w_5	$5.2333e^{-4}$	$8.3348e^{-7}$	$9.2354e^{-5}$
w_6	$1.7039e^{-4}$	$5.1261e^{-5}$	$2.4921e^{-5}$
w_7	$7.8766e^{-6}$	$2.9480e^{-4}$	$1.1288e^{-4}$
w_8	$6.1698e^{-4}$	$3.2716e^{-4}$	$3.6726e^{-2}$
w_9	$1.8203e^{-4}$	$3.3813e^{-2}$	$5.9150e^{-4}$
w_{10}	$4.0478e^{-6}$	$2.7660e^{-4}$	$6.2670e^{-5}$
w_{11}	$8.0719e^{-3}$	$5.4907e^{-5}$	$7.6960e^{-5}$
w_{12}	$9.4097e^{-5}$	$5.6892e^{-4}$	$7.3303e^{-7}$
w_{13}	$2.3533e^{-2}$	$2.6781e^{-4}$	$2.4188e^{-5}$
w_{14}	$1.7277e^{-1}$	$2.7978e^{-5}$	$2.1403e^{-4}$
w_{15}	$1.0689e^{-5}$	$2.4642e^{-5}$	$7.2050e^{-4}$
w_{16}	$1.5793e^{-5}$	$5.4348e^{-5}$	$7.4763e^{-5}$
w_{17}	$1.0180e^{-3}$	$7.0945e^{-5}$	$3.3575e^{-4}$
w_{18}	$8.1690e^{-6}$	$9.0659e^{-5}$	-
w_{19}	$6.4727e^{-3}$	-	-

products, which can be translated into a macroscopic reaction. Proceeding in this way, the set of 19 macroscopic reactions presented in Table 5.2 describes the main metabolic processes occurring during the growth phase.

Thus, the minimal set of EFMs obtained for the exponential growth phase has been translated into a set of macroscopic bioreactions, from which a general model can be deduced. At this point, it is worth noticing that each run of the model reduction algorithm will yield different minimal sets of EFMs, thus giving different sets of macroscopic reactions. The reader is reminded about vectors $\mathbf{h}_i$ and Equation ((5.16)) which states that the pseudo-steady state assumption and the constraints imposed by the extracellular measurements can be satisfied by different minimal flux distributions $\hat{v}_i$. Hence, each time the calculation procedure is launched, a particular vector $\mathbf{h}_i$ is found and in turn, a minimal flux distribution $\hat{v}_i$.

An estimation of the reaction rates for the macroreactions are obtained from Equation ((5.13)). As $\mathbf{N_m}\mathbf{E}$ is a $p \times p$ matrix, then $\mathbf{w}$ is easily obtained from:

$$\mathbf{w} = (\mathbf{N}_m E)^{-1} \mathbf{v}_m \tag{5.21}$$

The resulting reaction rates w_i for each of the macroscopic reactions taking place during the exponential growth phase are listed in Table 5.3.

In the same way, a minimal set of elementary vectors for the transition phase is obtained. The number of extreme rays $\mathbf{e_i}$ matches the number of entries in the vector $\mathbf{v_m}$. Thus, the 18 resulting elementary flux vectors are presented in Table 5.4, from which a set of macroscopic reactions is defined.

Table 5.4: Macroscopic reactions for the transition phase

EFM	Macroscopic Reaction
e_1	$Tyr \rightarrow NH_4^+ + 9\ CO_2$
e_2	$Gln \rightarrow 2\ NH_4^+ + 3\ CO_2$
e_3	$3\ Leu + Met \rightarrow 2\ Urea + 20\ CO_2$
e_4	$Ser \rightarrow Gly$
e_5	$Asn \rightarrow Urea + 3\ CO_2$
e_6	$13.7\ Lactate + 2.2\ Gln + Asn + 2.6\ Asp + 1.2\ Arg + 1.4\ Thr + 1.4\ Lys + 1.6\ Val + 1.3\ Ile$
	$+2.2\ Leu + 1.7\ Phe + Met + 1.9\ Ala + 4.5\ Glu + 1.2\ Pro + 0.3\ Trp + 0.5\ His + 0.2\ Etn + 0.4\ cho$
	$\rightarrow 25.8\ Biomass + 0.7\ Urea + 23.8\ CO_2$
e_7	$Ala + Asp \rightarrow Urea + 4\ CO_2$
e_8	$Val \rightarrow Gly + 2\ CO_2$
e_9	$Lactate \rightarrow 3\ CO_2$
e_{10}	$Ile + Leu \rightarrow Urea + 9\ CO_2$
e_{11}	$Lys + 2\ Phe \rightarrow 2\ Urea + 18\ CO_2$
e_{12}	$Gln \rightarrow Urea + 4\ CO_2$
e_{13}	$Lys + 2\ Glu \rightarrow 2\ Urea + 10\ CO_2$
e_{14}	$Lys + 2\ Val \rightarrow 2\ Urea + 10\ CO22$
e_{15}	$Thr + Ile \rightarrow Urea + 9\ CO_2$
e_{16}	$Thr + 1.5\ Lys \rightarrow 2\ Urea + 9\ CO_2$
e_{17}	$2\ Asp + Lys \rightarrow 2\ Urea + 8\ CO_2$
e_{18}	$Lys + 2\ Ile \rightarrow 2\ Urea + 12\ CO_2$

Notice that the metabolic changes corresponding to this phase of the culture are reflected by the macroscopic reactions obtained. Lactate, Alanine and Glutamate are now consumed as substrates, and since glucose is depleted, it no longer appears as a substrate. The estimated reaction rates w_i are listed in Table 5.3.

The same procedure is now applied to the reaction network defining the metabolism of the death phase of the culture. As vector $\mathbf{v_m}$ includes 17 experimental measurements, the same number of elementary vectors are obtained. This set of extreme rays generate the corresponding macroscopic bioreactions presented in Table 5.5. Now that cells are dying, there is no production of biomass any longer and the metabolism is centered in the production of energy with CO_2 as main product. The resulting reaction rates w_i are presented in Table 5.3.

5.5 A piecewise dynamic model of CHO-320 cells

An estimation of the maximum reaction rates have been obtained for each of the cell life phase (see Table 5.3). To take account of possible substrate limitations, and guarantee concentration positivity during model simulation, it is suggested to modulate these maximum rates with Monod factors.

$$r_i = w_i \frac{S_1}{(k_{s_1} + S_1)} \frac{S_2}{(k_{s_2} + S_2)} \ ...... \ \frac{S_z}{(k_{s_{n_i}} + S_{n_i})} \tag{5.22}$$

Subindex n_i indicates the number of substrates participating in reaction i.

Table 5.5: Macroscopic reactions for the death phase

EFM	Macroscopic Reaction
e_1	$Ala + Gly \rightarrow Asn$
e_2	$Lys + 2\,Gly \rightarrow 2\,Urea + 6\,CO_2$
e_3	$Asp + 3\,Leu + Pro \rightarrow Ser + Arg + 18\,CO_2$
e_4	$Gly \rightarrow NH_4^+ + CO_2$
e_5	$Thr \rightarrow NH_4^+ + 3\,CO_2$
e_6	$3\,Ala + 1\,Pro \rightarrow Arg + 8\,CO_2$
e_7	$Glu \rightarrow Ser + 2\,CO_2$
e_8	$Lactate \rightarrow 3\,CO_2$
e_9	$Gln \rightarrow 2\,NH_4^+ + 5\,CO_2$
e_{10}	$2\,Val \rightarrow Urea + 9\,CO_2$
e_{11}	$2\,Ile \rightarrow Urea + 11\,CO_2$
e_{12}	$Asp + Glu \rightarrow Urea + 8\,CO_2$
e_{13}	$2\,Phe \rightarrow Urea + 17\,CO_2$
e_{14}	$Glu \rightarrow NH_4^+ + 5\,CO_2$
e_{15}	$2\,Ala \rightarrow Urea + 5\,CO_2$
e_{16}	$Tyr \rightarrow NH_4^+ + 9\,CO_2$
e_{17}	$Ala \rightarrow NH_4^+ + 3\,CO_2$

Thus, the dynamical model can be rewritten as:

$$\frac{d\xi}{dt} = KrX. \tag{5.23}$$

In order to complete the model, it is necessary to select numerical values for the half-saturation constants of substrates. Our aim in this study is to propose a model structure and not to estimate these values from experimental data. Clearly, our database is insufficient for this latter purpose. Here, we select somewhat arbitrary values equal to 0.1 mM, i.e., values small enough to not interfere during the growth phase but large enough to avoid stiffness difficulties in the simulation of the model differential equations. The same idea has been used in [38].

Consequently, a local dynamic model is obtained for each of the life phases. In Figures 5.1 and 5.2 the prediction of the three different models is presented. As expected, all three models fit well the available data in their respective time span.

A global model describing the complete dynamics of a CHO-320 cell culture, can be defined as an interpolation between the three models obtained in the previous section for growth, transition and death phases. The influence of each model is controlled by means of weighting functions ϕ_g, ϕ_m and ϕ_d (see [31] for more on the multi-model approach), such that the global model is formulated as follows:

$$\frac{d\xi}{dt} = \phi_g \frac{d\xi_g}{dt} + \phi_m \frac{d\xi_m}{dt} + \phi_d \frac{d\xi_d}{dt}. \tag{5.24}$$

Many local basis functions could be used. One of the simplest option is provided by linear functions of time ϕ_g, ϕ_m and ϕ_d, as shown in Figure 5.3).
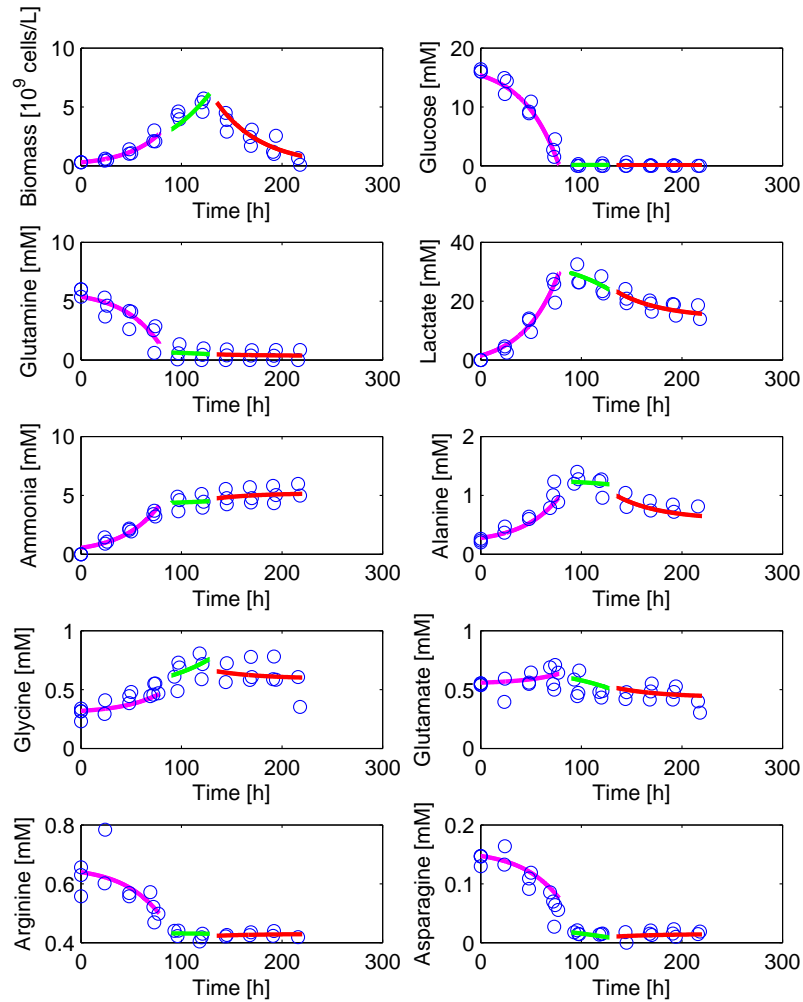
Figure 5.1: Prediction of the three different models.

In order to blend the three models, the first transition occurs in a time span starting from 75 hours until 95 hours, time of the culture at which glucose is depleted. The second transition starts at $t = 123$ hours and finishes at $t = 143$ hours, a time range where some kind of stress in the culture medium triggers cellular apoptosis or programmed cell death. The time selection for the first model transition is derived from the fact that the last measurement points of the growth phase occurs at 72-74 hours and the first measurement points of the transition phase are at 96-98 hours. In the same way, the time selection for the second transition comes from the last measurement points
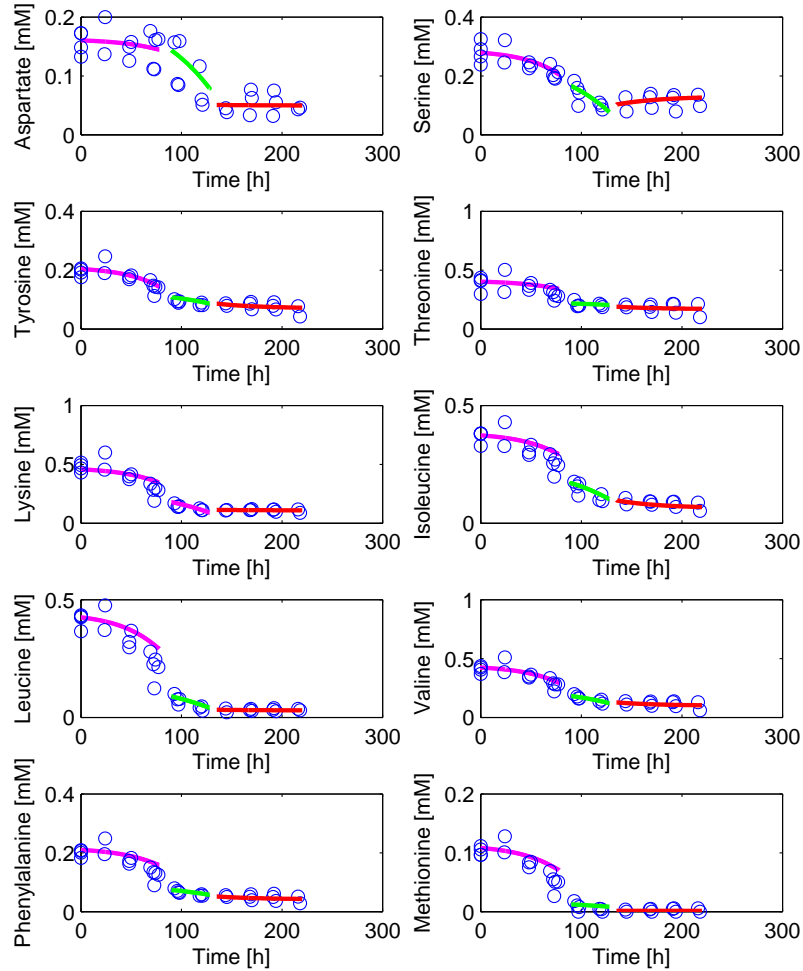
Figure 5.2: Prediction of the three different models.

of the transition phase and the first points of the death phase, at 120-122 hours and 144-145 hours, respectively. The simulation results are presented in Figures 5.4 and 5.5.

While the model reproduces quite well the evolution of cellular density and main substrates and products, it fails to provide good results for all metabolites. Indeed, at the end of the growth phase, the model stops predicting the consumption of certain amino acids such as Arginine, As-
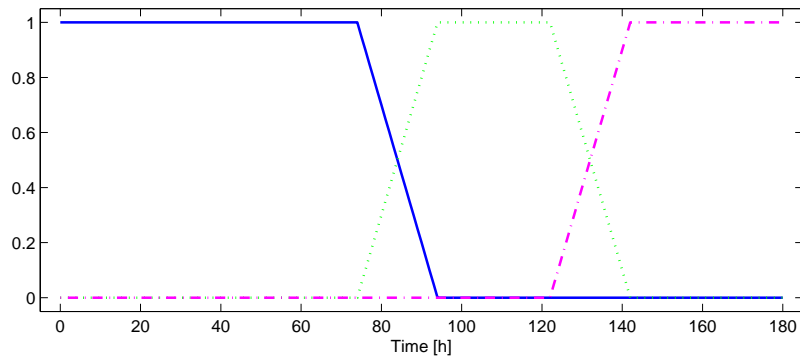
Figure 5.3: Linear switching functions.

paragine, Threonine, Leucine, Isoleucine, Valine, Phenylalanine and Methionine. Hence, the transition phase model starts with wrong initial concentrations and is not able to catch up with the real data.

To alleviate the problem of the erroneous model prediction for certain amino acids, we search for those macroscopic reactions where these amino acids participate. It appears that all nine amino acids participate in almost exactly the same reactions. In addition, in all these reactions glucose appears as a substrate. The kinetic expressions of the reaction rates r are modeled by Monod kinetics and thus, they depend on glucose concentration as a multiplication factor. Consequently, the concentration of these amino-acids do not vary any longer, as the glucose concentration depletes.

It is clear then that the early disappearance of glucose from the medium is the cause of this problem. The exponential growth phase model presented in Table 5.2 has been determined from the experimental measurements collected between 0 and 80 hours. Due to the reduced number of measurement points, the error in the determination of the specific uptake rate of glucose (and all other species) might be significant. Indeed, a smaller consumption rate of glucose would maybe yield a macroscopic model capable of a better fit for the amino acids in question. Thus, we selected from Table 5.1 the smaller specific uptake rate of glucose to compute a new minimal set of EFMs, and in turn, a new model for the exponential growth phase. The set of macroscopic reactions obtained along with their corresponding reaction rates w_i are presented in Table 5.6.

The global model is constructed as before using linear functions of time. Now, the first transition starts at $t = 85$ hours until $t = 100$ hours. In this way, the overlapping of the exponential growth and transition phase models occurs later, allowing the first to have an influence on the global model for a longer time. The time span of the second transition remains identical, starting at $t = 123$ hours and finishing at $t = 143$ hours. The simulation
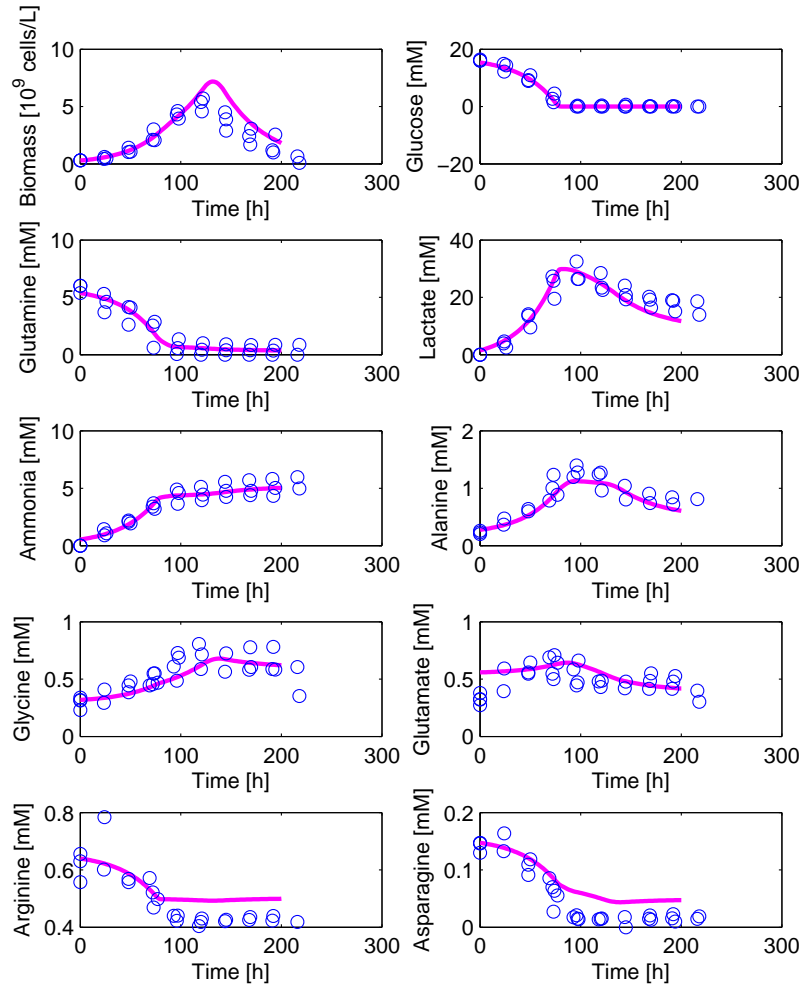
Figure 5.4: Global model validation (using linear weighting functions).
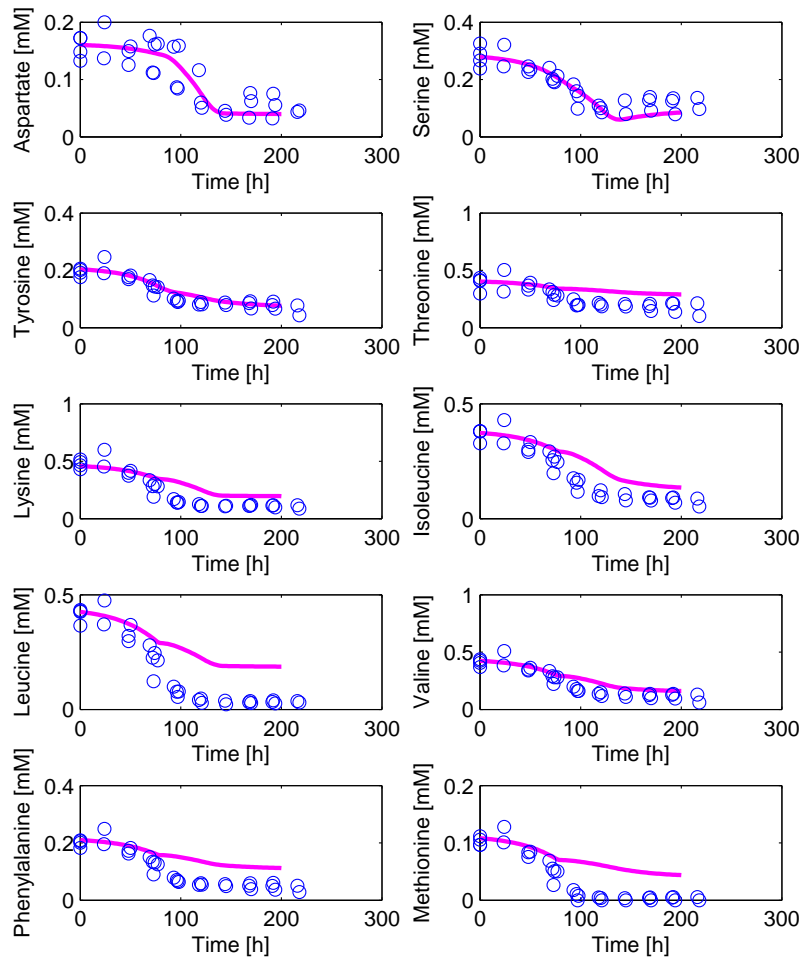
Figure 5.5: Global model validation (using linear weighting functions).

Table 5.6: Macroscopic Reactions for the exponential growth phase

EFM	Macroscopic Reaction	Reaction Rate w
e_1	16.2 $Glucose$ + 3.1 Gln + 1.9 Asn + 3.4 Asp + 2.2 Arg + 1.4 Tyr + 2.6 Thr $+15.4$ Lys + 2.9 Val + 2.3 Ile + 4 Leu + 1.7 Phe + Met + 3.1 Pro + 0.6 Trp $+His$ + 0.3 Eth + 0.8 cho → 47.1 $Biomass$ + 14.9 Gly + 43.6 CO_2	$3.3637e^{-3}$
e_2	$Lysine \rightarrow 2\ NH_4^+ + 6\ CO_2$	$1.2885e^{-3}$
e_3	$Val \rightarrow Lactate + NH_4^+ + 2\ CO_2$	$6.8944e^{-3}$
e_4	$Gln \rightarrow Lactate + 2\ NH_4^+ + 2\ CO_2$	$5.8354e^{-2}$
e_5	$Glucose \rightarrow 2\ Lactate$	$8.9550e^{-1}$
e_6	$Ser + Arg \rightarrow Ala + Glu + NH_4^+ + Urea$	$2.6505e^{-4}$
e_7	$Gln \rightarrow Ala + NH_4^+ + 2\ CO_2$	$3.2234e^{-3}$
e_8	$Ile \rightarrow Glu + CO_2$	$3.3120e^{-5}$
e_9	$Glucose \rightarrow 6\ CO_2$	$1.5911e^{-2}$
e_{10}	$Thr \rightarrow Gly + 2\ CO_2$	$6.4803e^{-5}$
e_{11}	$Asn + Arg \rightarrow 2\ Ala + 2\ Urea + 2\ CO_2$	$2.6428e^{-4}$
e_{12}	$Ser + 4\ Arg + Met \rightarrow 6\ Ala + 6\ Urea + 7\ CO_2$	$2.1242e^{-5}$
e_{13}	$Tyr + Thr \rightarrow Urea + 11\ CO_2$	$1.2274e^{-5}$
e_{14}	$Ser + 4\ Leu + Met \rightarrow 2\ Ala + 23\ CO_2$	$2.8599e^{-4}$
e_{15}	$Tyr \rightarrow Ala + 6\ CO_2$	$6.1860e^{-5}$
e_{16}	$Ile \rightarrow Ala + 3\ CO_2$	$1.3218e^{-4}$
e_{17}	$Gln \rightarrow Urea + 4\ CO_2$	$1.4200e^{-2}$
e_{18}	$Phe \rightarrow Ala + 6\ CO_2$	$1.2058e^{-4}$
e_{19}	$Ser + 2\ Phe + Met \rightarrow 2\ Urea + 23\ CO_2$	$4.9886e^-6$

results are presented in Figures 5.6 and 5.7.
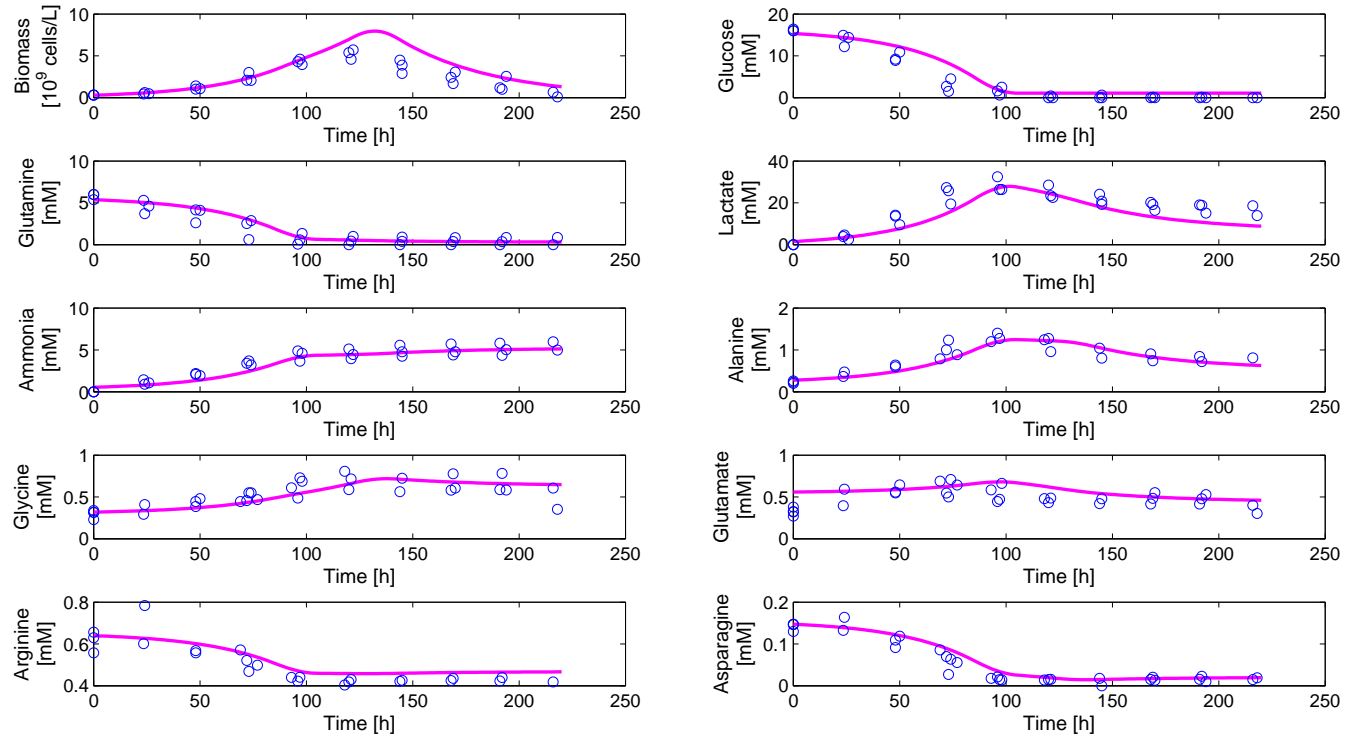
Figure 5.6: Global model validation using a smaller glucose uptake rate.
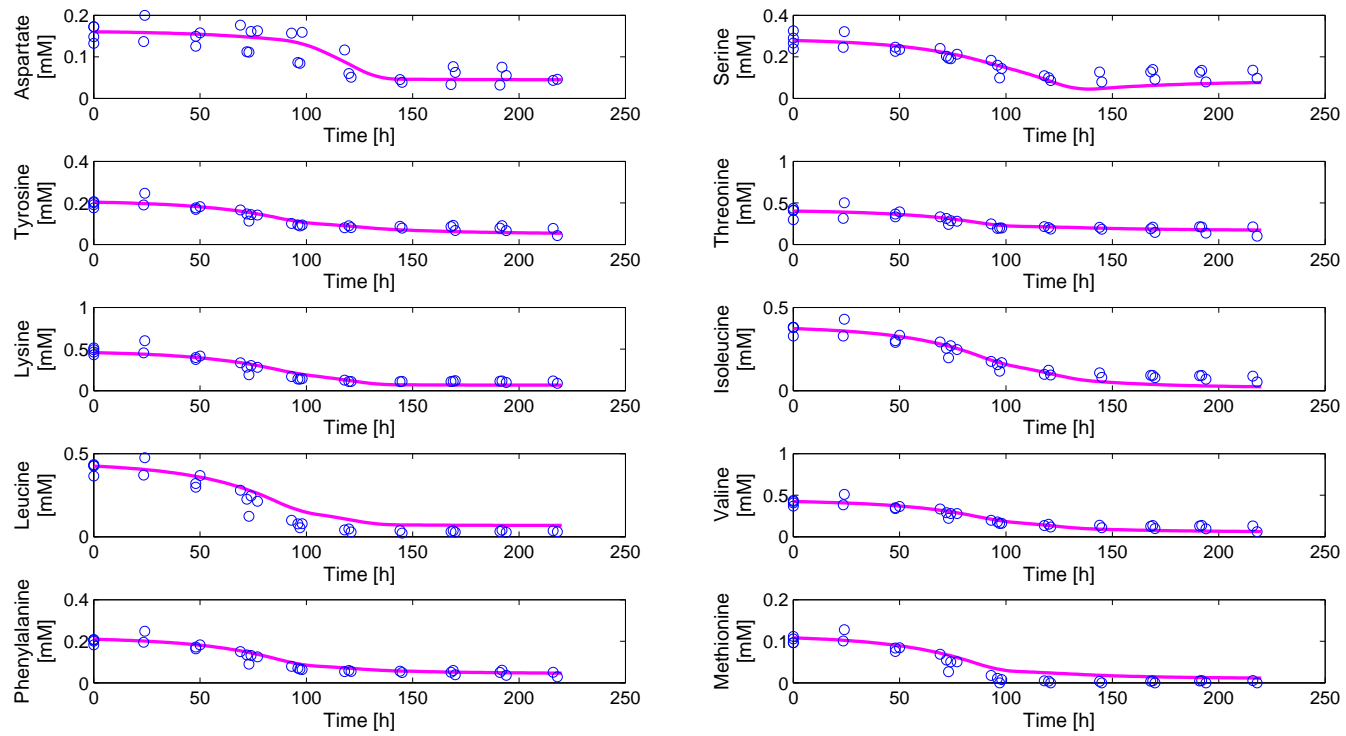
Figure 5.7: Global model validation using a smaller glucose uptake rate.

Chapter 6

Computational procedures - a dedicated Matlab toolbox

6.1 MFA Tools

This section aims at explaining in more details the computational procedures used for metabolic flux analysis in this work. Hopefully, this chapter will be useful for those who would like to reproduce parts of our results or pursue the research investigations with additional databases.

6.1.1 Preliminary Analysis

As commented in Section 3, a few tests must be preformed before hand to ensure the legitimacy of the metabolic network.

Elementary Mass Conservation

We have seen that if mass conservation applies, then

$$a^T \cdot M = 0$$

M is the $m_T \times n$ Stoichiometric matrix, where m_T is the number of all, internal and extracellular, metabolites. a is a $m_T \times 1$ mass indicator vector. In our case, a contains the number of carbon atoms of every internal and extracellular metabolite in matrix M. The idea is simply to verify that the number of total carbon atoms remains constant, so as to ensure that the mass conservation principle applies in the metabolic network.

The product of the above equation should yield a $1 \times n$ null vector if the mass conservation principle is verified. In the case where an inconsistency in the number of carbon atoms is found in one reaction, the position of a non-zero entry will determine the unbalanced reaction. For instance, if the product of $a^T \cdot M$ has a non-zero entry in the 44th position, there

is an inconsistency with the number of carbon atoms in reaction v_{44} (see Table 2.1). It should be verified that the number of carbon atoms in the substrates (methionine + serine) is exactly the same as the carbon atoms in the products (cysteine + $\alpha - Ketobutyrate + NH_4^+$). ATP and ADP are not considered for mass balances purposes since they only participate in the reaction as energetic cofactors.

For if we do the calculation, methionine has $5C$ and serine has $3C$. On the other side, cysteine has $3C$ and $\alpha - Ketobutyrate$ has only $4C$. Apparently, the mass balance conservation does not apply here. In fact, what happens here is that methionine donates its methyl group ($-CH_3$) to a tetrahydrofolate (H_4 folate) cofactor. H_4 folate serves as donor and acceptor of one-carbon units in a variety of metabolic reactions. It participates as well in reactions v_{27}, v_{29}, v_{51}, v_{57} and v_{74}.

Another issue in mass conservation arises when considering macromolecules as proteins, lipids and nucleic acids. It is known that the elementary composition of these macromolecules can vary widely depending on their function and on the organism that produces them. In proteins, lipids and nucleic acids, unlike amino acids and nucleotides, it is not possible to define a standard composition. In the same way, a standard composition of a single cell cannot be established either. At the same time, the macromolecule and biomass reaction synthesis are not chemical reactions in a strict sense, but an assembly of building blocks. In practice, these species (proteins, lipids, nucleic acids and biomass) can be either eliminated from matrix M and vector a or set as null the number of carbon atoms in a. In either case, one should expect to have non-zero entries in the positions corresponding to the reaction synthesis of proteins, lipids and nucleic acids.

Calculability Analysis

This is a simple way to evaluate *a priori* if there are any fluxes that might be uniquely determined for a particular system

$$\mathbf{0} = \mathbf{N}\mathbf{v} = \mathbf{N}_k\mathbf{v}_k + \mathbf{N}_u\mathbf{v}_u \Leftrightarrow \mathbf{N}_u\mathbf{v}_u = -\mathbf{N}_k\mathbf{v}_k.$$

The determination of the balanceable fluxes for the case study in Subsection 4.1.3 will serve as example of calculation. In this case study, in addition to the assumption regarding the no catabolism of Threonine, we assume that additional measurements of Cysteine and Proline are available.

The first step is to split vector $\mathbf{v}$ and matrix $\mathbf{N}$ in two: one containing the measured or known reaction rates and another containing the unmeasured or unknown reaction rates. Thus, for the case study herein considered $\mathbf{v}_k$ includes 22 reaction rates: v_1 (glucose), v_{15} (lactate), v_{77} to v_{86} (asp, cys, gly, ser, glu, tyr, ala, arg, asn, gln), v_{88} to v_{94} (ile, leu, lys, met, phe, pro, thr), v_{96} (val), v_{99} (NH_4^+) and v_{100} (CO_2). On the other hand, vector $\mathbf{v}_u$

considers 76 reaction rates instead of 78 since the catabolic reactions of threonine (v_{26} and v_{31}) have been eliminated. Hence, matrices $\mathbf{N}_k$ and $\mathbf{N}_u$ have dimensions 72×22 and 72×76, respectively.

One just needs to calculate the pseudo inverse matrix $\mathbf{N}_u^{\#}$ and the kernel $\mathbf{K}_u$ of matrix $\mathbf{N}_u$. Vector $\mathbf{a}$ must have $dim(\mathbf{v}_u) - rank(\mathbf{N}_u)$ arbitrary elements. For this particular case, where $\mathbf{v}_u$ has 76 elements and the rank of $\mathbf{N}_u$ is 72, vector $\mathbf{a}$ must consider 4 randomly chosen elements.

At least two different vectors $\mathbf{a}$ should be defined, so as to calculate at least two possible $\mathbf{v}_{u,s}$.

$$\mathbf{v}_{u,s} = -\mathbf{N}_u^{\#}\mathbf{N}_k\mathbf{v}_k + \mathbf{K}_u\mathbf{a}$$

Then, by comparing solutions $\mathbf{v}_{u1}$ and $\mathbf{v}_{u2}$ it is found that 40 metabolic fluxes have the exact same value, meaning that these are the calculable fluxes of the system as it is. The uniquely determined fluxes are v_{25}, v_{32}, v_{33}, v_{35}, v_{38} to v_{40}, v_{48} to v_{50}, v_{55} to v_{76}, v_{97} and v_{98}, the same fluxes uniquely determined through MFA in Subsection 4.1.3.

6.1.2 Metabolic Flux Analysis

Reaction Rates Determination

Cellular growth is understood as the division of one cell into two "daughter" cells. Hence, cell doubling takes place and the cell population undergoes exponential growth. This exponential growth depends on the specific growth rate of the cells μ. The specific growth rate is a key parameter for the description of biomass growth, substrate consumption and product formation. It is also known that μ varies with time and is influenced by many factors such as: substrate concentration, biomass concentration, product concentration, pH, temperature and dissolved oxygen, among others [5].

This specific growth rate can be experimentally calculated by measuring the cell density along a cellular culture. Assuming an exponential growth with constant specific growth rate operated in batch mode, the dynamics of cellular growth, substrate uptake and product excretion can be written as:

$$\frac{dX}{dt} = \mu X \tag{6.1a}$$

$$\frac{dS}{dt} = -\nu_S X \tag{6.1b}$$

$$\frac{dP}{dt} = \nu_P X \tag{6.1c}$$

The specific growth rate can be obtained by doing an exponential (or linear) regression (using the least squares method) of the biomass production data against the elapsed time of the culture (see equation (6.2)). This

exponential regression allows the determination of μ and at the same time give us an estimation of the the biomass concentration at the beginning of the culture X_0.

$$\frac{dX}{dt} = \mu t \quad \Rightarrow \quad X = X_0 e^{\mu t} \tag{6.2}$$

As an example, the specific growth rate for the exponential growth phase is calculated in Figure 6.1.
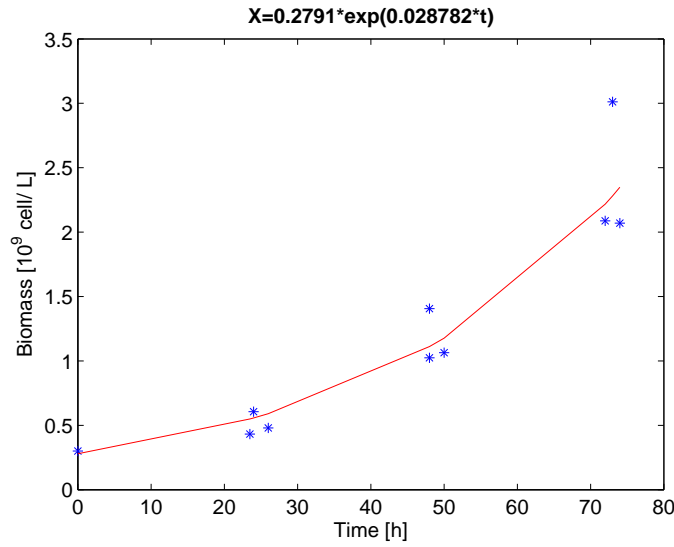
Figure 6.1: Exponential regression of the biomass production.

The specific rates of the extracellular species, whether substrates or products, can be determined from the experimental measurements collected through the culture. The specific uptake and excretion rates are assumed to be constant and are calculated by linear regression with respect to biomass. By integrating the last two equations of group 6.1, those describing the dynamics of substrates and products, the following linear regressions are obtained:

$$S = -\frac{\nu_S}{\mu}X + \frac{\nu_S X_0}{\mu} + S_0 \tag{6.3a}$$

$$P = \frac{\nu_P}{\mu}X - \frac{\nu_P X_0}{\mu} + P_0 \tag{6.3b}$$

In Figure 6.2, the specific uptake and excretion rates of the main substrates and products.
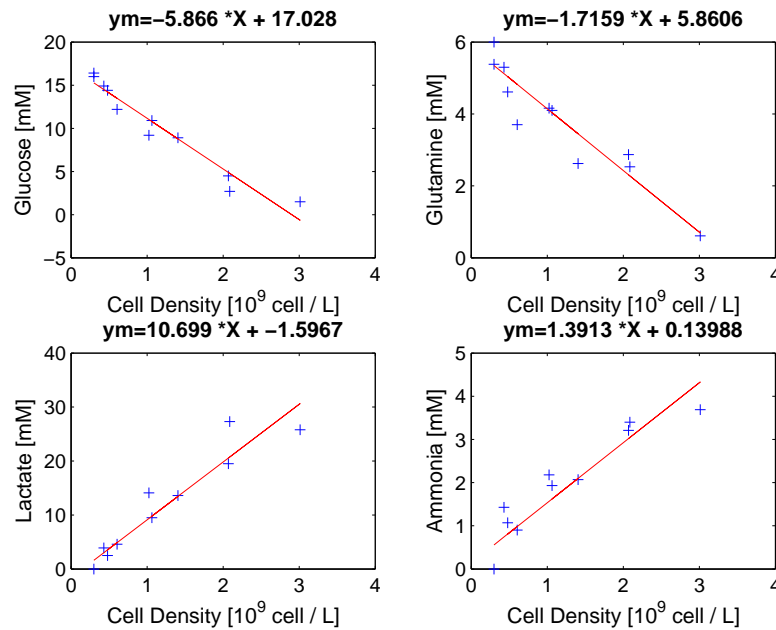
Figure 6.2: Linear regression of main substrates and products.

The slope obtained by linear regression, multiplied by the specific growth rate μ returns the specific uptake/excretion rate of that specific extracellular metabolite. In Table 4.1, Subsection 4.1.1, the calculated specific rates are listed.

It is worth to notice, that the calculated specific rates are prone to estimation errors, sometimes significant, and which may have an influence on the obtained results. We have seen the effect these errors induced in the dynamical modelling (Chapter 5). A confidence interval was calculated for each specific rate, for each life phase, so as to estimate this error. The specific uptake/excretion rates were presented in Table 5.1.

Other Operational Modalities   In the case where a cellular culture is operated in a different modality such as continuous, fed-batch or perfused, the determination of the specific reaction rates can become a bit harder. First of all the system is no longer isolated from the outside, meaning that inlet and outlet streams can be present. In Figure the 3 different culture modalities are depicted.

As the system is now open, there is an inlet flow F_{in} containing a substrate concentration S_{in}. Depending on the operation modality there may also be an outflow F_{out}, equal or not to the inflow. This causes that the volume of the culture may no longer be constant. In the case of a continuous or a perfusion culture the volume could be kept constant if one wishes to do

so while by definition in a fed-batch mode this would be impossible.

A variable D is introduced as the dilution rate. D is defined as the rate of inlet flow over the volume of culture in the bioreactor.

$$D = \frac{F}{V} \tag{6.4}$$

Normally, the equations describing the dynamics of cellular growth and substrate consumption are coupled as μ and ν_S, both depend on the substrate and biomass concentrations.

$$\frac{dX}{dt} = \mu\left(S, X\right) X - DX \tag{6.5a}$$

$$\frac{dS}{dt} = -\nu_S\left(S, X\right) X + D\left(S_{in} - S\right) \tag{6.5b}$$

In general, and to be able to solve this system, the hypothesis of constant μ and ν_S is adopted. We also consider that the biomass concentration X is an input to our system of equations. On this base, we obtain 2 uncoupled differential equations.

$$\frac{dX}{dt} = \left(\mu - D\right) X \tag{6.6a}$$

$$\frac{dS}{dt} = -DS - \nu_S X + DS_{in} \tag{6.6b}$$

We have seen that in the case of a batch culture the analytical resolution of these equations is quite simple. The dilution rate D is equal to zero and by means of a linear regression we are able to calculate μ and ν_S. For continuous, perfusion and fed-batch cultures to solve these equations is more difficult, though still feasible. If we integrate equation 6.6a we obtain:

$$\frac{X_2}{X_1} = e^{\mu(t_2 - t_1)} e^{-\int_{t_1}^{t_2} D(\tau) d\tau}$$

Then, μ is determined through the following expression:

$$\mu = \frac{ln\left(\frac{X_2}{X_1}\right)}{\left(t_2 - t_1\right)} + \frac{\int_{t_1}^{t_2} D(\tau) d\tau}{\left(t_2 - t_1\right)} \tag{6.7}$$

If the dilution rate D can be considered as a constant (for continuous or perfusion cultures), the expression is simplified to:

$$\mu - D = \frac{ln\left(\frac{X_2}{X_1}\right)}{(t_2 - t_1)}$$

It is easily verified that for a batch culture where D is equal to zero, equation 6.7 becomes equation 6.2.

In the same way, if we integrate equation 6.6b we obtain:

$$S(t) = \left[S(0) + \int_0^t (DS_{in} - \nu_S X)\, e^{\int_0^\tau D(\rho)d\rho} d\tau\right] e^{-\int_0^t D(\rho)d\rho} \qquad (6.8)$$

In order to calculate ν_S, we can rewrite equation (6.8) in the form

$$y(t) = \theta \cdot \varphi(t) \qquad (6.9)$$

where $y(t)$ are the measured variables, $\varphi(t)$ are the explicative variables and θ represents ν_S, the parameter we are looking for. Thus, we write equation (6.8) as

$$S(t) - U(t) = -\nu_S \left[e^{-\int_0^t D(\rho)d\rho} \int_0^t X\, e^{\int_0^\tau D(\rho)d\rho} d\tau\right] \qquad (6.10)$$

with

$$U(t) = S(0)\, e^{-\int_0^t D(\rho)d\rho} + e^{-\int_0^t D(\rho)d\rho} \int_0^t DS_{in}\, e^{\int_0^\tau D(\rho)d\rho} d\tau \qquad (6.11a)$$

$$S(t) - U(t) = y(t) \qquad (6.11b)$$

$$-\nu_S = \theta \qquad (6.11c)$$

$$\left[e^{-\int_0^t D(\rho)d\rho} \int_0^t X\, e^{\int_0^\tau D(\rho)d\rho} d\tau\right] = \varphi(t) \qquad (6.11d)$$

Equivalently, to calculate the specific growth rate μ through a parameter estimation we rewrite equation 6.7 in the form of 6.9.

$$ln\left(\frac{X_2}{X_1}\right) + \int_{t_1}^{t_2} D(\tau)d\tau = \mu\,(t_2 - t_1) \qquad (6.12)$$

with

$$ln\left(\frac{X_2}{X_1}\right) + \int_{t_1}^{t_2} D(\tau)d\tau = y(t) \qquad (6.13a)$$

$$\mu = \theta \qquad (6.13b)$$

$$(t_2 - t_1) = \varphi(t) \qquad (6.13c)$$

Metatool

Once the vector of measurements $\mathbf{v}_m$ has been calculated, we perform a flux analysis on the basis of the metabolic network $\mathbf{N}$ presented in Section 2.2. Matrix $\mathbf{N}$ has dimensions 100×72 (100 bioreactions and 72 internal metabolites) (see Appendix A).

The basis vectors $\mathbf{f}_i$ of the solution space $\mathcal{F}$ are obtained applying the software METATOOL [35, 44]. This software is freely available for academic users and allows the computation of elementary modes and other structural properties of biochemical reaction networks. It can be downloaded from the website http://pinguin.biologie.uni-jena.de/bioinformatik/networks/. The installation is straightforward: extract the script files into one directory and start Matlab into the directory where the files have been placed.

The starting point for the computation of the basis vectors is the following system

$$\begin{pmatrix} \mathbf{N} & \mathbf{0} \\ \mathbf{N}_m & -v_m \end{pmatrix} \cdot \begin{pmatrix} \mathbf{v} \\ \mathbf{1} \end{pmatrix} = 0 \tag{6.14}$$

and the matrix $\mathbf{A}$ which has to be defined within METATOOL

$$\mathbf{A} = \begin{pmatrix} \mathbf{N} & \mathbf{0} \\ \mathbf{N}_m & -\mathbf{v}_m \end{pmatrix}.$$

The standard input file format of METATOOL is ``file.dat``, meaning that matrix $\mathbf{A}$ should be written in this format. When the stoichiometric network has already been translated into a stoichiometric matrix (in Matlab or even Excel), it is also possible to use it directly. One simply has to set up a variable with two fields: `st` and `irrev_react`. `st` stands for the stoichiometric matrix $\mathbf{N}$ and `irrev_react` is a row vector which contains 0 for a reversible and 1 for an irreversible reaction.

Thus, the first step is to create a structure array. The specific fields are set by a dynamic link library (.dll) file present in the METATOOL directory. We can directly call:
`ex= parse('');`.
This command creates the array. Now, to define `st` and `irrev_react` we execute:
`ex.st= A;`
`ex.irrev_react= ones(101);`.
As stated before, all metabolic reactions are considered as irreversible in our study. Hence, `irrev_react` is defined as a vector of ones and, since matrix $\mathbf{A}$ has 101 columns, so does vector `irrev_react`.

To perform the calculations we need to call:

```
ex= metatool(ex);.
```
This will perform most of the operations that the stand-alone META-TOOL does and stores the results in the variable `ex`, which now contains several fields. When running METATOOL in this form, the elementary modes for the full system are not produced. To calculate the elementary modes we need to call:
```
ex.ems= ex.sub' * ex.rd_ems;,
```
where `ex.sub` and `ex.rd_ems` are both fields in `ex`. `ex.sub` stands for a subset matrix (rows correspond to the subsets, columns to the reactions in `st`) and `ex.rd_ems` houses the elementary modes of the reduced system (rows correspond to the subsets, columns are elementary modes).

It is important to pay attention to the results METATOOL displays in the Matlab command window. Eventually, one or maybe more errors can be found. In that case, the stoichiometric matrix $\mathbf{N}$ and the complete system (6.14) should be reviewed.

Once we have obtained the elementary modes matrix `ex.ems`, one should check for the presence of zero columns in it. As we have seen in Subsection 4.1.2, the presence of null columns means that there are as many unbounded paths as columns of zeros in the elementary modes matrix.

If everything is alright and no columns of zeros are found, we still need to normalize all elementary vectors so that the last element of each column is one. This is because of equation (6.14) where the last elements of vector $\begin{pmatrix} v \\ 1 \end{pmatrix}$ should be one.

This normalized matrix of elementary vectors, once the last row of ones is removed, contains the basis vectors $\mathbf{f}_i$ of system (6.14). From here it is now possible to determine the boundaries for each metabolic flux. One simply calculates the minimum and maximum flux values in each row and the flux intervals are obtained in a straightforward way.

6.1.3   Optimal Solution Determination

In this subsection we describe the optimization criterion used to calculate the flux distribution that maximizes the biomass production.

Matlab function `fmincon` is used as the optimization tool. The main function is `func_maxim_v`, that maximizes $\mathbf{v}$ with respect to the objective function `obj_func_biomass`. `fmincon` allows the minimization of the objective function under linear constraints. In our case, these constraints represent the mass balance system and require the definition of matrices $\mathbf{N}$, $\mathbf{N}_m$ and the vector of measurements $\mathbf{v}_m$.

Function `fmincon` needs a linear equation of the form $\mathbf{A}eq \times X = Beq$.

In our case, the equation to solve is

$$
\begin{bmatrix} N \\ N_m \end{bmatrix} \times X = \begin{bmatrix} 0 \\ v_m \end{bmatrix}
\tag{6.15}
$$

It is also necessary to define an arbitrary solution $\mathbf{v}_0$. A possible flux distribution can be obtained as the mean from the flux intervals determined with METATOOL.

```
func_maxim_v.m

Aeq = [N; Nm];
beq = [zeros(size(N,1),1) ; vm];
lB = zeros(length(v0),1);
x=fmincon(@obj_func_biomass,v0,[],[],Aeq,beq,lB,[],[]);
```

The objective function maximizes fluxes v_{55}, v_{63}, v_{68} and v_{75}, fluxes that correspond to protein, RNA, DNA and lipid synthesis, respectively. The reaction responsible for biomass production v_{76} synthesizes biomass from these macromolecules. Therefore, by maximizing the production of the elementary macromolecules, biomass production is also maximized.

```
function f=obj_func_biomass(v0)

a=zeros(1,length(v0));
a(55)= 0.9226;
a(63)= 0.013;
a(68)= 0.0052;
a(75)= 0.0297;
f=-a*v0;
```

All Matlab functions used for these calculations are listed in Appendix D.

6.2 Model Reduction Toolbox

This section is intended to give the reader a general idea of the model reduction procedure. In order to become familiar with the methodology used for this purpose, a small toolbox has been created. Through a series of steps, this toolbox allows the reduction of a metabolic network into a set of macroscopic bioreactions, which in turn can be translated into a dynamical model.

6.2.1 Overview

This application is composed mainly of four steps, all of them running in MATLAB environment. The intention of the first part is to calculate the specific growth rate of the cells and the specific consumption and excretion rates of substrates and extracellular products. In addition, an estimative of the initial concentration of these metabolite can also be calculated (S_0 or P_0). In a second step, the good agreement between the experimental data and the metabolic network is verified. The third part consists in the determination of the minimal set of elementary flux modes, which is further translated in a set of macroscopic reactions. These last macroreactions are used in the fourth and final stage of the application to built a dynamical model capable of reproducing the experimental data. A general diagram of the toolbox is presented in Figure 6.3.

6.2.2 Procedure

The determination of the specific growth rate and the specific consumption/production rates of the extracellular species has been explained in the previous chapter (see Subsubsection 6.1.2).

All the specific rates determined by linear regression conform vector $\mathbf{v}_m$ (the vector of measurements) and serve as inputs to determine the minimal set of elementary flux modes using the methodology described in Section 5.3, Chapter 5. Nevertheless, before calculating the minimal set of EFMs, it is necessary to check whether the metabolic network constructed to represent the metabolism of the cells is in agreement or not with the experimental measurements. The second part of the toolbox consists then in verifying that the phase of the cell life where the specific rates were calculated is well represented by the underlying stoichiometric matrix. Otherwise, a metabolite that may appear as being produced in the metabolic network, might be evidenced as consumed by the experimental measurements giving rise to an inconsistency. If this is the case, the metabolic network needs to be modified.

The next step is then the calculation of the minimal set of EFMs ($\mathbf{E_{min}}$). The methodology has been thoroughly described in Section 5.3. For more details on the algorithm and the reasoning behind, the reader is referred to [20]. The inputs to this third stage are: the stoichiometric matrices for the intracellular and extracellular metabolites $\mathbf{N}$ and $\mathbf{N}_m$, respectively and the vector of measurements $\mathbf{v}_m$. The decomposition of $\mathbf{v}_m$ in its basis vectors y_i, as we have seen, allows the determination of a small set of basis vectors e_i. This minimal set of EFMs is further translated into a set of macroscopic reactions, which we assume summarize the whole metabolism encoded in metabolic network $\mathbf{N}$. Along with this minimal set of EFMs, the specific reaction rates $\mathbf{w}$ for each of the macroscopic reactions are calculated.
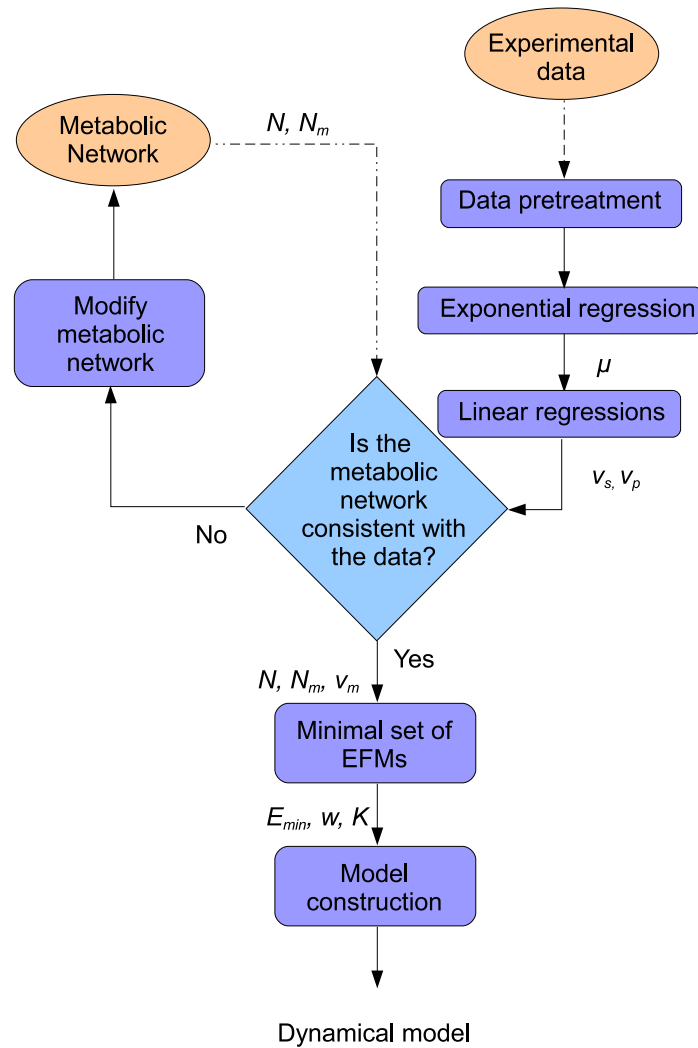
Figure 6.3: Model reduction toolbox flowchart.

The determination of the set of macroreactions and the set up of the dynamic model are done in the fourth and final stage. The macroreactions are encoded in stoichiometric matrix $\mathbf{K}$, resulting from the multiplication of matrix $\mathbf{N}_m$ times matrix $\mathbf{E_{min}}$ (see equation 5.8 in Section 5.2). Therefore, $\mathbf{K}$ is a $p \times p$ matrix (p being the number of extracellular measurements, either substrates or products) and it is translated into a set of p differential equations by means of a text generator. A text generator is a script file that, given the necessary informative parameters, produces a text file. In this case, the reaction rate expressions are generated thanks to the information extracted from matrix $\mathbf{K}$.

The way in which the set of reactions obtained are used to develop a dynamical model has been reviewed in Section 5.2. The final stage of this toolbox simply consists in building the dynamical model as it has been explained previously.

The reaction rates of the p macroreactions are chosen as Michaîlis-Menten kinetics:

$$r_i = w_i \frac{S_1}{(k_{s_1} + S_1)} \frac{S_2}{(k_{s_2} + S_2)} \; ...... \; \frac{S_z}{(k_{s_z} + S_z)}$$

Subindex z indicates the number of substrates participating in reaction i. The reaction rates have nearly constant values except when substrates approach to exhaustion.

Thus, the dynamical model is constructed as:

$$\frac{d\xi}{dt} = KrX$$

In the following, the toolbox is applied to a series of data obtained from a CHO-320 cell culture operated in batch mode. The intention is to generate a dynamical model for the exponential growth phase using the metabolic network described in Section 2.2 and the experimental measurements used in Subsection 4.2.1.

6.2.3 Application

Following the flowchart in Figure 6.3, the starting points are stoichiometric matrix **N** and the set of experimental measurements. Eventually, a pretreatment of the data set might be required when the number of measurement points differs from one metabolite to another. For instance, this occurs when not all the analysis have been performed for one of the samples taken or when the sampling time is different between duplicates. Ideally, the measurement points of the extracellular species should be the same as those of the biomass production.

Once this has been settled, the exponential regression of the biomass production curve is performed (see Figure 6.4).

From this operation, the specific growth rate μ and an estimation of the initial concentration of biomass X_0 are obtained. The specific growth rate is now used to calculate the specific uptake and excretion rates of the measured extracellular species. The linear regression obtained for substrates and products are presented in Figures 6.5, 6.6 and 6.7.

From this step, the specific uptake and excretion rates $\mathbf{v}_s$ and $\mathbf{v}_p$ are calculated. With this information it is now possible to see whether the
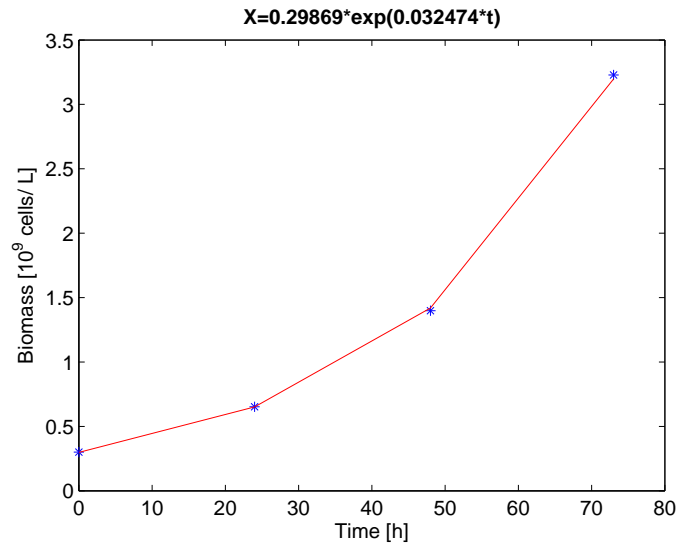
Figure 6.4: Exponential regression of the biomass production.
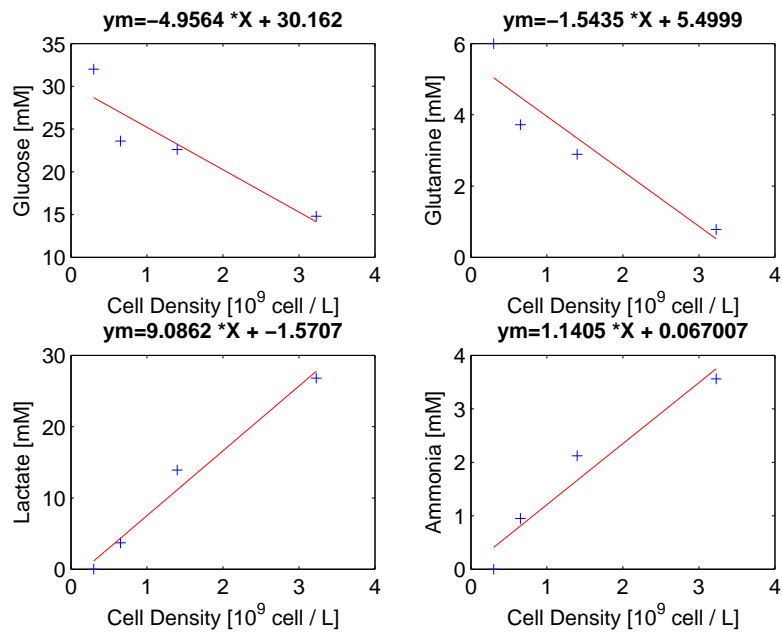
Figure 6.5: Linear regression of main substrates and products.

metabolic network is consistent with the experimental data or not. This verification step is easily done by comparing the sign of the entries in matrix $\mathbf{N}m$ ("-" for a substrate and "+" for a product) with the sign of the specific rates just calculated. The signs should be both, either positive or negative.
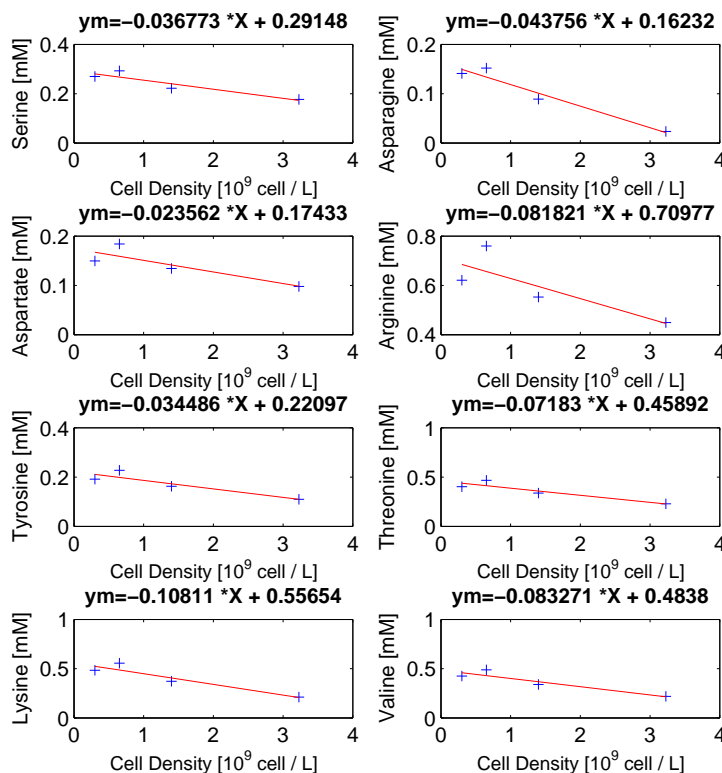
Figure 6.6: Linear regression of amino acids.

As the stoichiometric matrix is in perfect agreement with the specific rates calculated, the next stage is the computation of a minimal set of elementary flux modes $\mathbf{E}_{min}$. If any inconsistency were found, the stoichiometric matrix should be modified or even rebuilt until it agrees with the experimental data.

The inputs for the algorithm which calculates minimal sets of EFMs are the stoichiometric matrices $\mathbf{N}$ and $\mathbf{N}m$ and the vector of extracellular measurements $\mathbf{v}_m$, which assembles vectors $\mathbf{v}_s$ and $\mathbf{v}_p$. At this point it is important to bear in mind that each run of the algorithm will yield a different minimal set of EFMs. As it has been stated in Subsection 5.3.2, the minimal decomposition obtained in $\mathbf{E}_{min}$ is not unique.

The multiplication of stoichiometric matrix $\mathbf{N}m$ times matrix $\mathbf{E}_{min}$, encoding the minimal set of elementary paths, yields a stoichiometric matrix for a set of macroscopic reactions $\mathbf{K}$. This stoichiometric matrix and the vector of specific reaction rates $\mathbf{w}$ for each macroscopic reaction are presented

	e1	e2	e3	e4	e5	e6	e7	e8	e9	e10	e11	e12	e13	e14	e15	e16	e17	e18	e19
Glucose	0.00	-1.00	0.00	0.00	-1.00	-3.72	-13.03	-1.00	-1.86	0.00	0.00	-1.86	-9.38	-1.00	-6.41	-5.62	-5.75	-2.83	-13.03
Gln	0.00	-2.00	-1.00	0.00	0.00	-8.41	-7.68	0.00	-2.50	0.00	-1.00	-1.67	-7.68	0.00	-1.63	-1.63	-1.67	-1.67	-7.68
Ser	0.00	0.00	0.00	-1.00	0.00	0.00	0.00	0.00	0.00	0.00	0.00	0.00	0.00	0.00	0.00	0.00	0.00	0.00	0.00
Asn	0.00	0.00	0.00	0.00	0.00	-1.34	-4.71	0.00	-1.02	0.00	0.00	-2.89	-4.71	0.00	-1.00	-1.00	-2.07	-2.07	-4.71
Asp	0.00	0.00	0.00	0.00	0.00	-2.45	-8.58	0.00	-1.04	0.00	0.00	0.00	0.00	0.00	0.00	0.00	0.00	0.00	0.00
Arg	0.00	0.00	0.00	0.00	0.00	-1.59	-9.39	0.00	-1.21	0.00	0.00	-2.04	-21.07	-2.00	-2.00	-2.00	-2.04	-2.04	-14.19
Tyr	-1.00	0.00	0.00	0.00	0.00	-1.00	-3.50	0.00	0.00	0.00	0.00	0.00	0.00	0.00	0.00	0.00	0.00	0.00	0.00
Thr	0.00	0.00	0.00	0.00	0.00	-1.84	-6.46	0.00	-3.35	0.00	0.00	-3.35	-69.35	0.00	-1.37	-1.37	-1.40	-1.40	-6.46
Lys	0.00	0.00	0.00	0.00	0.00	-2.23	-14.06	0.00	-2.91	0.00	0.00	-2.49	-6.46	0.00	-8.05	-7.26	-6.39	-3.47	-13.55
Val	0.00	0.00	0.00	0.00	0.00	-2.06	-7.22	0.00	-1.57	-1.00	0.00	-1.57	-7.22	0.00	-1.53	-1.53	-1.57	-1.57	-7.22
Ile	0.00	0.00	0.00	0.00	0.00	-1.66	-5.80	0.00	-1.26	0.00	0.00	-10.82	-5.80	0.00	-1.23	-1.23	-1.26	-1.26	-5.80
Leu	0.00	0.00	0.00	0.00	0.00	-8.57	-9.96	0.00	-2.17	0.00	0.00	-2.17	-9.96	0.00	-2.12	-2.12	-2.17	-2.17	-9.96
Phe	0.00	0.00	0.00	0.00	0.00	-1.22	-4.27	0.00	-1.69	0.00	0.00	-1.69	-7.77	0.00	-1.65	-1.65	-1.69	-1.69	-7.77
Met	0.00	0.00	0.00	0.00	0.00	-1.31	-4.60	0.00	-1.00	0.00	0.00	-1.00	-4.60	0.00	-2.00	-2.00	-1.00	-1.00	-4.60
Lactate	0.00	2.00	1.00	0.00	1.67	0.00	3.77	2.00	0.00	0.00	0.00	0.00	0.00	0.00	0.00	0.00	0.00	0.00	0.00
Ala	0.00	0.00	0.00	0.00	0.00	3.77	15.31	0.00	2.51	1.00	1.00	8.52	0.00	4.00	5.48	0.00	0.00	2.92	15.82
Gly	0.00	0.00	0.00	1.00	0.00	0.00	0.00	0.00	0.00	0.00	0.00	0.00	53.93	0.00	0.00	4.68	5.84	0.00	0.00
Glu	1.00	0.00	0.00	0.00	0.00	0.00	0.00	0.00	0.00	0.00	0.00	0.00	0.00	0.00	0.00	0.00	0.00	0.00	0.00
NH4	0.00	4.00	0.00	0.00	0.00	6.50	1.00	0.00	1.05	0.00	1.00	2.08	1.00	0.00	2.25	2.25	1.26	1.26	1.00

Table 6.1: Stoichiometric Network for the macroscopic reactions.
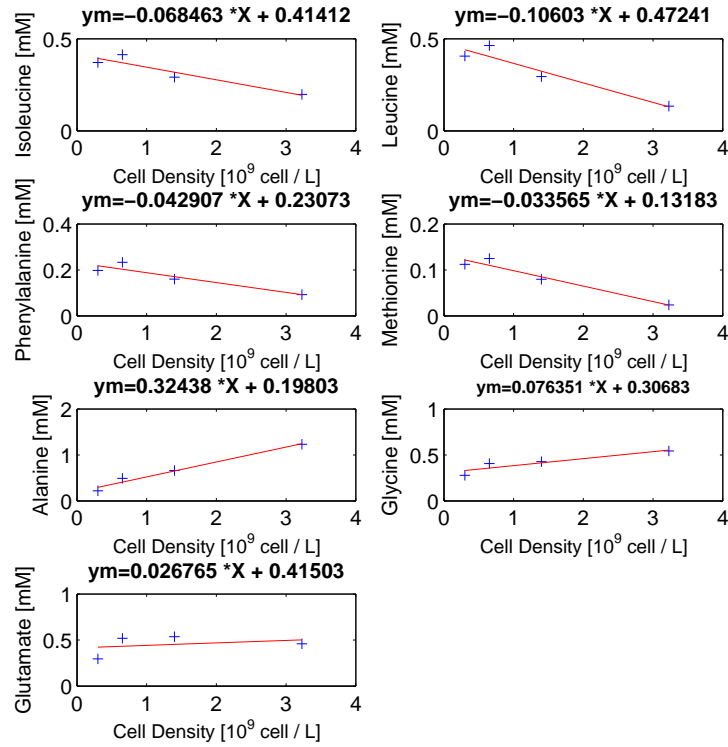
Figure 6.7: Linear regression of amino acids.

in Tables 6.2.3 and 6.2.3, respectively.

From stoichiometric matrix **K** the text generator identifies the position of the substrates taking part in each one of the 19 macroscopic reactions and then builds the reaction rate kinetic equations.

Reaction	w_i	Reaction	w_i
e1	$1.4772e^{-5}$	**e11**	$3.6602e^{-3}$
e2	$6.4504e^{-2}$	**e12**	$5.4817e^{-4}$
e3	$8.0929e^{-2}$	**e13**	$1.5650e^{-4}$
e4	$3.7485e^{-5}$	**e14**	$8.2605e^{-4}$
e5	$7.8179e^{-1}$	**e15**	$1.2298e^{-3}$
e6	$2.7201e^{-3}$	**e16**	$5.2730e^{-5}$
e7	$1.6900e^{-4}$	**e17**	$1.3929e^{-3}$
e8	$6.0614e^{-2}$	**e18**	$4.2699e^{-4}$
e9	$6.5741e^{-4}$	**e19**	$1.3841e^{-4}$
e10	$1.3301e^{-4}$		

Table 6.2: Macro-reaction rates

```
%reaction rate kinetic equations

r1 = mu1*tyr/((k_tyr+tyr));
r2 = mu2*G*gln/((k_G+G)*(k_gln+gln));
r3 = mu3*gln/((k_gln+gln));
r4 = mu4*ser/((k_ser+ser));
r5 = mu5*G/((k_G+G));
r6 = mu6*G*gln*asn*asp*arg*tyr*thr*lys*val*ile*leu*phe*met/((k_G+G)
*(k_gln+gln)*(k_asn+asn)*(k_asp+asp)*(k_arg+arg)*(k_tyr+tyr)*(k_thr+thr)
*(k_lys+lys)*(k_val+val)*(k_ile+ile)*(k_leu+leu)*(k_phe+phe)*(k_met+met));
r7 = mu7*G*gln*asn*asp*arg*tyr*thr*lys*val*ile*leu*phe*met/((k_G+G)
*(k_gln+gln)*(k_asn+asn)*(k_asp+asp)*(k_arg+arg)*(k_tyr+tyr)*(k_thr+thr)
*(k_lys+lys)*(k_val+val)*(k_ile+ile)*(k_leu+leu)*(k_phe+phe)*(k_met+met));
r8 = mu8*G/((k_G+G));
r9 = mu9*G*gln*asn*asp*arg*thr*lys*val*ile*leu*phe*met/((k_G+G)*(k_gln+gln)
*(k_asn+asn)*(k_asp+asp)*(k_arg+arg)*(k_thr+thr)*(k_lys+lys)*(k_val+val)
*(k_ile+ile)*(k_leu+leu)*(k_phe+phe)*(k_met+met));
r10 = mu10*val/((k_val+val));
r11 = mu11*gln/((k_gln+gln));
r12 = mu12*G*gln*asn*arg*thr*lys*val*ile*leu*phe*met/((k_G+G)*(k_gln+gln)
*(k_asn+asn)*(k_arg+arg)*(k_thr+thr)*(k_lys+lys)*(k_val+val)*(k_ile+ile)
*(k_leu+leu)*(k_phe+phe)*(k_met+met));
r13 = mu13*G*gln*asn*arg*thr*lys*val*ile*leu*phe*met/((k_G+G)*(k_gln+gln)
*(k_asn+asn)*(k_arg+arg)*(k_thr+thr)*(k_lys+lys)*(k_val+val)*(k_ile+ile)
*(k_leu+leu)*(k_phe+phe)*(k_met+met));
r14 = mu14*G*arg/((k_G+G)*(k_arg+arg));
r15 = mu15*G*gln*asn*arg*thr*lys*val*ile*leu*phe*met/((k_G+G)*(k_gln+gln)
*(k_asn+asn)*(k_arg+arg)*(k_thr+thr)*(k_lys+lys)*(k_val+val)*(k_ile+ile)
*(k_leu+leu)*(k_phe+phe)*(k_met+met));
r16 = mu16*G*gln*asn*arg*thr*lys*val*ile*leu*phe*met/((k_G+G)*(k_gln+gln)
*(k_asn+asn)*(k_arg+arg)*(k_thr+thr)*(k_lys+lys)*(k_val+val)*(k_ile+ile)
*(k_leu+leu)*(k_phe+phe)*(k_met+met));
r17 = mu17*G*gln*asn*arg*thr*lys*val*ile*leu*phe*met/((k_G+G)*(k_gln+gln)
*(k_asn+asn)*(k_arg+arg)*(k_thr+thr)*(k_lys+lys)*(k_val+val)*(k_ile+ile)
*(k_leu+leu)*(k_phe+phe)*(k_met+met));
r18 = mu18*G*gln*asn*arg*thr*lys*val*ile*leu*phe*met/((k_G+G)*(k_gln+gln)
*(k_asn+asn)*(k_arg+arg)*(k_thr+thr)*(k_lys+lys)*(k_val+val)*(k_ile+ile)
*(k_leu+leu)*(k_phe+phe)*(k_met+met));
r19 = mu19*G*gln*asn*arg*thr*lys*val*ile*leu*phe*met/((k_G+G)*(k_gln+gln)
*(k_asn+asn)*(k_arg+arg)*(k_thr+thr)*(k_lys+lys)*(k_val+val)*(k_ile+ile)
*(k_leu+leu)*(k_phe+phe)*(k_met+met));
```

With this, the set up of the dynamical model is complete and the simu-

lator can be ran. The fit of the model to the experimental data is presented
in Figures 6.8 and 6.9.
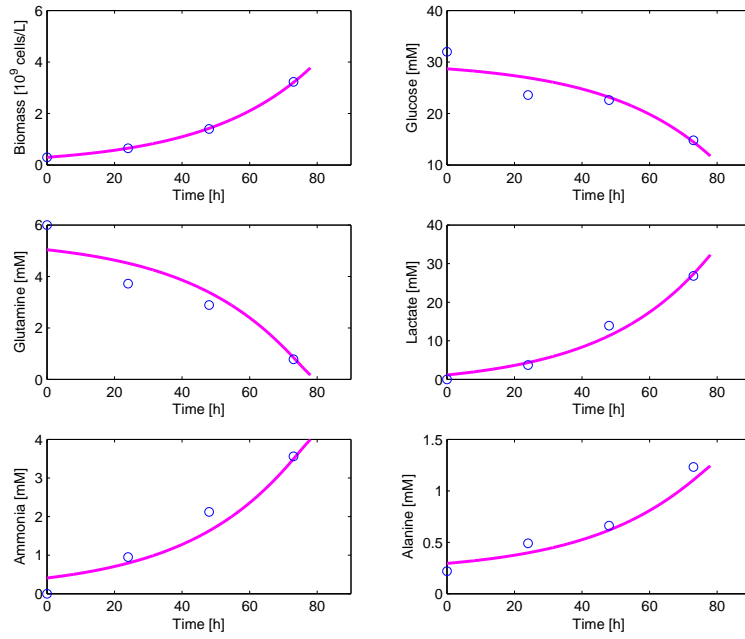
Figure 6.8: Simulation obtained from the model.

All Matlab functions used for these calculations are listed in Appendix
D.
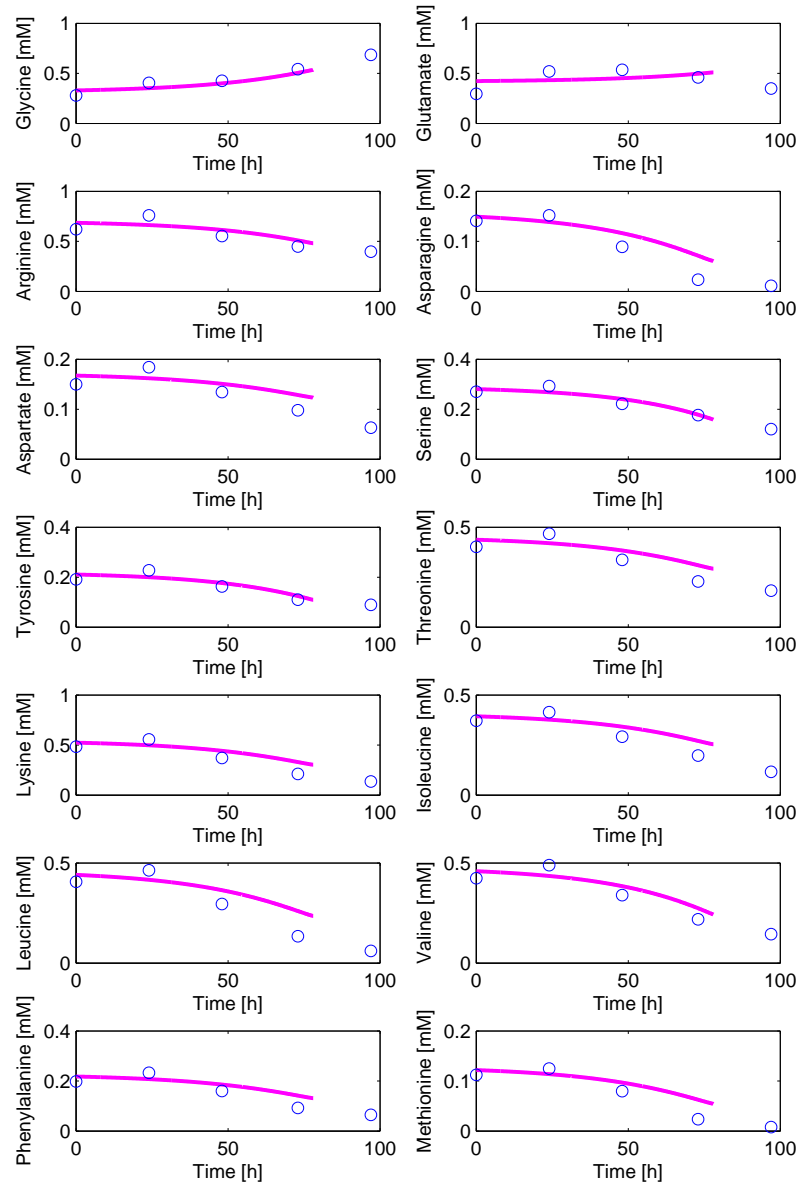
Figure 6.9: Simulation obtained from the model.

Chapter 7

Laboratory Setup and Cellular Culture Experiences

This chapter introduces the overall setup of an animal cell culture laboratory and the subsequent development of culture experiences. This laboratory is the outcome of the joint effort of the Applied Chemistry and Biochemistry Department and the Automatic Control Department of the University of Mons. The creation of this laboratory has been supported by the Engineering Faculty (laboratory and main equipments such as bioreactors) and by the OCPAM project (Hainaut Biomed) funded by FEDER and the Walloon Region for some specific instrumentation (NIR probe and UPLC). Our main goal is to obtain a more informative and modular data base, in the sense that we want to validate the metabolic flux analysis with different sets of experimental data but also to be capable of measuring the species pointed out as most informative. For instance, it has been shown how important the determination of the carbon dioxide measurement is for the well posedness of the system. Thus, the bioreactor setup considers the installation of a gas analyzer so as to determine the CO_2 production rate.

Firstly, the main features of the laboratory are highlighted, describing the utilized equipments and the analytic procedures which allow the realization of animal cellular cultures and hopefully in the future, the continuous monitoring of a perfused bioreactor. Afterwards, the actual cellular cultures that have been carried out in the laboratory are presented.

7.1 Laboratory Implementation

7.1.1 Cell Lines

A small cell bank has been established within our laboratory. Three types of CHO cell lines are currently available: CHO-320, CHO-S and CHO-S clone 4922-69. All of them are stored in liquid nitrogen (-196°C). CHO-320 cells

have been kindly provided by Professor Annie Marc (Institut national polytechnique de Lorraine (INPL) - Nancy, France). This cell line derives from CHO-K1 cells which were transfected to produce gamma-interferon. CHO-S cells and its clone have been provided by Dr Emmanuelle ADAM (Biology and Molecular Medicine Institute (IBMM), Université Libre de Bruxelles, Belgium). CHO-S also derives from CHO-K1, and has been adapted to grow in suspension. CHO-S clone 4922-69 corresponds to CHO-S transfected to produce Hypoallergenic *Pro Der P 1 FC* (precursor of *Der p 1* major dust mite allergen).

The cellular cultures presented in this thesis were carried out using the CHO-S cell line.

7.1.2 Culture Medium

The culture medium used for the cultivation of CHO-S is a defined medium called CD-CHO (Gibco). This medium should be complemented with glutamine (so as to achieve a 6 mM final concentration) and HT supplement at 1% (v/v) which provides preformed purines and pyrimidines. The culture medium for the CHO-320 is a BDM (Basal Defined Medium) described in [43] which is a 5:5:1 mixture of IMDM, Ham's F12, NCTC 135 media. This medium is supplemented with 0,1% (v/v) pluronic acid F68 (a surfactant for the protection of cells against hydrodynamical stresses), ferric citrate at 500 mM, ethanolamine at 60 μM and glutamine at 6 mM of final concentration.

7.1.3 Cellular Cultures

Flask Cultures

A series of cell cultures were carried out in 250mL spinner flasks (Fig. 7.1). These flasks provide a continuous agitation through a magnetic stirrer platform and allow an appropriate gas exchange between the culture medium and the incubator atmosphere. The incubator is set to a temperature of 37° C under a water-saturated atmosphere and 5% (v/v) of CO_2. The agitation set point is recommended not to be under 40 rpm. Aeration is allowed only via the surface of the liquid thus, a high ratio between liquid surface and liquid height will improved the gas transfer exchange.

Bioreactor Cultures

The bioreactor is a 2 liters vessel and its corresponding controller is a Sartorius Biostat B plus in exclusive flow configuration. This exclusive configuration, as shown in Figure 7.2, allows the inflow of a gas-mixing of air, oxygen, nitrogen and carbon dioxide through the sparger aeration. On the other side, only the inlet of air is possible through the overlay aeration. This

Figure 7.1: 250 mL spinner flask (Wheaton)

configuration is intended to be specially configured for cell culture applications.
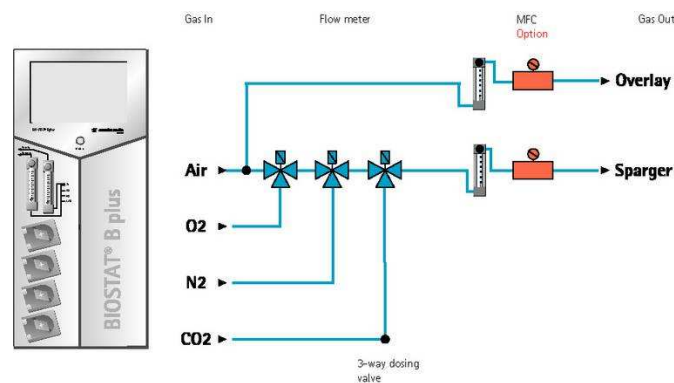
Figure 7.2: Exclusive Flow Configuration

The temperature of the culture is set to 36.5° C and the agitation to 60 rpm. These values are recommended as adequate set points to animal cell cultures in bioreactors [13].

Aeration In contrast with the aeration in flask cultures, the aeration in a bioreactor is done both through the surface and in the bottom of the culture media via a sparger device. This provides a more homogeneous and efficient gas transfer into the liquid. The recommended values for aeration via overlay are 0.1-1 vvm and via sparger 0.05-0.1 vvm (vvm = gas volume

per liquid volume per minute). Thus, for a working volume of 1.3 Liters, the inlet flow via overlay and sparger corresponds to 0.13 - 1.3 L/min and 0.065 - 0.13 L/min, respectively.

pO2 controler Dissolved oxygen (DO) is essential for cellular growth but at high concentrations it can be toxic due to the induction of oxidative stress. Recommended DO ranges in culture may vary widely depending on the cell line and type. For CHO cell cultures a common set point for the DO is 30% (Air saturation is equivalent to 100% or 8 ppm approximately).

The calibration of the DO probe (OXIFERM FDA, Hamilton) must be done each time before the bioreactor is launched. The setting of 0 percent DO can be done in two different ways, either by setting it as the electric zero (simply unplugging the probe from the controller) or by bubbling nitrogen (pure N_2) inside the bioreactor. For the 100 percent point a double calibration is done. First, 100% is set as the atmosphere air condition (before sterilization) and then, once the medium has been transfered into the bioreactor under sterile condition, oxygen is bubbled inside the bioreactor until saturation and the probe is reseted to 100%.

pH controler Cells are sensitive to environmental pH conditions since it influences the intracellular pH and so, all enzymatic activities. In general, pH ranges can span form 6,8 to 7,4 for cellular cultures, except for insect cells which require lower pH values. pH must remain stable and should be monitored all along the culture. pH is regulated with $NaHCO_3$ 1 M and CO_2 injection. pH probe (EASYFERM PLUS, Hamilton) is calibrated as a common pH meter with standard solutions of pH 4 and pH 7.

7.1.4   Analytical Methods

Cell Counting

Cell density and viability are determined by a dye exclusion method. The stain used is Trypan blue which permeates through the membrane of dead cells but not that of a viable cell. Hence, dead cells are shown as a distinctive blue colour under a microscope. The number of cells per unit volume of a suspension is determined using a specific type of counting chamber called Burker hemocytometer.

A Bürker hemocytometer has two counting chambers, each one divided in 9 large squares. Each large square has a surface of 1 mm^2 and a depth of 0.1 mm, resulting in a volume of 0.1 mm^3. The total number of cells can be determined by counting all or a certain number of these large squares. The
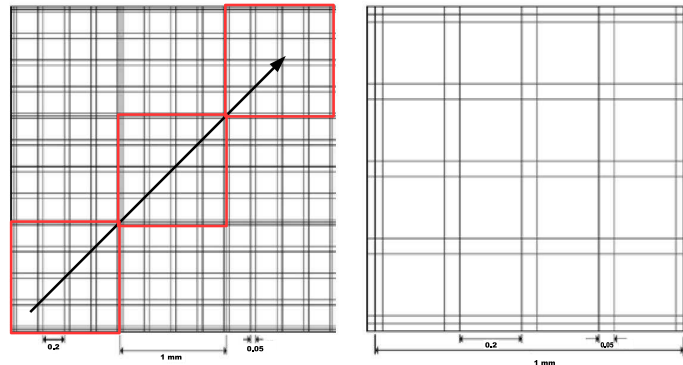
Figure 7.3: Bürker hemocytometer.

viable cell concentration is then given by:

$$Cell\ density\ \left[\frac{cells}{mL}\right] = \frac{number\ of\ cells}{number\ of\ squares} \times f \times 10^4 \qquad (7.1)$$

where f is the dilution factor of the sample in Trypan blue. The viability of the culture is given by the number of viable cells over the total number of cells.

$$Viability\ [\%] = \frac{number\ of\ viable\ cells}{Total\ number\ of\ cells} \times 100 \qquad (7.2)$$

UPLC

The amino acid measurements are done using a Waters ACQUITY UPLC ® System with the Acquity UPLC TUV detector. The UPLC or Ultra Performance Liquid Chromatography is an instrument allowing the performance of a much more efficient chromatography analysis than its predecessor the HPLC. Its main feature is that it has been conceived to work at a higher pressure so as to attain better defined and concentrated peaks and at the same time improving the analysis rate and reducing solvent consumption. The analysis method called AccQTag$^{\text{TM}}$, is based on a specific derivation which converts amino acids to stable fluorescent compounds. In this way, the monitoring of a certain number of amino acids during the cellular culture is possible through the analysis via UPLC. In Figure 7.4 the overlapping of 10 chromatograms obtained from the analysis of the same amino acid standard is presented, showing a good reproducibility of the analysis. The concentration of amino acids in this standard are very precise and as a result, the concentration of amino acids present in whatever sample of medium can be calculated.
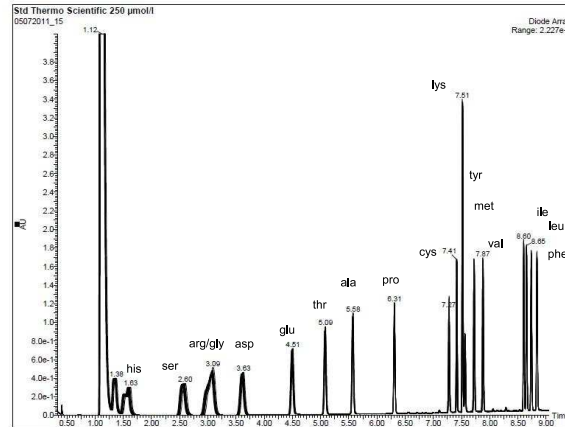
Figure 7.4: Chromatogram. Overlapping of ten standard analysis.

Any cellular remains should be removed from the sample before injection so as to avoid damaging the column.

Enzymatic Kits

The evolution of the concentration of the main metabolites present in the cell culture medium is followed by means of enzymatic kits. Glucose, Lactate, Glutamine and Ammonia concentrations are analyzed with D-Glucose (GOPOD Format), L-Lactic Acid (L-Lactate) and L-Glutamine / Ammonia (Rapid) Megazyme assay kits, respectively. Absorbances are read using a spectrophotometer.

7.2 Cell Culture Experiments

In this section, the cellular culture experiments carried out in our laboratory are described and presented. The cell cultures were performed both, in spinner flasks and in a bioreactor. A pre-culture preceding the actual experiments is common to both kinds of culture, flask and bioreactor cultures. A cellular culture must always begin by a pre-culture, usually a flask pre-culture so as to allow the proliferation of enough biomass to inoculate at the desired cell concentration.

7.2.1   Spinner Flask Cultures

First Series of Spinner Flask Cultures

A first series of CHO-S batch cultures was carried out in 250 mL spinner flasks for a period of 233 hours. Initial concentrations of glucose and glutamine were 6 g/L (33 mM) and 0,3 g/L (2mM), respectively. Cell cultures were performed in triplicate at 37°C, 42 rpm and 5% of CO_2 in a defined medium for CHO cells (CD-CHO, Gibco).

Figure 7.5: Batch cultures at glucose 33mM and glutamine 2mM.

Cellular density and viability were monitored all along the culture and further analysis of the evolution of glucose, lactate, ammonia and amino acid concentrations were performed afterwards. The sampling time was set to every 8 hours during the five first days and then set to every 12 hours. In Figure 7.6, the evolution of viable cell density, glucose and glutamine consumption and lactate, ammonia and alanine production are presented. Amino acid concentrations were determined via UPLC using the AccQTag^{TM}method. The evolution of the amino acid concentrations along the culture is shown in Figure 7.7.

Taking three samples per day allow us to have a good follow-up of the culture. The sampling time provides enough measurement points to have a good estimation of the evolution of the different metabolite concentrations. This experimental data could then be used for mathematical modelling purposes. Nevertheless, the analytical methods available (for the moment) in our laboratory allow us to determine the concentration of only 17 extracellu-
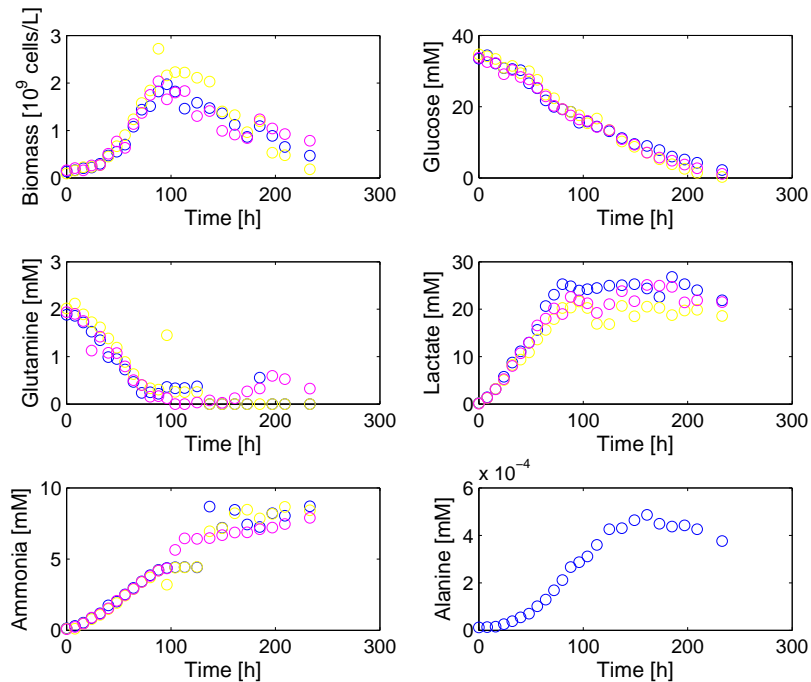
Figure 7.6: Cellular density and extracellular species.

lar species. As we have seen in Subsection 4.1.2, to perform a MFA with such a metabolic network as the one described in Section 2.2, at least 20 measurements are needed in order to assure the well-posedness of the system. In the future, more analytical methods, as the NIR probe and the gas analyzer, will be developed and clarified providing a richer set of experimental data.

Second Series of Spinner Flask Cultures

A second series of batch cultures using the same CHO cell line was carried out this time changing the initial concentration of glutamine while keeping the initial concentration of glucose at 33 mM. Initial glutamine concentrations considered were 6 mM, 10 mM and 14 mM. Cell cultures were performed at the same conditions as the preceding series, 37°C, 42 rpm and 5% of CO_2 in a defined medium for CHO cells (CD-CHO, Gibco). Cellular density and viability were followed through the culture and further analysis of the evolution of glucose, lactate, ammonia and urea concentrations were performed afterwards. Samples were taken two times a day every 8 and 16 hours. The evolution of viable cell density, glucose and glutamine consumption and lactate, ammonia and urea production are presented in Figure 7.8. Blue, yellow and red circles depict glutamine initial concentrations of 6 mM,

10mM and 14mM, respectively.

Although, the concentration of glutamine is different for the three cultures, no significant differences are noticed in the production of biomass. A slightly higher production of ammonia is the only outcome of this increase in the initial concentration of glutamine. Urea is one of the potential extra inputs of the metabolic network. As such, we measured it expecting to find some interesting results. Unfortunately, the production of urea appears to be negligible, at least when measured with an enzymatic kit. Maybe a more sensitive analytical method could yield more useful and interesting results.

7.2.2   Bioreactor Cell Cultures

A bioreactor culture was also carried out. Again the cell line used for this experience was CHO-S. The culture media was a defined medium CD-CHO (Gibco) which was further supplemented in glutamine so as to get initial concentrations of glucose and glutamine of 6 33 mM and 2mM, respectively. Cells were inoculated at a concentration of 0.39 cells per mL (5.08×10^8 cells) in 1.3 L of culture medium. The culture conditions were set to a temperature of 36.7°C, a stirring of 60 rpm, a pH of 7.24 and 30% of PO_2. The aeration was only supplied by the overlay as a mixture of air, oxygen and CO_2 at a flow of 0.6 L/min.

Cellular density and viability were monitored all along the culture using the Trypan Blue method. The evolution of glucose, lactate, ammonia and glutamine was determined in posteriori enzymatic assays. The sampling time was set to every 8 and 16 hours, taking two samples a day. In Figure 7.9, the measurements of the evolution of viable cell density, glucose and glutamine consumption and lactate and ammonia production are presented.

Even though these data are not likely to be used for flux analysis, modelling or control purposes, they represent our very first accomplishment. For the first time we were able to carry out a cellular culture in a bioreactor taking samples and controlling all the environmental condition cited above. We do not look at this experiment as a poor data base but as an asset of the group of people who have work very hard to make this a functional laboratory.
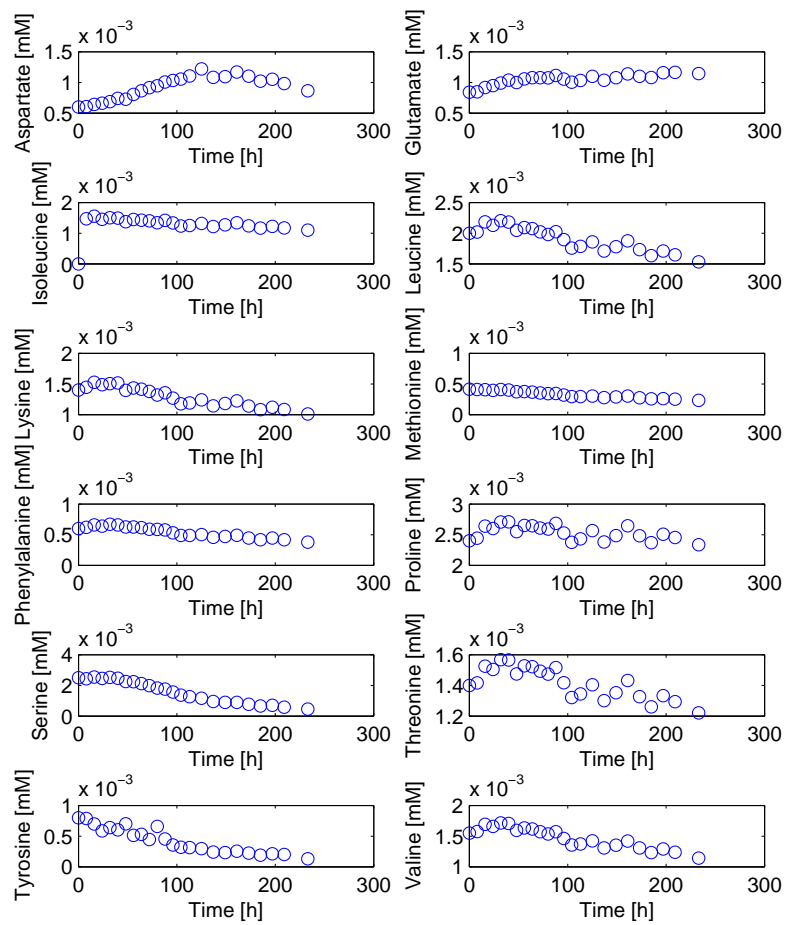
Figure 7.7: Amino acid uptake and excretion profiles.
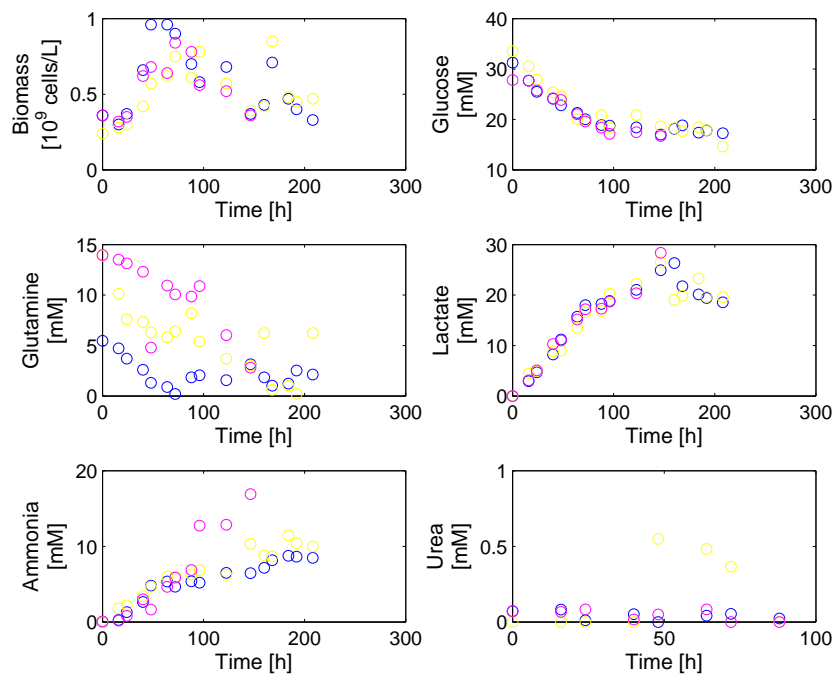
Figure 7.8: Cellular density and measured extracellular species.
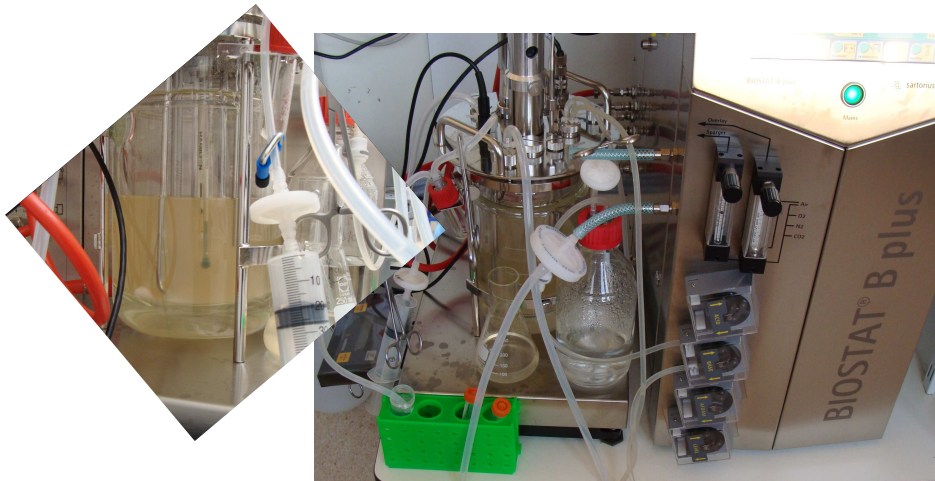
Figure 7.9: Batch bioreactor culture of CHO-S cells
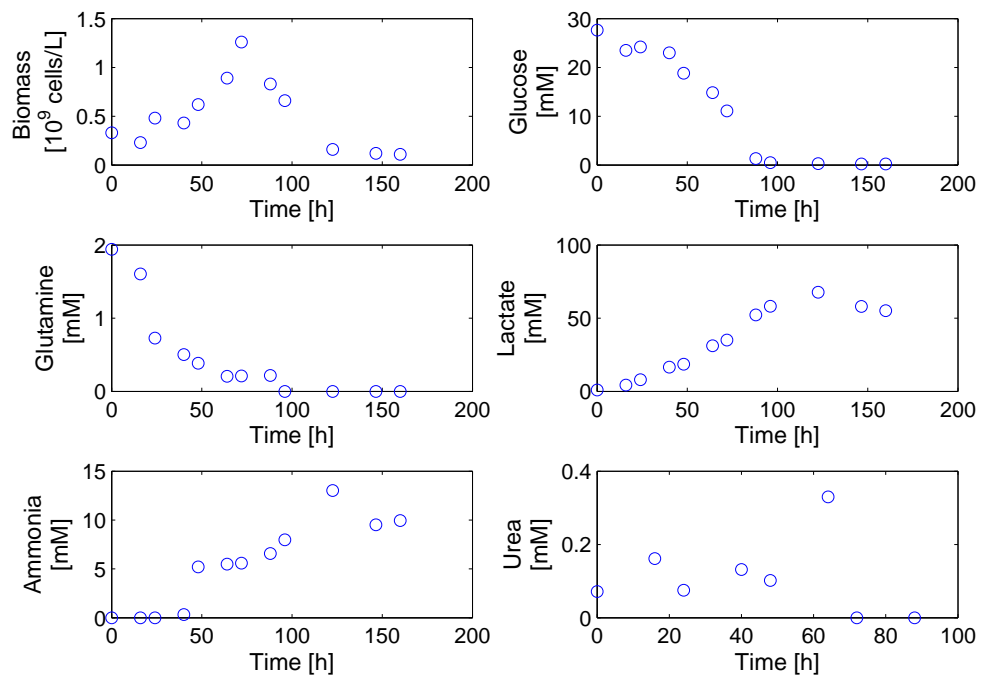
Figure 7.10: Batch bioreactor culture. Glucose: 33mM; Gln: 2mM.

Chapter 8

Conclusions

In this study, the MFA of a detailed metabolic network of $CHO - 320$ has been studied, using the classical quasi-steady state assumption and under the constraint of the measurements of the time evolution of a number of culture components. With commonly available measurements in today's laboratory practice, the mass balance system remains underdetermined due to an insufficient number of measurements. The analysis of the solution space of this underdetermined system allows to define admissible flux ranges for each metabolic reaction in the network, giving both a qualitative and quantitative idea of the metabolic state of the cells.

It is of capital importance to check that the mass balance system is well-posed, as it may occur that the estimated range for the fluxes along certain elementary routes in the network are not bounded due to the absence of measurements at their extreme points.

If the system is well-posed, the size of the flux intervals can be significantly reduced either by adding a few more extracellular measurements or by considering simple assumptions, such as the assumption of no Threonine catabolism. In all cases, where the problem is well posed, the computed flux intervals are bounded and a significant number of metabolic fluxes are uniquely determined. Nevertheless, the size of certain flux intervals cannot be reduced due to the existence of parallel pathways with fluxes in counterbalance.

A unique flux distribution maximizing the biomass production rate has been calculated for the initial set of measurements which appears to be equivalent to the solution space obtained when considering that threonine is only used for protein synthesis. The optimal fluxes are exactly identical to the uniquely determined fluxes obtained under the assumption of no catabolism of threonine. This is a nice example of two equivalent approaches for reducing the range of flux distributions: either to add theoretical linear constraints or to select an optimization criterion.

In short, we have seen that it is not absolutely necessary to have an

exactly determined system to be able to perform a flux analysis. Even though, several fluxes remain unknown and uncertain we still get a very good insight on the general metabolic state of the cell. This flux analysis, has also improved our understanding on the experimental measurements. It is possible to distinguish between very and poorly informative measurements, notably which set of experimental data would allow a well-posed system and which would not.

Regarding the model reduction procedure, the model reproduces the experimental data of biomass and main substrates and products without any special adjustment.

Each local model derived from their corresponding metabolic network fits the experimental data of that particular life phase of the cellular culture. This demonstrates the potential of the model reduction method presented in Chapter 5.

A global model can be obtained by a minor adjustment in the consumption rate of glucose. If glucose is considered to be consumed a little slower, the reaction rates of the macro reactions depending on glucose concentration become zero once the passage from the exponential growth phase model to the transition phase model is completed. The consideration of a smaller slope of glucose consumption allows the obtaining of a global model capable of reproducing the experimental data for the entire cell culture.

Perspectives

Many ways of action can be considered henceforth. The work presented in this thesis sets the path for further studies at an experimental level, regarding the analysis of metabolic fluxes and dynamic modelling, as well as for optimization and control purposes.

Concerning the cellular culture laboratory, there is still much work to do and many experiments to be done. The set of experimental measurements to be achieved in a short term includes the determination of CO_2 and O_2 in the exhausted gas stream which will provide important information about the internal balance of this gases to be used in MFA. It is also important to achieve the measurement of the 20 standard amino acids. Up to now, we have been able to measure only 15 amino acids due to overlapping problems, inexistent standard for instable amino acids such as glutamine and the incapability of the analytical method to differentiate cysteine from cystine. The measurements of this 5 missing amino acids might be achieved in the future either by improving the UPLC analytical method or via NIR analysis. This last method needs to be entirely developed and it is probably the subject of a whole PhD thesis. None the less, NIR is a powerful analysis and its set up would improve greatly the extracellular species capable to be measured.

In regard with the bioreactor cultures, there is a number of culture

modalities and environmental conditions to be tested. Notably, the passage from plain batch cultures to fed-batch or even perfused mode cultures is a step that should be taken soon enough. Along with fed-batch and perfused cultures, the measurements of the main substrates and products such as glucose, lactate and ammonia, should be performed on line.

Once a richer set of experimental data would be available, the metabolic network, the metabolic flux analysis and the methodology presented in this study should be validated. Furthermore, a more informative set of experimental data could also serve to the development of a dynamical model in a similar way (or not) as the one presented in this thesis. Depending on the use the dynamical model would be given, a more complex or simple model could be established. Possible ways of exploitation of a dynamical model for cell cultures could be the optimization of the production of a metabolite of interest or the development of state observer or controllers.

Bibliography

[1] Y-J. Schneider A. Provost, G. Bastin. From metabolic networks to minimal dynamic bioreaction models. In 10th International IFAC Symposium on Computer Applications in Biotechnology. IFAC, June 2007.

[2] C. Altamirano, A. Illanes, S. Becerra, J.J. Cairó, and F. Gòdia. Considerations on the lactate consumption by CHO cells in the presence of galactose. Journal of Biotechnology, 125:547–556, 2006.

[3] Maciek R. Antoniewicz, Joanne K. Kelleher, and Gregory Stephanopoulos. Determination of confidence intervals of metabolic fluxes estimated from stable isotope measurements. Metabolic Engineering, 8:324–337, 2006.

[4] Nilou Arden and Michael J. Betenbaugh. Life and death in mammalian cell culture: strategies for apoptosis inhibition. Trends in Biotechnology, 22:174–180, 2004.

[5] G. Bastin and D. Dochain. On-line Estimation and Adaptive Control of Bioreactors. 1990.

[6] Olivier Bernard and Georges Bastin. On the estimation of the pseudo-stoichiometric matrix for macroscopic mass balance modelling of biotechnological processes. Mathematical Biosciences, 193:51–77, 2005.

[7] Brett A. Boghigian, Gargi Seth, Robert Kiss, and Blaine A. Pfeifer. Metabolic flux analysis and pharmaceutical production. Metabolic Engineering, doi:10.1016/j.ymben.2009.10.004, 2009.

[8] H. P. J. Bonarius, V. Hatzimanikatis, K.P.H. Meesters, C.D.de Goojier, G. Schimd, and J. Tramper. Metabolic flux analysis of hybridoma cells in different culture media using mass balances. Biotechnology and Bioengineering, 50:299–318, 1996.

[9] Hendrik P. J. Bonarius, José H.M. Houtman, Cornelis D. de Gooijer, JohannesTramper, and Georg Schmid. Activity of glutamate dehydro-

genase is increased in ammonia-stressed hybridoma cells. Biotechnology and Bioengineering, 57:447–453, 1998.

[10] Hendrik P. J. Bonarius, José H.M. Houtman, Georg Schmid, Cornelis D. de Gooijer, and Johannes Tramper. Metabolic flux analysis of hybridoma cells under oxidative and reductive stress using mas balances. Cytotechnology, 32:97–107, 2000.

[11] Hendrik P. J. Bonarius, Georg Schmid, and Johannes Tramper. Flux analysis of underdetermined metabolic networks: the quest for the missing constraints. TIBTECH, 15:308–314, August 1997.

[12] L. Chen and G. Bastin. Structural identifiability of the yield coefficients in bioprocess models when the reaction rates are unknown. Mathematical Biosciences, 132:35–67, 1996.

[13] J.C. Drugmand, V. Meriaux, N. Mazouz, and A. Engrand. Technologie des cellules animales. Technical report, Cefochim and Culture in Vivo, 2011.

[14] A. K. Gombert and J. Nielsen. Mathematical modelling of metabolism. Biochemical engineering, 11:180–186, 2000.

[15] Jens E. Haag, Alain Vande Wouwer, and Philippe Bogaerts. Dynamic modeling of complex biological systems: a link between metabolic and macroscopic description. Mathematical Biosciences, 193:25–49, 2005.

[16] O. Henry, M. Perrier, and A. Kamen. Metabolic flux analysis of HEK-293 cells in perfusion cultures for the production of adenoviral vectors. Metabolic Engineering, 7:467–476, 2005.

[17] Wei-Shou Hu. Cell biology for process engineering. Technical report, Cellular Bioprocess Technology. University of Minnesota, 2004.

[18] X. Hulhoven, A. Vande Wouwer, and Ph. Bogaerts. On a systematic procedure for the predetermination of macroscopic reaction schemes. Bioprocess Biosystem Engineering, 27(5):283–291, 2005.

[19] K.P. Jayapal, K.F. Wlaschin, W-S. Hu, and Yap M.G.S. Recombinant protein therapeutics from cho cells - 20 years and counting. CHO Consortium SBE Special Section, pages 40–47, 2010.

[20] Raphael M. Jungers, Francisca Zamorano, Vincent D. Blondel, Alain Vande Wouwer, and Georges Bastin. Fast computation of minimal elementary decompositions of metabolic flux vectors. Automatica, 47:1255–1259, 2011.

[21] R.M. Jungers, F. Zamorano, V.D. Blondel, A. Vande Wouwer, and G. Bastin. A fast algorithm for computing a minimal decomposition of a metabolic flux vector in terms of elementary flux vectors. MATHMOD, 2009.

[22] Fa-Ten Kao and Theodore T. Puck. Genetics of somatic mammalian cells, IV. properties of chinese hamster cell mutants with respect to the requirement for proline. Genetics, 55:513–524, 1967.

[23] Fa-Ten Kao and Theodore T. Puck. Genetics of somatic mammalian cells, VII. induction and isolation of nutritional mutants in chinese hamster cells. Proceedings of the National Academy of Sciences of the United States of America, 60:1275–1281, 1968.

[24] KEGG. Kyoto encyclopedia of genes and genomes. online, 2008.

[25] S. Klamt, J. Saez-Rodriguez, and ED. Gilles. Structural and functional analysis of cellular networks with *CellNetAnalyzer*. BMC Systems Biology, 1:2, 2007.

[26] S. Klamt and S. Schuster. Calculating as many fluxes as possible in underdetermined metabolic networks. Molecular Biology Reports, 29:243–248, 2002.

[27] S. Klamt, S. Schuster, and E. D. Gilles. Calculability analysis in underdetermined metabolic networks illustrated by a model of the central metabolism in purple nonsulfur bacteria. Biotechnology and Bioengineering, 77(7):734–751, 2002.

[28] F. Llaneras and J. Picó. An interval approach for dealing with flux distributions and elementarymodesactivity patterns. Journal of Theoretical Biology, 246:290–308, 2007.

[29] George Lovrecz and Peter Gray. Use of on-line gas analysis to monitor recombinant mammalian cell cultures. pages 167–175, 1994.

[30] Christophe Mocquet, Olivier Bernard, and Antoine Sciandra. Cell cycle modelling of microalgae grown under a light-dark signal. CAB 2010, 2010.

[31] Roderick Murray-Smith and Tor Arne Johansen. Multiple model approaches to modelling and control. 1997.

[32] I. Nadeau, J. Sabatié, M. Koehl, M. Perrier, and A. Kamen. Human 293 cell metabolism in low glutamine-supplied culture: Interpretation of metabolic changes through metabolic flux analysis. Metabolic Engineering, 2:277–292, 2000.

[33] D.L. Nelson and M.M. Cox. Lehninger, Principles of Biochemistry. Fourth edition edition, 2005.

[34] Gregg B. Nyberg, Robert Balcarcel, Brian D. Follstad, Gregory Stephanopoulos, and Daniel I. C. Wang. Metabolism of peptide amino acids by chinese hamster ovary cells grown in a complex medium. Biotechnology and Bioengineering, 62:321–335, 1999.

[35] T. Pfeiffer, I. Sánchez-Valdenebro, J.C. Nuño, F. Montero, and S. Schuster. METATOOL: for studying metabolic networks. Bioinformatics, 15(3):251–257, Mar 1999.

[36] A. Provost. Metabolic Design of Dynamic Bioreaction Models. PhD thesis, Université Catholique de Louvain, 2006.

[37] A. Provost and G. Bastin. Dynamical metabolic modelling of biological processes. Fourth International Symposium on Mathematical Modelling, February 2003.

[38] A. Provost and G. Bastin. Dynamic metabolic modelling under the balanced growth condition. Journal of Process Control, 14:717–728, 2004.

[39] A. Provost, G Bastin, and YJ. Schneider. From metabolic networks to minimal dynamic bioreaction models. 10th International IFAC Symposium on Computer Applications in Biotechnology, June 2007.

[40] Joanne M. Savinell and Bernhard O. Palsson. Optimal selection of metabolic fluxes for in vivo measurement. I. development of mathematical methods. Journal of Theoretical Biology, 155:201–214, 1992.

[41] Joanne M. Savinell and Bernhard O. Palsson. Optimal selection of metabolic fluxes for in vivo measurement. II. application to escherichia coli and hybridoma cell metabolism. Journal of Theoretical Biology, 155:215–242, 1992.

[42] Markus Schneider, Ian W. Marison, and Urs von Stockar. The importance of ammonia in mammalian cell culture. Journal of Biotechnology, 46:161–185, 1996.

[43] Yves-Jacques Schneider. Optimisation of hybridoma cell growth and monoclonal antibody secretion in a chemically defined, serum- and protein-free culture medium. Journal of Immunological Methods, 116:65–77, 1989.

[44] S. Schuster, T. Dandekar, and D. A. Fell. Detection of elementary flux modes in biochemical networks: a promising tool for pathway analysis and metabolic engineering. TIBTECH, 17:53–60, 1999.

[45] Noboru Seoka. Directional mutation preassure and neutral molecular evolution. Proc.Natl. Acad. Sci. USA, 85:2653–2657, 1988.

[46] Y. Sidorenko, A. Wahl, M. Dauner, Y. Genzel, and U. Reichl. Comparison of metabolic flux distributions for MDCK cell growth in glutamine- and pyruvate-containing media. Biotechnol. Prog., 24:311–320, 2008.

[47] Ilse Smets. Analysis and synthesis of mathematical algorithms for optimization and control of complex biochemical conversion processes. PhD thesis, Department of Chemical Engineering, 2002.

[48] G. N. Stephanopoulos, A. A. Aristidou, and J. Nielsen. Metabolic Engineering: Principles and Methodologies. 1998.

[49] Noboru Sueoka. Correlation between base composition of deoxyribonucleic acid and amino acid composition of protein. Proc.Natl. Acad. Sci. USA, 47:1141–1149, 1961.

[50] Noboru Sueoka. On genetic basis of variation and heterogeneity of DNA base composition. Proc.Natl. Acad. Sci. USA, 48:582–592, 1962.

[51] R.T.J.M. van der Heijden, J.J. Heijnen, C. Hellinga, B. Romein, and K.Ch.A.M. Luyben. Linear constraint relations in biochemical reaction systems: I. classification of the calculability and the balanceability of conversion rates. Biotechnology and Bioengineering, 43:3–10, 1994.

[52] Aljoscha Wahl, Yury Sidorenko, Michael Dauner, Yvonne Genzel, and Udo Reichl. Metabolic flux model for an anchorage-dependent MDCK cell line. Biotechnology and Bioengineering, 101:135–152, 2008.

[53] Liangzhi Xie and Daniel I.C. Wang. Applications of improved stoichiometric model in medium design and fed-batch cultivation of animal cells in bioreactor. Cytotechnology, 15:17–29, 1994.

[54] Liangzhi Xie and Daniel I.C. Wang. Material balance studies on animall cell metabolism using stoichiometrically based reaction network. Biotechnology and Bioengineering, 52:579–590, 1996a.

[55] Liangzhi Xie and Daniel I.C. Wang. Energy metabolism and ATP balance in animall cell cultivation using a stoichiometrically based reaction network. Biotechnology and Bioengineering, 52:591–601, 1996b.

[56] Francisca Zamorano, Alain Vande Wouwer, and Georges Bastin. A detailed metabolic flux analysis of an underdetermined network of cho cells. Journal of Biotechnology, 150:497–508, 2010.

[57] Craig Zupke and Gregory Stephanopoulos. Intracellular flux analysis in hybridomas using mass balances and in vitro ^{13}C NMR. Biotechnology and Bioengineering, 45:292–303, 1995.

Appendix A

Stoichiometric Matrices

A.1 Stoichiometric Matrix N for the internal metabolites

A.2 Stoichiometric Matrix N_m for the extracellular measurements

	v1	v2	v3	v4	v5	v6	v7	v8	v9	v10	v11	v12	v13	v14	v15	v16	v17	v18	v19	v20
G6P	1.00	-1.00	0.00	0.00	0.00	0.00	0.00	0.00	0.00	0.00	0.00	0.00	0.00	0.00	0.00	0.00	-1.00	0.00	0.00	0.00
F6P	0.00	1.00	-1.00	0.00	0.00	0.00	0.00	0.00	0.00	0.00	0.00	0.00	0.00	0.00	0.00	0.00	0.00	0.00	0.00	1.00
DHAP	0.00	0.00	1.00	-1.00	0.00	0.00	0.00	0.00	0.00	0.00	0.00	0.00	0.00	0.00	0.00	0.00	0.00	0.00	0.00	0.00
GA3P	0.00	0.00	1.00	1.00	-1.00	0.00	0.00	0.00	0.00	0.00	0.00	0.00	0.00	0.00	0.00	0.00	0.00	0.00	0.00	0.00
3PG	0.00	0.00	0.00	0.00	1.00	-1.00	0.00	0.00	0.00	0.00	0.00	0.00	0.00	0.00	0.00	0.00	0.00	0.00	0.00	0.00
PYR	0.00	0.00	0.00	0.00	0.00	1.00	-1.00	0.00	0.00	0.00	0.00	0.00	0.00	0.00	-1.00	-1.00	0.00	0.00	0.00	0.00
AcCoA	0.00	0.00	0.00	0.00	0.00	0.00	1.00	-1.00	0.00	0.00	0.00	0.00	0.00	0.00	0.00	0.00	0.00	0.00	0.00	0.00
Cit	0.00	0.00	0.00	0.00	0.00	0.00	0.00	1.00	-1.00	0.00	0.00	0.00	0.00	0.00	0.00	0.00	0.00	0.00	0.00	0.00
α KG	0.00	0.00	0.00	0.00	0.00	0.00	0.00	0.00	1.00	-1.00	0.00	0.00	0.00	0.00	0.00	1.00	0.00	0.00	0.00	0.00
SucCoA	0.00	0.00	0.00	0.00	0.00	0.00	0.00	0.00	0.00	1.00	-1.00	0.00	0.00	0.00	0.00	0.00	0.00	0.00	0.00	0.00
Succ	0.00	0.00	0.00	0.00	0.00	0.00	0.00	0.00	0.00	0.00	1.00	-1.00	0.00	0.00	0.00	0.00	0.00	0.00	0.00	0.00
Fum	0.00	0.00	0.00	0.00	0.00	0.00	0.00	0.00	0.00	0.00	0.00	1.00	-1.00	0.00	0.00	0.00	0.00	0.00	0.00	0.00
Mal	0.00	0.00	0.00	0.00	0.00	0.00	0.00	0.00	0.00	0.00	0.00	0.00	1.00	-1.00	0.00	0.00	0.00	0.00	0.00	0.00
Oxa	0.00	0.00	0.00	0.00	0.00	0.00	0.00	-1.00	0.00	0.00	0.00	0.00	0.00	1.00	0.00	0.00	0.00	0.00	0.00	0.00
Rl5P	0.00	0.00	0.00	0.00	0.00	0.00	0.00	0.00	0.00	0.00	0.00	0.00	0.00	0.00	0.00	0.00	1.00	-1.00	-1.00	0.00
R5P	0.00	0.00	0.00	0.00	0.00	0.00	0.00	0.00	0.00	0.00	0.00	0.00	0.00	0.00	0.00	0.00	0.00	1.00	0.00	-1.00
X5P	0.00	0.00	0.00	0.00	0.00	0.00	0.00	0.00	0.00	0.00	0.00	0.00	0.00	0.00	0.00	0.00	0.00	0.00	1.00	-1.00
E4P	0.00	0.00	0.00	0.00	0.00	0.00	0.00	0.00	0.00	0.00	0.00	0.00	0.00	0.00	0.00	0.00	0.00	0.00	0.00	1.00
Glu	0.00	0.00	0.00	0.00	0.00	0.00	0.00	0.00	0.00	0.00	0.00	0.00	0.00	0.00	0.00	-1.00	0.00	0.00	0.00	0.00
Asp	0.00	0.00	0.00	0.00	0.00	0.00	0.00	0.00	0.00	0.00	0.00	0.00	0.00	0.00	0.00	0.00	0.00	0.00	0.00	0.00
Gly	0.00	0.00	0.00	0.00	0.00	0.00	0.00	0.00	0.00	0.00	0.00	0.00	0.00	0.00	0.00	0.00	0.00	0.00	0.00	0.00
Ser	0.00	0.00	0.00	0.00	0.00	0.00	0.00	0.00	0.00	0.00	0.00	0.00	0.00	0.00	0.00	0.00	0.00	0.00	0.00	0.00
Tyr	0.00	0.00	0.00	0.00	0.00	0.00	0.00	0.00	0.00	0.00	0.00	0.00	0.00	0.00	0.00	0.00	0.00	0.00	0.00	0.00
Cys	0.00	0.00	0.00	0.00	0.00	0.00	0.00	0.00	0.00	0.00	0.00	0.00	0.00	0.00	0.00	0.00	0.00	0.00	0.00	0.00
Ala	0.00	0.00	0.00	0.00	0.00	0.00	0.00	0.00	0.00	0.00	0.00	0.00	0.00	0.00	0.00	1.00	0.00	0.00	0.00	0.00
Arg	0.00	0.00	0.00	0.00	0.00	0.00	0.00	0.00	0.00	0.00	0.00	0.00	0.00	0.00	0.00	0.00	0.00	0.00	0.00	0.00
Asn	0.00	0.00	0.00	0.00	0.00	0.00	0.00	0.00	0.00	0.00	0.00	0.00	0.00	0.00	0.00	0.00	0.00	0.00	0.00	0.00
Gln	0.00	0.00	0.00	0.00	0.00	0.00	0.00	0.00	0.00	0.00	0.00	0.00	0.00	0.00	0.00	0.00	0.00	0.00	0.00	0.00
His	0.00	0.00	0.00	0.00	0.00	0.00	0.00	0.00	0.00	0.00	0.00	0.00	0.00	0.00	0.00	0.00	0.00	0.00	0.00	0.00
Ile	0.00	0.00	0.00	0.00	0.00	0.00	0.00	0.00	0.00	0.00	0.00	0.00	0.00	0.00	0.00	0.00	0.00	0.00	0.00	0.00
Leu	0.00	0.00	0.00	0.00	0.00	0.00	0.00	0.00	0.00	0.00	0.00	0.00	0.00	0.00	0.00	0.00	0.00	0.00	0.00	0.00
Lys	0.00	0.00	0.00	0.00	0.00	0.00	0.00	0.00	0.00	0.00	0.00	0.00	0.00	0.00	0.00	0.00	0.00	0.00	0.00	0.00
Met	0.00	0.00	0.00	0.00	0.00	0.00	0.00	0.00	0.00	0.00	0.00	0.00	0.00	0.00	0.00	0.00	0.00	0.00	0.00	0.00
Phe	0.00	0.00	0.00	0.00	0.00	0.00	0.00	0.00	0.00	0.00	0.00	0.00	0.00	0.00	0.00	0.00	0.00	0.00	0.00	0.00
Pro	0.00	0.00	0.00	0.00	0.00	0.00	0.00	0.00	0.00	0.00	0.00	0.00	0.00	0.00	0.00	0.00	0.00	0.00	0.00	0.00
Thr	0.00	0.00	0.00	0.00	0.00	0.00	0.00	0.00	0.00	0.00	0.00	0.00	0.00	0.00	0.00	0.00	0.00	0.00	0.00	0.00
Trp	0.00	0.00	0.00	0.00	0.00	0.00	0.00	0.00	0.00	0.00	0.00	0.00	0.00	0.00	0.00	0.00	0.00	0.00	0.00	0.00
Val	0.00	0.00	0.00	0.00	0.00	0.00	0.00	0.00	0.00	0.00	0.00	0.00	0.00	0.00	0.00	0.00	0.00	0.00	0.00	0.00
α KBut	0.00	0.00	0.00	0.00	0.00	0.00	0.00	0.00	0.00	0.00	0.00	0.00	0.00	0.00	0.00	0.00	0.00	0.00	0.00	0.00
PropCoA	0.00	0.00	0.00	0.00	0.00	0.00	0.00	0.00	0.00	0.00	0.00	0.00	0.00	0.00	0.00	0.00	0.00	0.00	0.00	0.00

Table A.1: Stoichiometric Matrix **N** for the internal metabolites.

	v1	v2	v3	v4	v5	v6	v7	v8	v9	v10	v11	v12	v13	v14	v15	v16	v17	v18	v19	v20
α KAd	0.00	0.00	0.00	0.00	0.00	0.00	0.00	0.00	0.00	0.00	0.00	0.00	0.00	0.00	0.00	0.00	0.00	0.00	0.00	0.00
AcetoacCoA	0.00	0.00	0.00	0.00	0.00	0.00	0.00	0.00	0.00	0.00	0.00	0.00	0.00	0.00	0.00	0.00	0.00	0.00	0.00	0.00
Acetoac	0.00	0.00	0.00	0.00	0.00	0.00	0.00	0.00	0.00	0.00	0.00	0.00	0.00	0.00	0.00	0.00	0.00	0.00	0.00	0.00
Glu γ sa	0.00	0.00	0.00	0.00	0.00	0.00	0.00	0.00	0.00	0.00	0.00	0.00	0.00	0.00	0.00	0.00	0.00	0.00	0.00	0.00
Orn	0.00	0.00	0.00	0.00	0.00	0.00	0.00	0.00	0.00	0.00	0.00	0.00	0.00	0.00	0.00	0.00	0.00	0.00	0.00	0.00
Cln	0.00	0.00	0.00	0.00	0.00	0.00	0.00	0.00	0.00	0.00	0.00	0.00	0.00	0.00	0.00	0.00	0.00	0.00	0.00	0.00
Argsucc	0.00	0.00	0.00	0.00	0.00	0.00	0.00	0.00	0.00	0.00	0.00	0.00	0.00	0.00	0.00	0.00	0.00	0.00	0.00	0.00
PRPP	0.00	0.00	0.00	0.00	0.00	0.00	0.00	0.00	0.00	0.00	0.00	0.00	0.00	0.00	0.00	0.00	0.00	0.00	0.00	0.00
IMP	0.00	0.00	0.00	0.00	0.00	0.00	0.00	0.00	0.00	0.00	0.00	0.00	0.00	0.00	0.00	0.00	0.00	0.00	0.00	0.00
Orot	0.00	0.00	0.00	0.00	0.00	0.00	0.00	0.00	0.00	0.00	0.00	0.00	0.00	0.00	0.00	0.00	0.00	0.00	0.00	0.00
UTPrn	0.00	0.00	0.00	0.00	0.00	0.00	0.00	0.00	0.00	0.00	0.00	0.00	0.00	0.00	0.00	0.00	0.00	0.00	0.00	0.00
ATPrn	0.00	0.00	0.00	0.00	0.00	0.00	0.00	0.00	0.00	0.00	0.00	0.00	0.00	0.00	0.00	0.00	0.00	0.00	0.00	0.00
GTPrn	0.00	0.00	0.00	0.00	0.00	0.00	0.00	0.00	0.00	0.00	0.00	0.00	0.00	0.00	0.00	0.00	0.00	0.00	0.00	0.00
CTPrn	0.00	0.00	0.00	0.00	0.00	0.00	0.00	0.00	0.00	0.00	0.00	0.00	0.00	0.00	0.00	0.00	0.00	0.00	0.00	0.00
dATP	0.00	0.00	0.00	0.00	0.00	0.00	0.00	0.00	0.00	0.00	0.00	0.00	0.00	0.00	0.00	0.00	0.00	0.00	0.00	0.00
dGTP	0.00	0.00	0.00	0.00	0.00	0.00	0.00	0.00	0.00	0.00	0.00	0.00	0.00	0.00	0.00	0.00	0.00	0.00	0.00	0.00
dTTP	0.00	0.00	0.00	0.00	0.00	0.00	0.00	0.00	0.00	0.00	0.00	0.00	0.00	0.00	0.00	0.00	0.00	0.00	0.00	0.00
dCTP	0.00	0.00	0.00	0.00	0.00	0.00	0.00	0.00	0.00	0.00	0.00	0.00	0.00	0.00	0.00	0.00	0.00	0.00	0.00	0.00
Ethn	0.00	0.00	0.00	0.00	0.00	0.00	0.00	0.00	0.00	0.00	0.00	0.00	0.00	0.00	0.00	0.00	0.00	0.00	0.00	0.00
Cho	0.00	0.00	0.00	0.00	0.00	0.00	0.00	0.00	0.00	0.00	0.00	0.00	0.00	0.00	0.00	0.00	0.00	0.00	0.00	0.00
Glyc3P	0.00	0.00	0.00	0.00	0.00	0.00	0.00	0.00	0.00	0.00	0.00	0.00	0.00	0.00	0.00	0.00	0.00	0.00	0.00	0.00
PhosphE	0.00	0.00	0.00	0.00	0.00	0.00	0.00	0.00	0.00	0.00	0.00	0.00	0.00	0.00	0.00	0.00	0.00	0.00	0.00	0.00
PhosphC	0.00	0.00	0.00	0.00	0.00	0.00	0.00	0.00	0.00	0.00	0.00	0.00	0.00	0.00	0.00	0.00	0.00	0.00	0.00	0.00
PhosphS	0.00	0.00	0.00	0.00	0.00	0.00	0.00	0.00	0.00	0.00	0.00	0.00	0.00	0.00	0.00	0.00	0.00	0.00	0.00	0.00
Sphm	0.00	0.00	0.00	0.00	0.00	0.00	0.00	0.00	0.00	0.00	0.00	0.00	0.00	0.00	0.00	0.00	0.00	0.00	0.00	0.00
Cholesterol	0.00	0.00	0.00	0.00	0.00	0.00	0.00	0.00	0.00	0.00	0.00	0.00	0.00	0.00	0.00	0.00	0.00	0.00	0.00	0.00
Proteins	0.00	0.00	0.00	0.00	0.00	0.00	0.00	0.00	0.00	0.00	0.00	0.00	0.00	0.00	0.00	0.00	0.00	0.00	0.00	0.00
ADN	0.00	0.00	0.00	0.00	0.00	0.00	0.00	0.00	0.00	0.00	0.00	0.00	0.00	0.00	0.00	0.00	0.00	0.00	0.00	0.00
ARN	0.00	0.00	0.00	0.00	0.00	0.00	0.00	0.00	0.00	0.00	0.00	0.00	0.00	0.00	0.00	0.00	0.00	0.00	0.00	0.00
Lipids	0.00	0.00	0.00	0.00	0.00	0.00	0.00	0.00	0.00	0.00	0.00	0.00	0.00	0.00	0.00	0.00	0.00	0.00	0.00	0.00
NH_4^+	0.00	0.00	0.00	0.00	0.00	0.00	0.00	0.00	0.00	0.00	0.00	0.00	0.00	0.00	0.00	0.00	0.00	0.00	0.00	0.00
CO_2	0.00	0.00	0.00	0.00	0.00	0.00	1.00	0.00	1.00	1.00	0.00	0.00	0.00	0.00	0.00	0.00	1.00	0.00	0.00	0.00

	v21	v22	v23	v24	v25	v26	v27	v28	v29	v30	v31	v32	v33	v34	v35	v36	v37	v38	v39	v40
G6P	0.00	0.00	0.00	0.00	0.00	0.00	0.00	0.00	0.00	0.00	0.00	0.00	0.00	0.00	0.00	0.00	0.00	0.00	0.00	0.00
F6P	1.00	0.00	0.00	0.00	0.00	0.00	0.00	0.00	0.00	0.00	0.00	0.00	0.00	0.00	0.00	0.00	0.00	0.00	0.00	0.00
DHAP	0.00	0.00	0.00	0.00	0.00	0.00	0.00	0.00	0.00	0.00	0.00	0.00	0.00	0.00	0.00	0.00	0.00	0.00	0.00	0.00
GA3P	1.00	0.00	0.00	0.00	0.00	0.00	0.00	0.00	0.00	0.00	0.00	0.00	0.00	0.00	0.00	0.00	0.00	0.00	0.00	0.00
3PG	0.00	0.00	0.00	0.00	0.00	0.00	0.00	-1.00	0.00	0.00	0.00	0.00	0.00	0.00	0.00	0.00	0.00	0.00	0.00	0.00
PYR	0.00	1.00	0.00	0.00	0.00	0.00	0.00	0.00	0.00	1.00	0.00	0.00	0.00	0.00	0.00	0.00	0.00	0.00	0.00	0.00
AcCoA	0.00	0.00	0.00	0.00	0.00	1.00	0.00	0.00	0.00	0.00	0.00	0.00	0.00	0.00	0.00	0.00	2.00	0.00	1.00	1.00
Cit	0.00	0.00	0.00	0.00	0.00	0.00	0.00	0.00	0.00	0.00	0.00	0.00	0.00	0.00	0.00	0.00	0.00	0.00	0.00	0.00
α KG	0.00	0.00	1.00	1.00	0.00	0.00	0.00	1.00	0.00	0.00	0.00	0.00	0.00	0.00	-2.00	0.00	0.00	-1.00	-1.00	-1.00
SucCoA	0.00	0.00	0.00	0.00	0.00	0.00	0.00	0.00	0.00	0.00	0.00	0.00	1.00	0.00	0.00	0.00	0.00	0.00	0.00	0.00
Succ	0.00	0.00	0.00	0.00	0.00	0.00	0.00	0.00	0.00	0.00	0.00	0.00	0.00	0.00	0.00	0.00	0.00	0.00	0.00	0.00
Fum	0.00	0.00	0.00	0.00	0.00	0.00	0.00	0.00	0.00	0.00	0.00	0.00	0.00	0.00	0.00	0.00	0.00	0.00	0.00	0.00
Mal	0.00	-1.00	0.00	0.00	0.00	0.00	0.00	0.00	0.00	0.00	0.00	0.00	0.00	0.00	0.00	0.00	0.00	0.00	0.00	0.00
Oxa	0.00	0.00	0.00	-1.00	0.00	0.00	0.00	0.00	0.00	0.00	0.00	0.00	0.00	0.00	0.00	0.00	0.00	0.00	0.00	0.00
Rl5P	0.00	0.00	0.00	0.00	0.00	0.00	0.00	0.00	0.00	0.00	0.00	0.00	0.00	0.00	0.00	0.00	0.00	0.00	0.00	0.00
R5P	0.00	0.00	0.00	0.00	0.00	0.00	0.00	0.00	0.00	0.00	0.00	0.00	0.00	0.00	0.00	0.00	0.00	0.00	0.00	0.00
X5P	-1.00	0.00	0.00	0.00	0.00	0.00	0.00	0.00	0.00	0.00	0.00	0.00	0.00	0.00	0.00	0.00	0.00	0.00	0.00	0.00
E4P	-1.00	0.00	0.00	0.00	0.00	0.00	0.00	0.00	0.00	0.00	0.00	0.00	0.00	0.00	0.00	0.00	0.00	0.00	0.00	0.00
Glu	0.00	0.00	-1.00	-1.00	1.00	0.00	0.00	-1.00	0.00	0.00	0.00	0.00	0.00	0.00	2.00	0.00	0.00	1.00	1.00	1.00
Asp	0.00	0.00	0.00	1.00	0.00	0.00	0.00	0.00	0.00	0.00	0.00	0.00	0.00	0.00	0.00	0.00	0.00	0.00	0.00	0.00
Gly	0.00	0.00	0.00	0.00	0.00	1.00	1.00	0.00	-1.00	0.00	0.00	0.00	0.00	0.00	0.00	0.00	0.00	0.00	0.00	0.00
Ser	0.00	0.00	0.00	0.00	0.00	0.00	-1.00	1.00	0.00	-1.00	0.00	0.00	0.00	0.00	0.00	0.00	0.00	0.00	0.00	0.00
Tyr	0.00	0.00	0.00	0.00	0.00	0.00	0.00	0.00	0.00	0.00	0.00	0.00	0.00	0.00	0.00	0.00	0.00	0.00	0.00	0.00
Cys	0.00	0.00	0.00	0.00	0.00	0.00	0.00	0.00	0.00	0.00	0.00	0.00	0.00	0.00	0.00	0.00	0.00	0.00	0.00	0.00
Ala	0.00	0.00	0.00	0.00	0.00	0.00	0.00	0.00	0.00	0.00	0.00	0.00	0.00	1.00	0.00	0.00	0.00	0.00	0.00	0.00
Arg	0.00	0.00	0.00	0.00	0.00	0.00	0.00	0.00	0.00	0.00	0.00	0.00	0.00	0.00	0.00	0.00	0.00	0.00	0.00	0.00
Asn	0.00	0.00	0.00	0.00	0.00	0.00	0.00	0.00	0.00	0.00	0.00	0.00	0.00	0.00	0.00	0.00	0.00	0.00	0.00	0.00
Gln	0.00	0.00	0.00	0.00	-1.00	0.00	0.00	0.00	0.00	0.00	0.00	0.00	0.00	0.00	0.00	0.00	0.00	0.00	0.00	0.00
His	0.00	0.00	0.00	0.00	0.00	0.00	0.00	0.00	0.00	0.00	0.00	0.00	0.00	0.00	0.00	0.00	0.00	0.00	0.00	0.00
Ile	0.00	0.00	0.00	0.00	0.00	0.00	0.00	0.00	0.00	0.00	0.00	0.00	0.00	0.00	0.00	0.00	0.00	0.00	-1.00	0.00
Leu	0.00	0.00	0.00	0.00	0.00	0.00	0.00	0.00	0.00	0.00	0.00	0.00	0.00	0.00	0.00	0.00	0.00	0.00	0.00	-1.00
Lys	0.00	0.00	0.00	0.00	0.00	0.00	0.00	0.00	0.00	0.00	0.00	0.00	0.00	0.00	-1.00	0.00	0.00	0.00	0.00	0.00
Met	0.00	0.00	0.00	0.00	0.00	0.00	0.00	0.00	0.00	0.00	0.00	0.00	0.00	0.00	0.00	0.00	0.00	0.00	0.00	0.00
Phe	0.00	0.00	0.00	0.00	0.00	0.00	0.00	0.00	0.00	0.00	0.00	0.00	0.00	0.00	0.00	0.00	0.00	0.00	0.00	0.00
Pro	0.00	0.00	0.00	0.00	0.00	0.00	0.00	0.00	0.00	0.00	0.00	0.00	0.00	0.00	0.00	0.00	0.00	0.00	0.00	0.00
Thr	0.00	0.00	0.00	0.00	0.00	-1.00	0.00	0.00	0.00	0.00	-1.00	0.00	0.00	0.00	0.00	0.00	0.00	0.00	0.00	0.00
Trp	0.00	0.00	0.00	0.00	0.00	0.00	0.00	0.00	0.00	0.00	0.00	0.00	0.00	-1.00	0.00	0.00	0.00	0.00	0.00	0.00
Val	0.00	0.00	0.00	0.00	0.00	0.00	0.00	0.00	0.00	0.00	0.00	0.00	0.00	0.00	0.00	0.00	0.00	-1.00	0.00	0.00
α KBut	0.00	0.00	0.00	0.00	0.00	0.00	0.00	0.00	0.00	0.00	1.00	-1.00	0.00	0.00	0.00	0.00	0.00	0.00	0.00	0.00
PropCoA	0.00	0.00	0.00	0.00	0.00	0.00	0.00	0.00	0.00	0.00	0.00	1.00	-1.00	0.00	0.00	0.00	0.00	1.00	1.00	0.00

	v21	v22	v23	v24	v25	v26	v27	v28	v29	v30	v31	v32	v33	v34	v35	v36	v37	v38	v39	v40
α KAd	0.00	0.00	0.00	0.00	0.00	0.00	0.00	0.00	0.00	0.00	0.00	0.00	0.00	1.00	1.00	-1.00	0.00	0.00	0.00	0.00
AcetoacCoA	0.00	0.00	0.00	0.00	0.00	0.00	0.00	0.00	0.00	0.00	0.00	0.00	0.00	0.00	0.00	1.00	-1.00	0.00	0.00	0.00
Acetoac	0.00	0.00	0.00	0.00	0.00	0.00	0.00	0.00	0.00	0.00	0.00	0.00	0.00	0.00	0.00	0.00	0.00	0.00	0.00	1.00
Glu γ sa	0.00	0.00	0.00	0.00	0.00	0.00	0.00	0.00	0.00	0.00	0.00	0.00	0.00	0.00	0.00	0.00	0.00	0.00	0.00	0.00
Orn	0.00	0.00	0.00	0.00	0.00	0.00	0.00	0.00	0.00	0.00	0.00	0.00	0.00	0.00	0.00	0.00	0.00	0.00	0.00	0.00
Cln	0.00	0.00	0.00	0.00	0.00	0.00	0.00	0.00	0.00	0.00	0.00	0.00	0.00	0.00	0.00	0.00	0.00	0.00	0.00	0.00
Argsucc	0.00	0.00	0.00	0.00	0.00	0.00	0.00	0.00	0.00	0.00	0.00	0.00	0.00	0.00	0.00	0.00	0.00	0.00	0.00	0.00
PRPP	0.00	0.00	0.00	0.00	0.00	0.00	0.00	0.00	0.00	0.00	0.00	0.00	0.00	0.00	0.00	0.00	0.00	0.00	0.00	0.00
IMP	0.00	0.00	0.00	0.00	0.00	0.00	0.00	0.00	0.00	0.00	0.00	0.00	0.00	0.00	0.00	0.00	0.00	0.00	0.00	0.00
Orot	0.00	0.00	0.00	0.00	0.00	0.00	0.00	0.00	0.00	0.00	0.00	0.00	0.00	0.00	0.00	0.00	0.00	0.00	0.00	0.00
UTPrn	0.00	0.00	0.00	0.00	0.00	0.00	0.00	0.00	0.00	0.00	0.00	0.00	0.00	0.00	0.00	0.00	0.00	0.00	0.00	0.00
ATPrn	0.00	0.00	0.00	0.00	0.00	0.00	0.00	0.00	0.00	0.00	0.00	0.00	0.00	0.00	0.00	0.00	0.00	0.00	0.00	0.00
GTPrn	0.00	0.00	0.00	0.00	0.00	0.00	0.00	0.00	0.00	0.00	0.00	0.00	0.00	0.00	0.00	0.00	0.00	0.00	0.00	0.00
CTPrn	0.00	0.00	0.00	0.00	0.00	0.00	0.00	0.00	0.00	0.00	0.00	0.00	0.00	0.00	0.00	0.00	0.00	0.00	0.00	0.00
dATP	0.00	0.00	0.00	0.00	0.00	0.00	0.00	0.00	0.00	0.00	0.00	0.00	0.00	0.00	0.00	0.00	0.00	0.00	0.00	0.00
dGTP	0.00	0.00	0.00	0.00	0.00	0.00	0.00	0.00	0.00	0.00	0.00	0.00	0.00	0.00	0.00	0.00	0.00	0.00	0.00	0.00
dTTP	0.00	0.00	0.00	0.00	0.00	0.00	0.00	0.00	0.00	0.00	0.00	0.00	0.00	0.00	0.00	0.00	0.00	0.00	0.00	0.00
dCTP	0.00	0.00	0.00	0.00	0.00	0.00	0.00	0.00	0.00	0.00	0.00	0.00	0.00	0.00	0.00	0.00	0.00	0.00	0.00	0.00
Ethn	0.00	0.00	0.00	0.00	0.00	0.00	0.00	0.00	0.00	0.00	0.00	0.00	0.00	0.00	0.00	0.00	0.00	0.00	0.00	0.00
Cho	0.00	0.00	0.00	0.00	0.00	0.00	0.00	0.00	0.00	0.00	0.00	0.00	0.00	0.00	0.00	0.00	0.00	0.00	0.00	0.00
Glyc3P	0.00	0.00	0.00	0.00	0.00	0.00	0.00	0.00	0.00	0.00	0.00	0.00	0.00	0.00	0.00	0.00	0.00	0.00	0.00	0.00
PhosphE	0.00	0.00	0.00	0.00	0.00	0.00	0.00	0.00	0.00	0.00	0.00	0.00	0.00	0.00	0.00	0.00	0.00	0.00	0.00	0.00
PhosphC	0.00	0.00	0.00	0.00	0.00	0.00	0.00	0.00	0.00	0.00	0.00	0.00	0.00	0.00	0.00	0.00	0.00	0.00	0.00	0.00
PhosphS	0.00	0.00	0.00	0.00	0.00	0.00	0.00	0.00	0.00	0.00	0.00	0.00	0.00	0.00	0.00	0.00	0.00	0.00	0.00	0.00
Sphm	0.00	0.00	0.00	0.00	0.00	0.00	0.00	0.00	0.00	0.00	0.00	0.00	0.00	0.00	0.00	0.00	0.00	0.00	0.00	0.00
Cholesterol	0.00	0.00	0.00	0.00	0.00	0.00	0.00	0.00	0.00	0.00	0.00	0.00	0.00	0.00	0.00	0.00	0.00	0.00	0.00	0.00
Proteins	0.00	0.00	0.00	0.00	0.00	0.00	0.00	0.00	0.00	0.00	0.00	0.00	0.00	0.00	0.00	0.00	0.00	0.00	0.00	0.00
ADN	0.00	0.00	0.00	0.00	0.00	0.00	0.00	0.00	0.00	0.00	0.00	0.00	0.00	0.00	0.00	0.00	0.00	0.00	0.00	0.00
ARN	0.00	0.00	0.00	0.00	0.00	0.00	0.00	0.00	0.00	0.00	0.00	0.00	0.00	0.00	0.00	0.00	0.00	0.00	0.00	0.00
Lipids	0.00	0.00	0.00	0.00	0.00	0.00	0.00	0.00	0.00	0.00	0.00	0.00	0.00	0.00	0.00	0.00	0.00	0.00	0.00	0.00
NH_4^+	0.00	0.00	1.00	0.00	1.00	0.00	0.00	0.00	1.00	1.00	1.00	0.00	0.00	0.00	0.00	0.00	0.00	0.00	0.00	0.00
CO_2	0.00	1.00	0.00	0.00	0.00	0.00	0.00	0.00	1.00	0.00	0.00	1.00	-1.00	2.00	0.00	2.00	0.00	2.00	1.00	0.00

	v41	v42	v43	v44	v45	v46	v47	v48	v49	v50	v51	v52	v53	v54	v55	v56	v57	v58	v59	v60
G6P	0.00	0.00	0.00	0.00	0.00	0.00	0.00	0.00	0.00	0.00	0.00	0.00	0.00	0.00	0.00	0.00	0.00	0.00	0.00	0.00
F6P	0.00	0.00	0.00	0.00	0.00	0.00	0.00	0.00	0.00	0.00	0.00	0.00	0.00	0.00	0.00	0.00	0.00	0.00	0.00	0.00
DHAP	0.00	0.00	0.00	0.00	0.00	0.00	0.00	0.00	0.00	0.00	0.00	0.00	0.00	0.00	0.00	0.00	0.00	0.00	0.00	0.00
GA3P	0.00	0.00	0.00	0.00	0.00	0.00	0.00	0.00	0.00	0.00	0.00	0.00	0.00	0.00	0.00	0.00	0.00	0.00	0.00	0.00
3PG	0.00	0.00	0.00	0.00	0.00	0.00	0.00	0.00	0.00	0.00	0.00	0.00	0.00	0.00	0.00	0.00	0.00	0.00	0.00	0.00
PYR	0.00	0.00	0.00	0.00	1.00	0.00	0.00	0.00	0.00	0.00	0.00	0.00	0.00	0.00	0.00	0.00	0.00	0.00	0.00	0.00
AcCoA	0.00	0.00	0.00	0.00	0.00	0.00	0.00	0.00	0.00	0.00	0.00	0.00	0.00	0.00	0.00	0.00	0.00	0.00	0.00	0.00
Cit	0.00	0.00	0.00	0.00	0.00	0.00	0.00	0.00	0.00	0.00	0.00	0.00	0.00	0.00	0.00	0.00	0.00	0.00	0.00	0.00
α KG	0.00	0.00	-1.00	0.00	0.00	0.00	0.00	-1.00	0.00	0.00	0.00	0.00	0.00	0.00	0.00	0.00	0.00	0.00	0.00	0.00
SucCoA	-1.00	0.00	0.00	0.00	0.00	0.00	0.00	0.00	0.00	0.00	0.00	0.00	0.00	0.00	0.00	0.00	-1.00	0.00	0.00	0.00
Succ	1.00	0.00	0.00	0.00	0.00	0.00	0.00	0.00	0.00	0.00	0.00	0.00	0.00	0.00	0.00	0.00	0.00	0.00	0.00	0.00
Fum	0.00	0.00	1.00	0.00	0.00	0.00	0.00	0.00	0.00	0.00	0.00	0.00	0.00	1.00	0.00	0.00	1.00	1.00	0.00	0.00
Mal	0.00	0.00	0.00	0.00	0.00	0.00	0.00	0.00	0.00	0.00	0.00	0.00	0.00	0.00	0.00	0.00	0.00	0.00	0.00	0.00
Oxa	0.00	0.00	0.00	0.00	0.00	0.00	0.00	0.00	0.00	0.00	0.00	0.00	0.00	0.00	0.00	0.00	0.00	0.00	0.00	0.00
Rl5P	0.00	0.00	0.00	0.00	0.00	0.00	0.00	0.00	0.00	0.00	0.00	0.00	0.00	0.00	0.00	0.00	0.00	0.00	0.00	0.00
R5P	0.00	0.00	0.00	0.00	0.00	0.00	0.00	0.00	0.00	0.00	0.00	0.00	0.00	0.00	0.00	-1.00	0.00	0.00	0.00	0.00
X5P	0.00	0.00	0.00	0.00	0.00	0.00	0.00	0.00	0.00	0.00	0.00	0.00	0.00	0.00	0.00	0.00	0.00	0.00	0.00	0.00
E4P	0.00	0.00	0.00	0.00	0.00	0.00	0.00	0.00	0.00	0.00	0.00	0.00	0.00	0.00	0.00	0.00	0.00	0.00	0.00	0.00
Glu	0.00	0.00	1.00	0.00	0.00	0.00	0.00	1.00	0.00	1.00	1.00	0.00	0.00	0.00	-0.06	0.00	2.00	0.00	1.00	0.00
Asp	0.00	0.00	0.00	0.00	0.00	1.00	0.00	0.00	0.00	0.00	0.00	0.00	-1.00	0.00	-0.05	0.00	-1.00	-1.00	0.00	-1.00
Gly	0.00	0.00	0.00	0.00	0.00	0.00	0.00	0.00	0.00	0.00	0.00	0.00	0.00	0.00	-0.07	0.00	-1.00	0.00	0.00	0.00
Ser	0.00	0.00	0.00	-1.00	0.00	0.00	0.00	0.00	0.00	0.00	0.00	0.00	0.00	0.00	-0.07	0.00	0.00	0.00	0.00	0.00
Tyr	0.00	1.00	-1.00	0.00	0.00	0.00	0.00	0.00	0.00	0.00	0.00	0.00	0.00	0.00	-0.03	0.00	0.00	0.00	0.00	0.00
Cys	0.00	0.00	0.00	1.00	-1.00	0.00	0.00	0.00	0.00	0.00	0.00	0.00	0.00	0.00	-0.02	0.00	0.00	0.00	0.00	0.00
Ala	0.00	0.00	0.00	0.00	0.00	0.00	0.00	0.00	0.00	0.00	0.00	0.00	0.00	0.00	-0.08	0.00	0.00	0.00	0.00	0.00
Arg	0.00	0.00	0.00	0.00	0.00	0.00	-1.00	0.00	0.00	0.00	0.00	0.00	0.00	1.00	-0.05	0.00	0.00	0.00	0.00	0.00
Asn	0.00	0.00	0.00	0.00	0.00	-1.00	0.00	0.00	0.00	0.00	0.00	0.00	0.00	0.00	-0.04	0.00	0.00	0.00	0.00	0.00
Gln	0.00	0.00	0.00	0.00	0.00	0.00	0.00	0.00	0.00	0.00	0.00	0.00	0.00	0.00	-0.04	0.00	-2.00	0.00	-1.00	0.00
His	0.00	0.00	0.00	0.00	0.00	0.00	0.00	0.00	0.00	0.00	-1.00	0.00	0.00	0.00	-0.02	0.00	0.00	0.00	0.00	0.00
Ile	0.00	0.00	0.00	0.00	0.00	0.00	0.00	0.00	0.00	0.00	0.00	0.00	0.00	0.00	-0.05	0.00	0.00	0.00	0.00	0.00
Leu	0.00	0.00	0.00	0.00	0.00	0.00	0.00	0.00	0.00	0.00	0.00	0.00	0.00	0.00	-0.09	0.00	0.00	0.00	0.00	0.00
Lys	0.00	0.00	0.00	0.00	0.00	0.00	0.00	0.00	0.00	0.00	0.00	0.00	0.00	0.00	-0.06	0.00	0.00	0.00	0.00	0.00
Met	0.00	0.00	0.00	-1.00	0.00	0.00	0.00	0.00	0.00	0.00	0.00	0.00	0.00	0.00	-0.02	0.00	0.00	0.00	0.00	0.00
Phe	0.00	-1.00	0.00	0.00	0.00	0.00	0.00	0.00	0.00	0.00	0.00	0.00	0.00	0.00	-0.04	0.00	0.00	0.00	0.00	0.00
Pro	0.00	0.00	0.00	0.00	0.00	0.00	0.00	0.00	-1.00	0.00	0.00	0.00	0.00	0.00	-0.05	0.00	0.00	0.00	0.00	0.00
Thr	0.00	0.00	0.00	0.00	0.00	0.00	0.00	0.00	0.00	0.00	0.00	0.00	0.00	0.00	-0.06	0.00	0.00	0.00	0.00	0.00
Trp	0.00	0.00	0.00	0.00	0.00	0.00	0.00	0.00	0.00	0.00	0.00	0.00	0.00	0.00	-0.01	0.00	0.00	0.00	0.00	0.00
Val	0.00	0.00	0.00	0.00	0.00	0.00	0.00	0.00	0.00	0.00	0.00	0.00	0.00	0.00	-0.07	0.00	0.00	0.00	0.00	0.00
α KBut	0.00	0.00	0.00	1.00	0.00	0.00	0.00	0.00	0.00	0.00	0.00	0.00	0.00	0.00	0.00	0.00	0.00	0.00	0.00	0.00
PropCoA	0.00	0.00	0.00	0.00	0.00	0.00	0.00	0.00	0.00	0.00	0.00	0.00	0.00	0.00	0.00	0.00	0.00	0.00	0.00	0.00

	v41	v42	v43	v44	v45	v46	v47	v48	v49	v50	v51	v52	v53	v54	v55	v56	v57	v58	v59	v60
α KAd	0.00	0.00	0.00	0.00	0.00	0.00	0.00	0.00	0.00	0.00	0.00	0.00	0.00	0.00	0.00	0.00	0.00	0.00	0.00	0.00
AcetoacCoA	1.00	0.00	0.00	0.00	0.00	0.00	0.00	0.00	0.00	0.00	0.00	0.00	0.00	0.00	0.00	0.00	0.00	0.00	0.00	0.00
Acetoac	-1.00	0.00	1.00	0.00	0.00	0.00	0.00	0.00	0.00	0.00	0.00	0.00	0.00	0.00	0.00	0.00	0.00	0.00	0.00	0.00
Glu γ sa	0.00	0.00	0.00	0.00	0.00	0.00	0.00	1.00	1.00	-1.00	0.00	0.00	0.00	0.00	0.00	0.00	0.00	0.00	0.00	0.00
Orn	0.00	0.00	0.00	0.00	0.00	0.00	1.00	-1.00	0.00	0.00	0.00	-1.00	0.00	0.00	0.00	0.00	0.00	0.00	0.00	0.00
Cln	0.00	0.00	0.00	0.00	0.00	0.00	0.00	0.00	0.00	0.00	0.00	1.00	-1.00	0.00	0.00	0.00	0.00	0.00	0.00	0.00
Argsucc	0.00	0.00	0.00	0.00	0.00	0.00	0.00	0.00	0.00	0.00	0.00	0.00	1.00	-1.00	0.00	0.00	0.00	0.00	0.00	0.00
PRPP	0.00	0.00	0.00	0.00	0.00	0.00	0.00	0.00	0.00	0.00	0.00	0.00	0.00	0.00	0.00	1.00	-1.00	0.00	0.00	0.00
IMP	0.00	0.00	0.00	0.00	0.00	0.00	0.00	0.00	0.00	0.00	0.00	0.00	0.00	0.00	0.00	0.00	1.00	-1.00	-1.00	0.00
Orot	0.00	0.00	0.00	0.00	0.00	0.00	0.00	0.00	0.00	0.00	0.00	0.00	0.00	0.00	0.00	0.00	0.00	0.00	0.00	1.00
UTPrn	0.00	0.00	0.00	0.00	0.00	0.00	0.00	0.00	0.00	0.00	0.00	0.00	0.00	0.00	0.00	0.00	0.00	0.00	0.00	0.00
ATPrn	0.00	0.00	0.00	0.00	0.00	0.00	0.00	0.00	0.00	0.00	0.00	0.00	0.00	0.00	0.00	0.00	0.00	1.00	0.00	0.00
GTPrn	0.00	0.00	0.00	0.00	0.00	0.00	0.00	0.00	0.00	0.00	0.00	0.00	0.00	0.00	0.00	0.00	0.00	0.00	1.00	0.00
CTPrn	0.00	0.00	0.00	0.00	0.00	0.00	0.00	0.00	0.00	0.00	0.00	0.00	0.00	0.00	0.00	0.00	0.00	0.00	0.00	0.00
dATP	0.00	0.00	0.00	0.00	0.00	0.00	0.00	0.00	0.00	0.00	0.00	0.00	0.00	0.00	0.00	0.00	0.00	0.00	0.00	0.00
dGTP	0.00	0.00	0.00	0.00	0.00	0.00	0.00	0.00	0.00	0.00	0.00	0.00	0.00	0.00	0.00	0.00	0.00	0.00	0.00	0.00
dTTP	0.00	0.00	0.00	0.00	0.00	0.00	0.00	0.00	0.00	0.00	0.00	0.00	0.00	0.00	0.00	0.00	0.00	0.00	0.00	0.00
dCTP	0.00	0.00	0.00	0.00	0.00	0.00	0.00	0.00	0.00	0.00	0.00	0.00	0.00	0.00	0.00	0.00	0.00	0.00	0.00	0.00
Ethn	0.00	0.00	0.00	0.00	0.00	0.00	0.00	0.00	0.00	0.00	0.00	0.00	0.00	0.00	0.00	0.00	0.00	0.00	0.00	0.00
Cho	0.00	0.00	0.00	0.00	0.00	0.00	0.00	0.00	0.00	0.00	0.00	0.00	0.00	0.00	0.00	0.00	0.00	0.00	0.00	0.00
Glyc3P	0.00	0.00	0.00	0.00	0.00	0.00	0.00	0.00	0.00	0.00	0.00	0.00	0.00	0.00	0.00	0.00	0.00	0.00	0.00	0.00
PhosphE	0.00	0.00	0.00	0.00	0.00	0.00	0.00	0.00	0.00	0.00	0.00	0.00	0.00	0.00	0.00	0.00	0.00	0.00	0.00	0.00
PhosphC	0.00	0.00	0.00	0.00	0.00	0.00	0.00	0.00	0.00	0.00	0.00	0.00	0.00	0.00	0.00	0.00	0.00	0.00	0.00	0.00
PhosphS	0.00	0.00	0.00	0.00	0.00	0.00	0.00	0.00	0.00	0.00	0.00	0.00	0.00	0.00	0.00	0.00	0.00	0.00	0.00	0.00
Sphm	0.00	0.00	0.00	0.00	0.00	0.00	0.00	0.00	0.00	0.00	0.00	0.00	0.00	0.00	0.00	0.00	0.00	0.00	0.00	0.00
Cholesterol	0.00	0.00	0.00	0.00	0.00	0.00	0.00	0.00	0.00	0.00	0.00	0.00	0.00	0.00	0.00	0.00	0.00	0.00	0.00	0.00
Proteins	0.00	0.00	0.00	0.00	0.00	0.00	0.00	0.00	0.00	0.00	0.00	0.00	0.00	0.00	1.00	0.00	0.00	0.00	0.00	0.00
ADN	0.00	0.00	0.00	0.00	0.00	0.00	0.00	0.00	0.00	0.00	0.00	0.00	0.00	0.00	0.00	0.00	0.00	0.00	0.00	0.00
ARN	0.00	0.00	0.00	0.00	0.00	0.00	0.00	0.00	0.00	0.00	0.00	0.00	0.00	0.00	0.00	0.00	0.00	0.00	0.00	0.00
Lipids	0.00	0.00	0.00	0.00	0.00	0.00	0.00	0.00	0.00	0.00	0.00	0.00	0.00	0.00	0.00	0.00	0.00	0.00	0.00	0.00
NH_4^+	0.00	0.00	0.00	1.00	1.00	1.00	0.00	0.00	0.00	0.00	1.00	-1.00	0.00	0.00	0.00	0.00	0.00	0.00	0.00	-1.00
CO_2	0.00	0.00	1.00	0.00	0.00	0.00	0.00	0.00	0.00	0.00	0.00	-1.00	0.00	0.00	0.00	0.00	-1.00	0.00	0.00	-1.00

	v61	v62	v63	v64	v65	v66	v67	v68	v69	v70	v71	v72	v73	v74	v75	v76	v77	v78	v79	v80
G6P	0.00	0.00	0.00	0.00	0.00	0.00	0.00	0.00	0.00	0.00	0.00	0.00	0.00	0.00	0.00	0.00	0.00	0.00	0.00	0.00
F6P	0.00	0.00	0.00	0.00	0.00	0.00	0.00	0.00	0.00	0.00	0.00	0.00	0.00	0.00	0.00	0.00	0.00	0.00	0.00	0.00
DHAP	0.00	0.00	0.00	0.00	0.00	0.00	0.00	0.00	-1.00	0.00	0.00	0.00	0.00	0.00	0.00	0.00	0.00	0.00	0.00	0.00
GA3P	0.00	0.00	0.00	0.00	0.00	0.00	0.00	0.00	0.00	0.00	0.00	0.00	0.00	0.00	0.00	0.00	0.00	0.00	0.00	0.00
3PG	0.00	0.00	0.00	0.00	0.00	0.00	0.00	0.00	0.00	0.00	0.00	0.00	0.00	0.00	0.00	0.00	0.00	0.00	0.00	0.00
PYR	0.00	0.00	0.00	0.00	0.00	0.00	0.00	0.00	0.00	0.00	0.00	0.00	0.00	0.00	0.00	0.00	0.00	0.00	0.00	0.00
AcCoA	0.00	0.00	0.00	0.00	0.00	0.00	0.00	0.00	0.00	-18.00	-18.00	0.00	-16.00	-18.00	0.00	0.00	0.00	0.00	0.00	0.00
Cit	0.00	0.00	0.00	0.00	0.00	0.00	0.00	0.00	0.00	0.00	0.00	0.00	0.00	0.00	0.00	0.00	0.00	0.00	0.00	0.00
α KG	0.00	0.00	0.00	0.00	0.00	0.00	0.00	0.00	0.00	0.00	0.00	0.00	0.00	0.00	0.00	0.00	0.00	0.00	0.00	0.00
SucCoA	0.00	0.00	0.00	0.00	0.00	0.00	0.00	0.00	0.00	0.00	0.00	0.00	0.00	0.00	0.00	0.00	0.00	0.00	0.00	0.00
Succ	0.00	0.00	0.00	0.00	0.00	0.00	0.00	0.00	0.00	0.00	0.00	0.00	0.00	0.00	0.00	0.00	0.00	0.00	0.00	0.00
Fum	0.00	0.00	0.00	0.00	0.00	0.00	0.00	0.00	0.00	0.00	0.00	0.00	0.00	0.00	0.00	0.00	0.00	0.00	0.00	0.00
Mal	0.00	0.00	0.00	0.00	0.00	0.00	0.00	0.00	0.00	0.00	0.00	0.00	0.00	0.00	0.00	0.00	0.00	0.00	0.00	0.00
Oxa	0.00	0.00	0.00	0.00	0.00	0.00	0.00	0.00	0.00	0.00	0.00	0.00	0.00	0.00	0.00	0.00	0.00	0.00	0.00	0.00
Rl5P	0.00	0.00	0.00	0.00	0.00	0.00	0.00	0.00	0.00	0.00	0.00	0.00	0.00	0.00	0.00	0.00	0.00	0.00	0.00	0.00
R5P	0.00	0.00	0.00	0.00	0.00	0.00	0.00	0.00	0.00	0.00	0.00	0.00	0.00	0.00	0.00	0.00	0.00	0.00	0.00	0.00
X5P	0.00	0.00	0.00	0.00	0.00	0.00	0.00	0.00	0.00	0.00	0.00	0.00	0.00	0.00	0.00	0.00	0.00	0.00	0.00	0.00
E4P	0.00	0.00	0.00	0.00	0.00	0.00	0.00	0.00	0.00	0.00	0.00	0.00	0.00	0.00	0.00	0.00	0.00	0.00	0.00	0.00
Glu	0.00	1.00	0.00	0.00	0.00	0.00	0.00	0.00	0.00	0.00	0.00	0.00	0.00	0.00	0.00	0.00	0.00	0.00	0.00	0.00
Asp	0.00	0.00	0.00	0.00	0.00	0.00	0.00	0.00	0.00	0.00	0.00	0.00	0.00	0.00	0.00	0.00	1.00	0.00	0.00	0.00
Gly	0.00	0.00	0.00	0.00	0.00	0.00	0.00	0.00	0.00	0.00	0.00	0.00	0.00	0.00	0.00	0.00	0.00	0.00	-1.00	0.00
Ser	0.00	0.00	0.00	0.00	0.00	0.00	0.00	0.00	0.00	0.00	0.00	-1.00	-1.00	0.00	0.00	0.00	0.00	0.00	0.00	1.00
Tyr	0.00	0.00	0.00	0.00	0.00	0.00	0.00	0.00	0.00	0.00	0.00	0.00	0.00	0.00	0.00	0.00	0.00	0.00	0.00	0.00
Cys	0.00	0.00	0.00	0.00	0.00	0.00	0.00	0.00	0.00	0.00	0.00	0.00	0.00	0.00	0.00	0.00	0.00	1.00	0.00	0.00
Ala	0.00	0.00	0.00	0.00	0.00	0.00	0.00	0.00	0.00	0.00	0.00	0.00	0.00	0.00	0.00	0.00	0.00	0.00	0.00	0.00
Arg	0.00	0.00	0.00	0.00	0.00	0.00	0.00	0.00	0.00	0.00	0.00	0.00	0.00	0.00	0.00	0.00	0.00	0.00	0.00	0.00
Asn	0.00	0.00	0.00	0.00	0.00	0.00	0.00	0.00	0.00	0.00	0.00	0.00	0.00	0.00	0.00	0.00	0.00	0.00	0.00	0.00
Gln	0.00	-1.00	0.00	0.00	0.00	0.00	0.00	0.00	0.00	0.00	0.00	0.00	0.00	0.00	0.00	0.00	0.00	0.00	0.00	0.00
His	0.00	0.00	0.00	0.00	0.00	0.00	0.00	0.00	0.00	0.00	0.00	0.00	0.00	0.00	0.00	0.00	0.00	0.00	0.00	0.00
Ile	0.00	0.00	0.00	0.00	0.00	0.00	0.00	0.00	0.00	0.00	0.00	0.00	0.00	0.00	0.00	0.00	0.00	0.00	0.00	0.00
Leu	0.00	0.00	0.00	0.00	0.00	0.00	0.00	0.00	0.00	0.00	0.00	0.00	0.00	0.00	0.00	0.00	0.00	0.00	0.00	0.00
Lys	0.00	0.00	0.00	0.00	0.00	0.00	0.00	0.00	0.00	0.00	0.00	0.00	0.00	0.00	0.00	0.00	0.00	0.00	0.00	0.00
Met	0.00	0.00	0.00	0.00	0.00	0.00	0.00	0.00	0.00	0.00	0.00	0.00	0.00	0.00	0.00	0.00	0.00	0.00	0.00	0.00
Phe	0.00	0.00	0.00	0.00	0.00	0.00	0.00	0.00	0.00	0.00	0.00	0.00	0.00	0.00	0.00	0.00	0.00	0.00	0.00	0.00
Pro	0.00	0.00	0.00	0.00	0.00	0.00	0.00	0.00	0.00	0.00	0.00	0.00	0.00	0.00	0.00	0.00	0.00	0.00	0.00	0.00
Thr	0.00	0.00	0.00	0.00	0.00	0.00	0.00	0.00	0.00	0.00	0.00	0.00	0.00	0.00	0.00	0.00	0.00	0.00	0.00	0.00
Trp	0.00	0.00	0.00	0.00	0.00	0.00	0.00	0.00	0.00	0.00	0.00	0.00	0.00	0.00	0.00	0.00	0.00	0.00	0.00	0.00
Val	0.00	0.00	0.00	0.00	0.00	0.00	0.00	0.00	0.00	0.00	0.00	0.00	0.00	0.00	0.00	0.00	0.00	0.00	0.00	0.00
α KBut	0.00	0.00	0.00	0.00	0.00	0.00	0.00	0.00	0.00	0.00	0.00	0.00	0.00	0.00	0.00	0.00	0.00	0.00	0.00	0.00
PropCoA	0.00	0.00	0.00	0.00	0.00	0.00	0.00	0.00	0.00	0.00	0.00	0.00	0.00	0.00	0.00	0.00	0.00	0.00	0.00	0.00

	v61	v62	v63	v64	v65	v66	v67	v68	v69	v70	v71	v72	v73	v74	v75	v76	v77	v78	v79	v80
α KAd	0.00	0.00	0.00	0.00	0.00	0.00	0.00	0.00	0.00	0.00	0.00	0.00	0.00	0.00	0.00	0.00	0.00	0.00	0.00	0.00
AcetoacCoA	0.00	0.00	0.00	0.00	0.00	0.00	0.00	0.00	0.00	0.00	0.00	0.00	0.00	0.00	0.00	0.00	0.00	0.00	0.00	0.00
Acetoac	0.00	0.00	0.00	0.00	0.00	0.00	0.00	0.00	0.00	0.00	0.00	0.00	0.00	0.00	0.00	0.00	0.00	0.00	0.00	0.00
Glu γ sa	0.00	0.00	0.00	0.00	0.00	0.00	0.00	0.00	0.00	0.00	0.00	0.00	0.00	0.00	0.00	0.00	0.00	0.00	0.00	0.00
Orn	0.00	0.00	0.00	0.00	0.00	0.00	0.00	0.00	0.00	0.00	0.00	0.00	0.00	0.00	0.00	0.00	0.00	0.00	0.00	0.00
Cln	0.00	0.00	0.00	0.00	0.00	0.00	0.00	0.00	0.00	0.00	0.00	0.00	0.00	0.00	0.00	0.00	0.00	0.00	0.00	0.00
Argsucc	0.00	0.00	0.00	0.00	0.00	0.00	0.00	0.00	0.00	0.00	0.00	0.00	0.00	0.00	0.00	0.00	0.00	0.00	0.00	0.00
PRPP	-1.00	0.00	0.00	0.00	0.00	0.00	0.00	0.00	0.00	0.00	0.00	0.00	0.00	0.00	0.00	0.00	0.00	0.00	0.00	0.00
IMP	0.00	0.00	0.00	0.00	0.00	0.00	0.00	0.00	0.00	0.00	0.00	0.00	0.00	0.00	0.00	0.00	0.00	0.00	0.00	0.00
Orot	-1.00	0.00	0.00	0.00	0.00	0.00	0.00	0.00	0.00	0.00	0.00	0.00	0.00	0.00	0.00	0.00	0.00	0.00	0.00	0.00
UTPrn	1.00	-1.00	-0.28	0.00	0.00	-1.00	0.00	0.00	0.00	0.00	0.00	0.00	0.00	0.00	0.00	0.00	0.00	0.00	0.00	0.00
ATPrn	0.00	0.00	-0.28	-1.00	0.00	0.00	0.00	0.00	0.00	0.00	0.00	0.00	0.00	0.00	0.00	0.00	0.00	0.00	0.00	0.00
GTPrn	0.00	0.00	-0.22	0.00	-1.00	0.00	0.00	0.00	0.00	0.00	0.00	0.00	0.00	0.00	0.00	0.00	0.00	0.00	0.00	0.00
CTPrn	0.00	1.00	-0.22	0.00	0.00	0.00	-1.00	0.00	0.00	0.00	0.00	0.00	0.00	0.00	0.00	0.00	0.00	0.00	0.00	0.00
dATP	0.00	0.00	0.00	1.00	0.00	0.00	0.00	-0.28	0.00	0.00	0.00	0.00	0.00	0.00	0.00	0.00	0.00	0.00	0.00	0.00
dGTP	0.00	0.00	0.00	0.00	1.00	0.00	0.00	-0.22	0.00	0.00	0.00	0.00	0.00	0.00	0.00	0.00	0.00	0.00	0.00	0.00
dTTP	0.00	0.00	0.00	0.00	0.00	1.00	0.00	-0.28	0.00	0.00	0.00	0.00	0.00	0.00	0.00	0.00	0.00	0.00	0.00	0.00
dCTP	0.00	0.00	0.00	0.00	0.00	0.00	1.00	-0.22	0.00	0.00	0.00	0.00	0.00	0.00	0.00	0.00	0.00	0.00	0.00	0.00
Ethn	0.00	0.00	0.00	0.00	0.00	0.00	0.00	0.00	0.00	0.00	-1.00	1.00	0.00	0.00	0.00	0.00	0.00	0.00	0.00	0.00
Cho	0.00	0.00	0.00	0.00	0.00	0.00	0.00	0.00	0.00	-1.00	0.00	0.00	-1.00	0.00	0.00	0.00	0.00	0.00	0.00	0.00
Glyc3P	0.00	0.00	0.00	0.00	0.00	0.00	0.00	0.00	1.00	-1.00	-1.00	0.00	0.00	0.00	0.00	0.00	0.00	0.00	0.00	0.00
PhosphE	0.00	0.00	0.00	0.00	0.00	0.00	0.00	0.00	0.00	0.00	1.00	-1.00	0.00	0.00	-0.20	0.00	0.00	0.00	0.00	0.00
PhosphC	0.00	0.00	0.00	0.00	0.00	0.00	0.00	0.00	0.00	1.00	0.00	0.00	0.00	0.00	-0.50	0.00	0.00	0.00	0.00	0.00
PhosphS	0.00	0.00	0.00	0.00	0.00	0.00	0.00	0.00	0.00	0.00	0.00	0.00	1.00	0.00	-0.07	0.00	0.00	0.00	0.00	0.00
Sphm	0.00	0.00	0.00	0.00	0.00	0.00	0.00	0.00	0.00	0.00	0.00	0.00	1.00	0.00	-0.07	0.00	0.00	0.00	0.00	0.00
Cholesterol	0.00	0.00	0.00	0.00	0.00	0.00	0.00	0.00	0.00	0.00	0.00	0.00	0.00	1.00	-0.15	0.00	0.00	0.00	0.00	0.00
Proteins	0.00	0.00	0.00	0.00	0.00	0.00	0.00	0.00	0.00	0.00	0.00	0.00	0.00	0.00	0.00	-0.92	0.00	0.00	0.00	0.00
ADN	0.00	0.00	0.00	0.00	0.00	0.00	0.00	1.00	0.00	0.00	0.00	0.00	0.00	0.00	0.00	-0.01	0.00	0.00	0.00	0.00
ARN	0.00	0.00	1.00	0.00	0.00	0.00	0.00	0.00	0.00	0.00	0.00	0.00	0.00	0.00	0.00	-0.01	0.00	0.00	0.00	0.00
Lipids	0.00	0.00	0.00	0.00	0.00	0.00	0.00	0.00	0.00	0.00	0.00	0.00	0.00	0.00	1.00	-0.03	0.00	0.00	0.00	0.00
NH_4^+	0.00	0.00	0.00	0.00	0.00	0.00	0.00	0.00	0.00	0.00	0.00	0.00	0.00	0.00	0.00	0.00	0.00	0.00	0.00	0.00
CO_2	1.00	0.00	0.00	0.00	0.00	0.00	0.00	0.00	0.00	0.00	0.00	0.00	2.00	6.00	0.00	0.00	0.00	0.00	0.00	0.00

	v81	v82	v83	v84	v85	v86	v87	v88	v89	v90	v91	v92	v93	v94	v95	v96	v97	v98	v99	v100
G6P	0.00	0.00	0.00	0.00	0.00	0.00	0.00	0.00	0.00	0.00	0.00	0.00	0.00	0.00	0.00	0.00	0.00	0.00	0.00	0.00
F6P	0.00	0.00	0.00	0.00	0.00	0.00	0.00	0.00	0.00	0.00	0.00	0.00	0.00	0.00	0.00	0.00	0.00	0.00	0.00	0.00
DHAP	0.00	0.00	0.00	0.00	0.00	0.00	0.00	0.00	0.00	0.00	0.00	0.00	0.00	0.00	0.00	0.00	0.00	0.00	0.00	0.00
GA3P	0.00	0.00	0.00	0.00	0.00	0.00	0.00	0.00	0.00	0.00	0.00	0.00	0.00	0.00	0.00	0.00	0.00	0.00	0.00	0.00
3PG	0.00	0.00	0.00	0.00	0.00	0.00	0.00	0.00	0.00	0.00	0.00	0.00	0.00	0.00	0.00	0.00	0.00	0.00	0.00	0.00
PYR	0.00	0.00	0.00	0.00	0.00	0.00	0.00	0.00	0.00	0.00	0.00	0.00	0.00	0.00	0.00	0.00	0.00	0.00	0.00	0.00
AcCoA	0.00	0.00	0.00	0.00	0.00	0.00	0.00	0.00	0.00	0.00	0.00	0.00	0.00	0.00	0.00	0.00	0.00	0.00	0.00	0.00
Cit	0.00	0.00	0.00	0.00	0.00	0.00	0.00	0.00	0.00	0.00	0.00	0.00	0.00	0.00	0.00	0.00	0.00	0.00	0.00	0.00
α KG	0.00	0.00	0.00	0.00	0.00	0.00	0.00	0.00	0.00	0.00	0.00	0.00	0.00	0.00	0.00	0.00	0.00	0.00	0.00	0.00
SucCoA	0.00	0.00	0.00	0.00	0.00	0.00	0.00	0.00	0.00	0.00	0.00	0.00	0.00	0.00	0.00	0.00	0.00	0.00	0.00	0.00
Succ	0.00	0.00	0.00	0.00	0.00	0.00	0.00	0.00	0.00	0.00	0.00	0.00	0.00	0.00	0.00	0.00	0.00	0.00	0.00	0.00
Fum	0.00	0.00	0.00	0.00	0.00	0.00	0.00	0.00	0.00	0.00	0.00	0.00	0.00	0.00	0.00	0.00	0.00	0.00	0.00	0.00
Mal	0.00	0.00	0.00	0.00	0.00	0.00	0.00	0.00	0.00	0.00	0.00	0.00	0.00	0.00	0.00	0.00	0.00	0.00	0.00	0.00
Oxa	0.00	0.00	0.00	0.00	0.00	0.00	0.00	0.00	0.00	0.00	0.00	0.00	0.00	0.00	0.00	0.00	0.00	0.00	0.00	0.00
Rl5P	0.00	0.00	0.00	0.00	0.00	0.00	0.00	0.00	0.00	0.00	0.00	0.00	0.00	0.00	0.00	0.00	0.00	0.00	0.00	0.00
R5P	0.00	0.00	0.00	0.00	0.00	0.00	0.00	0.00	0.00	0.00	0.00	0.00	0.00	0.00	0.00	0.00	0.00	0.00	0.00	0.00
X5P	0.00	0.00	0.00	0.00	0.00	0.00	0.00	0.00	0.00	0.00	0.00	0.00	0.00	0.00	0.00	0.00	0.00	0.00	0.00	0.00
E4P	0.00	0.00	0.00	0.00	0.00	0.00	0.00	0.00	0.00	0.00	0.00	0.00	0.00	0.00	0.00	0.00	0.00	0.00	0.00	0.00
Glu	-1.00	0.00	0.00	0.00	0.00	0.00	0.00	0.00	0.00	0.00	0.00	0.00	0.00	0.00	0.00	0.00	0.00	0.00	0.00	0.00
Asp	0.00	0.00	0.00	0.00	0.00	0.00	0.00	0.00	0.00	0.00	0.00	0.00	0.00	0.00	0.00	0.00	0.00	0.00	0.00	0.00
Gly	0.00	0.00	0.00	0.00	0.00	0.00	0.00	0.00	0.00	0.00	0.00	0.00	0.00	0.00	0.00	0.00	0.00	0.00	0.00	0.00
Ser	0.00	0.00	0.00	0.00	0.00	0.00	0.00	0.00	0.00	0.00	0.00	0.00	0.00	0.00	0.00	0.00	0.00	0.00	0.00	0.00
Tyr	0.00	1.00	0.00	0.00	0.00	0.00	0.00	0.00	0.00	0.00	0.00	0.00	0.00	0.00	0.00	0.00	0.00	0.00	0.00	0.00
Cys	0.00	0.00	0.00	0.00	0.00	0.00	0.00	0.00	0.00	0.00	0.00	0.00	0.00	0.00	0.00	0.00	0.00	0.00	0.00	0.00
Ala	0.00	0.00	-1.00	0.00	0.00	0.00	0.00	0.00	0.00	0.00	0.00	0.00	0.00	0.00	0.00	0.00	0.00	0.00	0.00	0.00
Arg	0.00	0.00	0.00	1.00	0.00	0.00	0.00	0.00	0.00	0.00	0.00	0.00	0.00	0.00	0.00	0.00	0.00	0.00	0.00	0.00
Asn	0.00	0.00	0.00	0.00	1.00	0.00	0.00	0.00	0.00	0.00	0.00	0.00	0.00	0.00	0.00	0.00	0.00	0.00	0.00	0.00
Gln	0.00	0.00	0.00	0.00	0.00	1.00	0.00	0.00	0.00	0.00	0.00	0.00	0.00	0.00	0.00	0.00	0.00	0.00	0.00	0.00
His	0.00	0.00	0.00	0.00	0.00	0.00	1.00	0.00	0.00	0.00	0.00	0.00	0.00	0.00	0.00	0.00	0.00	0.00	0.00	0.00
Ile	0.00	0.00	0.00	0.00	0.00	0.00	0.00	1.00	0.00	0.00	0.00	0.00	0.00	0.00	0.00	0.00	0.00	0.00	0.00	0.00
Leu	0.00	0.00	0.00	0.00	0.00	0.00	0.00	0.00	1.00	0.00	0.00	0.00	0.00	0.00	0.00	0.00	0.00	0.00	0.00	0.00
Lys	0.00	0.00	0.00	0.00	0.00	0.00	0.00	0.00	0.00	1.00	0.00	0.00	0.00	0.00	0.00	0.00	0.00	0.00	0.00	0.00
Met	0.00	0.00	0.00	0.00	0.00	0.00	0.00	0.00	0.00	0.00	1.00	0.00	0.00	0.00	0.00	0.00	0.00	0.00	0.00	0.00
Phe	0.00	0.00	0.00	0.00	0.00	0.00	0.00	0.00	0.00	0.00	0.00	1.00	0.00	0.00	0.00	0.00	0.00	0.00	0.00	0.00
Pro	0.00	0.00	0.00	0.00	0.00	0.00	0.00	0.00	0.00	0.00	0.00	0.00	1.00	0.00	0.00	0.00	0.00	0.00	0.00	0.00
Thr	0.00	0.00	0.00	0.00	0.00	0.00	0.00	0.00	0.00	0.00	0.00	0.00	0.00	1.00	0.00	0.00	0.00	0.00	0.00	0.00
Trp	0.00	0.00	0.00	0.00	0.00	0.00	0.00	0.00	0.00	0.00	0.00	0.00	0.00	0.00	1.00	0.00	0.00	0.00	0.00	0.00
Val	0.00	0.00	0.00	0.00	0.00	0.00	0.00	0.00	0.00	0.00	0.00	0.00	0.00	0.00	0.00	1.00	0.00	0.00	0.00	0.00
α KBut	0.00	0.00	0.00	0.00	0.00	0.00	0.00	0.00	0.00	0.00	0.00	0.00	0.00	0.00	0.00	0.00	0.00	0.00	0.00	0.00
PropCoA	0.00	0.00	0.00	0.00	0.00	0.00	0.00	0.00	0.00	0.00	0.00	0.00	0.00	0.00	0.00	0.00	0.00	0.00	0.00	0.00

	v81	v82	v83	v84	v85	v86	v87	v88	v89	v90	v91	v92	v93	v94	v95	v96	v97	v98	v99	v100
α KAd	0.00	0.00	0.00	0.00	0.00	0.00	0.00	0.00	0.00	0.00	0.00	0.00	0.00	0.00	0.00	0.00	0.00	0.00	0.00	0.00
AcetoacCoA	0.00	0.00	0.00	0.00	0.00	0.00	0.00	0.00	0.00	0.00	0.00	0.00	0.00	0.00	0.00	0.00	0.00	0.00	0.00	0.00
Acetoac	0.00	0.00	0.00	0.00	0.00	0.00	0.00	0.00	0.00	0.00	0.00	0.00	0.00	0.00	0.00	0.00	0.00	0.00	0.00	0.00
Glu γ sa	0.00	0.00	0.00	0.00	0.00	0.00	0.00	0.00	0.00	0.00	0.00	0.00	0.00	0.00	0.00	0.00	0.00	0.00	0.00	0.00
Orn	0.00	0.00	0.00	0.00	0.00	0.00	0.00	0.00	0.00	0.00	0.00	0.00	0.00	0.00	0.00	0.00	0.00	0.00	0.00	0.00
Cln	0.00	0.00	0.00	0.00	0.00	0.00	0.00	0.00	0.00	0.00	0.00	0.00	0.00	0.00	0.00	0.00	0.00	0.00	0.00	0.00
Argsucc	0.00	0.00	0.00	0.00	0.00	0.00	0.00	0.00	0.00	0.00	0.00	0.00	0.00	0.00	0.00	0.00	0.00	0.00	0.00	0.00
PRPP	0.00	0.00	0.00	0.00	0.00	0.00	0.00	0.00	0.00	0.00	0.00	0.00	0.00	0.00	0.00	0.00	0.00	0.00	0.00	0.00
IMP	0.00	0.00	0.00	0.00	0.00	0.00	0.00	0.00	0.00	0.00	0.00	0.00	0.00	0.00	0.00	0.00	0.00	0.00	0.00	0.00
Orot	0.00	0.00	0.00	0.00	0.00	0.00	0.00	0.00	0.00	0.00	0.00	0.00	0.00	0.00	0.00	0.00	0.00	0.00	0.00	0.00
UTPrn	0.00	0.00	0.00	0.00	0.00	0.00	0.00	0.00	0.00	0.00	0.00	0.00	0.00	0.00	0.00	0.00	0.00	0.00	0.00	0.00
ATPrn	0.00	0.00	0.00	0.00	0.00	0.00	0.00	0.00	0.00	0.00	0.00	0.00	0.00	0.00	0.00	0.00	0.00	0.00	0.00	0.00
GTPrn	0.00	0.00	0.00	0.00	0.00	0.00	0.00	0.00	0.00	0.00	0.00	0.00	0.00	0.00	0.00	0.00	0.00	0.00	0.00	0.00
CTPrn	0.00	0.00	0.00	0.00	0.00	0.00	0.00	0.00	0.00	0.00	0.00	0.00	0.00	0.00	0.00	0.00	0.00	0.00	0.00	0.00
dATP	0.00	0.00	0.00	0.00	0.00	0.00	0.00	0.00	0.00	0.00	0.00	0.00	0.00	0.00	0.00	0.00	0.00	0.00	0.00	0.00
dGTP	0.00	0.00	0.00	0.00	0.00	0.00	0.00	0.00	0.00	0.00	0.00	0.00	0.00	0.00	0.00	0.00	0.00	0.00	0.00	0.00
dTTP	0.00	0.00	0.00	0.00	0.00	0.00	0.00	0.00	0.00	0.00	0.00	0.00	0.00	0.00	0.00	0.00	0.00	0.00	0.00	0.00
dCTP	0.00	0.00	0.00	0.00	0.00	0.00	0.00	0.00	0.00	0.00	0.00	0.00	0.00	0.00	0.00	0.00	0.00	0.00	0.00	0.00
Ethn	0.00	0.00	0.00	0.00	0.00	0.00	0.00	0.00	0.00	0.00	0.00	0.00	0.00	0.00	0.00	0.00	1.00	0.00	0.00	0.00
Cho	0.00	0.00	0.00	0.00	0.00	0.00	0.00	0.00	0.00	0.00	0.00	0.00	0.00	0.00	0.00	0.00	0.00	1.00	0.00	0.00
Glyc3P	0.00	0.00	0.00	0.00	0.00	0.00	0.00	0.00	0.00	0.00	0.00	0.00	0.00	0.00	0.00	0.00	0.00	0.00	0.00	0.00
PhosphE	0.00	0.00	0.00	0.00	0.00	0.00	0.00	0.00	0.00	0.00	0.00	0.00	0.00	0.00	0.00	0.00	0.00	0.00	0.00	0.00
PhosphC	0.00	0.00	0.00	0.00	0.00	0.00	0.00	0.00	0.00	0.00	0.00	0.00	0.00	0.00	0.00	0.00	0.00	0.00	0.00	0.00
PhosphS	0.00	0.00	0.00	0.00	0.00	0.00	0.00	0.00	0.00	0.00	0.00	0.00	0.00	0.00	0.00	0.00	0.00	0.00	0.00	0.00
Sphm	0.00	0.00	0.00	0.00	0.00	0.00	0.00	0.00	0.00	0.00	0.00	0.00	0.00	0.00	0.00	0.00	0.00	0.00	0.00	0.00
Cholesterol	0.00	0.00	0.00	0.00	0.00	0.00	0.00	0.00	0.00	0.00	0.00	0.00	0.00	0.00	0.00	0.00	0.00	0.00	0.00	0.00
Proteins	0.00	0.00	0.00	0.00	0.00	0.00	0.00	0.00	0.00	0.00	0.00	0.00	0.00	0.00	0.00	0.00	0.00	0.00	0.00	0.00
ADN	0.00	0.00	0.00	0.00	0.00	0.00	0.00	0.00	0.00	0.00	0.00	0.00	0.00	0.00	0.00	0.00	0.00	0.00	0.00	0.00
ARN	0.00	0.00	0.00	0.00	0.00	0.00	0.00	0.00	0.00	0.00	0.00	0.00	0.00	0.00	0.00	0.00	0.00	0.00	0.00	0.00
Lipids	0.00	0.00	0.00	0.00	0.00	0.00	0.00	0.00	0.00	0.00	0.00	0.00	0.00	0.00	0.00	0.00	0.00	0.00	0.00	0.00
NH_4^+	0.00	0.00	0.00	0.00	0.00	0.00	0.00	0.00	0.00	0.00	0.00	0.00	0.00	0.00	0.00	0.00	0.00	0.00	-1.00	0.00
CO_2	0.00	0.00	0.00	0.00	0.00	0.00	0.00	0.00	0.00	0.00	0.00	0.00	0.00	0.00	0.00	0.00	0.00	0.00	0.00	-1.00

	v1	v2	v3	v4	v5	v6	v7	v8	v9	v10	v11	v12	v13	v14	v15	v16	v17	v18	v19	v20
Glucose	-1.00	0.00	0.00	0.00	0.00	0.00	0.00	0.00	0.00	0.00	0.00	0.00	0.00	0.00	0.00	0.00	0.00	0.00	0.00	0.00
Gln	0.00	0.00	0.00	0.00	0.00	0.00	0.00	0.00	0.00	0.00	0.00	0.00	0.00	0.00	0.00	0.00	0.00	0.00	0.00	0.00
Ser	0.00	0.00	0.00	0.00	0.00	0.00	0.00	0.00	0.00	0.00	0.00	0.00	0.00	0.00	0.00	0.00	0.00	0.00	0.00	0.00
Asn	0.00	0.00	0.00	0.00	0.00	0.00	0.00	0.00	0.00	0.00	0.00	0.00	0.00	0.00	0.00	0.00	0.00	0.00	0.00	0.00
Asp	0.00	0.00	0.00	0.00	0.00	0.00	0.00	0.00	0.00	0.00	0.00	0.00	0.00	0.00	0.00	0.00	0.00	0.00	0.00	0.00
Arg	0.00	0.00	0.00	0.00	0.00	0.00	0.00	0.00	0.00	0.00	0.00	0.00	0.00	0.00	0.00	0.00	0.00	0.00	0.00	0.00
Tyr	0.00	0.00	0.00	0.00	0.00	0.00	0.00	0.00	0.00	0.00	0.00	0.00	0.00	0.00	0.00	0.00	0.00	0.00	0.00	0.00
Thr	0.00	0.00	0.00	0.00	0.00	0.00	0.00	0.00	0.00	0.00	0.00	0.00	0.00	0.00	0.00	0.00	0.00	0.00	0.00	0.00
Lys	0.00	0.00	0.00	0.00	0.00	0.00	0.00	0.00	0.00	0.00	0.00	0.00	0.00	0.00	0.00	0.00	0.00	0.00	0.00	0.00
Val	0.00	0.00	0.00	0.00	0.00	0.00	0.00	0.00	0.00	0.00	0.00	0.00	0.00	0.00	0.00	0.00	0.00	0.00	0.00	0.00
Ile	0.00	0.00	0.00	0.00	0.00	0.00	0.00	0.00	0.00	0.00	0.00	0.00	0.00	0.00	0.00	0.00	0.00	0.00	0.00	0.00
Leu	0.00	0.00	0.00	0.00	0.00	0.00	0.00	0.00	0.00	0.00	0.00	0.00	0.00	0.00	0.00	0.00	0.00	0.00	0.00	0.00
Phe	0.00	0.00	0.00	0.00	0.00	0.00	0.00	0.00	0.00	0.00	0.00	0.00	0.00	0.00	0.00	0.00	0.00	0.00	0.00	0.00
Met	0.00	0.00	0.00	0.00	0.00	0.00	0.00	0.00	0.00	0.00	0.00	0.00	0.00	0.00	0.00	0.00	0.00	0.00	0.00	0.00
Lactate	0.00	0.00	0.00	0.00	0.00	0.00	0.00	0.00	0.00	0.00	0.00	0.00	0.00	0.00	1.00	0.00	0.00	0.00	0.00	0.00
Ala	0.00	0.00	0.00	0.00	0.00	0.00	0.00	0.00	0.00	0.00	0.00	0.00	0.00	0.00	0.00	0.00	0.00	0.00	0.00	0.00
Gly	0.00	0.00	0.00	0.00	0.00	0.00	0.00	0.00	0.00	0.00	0.00	0.00	0.00	0.00	0.00	0.00	0.00	0.00	0.00	0.00
Glu	0.00	0.00	0.00	0.00	0.00	0.00	0.00	0.00	0.00	0.00	0.00	0.00	0.00	0.00	0.00	0.00	0.00	0.00	0.00	0.00
NH4	0.00	0.00	0.00	0.00	0.00	0.00	0.00	0.00	0.00	0.00	0.00	0.00	0.00	0.00	0.00	0.00	0.00	0.00	0.00	0.00
CO2	0.00	0.00	0.00	0.00	0.00	0.00	0.00	0.00	0.00	0.00	0.00	0.00	0.00	0.00	0.00	0.00	0.00	0.00	0.00	0.00

	v21	v22	v23	v24	v25	v26	v27	v28	v29	v30	v31	v32	v33	v34	v35	v36	v37	v38	v39	v40
Glucose	0.00	0.00	0.00	0.00	0.00	0.00	0.00	0.00	0.00	0.00	0.00	0.00	0.00	0.00	0.00	0.00	0.00	0.00	0.00	0.00
Gln	0.00	0.00	0.00	0.00	0.00	0.00	0.00	0.00	0.00	0.00	0.00	0.00	0.00	0.00	0.00	0.00	0.00	0.00	0.00	0.00
Ser	0.00	0.00	0.00	0.00	0.00	0.00	0.00	0.00	0.00	0.00	0.00	0.00	0.00	0.00	0.00	0.00	0.00	0.00	0.00	0.00
Asn	0.00	0.00	0.00	0.00	0.00	0.00	0.00	0.00	0.00	0.00	0.00	0.00	0.00	0.00	0.00	0.00	0.00	0.00	0.00	0.00
Asp	0.00	0.00	0.00	0.00	0.00	0.00	0.00	0.00	0.00	0.00	0.00	0.00	0.00	0.00	0.00	0.00	0.00	0.00	0.00	0.00
Arg	0.00	0.00	0.00	0.00	0.00	0.00	0.00	0.00	0.00	0.00	0.00	0.00	0.00	0.00	0.00	0.00	0.00	0.00	0.00	0.00
Tyr	0.00	0.00	0.00	0.00	0.00	0.00	0.00	0.00	0.00	0.00	0.00	0.00	0.00	0.00	0.00	0.00	0.00	0.00	0.00	0.00
Thr	0.00	0.00	0.00	0.00	0.00	0.00	0.00	0.00	0.00	0.00	0.00	0.00	0.00	0.00	0.00	0.00	0.00	0.00	0.00	0.00
Lys	0.00	0.00	0.00	0.00	0.00	0.00	0.00	0.00	0.00	0.00	0.00	0.00	0.00	0.00	0.00	0.00	0.00	0.00	0.00	0.00
Val	0.00	0.00	0.00	0.00	0.00	0.00	0.00	0.00	0.00	0.00	0.00	0.00	0.00	0.00	0.00	0.00	0.00	0.00	0.00	0.00
Ile	0.00	0.00	0.00	0.00	0.00	0.00	0.00	0.00	0.00	0.00	0.00	0.00	0.00	0.00	0.00	0.00	0.00	0.00	0.00	0.00
Leu	0.00	0.00	0.00	0.00	0.00	0.00	0.00	0.00	0.00	0.00	0.00	0.00	0.00	0.00	0.00	0.00	0.00	0.00	0.00	0.00
Phe	0.00	0.00	0.00	0.00	0.00	0.00	0.00	0.00	0.00	0.00	0.00	0.00	0.00	0.00	0.00	0.00	0.00	0.00	0.00	0.00
Met	0.00	0.00	0.00	0.00	0.00	0.00	0.00	0.00	0.00	0.00	0.00	0.00	0.00	0.00	0.00	0.00	0.00	0.00	0.00	0.00
Lactate	0.00	0.00	0.00	0.00	0.00	0.00	0.00	0.00	0.00	0.00	0.00	0.00	0.00	0.00	0.00	0.00	0.00	0.00	0.00	0.00
Ala	0.00	0.00	0.00	0.00	0.00	0.00	0.00	0.00	0.00	0.00	0.00	0.00	0.00	0.00	0.00	0.00	0.00	0.00	0.00	0.00
Gly	0.00	0.00	0.00	0.00	0.00	0.00	0.00	0.00	0.00	0.00	0.00	0.00	0.00	0.00	0.00	0.00	0.00	0.00	0.00	0.00
Glu	0.00	0.00	0.00	0.00	0.00	0.00	0.00	0.00	0.00	0.00	0.00	0.00	0.00	0.00	0.00	0.00	0.00	0.00	0.00	0.00
NH4	0.00	0.00	0.00	0.00	0.00	0.00	0.00	0.00	0.00	0.00	0.00	0.00	0.00	0.00	0.00	0.00	0.00	0.00	0.00	0.00
CO2	0.00	0.00	0.00	0.00	0.00	0.00	0.00	0.00	0.00	0.00	0.00	0.00	0.00	0.00	0.00	0.00	0.00	0.00	0.00	0.00

Table A.2: Stoichiometric Matrix $\mathbf{N}_m$ for the extracellular measurements.

	v41	v42	v43	v44	v45	v46	v47	v48	v49	v50	v51	v52	v53	v54	v55	v56	v57	v58	v59	v60
Glucose	0.00	0.00	0.00	0.00	0.00	0.00	0.00	0.00	0.00	0.00	0.00	0.00	0.00	0.00	0.00	0.00	0.00	0.00	0.00	0.00
Gln	0.00	0.00	0.00	0.00	0.00	0.00	0.00	0.00	0.00	0.00	0.00	0.00	0.00	0.00	0.00	0.00	0.00	0.00	0.00	0.00
Ser	0.00	0.00	0.00	0.00	0.00	0.00	0.00	0.00	0.00	0.00	0.00	0.00	0.00	0.00	0.00	0.00	0.00	0.00	0.00	0.00
Asn	0.00	0.00	0.00	0.00	0.00	0.00	0.00	0.00	0.00	0.00	0.00	0.00	0.00	0.00	0.00	0.00	0.00	0.00	0.00	0.00
Asp	0.00	0.00	0.00	0.00	0.00	0.00	0.00	0.00	0.00	0.00	0.00	0.00	0.00	0.00	0.00	0.00	0.00	0.00	0.00	0.00
Arg	0.00	0.00	0.00	0.00	0.00	0.00	0.00	0.00	0.00	0.00	0.00	0.00	0.00	0.00	0.00	0.00	0.00	0.00	0.00	0.00
Tyr	0.00	0.00	0.00	0.00	0.00	0.00	0.00	0.00	0.00	0.00	0.00	0.00	0.00	0.00	0.00	0.00	0.00	0.00	0.00	0.00
Thr	0.00	0.00	0.00	0.00	0.00	0.00	0.00	0.00	0.00	0.00	0.00	0.00	0.00	0.00	0.00	0.00	0.00	0.00	0.00	0.00
Lys	0.00	0.00	0.00	0.00	0.00	0.00	0.00	0.00	0.00	0.00	0.00	0.00	0.00	0.00	0.00	0.00	0.00	0.00	0.00	0.00
Val	0.00	0.00	0.00	0.00	0.00	0.00	0.00	0.00	0.00	0.00	0.00	0.00	0.00	0.00	0.00	0.00	0.00	0.00	0.00	0.00
Ile	0.00	0.00	0.00	0.00	0.00	0.00	0.00	0.00	0.00	0.00	0.00	0.00	0.00	0.00	0.00	0.00	0.00	0.00	0.00	0.00
Leu	0.00	0.00	0.00	0.00	0.00	0.00	0.00	0.00	0.00	0.00	0.00	0.00	0.00	0.00	0.00	0.00	0.00	0.00	0.00	0.00
Phe	0.00	0.00	0.00	0.00	0.00	0.00	0.00	0.00	0.00	0.00	0.00	0.00	0.00	0.00	0.00	0.00	0.00	0.00	0.00	0.00
Met	0.00	0.00	0.00	0.00	0.00	0.00	0.00	0.00	0.00	0.00	0.00	0.00	0.00	0.00	0.00	0.00	0.00	0.00	0.00	0.00
Lactate	0.00	0.00	0.00	0.00	0.00	0.00	0.00	0.00	0.00	0.00	0.00	0.00	0.00	0.00	0.00	0.00	0.00	0.00	0.00	0.00
Ala	0.00	0.00	0.00	0.00	0.00	0.00	0.00	0.00	0.00	0.00	0.00	0.00	0.00	0.00	0.00	0.00	0.00	0.00	0.00	0.00
Gly	0.00	0.00	0.00	0.00	0.00	0.00	0.00	0.00	0.00	0.00	0.00	0.00	0.00	0.00	0.00	0.00	0.00	0.00	0.00	0.00
Glu	0.00	0.00	0.00	0.00	0.00	0.00	0.00	0.00	0.00	0.00	0.00	0.00	0.00	0.00	0.00	0.00	0.00	0.00	0.00	0.00
NH4	0.00	0.00	0.00	0.00	0.00	0.00	0.00	0.00	0.00	0.00	0.00	0.00	0.00	0.00	0.00	0.00	0.00	0.00	0.00	0.00
CO2	0.00	0.00	0.00	0.00	0.00	0.00	0.00	0.00	0.00	0.00	0.00	0.00	0.00	0.00	0.00	0.00	0.00	0.00	0.00	0.00

	v61	v62	v63	v64	v65	v66	v67	v68	v69	v70	v71	v72	v73	v74	v75	v76	v77	v78	v79	v80
Glucose	0.00	0.00	0.00	0.00	0.00	0.00	0.00	0.00	0.00	0.00	0.00	0.00	0.00	0.00	0.00	0.00	0.00	0.00	0.00	0.00
Gln	0.00	0.00	0.00	0.00	0.00	0.00	0.00	0.00	0.00	0.00	0.00	0.00	0.00	0.00	0.00	0.00	0.00	0.00	0.00	0.00
Ser	0.00	0.00	0.00	0.00	0.00	0.00	0.00	0.00	0.00	0.00	0.00	0.00	0.00	0.00	0.00	0.00	0.00	0.00	0.00	-1.00
Asn	0.00	0.00	0.00	0.00	0.00	0.00	0.00	0.00	0.00	0.00	0.00	0.00	0.00	0.00	0.00	0.00	0.00	0.00	0.00	0.00
Asp	0.00	0.00	0.00	0.00	0.00	0.00	0.00	0.00	0.00	0.00	0.00	0.00	0.00	0.00	0.00	0.00	-1.00	0.00	0.00	0.00
Arg	0.00	0.00	0.00	0.00	0.00	0.00	0.00	0.00	0.00	0.00	0.00	0.00	0.00	0.00	0.00	0.00	0.00	0.00	0.00	0.00
Tyr	0.00	0.00	0.00	0.00	0.00	0.00	0.00	0.00	0.00	0.00	0.00	0.00	0.00	0.00	0.00	0.00	0.00	0.00	0.00	0.00
Thr	0.00	0.00	0.00	0.00	0.00	0.00	0.00	0.00	0.00	0.00	0.00	0.00	0.00	0.00	0.00	0.00	0.00	0.00	0.00	0.00
Lys	0.00	0.00	0.00	0.00	0.00	0.00	0.00	0.00	0.00	0.00	0.00	0.00	0.00	0.00	0.00	0.00	0.00	0.00	0.00	0.00
Val	0.00	0.00	0.00	0.00	0.00	0.00	0.00	0.00	0.00	0.00	0.00	0.00	0.00	0.00	0.00	0.00	0.00	0.00	0.00	0.00
Ile	0.00	0.00	0.00	0.00	0.00	0.00	0.00	0.00	0.00	0.00	0.00	0.00	0.00	0.00	0.00	0.00	0.00	0.00	0.00	0.00
Leu	0.00	0.00	0.00	0.00	0.00	0.00	0.00	0.00	0.00	0.00	0.00	0.00	0.00	0.00	0.00	0.00	0.00	0.00	0.00	0.00
Phe	0.00	0.00	0.00	0.00	0.00	0.00	0.00	0.00	0.00	0.00	0.00	0.00	0.00	0.00	0.00	0.00	0.00	0.00	0.00	0.00
Met	0.00	0.00	0.00	0.00	0.00	0.00	0.00	0.00	0.00	0.00	0.00	0.00	0.00	0.00	0.00	0.00	0.00	0.00	0.00	0.00
Lactate	0.00	0.00	0.00	0.00	0.00	0.00	0.00	0.00	0.00	0.00	0.00	0.00	0.00	0.00	0.00	0.00	0.00	0.00	0.00	0.00
Ala	0.00	0.00	0.00	0.00	0.00	0.00	0.00	0.00	0.00	0.00	0.00	0.00	0.00	0.00	0.00	0.00	0.00	0.00	0.00	0.00
Gly	0.00	0.00	0.00	0.00	0.00	0.00	0.00	0.00	0.00	0.00	0.00	0.00	0.00	0.00	0.00	0.00	0.00	0.00	1.00	0.00
Glu	0.00	0.00	0.00	0.00	0.00	0.00	0.00	0.00	0.00	0.00	0.00	0.00	0.00	0.00	0.00	0.00	0.00	0.00	0.00	0.00
NH4	0.00	0.00	0.00	0.00	0.00	0.00	0.00	0.00	0.00	0.00	0.00	0.00	0.00	0.00	0.00	0.00	0.00	0.00	0.00	0.00
CO2	0.00	0.00	0.00	0.00	0.00	0.00	0.00	0.00	0.00	0.00	0.00	0.00	0.00	0.00	0.00	0.00	0.00	0.00	0.00	0.00

	v81	v82	v83	v84	v85	v86	v87	v88	v89	v90	v91	v92	v93	v94	v95	v96	v97	v98	v99	v100
Glucose	0.00	0.00	0.00	0.00	0.00	0.00	0.00	0.00	0.00	0.00	0.00	0.00	0.00	0.00	0.00	0.00	0.00	0.00	0.00	0.00
Gln	0.00	0.00	0.00	0.00	0.00	-1.00	0.00	0.00	0.00	0.00	0.00	0.00	0.00	0.00	0.00	0.00	0.00	0.00	0.00	0.00
Ser	0.00	0.00	0.00	0.00	0.00	0.00	0.00	0.00	0.00	0.00	0.00	0.00	0.00	0.00	0.00	0.00	0.00	0.00	0.00	0.00
Asn	0.00	0.00	0.00	0.00	-1.00	0.00	0.00	0.00	0.00	0.00	0.00	0.00	0.00	0.00	0.00	0.00	0.00	0.00	0.00	0.00
Asp	0.00	0.00	0.00	0.00	0.00	0.00	0.00	0.00	0.00	0.00	0.00	0.00	0.00	0.00	0.00	0.00	0.00	0.00	0.00	0.00
Arg	0.00	0.00	0.00	-1.00	0.00	0.00	0.00	0.00	0.00	0.00	0.00	0.00	0.00	0.00	0.00	0.00	0.00	0.00	0.00	0.00
Tyr	0.00	-1.00	0.00	0.00	0.00	0.00	0.00	0.00	0.00	0.00	0.00	0.00	0.00	0.00	0.00	0.00	0.00	-1.00	0.00	0.00
Thr	0.00	0.00	0.00	0.00	0.00	0.00	0.00	0.00	0.00	0.00	0.00	0.00	0.00	-1.00	0.00	0.00	0.00	0.00	0.00	0.00
Lys	0.00	0.00	0.00	0.00	0.00	0.00	0.00	0.00	0.00	-1.00	0.00	0.00	0.00	0.00	0.00	0.00	0.00	0.00	0.00	0.00
Val	0.00	0.00	0.00	0.00	0.00	0.00	0.00	0.00	0.00	0.00	0.00	0.00	0.00	0.00	0.00	-1.00	0.00	0.00	0.00	0.00
Ile	0.00	0.00	0.00	0.00	0.00	0.00	0.00	-1.00	0.00	0.00	0.00	0.00	0.00	0.00	0.00	0.00	0.00	0.00	0.00	0.00
Leu	0.00	0.00	0.00	0.00	0.00	0.00	0.00	0.00	-1.00	0.00	0.00	0.00	0.00	0.00	0.00	0.00	0.00	0.00	0.00	0.00
Phe	0.00	0.00	0.00	0.00	0.00	0.00	0.00	0.00	0.00	0.00	0.00	-1.00	0.00	0.00	0.00	0.00	0.00	0.00	0.00	0.00
Met	0.00	0.00	0.00	0.00	0.00	0.00	0.00	0.00	0.00	0.00	-1.00	0.00	0.00	0.00	0.00	0.00	0.00	0.00	0.00	0.00
Lactate	0.00	0.00	0.00	0.00	0.00	0.00	0.00	0.00	0.00	0.00	0.00	0.00	0.00	0.00	0.00	0.00	0.00	0.00	0.00	0.00
Ala	0.00	0.00	1.00	0.00	0.00	0.00	0.00	0.00	0.00	0.00	0.00	0.00	0.00	0.00	0.00	0.00	0.00	0.00	0.00	0.00
Gly	0.00	0.00	0.00	0.00	0.00	0.00	0.00	0.00	0.00	0.00	0.00	0.00	0.00	0.00	0.00	0.00	0.00	0.00	0.00	0.00
Glu	1.00	0.00	0.00	0.00	0.00	0.00	0.00	0.00	0.00	0.00	0.00	0.00	0.00	0.00	0.00	0.00	0.00	0.00	0.00	0.00
NH4	0.00	0.00	0.00	0.00	0.00	0.00	0.00	0.00	0.00	0.00	0.00	0.00	0.00	0.00	0.00	0.00	0.00	0.00	1.00	0.00
CO2	0.00	0.00	0.00	0.00	0.00	0.00	0.00	0.00	0.00	0.00	0.00	0.00	0.00	0.00	0.00	0.00	0.00	0.00	0.00	1.00

Appendix B

Error Distributions

B.1   Error Distribution considering 5% Error Measurements
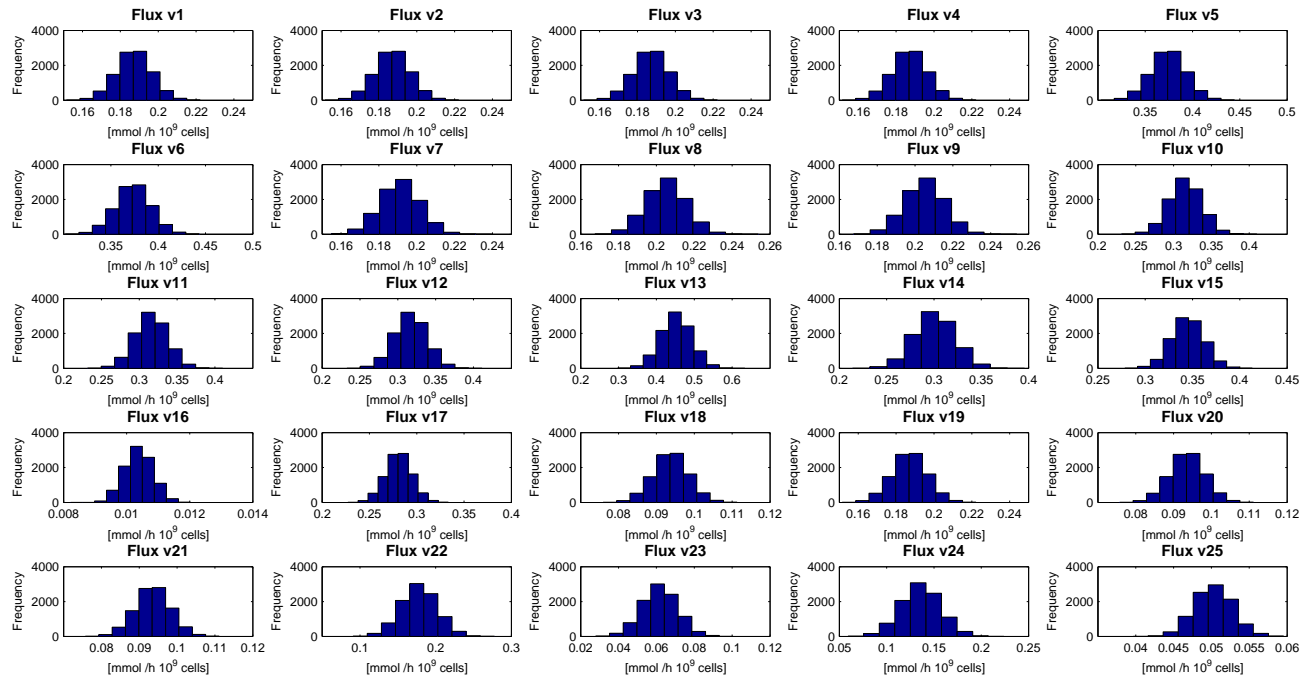
Figure B.1: Error distributions for the upper bounds.
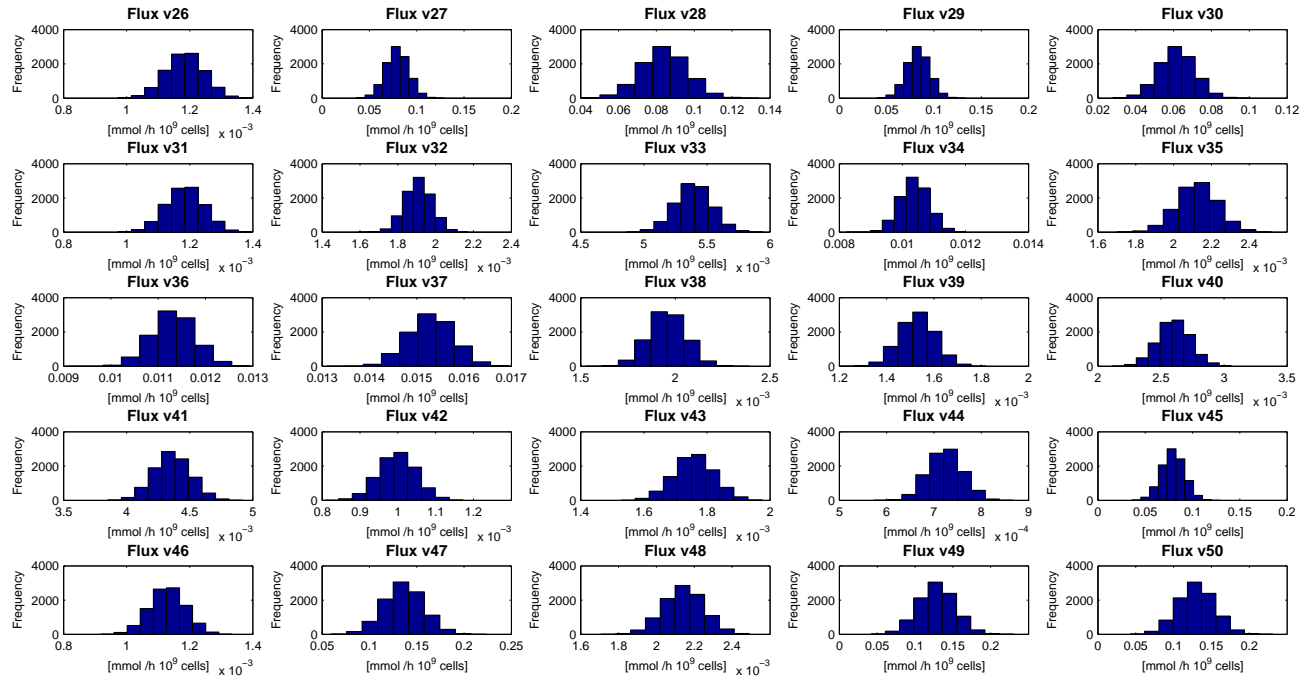
Figure B.2: Error distributions for the upper bounds (continuation).
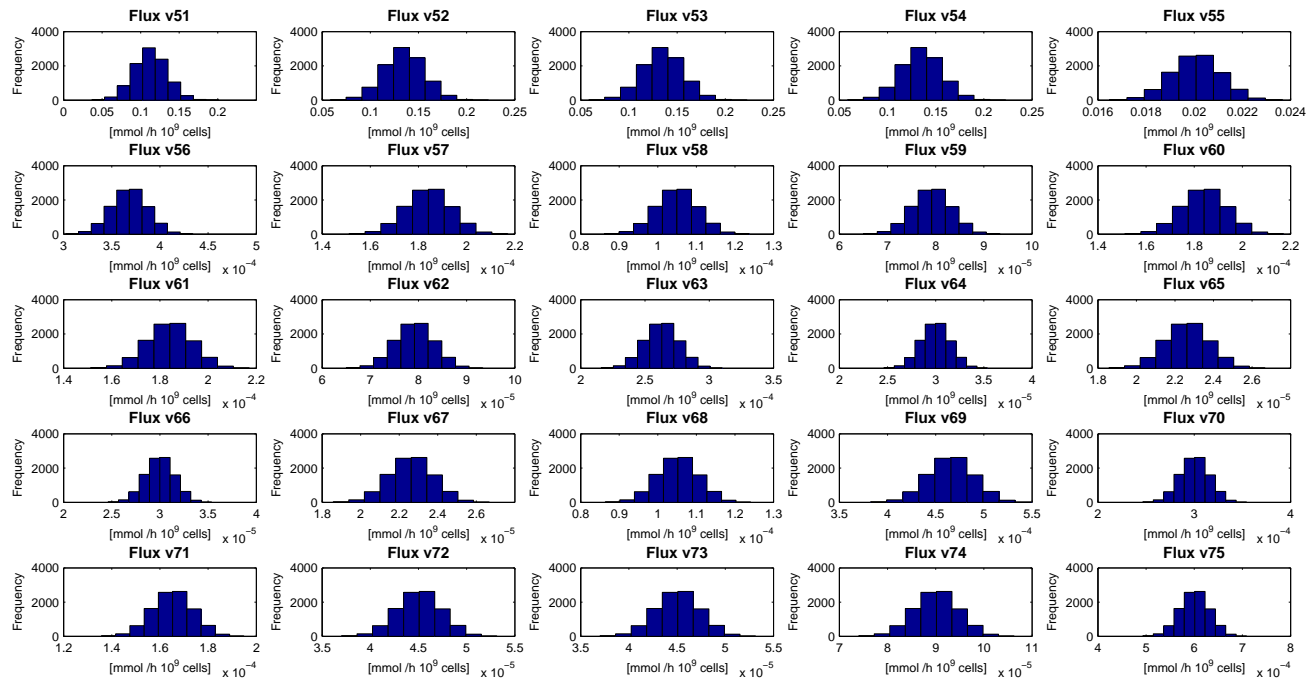
Figure B.3: Error distributions for the upper bounds (continuation).
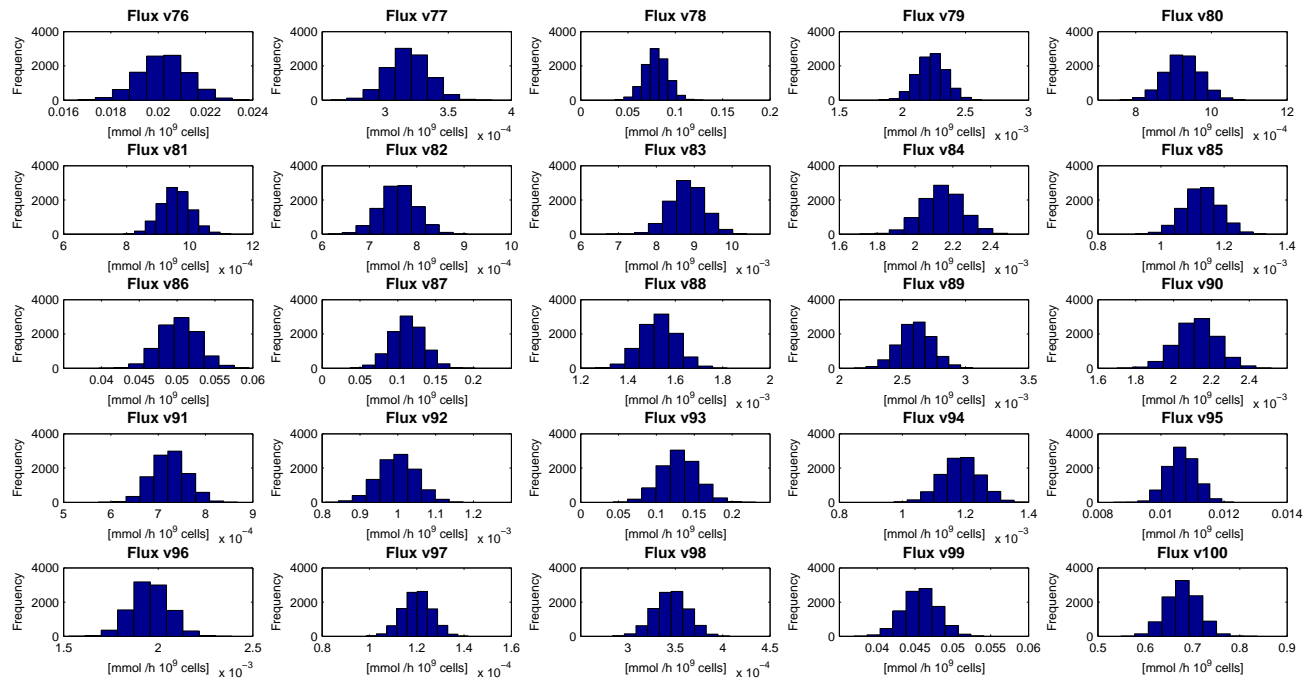
Figure B.4: Error distributions for the upper bounds (continuation).
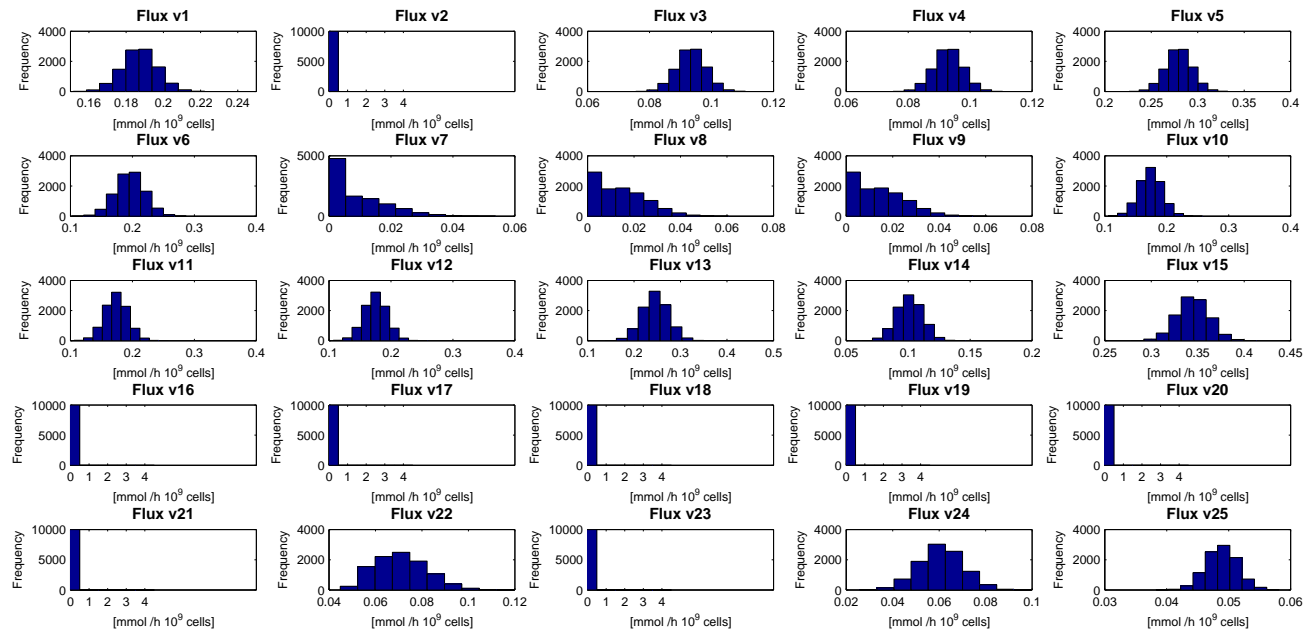
Figure B.5: Error distributions for the lower bounds.
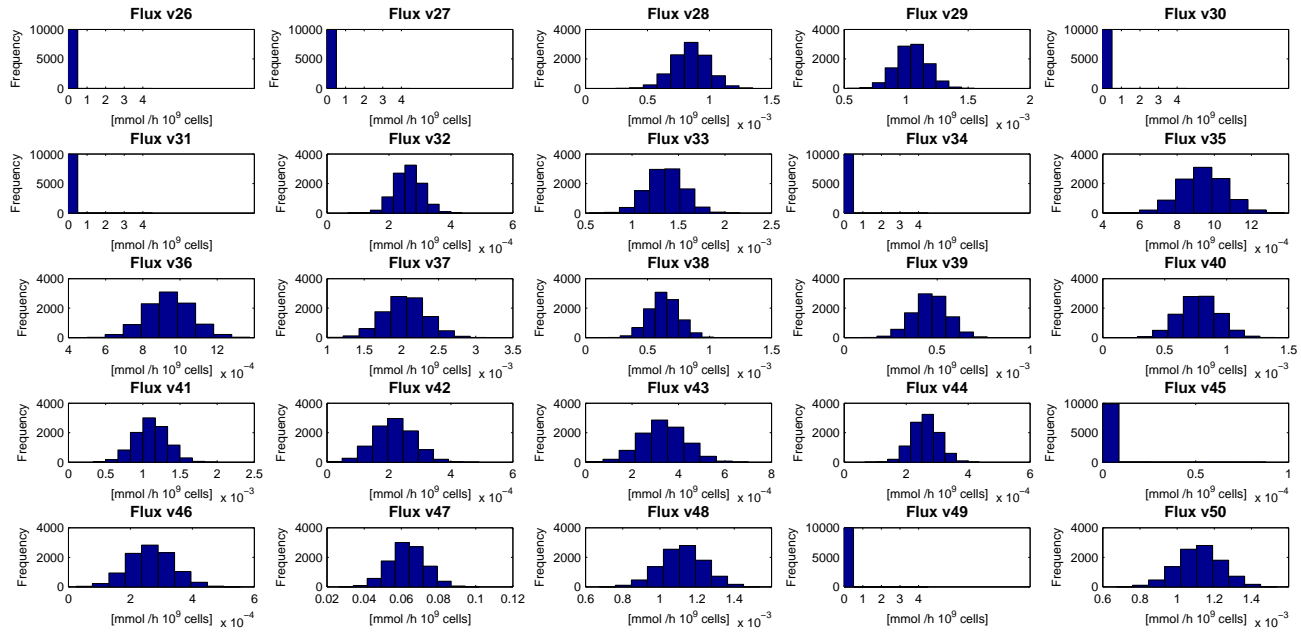
Figure B.6: Error distributions for the lower bounds (continuation).
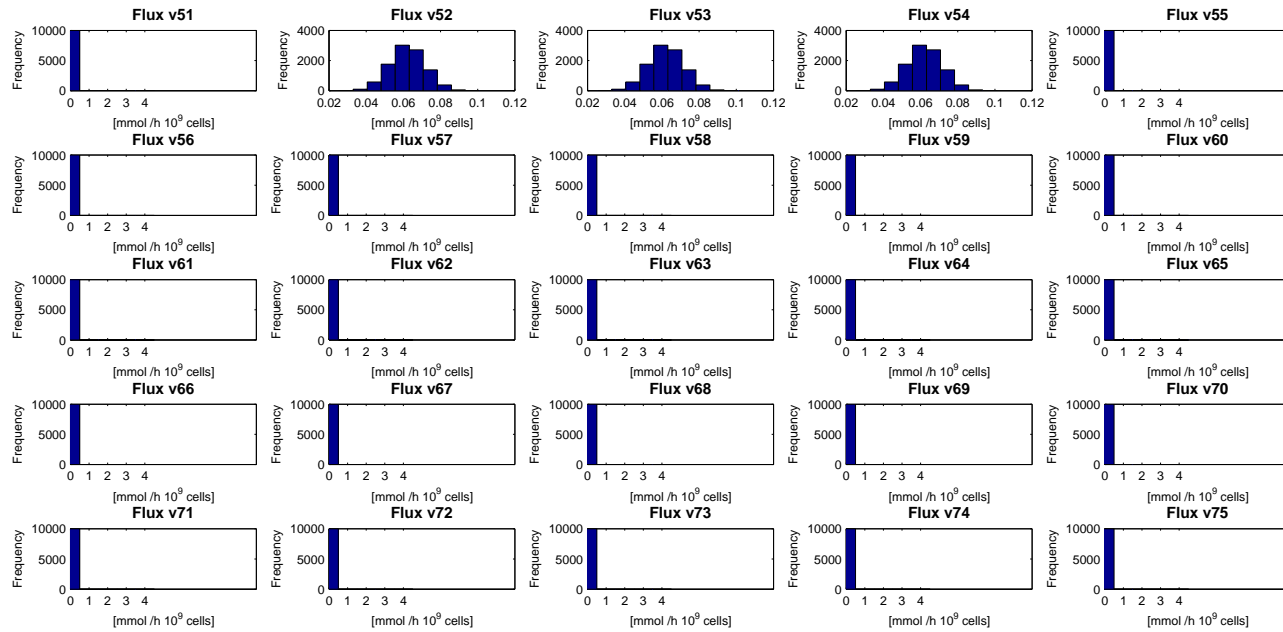
Figure B.7: Error distributions for the lower bounds (continuation).
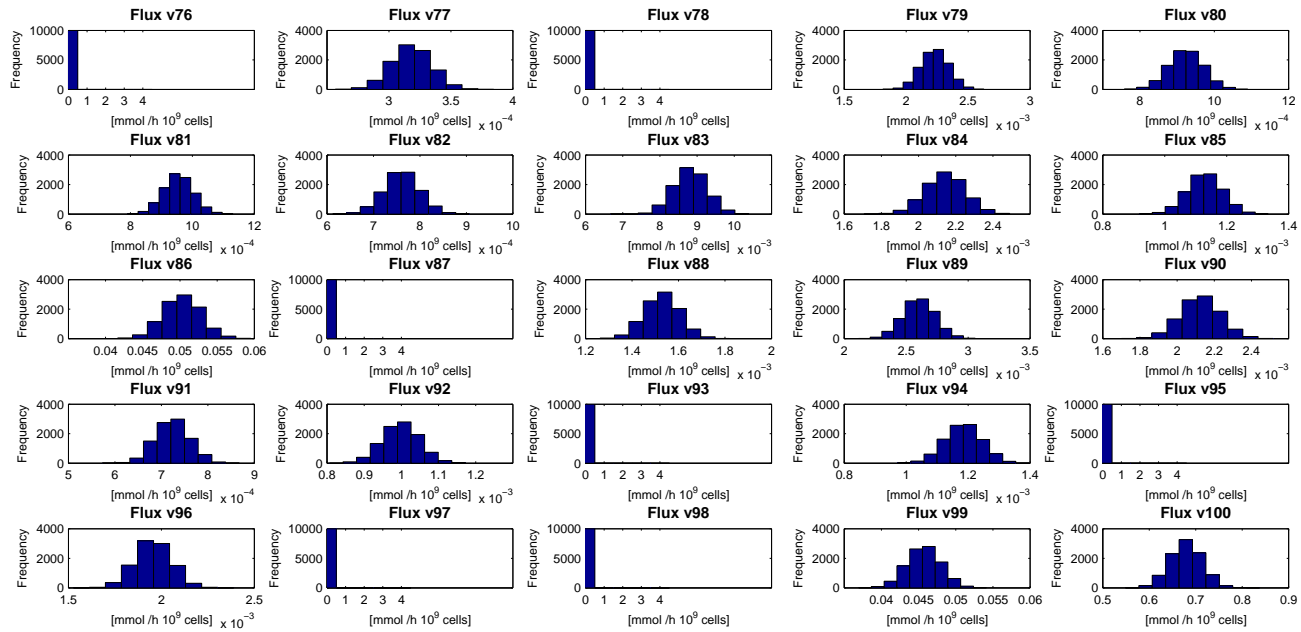
Figure B.8: Error distributions for the lower bounds (continuation).

Appendix C

Minimal Set of EFMs

C.1 Minimal Set of EFM for the Exponential Growth Phase

C.2 Minimal Set of EFMs for the Transition Phase

C.3 Minimal Set of EFMs for the Death Phase

	e1	e2	e3	e4	e5	e6	e7	e8	e9	e10	e11	e12	e13	e14	e15	e16	e17	e18	e19
v1	0.00	0.16	0.00	0.00	0.00	0.43	0.68	0.11	0.56	0.23	0.00	0.66	0.00	0.21	0.26	0.78	0.14	0.31	0.10
v2	0.00	0.00	0.00	0.00	0.00	0.00	0.00	0.00	0.00	0.00	0.00	0.00	0.00	0.00	0.00	0.00	0.00	0.00	0.00
v3	0.00	0.11	0.00	0.00	0.00	0.24	0.39	0.07	0.29	0.13	0.00	0.41	0.00	0.14	0.16	0.50	0.09	0.20	0.07
v4	0.00	0.11	0.00	0.00	0.00	0.17	0.27	0.07	0.13	0.09	0.00	0.35	0.00	0.14	0.14	0.46	0.09	0.17	0.07
v5	0.00	0.26	0.00	0.00	0.00	0.53	0.85	0.19	0.57	0.29	0.00	0.97	0.00	0.35	0.39	1.20	0.23	0.47	0.17
v6	0.00	0.00	0.00	0.00	0.00	0.00	0.00	0.00	0.00	0.00	0.00	0.00	0.00	0.35	0.00	0.00	0.00	0.00	0.00
v7	0.00	0.00	0.00	0.00	0.00	0.00	0.00	0.00	0.00	0.00	0.00	0.00	0.00	0.00	0.00	0.00	0.00	0.00	0.00
v8	184.67	0.00	0.00	0.00	0.00	0.00	0.00	0.00	0.00	0.00	0.00	0.00	0.00	0.00	0.00	0.00	0.00	0.00	0.00
v9	184.67	0.00	0.00	0.00	0.00	0.00	0.00	0.00	0.00	0.00	0.00	0.00	0.00	0.00	0.00	0.00	0.00	0.00	0.00
v10	92.34	0.26	0.00	0.00	0.00	0.50	0.21	0.00	0.00	0.00	1.51	0.00	0.40	0.00	0.16	0.21	0.12	0.04	0.17
v11	0.00	0.26	0.00	0.00	0.00	0.00	0.31	0.19	0.11	1.00	1.51	0.19	0.40	0.00	0.00	0.24	0.12	0.06	0.17
v12	92.34	0.26	0.00	0.00	0.00	0.56	0.31	0.19	0.87	1.00	1.51	0.19	0.40	0.00	0.18	0.24	0.12	0.06	0.17
v13	184.67	0.26	0.00	0.00	0.46	0.61	0.38	0.19	0.97	1.03	1.51	0.22	0.80	0.00	0.19	0.27	0.12	0.08	0.17
v14	184.67	0.00	0.00	0.00	0.00	0.00	0.38	0.00	0.49	0.13	0.00	0.18	0.40	0.00	0.07	0.14	0.00	0.08	0.00
v15	0.00	0.26	0.00	0.00	0.46	0.00	0.00	0.37	0.00	0.29	0.00	0.00	0.40	0.35	0.27	0.00	0.35	0.21	0.34
v16	0.00	0.00	0.00	0.00	0.00	0.61	0.00	0.00	0.48	0.60	1.51	0.18	0.00	0.00	0.07	0.13	0.00	0.08	0.00
v17	0.00	0.16	0.00	0.00	0.00	0.43	0.68	0.11	0.56	0.23	0.00	0.66	0.00	0.21	0.26	0.78	0.14	0.31	0.10
v18	0.00	0.05	0.00	0.00	0.00	0.18	0.29	0.04	0.27	0.10	0.00	0.25	0.00	0.07	0.10	0.28	0.05	0.12	0.03
v19	0.00	0.11	0.00	0.00	0.00	0.24	0.39	0.07	0.29	0.13	0.00	0.41	0.00	0.14	0.16	0.50	0.09	0.20	0.07
v20	0.00	0.05	0.00	0.00	0.00	0.12	0.19	0.04	0.14	0.07	0.00	0.21	0.00	0.07	0.08	0.25	0.05	0.10	0.03
v21	0.00	0.05	0.00	0.00	0.00	0.12	0.19	0.04	0.14	0.07	0.00	0.21	0.00	0.07	0.08	0.25	0.05	0.10	0.03
v22	0.00	0.26	0.00	0.00	0.46	0.61	0.00	0.19	0.48	0.89	1.51	0.04	0.40	0.00	0.12	0.13	0.12	0.00	0.17
v23	0.00	0.00	0.00	0.00	0.00	0.00	0.00	0.00	0.00	0.00	0.00	0.00	0.00	0.00	0.00	0.00	0.00	0.00	0.00
v24	0.00	0.00	0.00	0.00	0.00	0.00	0.38	0.00	0.49	0.13	0.00	0.18	0.40	0.00	0.07	0.14	0.00	0.08	0.00
v25	0.00	0.26	1.63	0.00	0.00	0.61	0.00	0.00	0.22	0.00	1.51	0.08	0.40	0.00	0.00	0.00	0.00	0.08	0.17
v26	0.00	0.00	0.00	0.00	0.00	0.00	0.00	0.00	0.51	0.00	0.00	0.00	0.00	0.00	0.00	0.00	0.00	0.00	0.00
v27	0.00	0.26	0.00	50.25	0.00	0.25	0.40	0.00	0.00	0.14	0.00	0.62	0.00	0.00	0.08	1.05	0.00	0.08	0.00
v28	0.00	0.26	0.00	0.00	0.00	0.53	0.85	0.19	0.57	0.29	0.00	0.97	0.00	0.00	0.39	1.20	0.23	0.47	0.17
v29	0.00	0.26	0.00	0.00	0.00	0.00	0.00	0.00	0.00	0.00	0.00	0.00	0.00	0.00	0.00	0.00	0.00	0.00	0.00
v30	0.00	0.00	0.00	0.00	0.00	0.00	0.00	0.19	0.00	0.00	0.00	0.00	0.00	0.00	0.22	0.00	0.23	0.29	0.17
v31	0.00	0.00	0.00	0.00	0.00	0.00	0.00	0.00	0.00	0.00	0.00	0.00	0.00	0.00	0.00	0.00	0.00	0.00	0.00
v32	0.00	0.00	0.00	0.00	0.00	0.06	0.09	0.00	0.12	0.03	0.00	0.19	0.00	0.00	0.02	0.03	0.00	0.02	0.00
v33	0.00	0.00	0.00	0.00	0.00	0.06	0.09	0.19	0.87	1.00	0.00	0.19	0.00	0.00	0.02	0.03	0.00	0.02	0.00
v34	0.00	0.00	0.00	0.00	0.00	0.00	1.09	0.00	0.00	0.00	0.00	0.00	0.00	0.00	0.00	0.00	0.00	0.00	0.00
v35	0.00	0.00	0.00	0.00	0.00	0.04	0.32	0.00	0.01	0.00	0.00	0.67	0.00	0.00	0.00	0.50	0.00	0.29	0.00
v36	0.00	0.00	0.00	0.00	0.00	0.04	1.40	0.00	0.01	0.00	0.00	0.67	0.00	0.00	0.00	0.50	0.00	0.29	0.00
v37	92.34	0.00	0.00	0.00	0.00	0.60	1.40	0.00	0.77	0.00	0.00	0.67	0.00	0.00	0.18	0.50	0.00	0.29	0.00
v38	0.00	0.00	0.00	0.00	0.00	0.00	0.00	0.19	0.00	0.00	0.00	0.00	0.00	0.00	0.00	0.00	0.00	0.00	0.00
v39	0.00	0.00	0.00	0.00	0.00	0.00	0.00	0.00	0.75	0.97	0.00	0.00	0.00	0.00	0.00	0.00	0.00	0.00	0.00
v40	0.00	0.00	0.00	0.00	0.00	0.56	0.00	0.00	0.76	0.00	0.00	0.00	0.00	0.00	0.18	0.00	0.00	0.00	0.00
v41	92.34	0.00	0.00	0.00	0.00	0.56	0.00	0.00	0.76	0.00	0.00	0.00	0.00	0.00	0.18	0.00	0.00	0.00	0.00
v42	0.00	0.00	0.00	0.00	0.00	0.10	0.16	0.00	0.20	0.05	0.00	0.07	0.00	0.00	0.03	0.06	0.00	0.03	0.00
v43	92.34	0.00	0.00	0.00	0.00	0.00	0.00	0.00	0.00	0.00	0.00	0.00	0.00	0.00	0.00	0.00	0.00	0.00	0.00
v44	0.00	0.00	0.00	0.00	0.00	0.06	0.09	0.00	0.12	0.03	0.00	0.19	0.00	0.00	0.02	0.03	0.00	0.02	0.00
v45	0.00	0.00	0.00	0.00	0.00	0.00	0.00	0.00	0.00	0.00	0.00	0.14	0.00	0.00	0.00	0.00	0.00	0.00	0.00
v46	0.00	0.00	0.00	0.00	0.46	0.00	0.00	0.00	0.00	0.00	0.00	0.00	0.00	0.00	0.00	0.00	0.00	0.00	0.00
v47	0.00	0.00	0.00	0.00	0.46	0.00	0.38	0.00	0.00	0.06	0.00	0.00	0.40	0.00	0.19	0.27	0.12	0.00	0.00
v48	0.00	0.00	0.00	0.00	0.00	0.00	0.38	0.00	0.00	0.06	0.00	0.00	0.00	0.00	0.19	0.27	0.12	0.00	0.00
v49	0.00	0.00	0.00	0.00	0.00	0.00	0.00	0.00	0.00	0.00	0.00	0.00	0.00	0.00	0.00	0.00	0.00	0.00	0.00
v50	0.00	0.00	0.00	0.00	0.00	0.00	0.38	0.00	0.00	0.06	0.00	0.00	0.00	0.00	0.19	0.27	0.12	0.00	0.00

Table C.1: EFMs for the Exponential Growth Phase.

	e1	e2	e3	e4	e5	e6	e7	e8	e9	e10	e11	e12	e13	e14	e15	e16	e17	e18	e19
v51	0.00	0.00	0.00	0.00	0.00	0.00	0.00	0.00	0.00	0.00	0.00	0.00	0.00	0.00	0.00	0.00	0.00	0.00	0.00
v52	0.00	0.00	0.00	0.00	0.46	0.00	0.00	0.00	0.00	0.00	0.00	0.00	0.40	0.00	0.00	0.00	0.00	0.00	0.00
v53	0.00	0.00	0.00	0.00	0.46	0.00	0.00	0.00	0.00	0.00	0.00	0.00	0.40	0.00	0.00	0.00	0.00	0.00	0.00
v54	0.00	0.00	0.00	0.00	0.46	0.00	0.00	0.00	0.00	0.00	0.00	0.00	0.40	0.00	0.00	0.00	0.00	0.00	0.00
v55	0.00	0.00	0.00	0.00	0.00	3.07	4.89	0.00	6.19	1.69	0.00	2.32	0.00	0.00	0.93	1.73	0.00	1.01	0.00
v56	0.00	0.00	0.00	0.00	0.00	0.06	0.10	0.00	0.12	0.03	0.00	0.05	0.00	0.00	0.02	0.03	0.00	0.02	0.00
v57	0.00	0.00	0.00	0.00	0.00	0.03	0.05	0.00	0.06	0.02	0.00	0.02	0.00	0.00	0.01	0.02	0.00	0.01	0.00
v58	0.00	0.00	0.00	0.00	0.00	0.02	0.03	0.00	0.03	0.01	0.00	0.01	0.00	0.00	0.01	0.01	0.00	0.01	0.00
v59	0.00	0.00	0.00	0.00	0.00	0.01	0.02	0.00	0.03	0.01	0.00	0.01	0.00	0.00	0.00	0.01	0.00	0.00	0.00
v60	0.00	0.00	0.00	0.00	0.00	0.03	0.05	0.00	0.06	0.02	0.00	0.02	0.00	0.00	0.01	0.02	0.00	0.01	0.00
v61	0.00	0.00	0.00	0.00	0.00	0.03	0.05	0.00	0.06	0.02	0.00	0.02	0.00	0.00	0.01	0.02	0.00	0.01	0.00
v62	0.00	0.00	0.00	0.00	0.00	0.01	0.02	0.00	0.03	0.01	0.00	0.01	0.00	0.00	0.00	0.01	0.00	0.00	0.00
v63	0.00	0.00	0.00	0.00	0.00	0.04	0.07	0.00	0.09	0.02	0.00	0.03	0.00	0.00	0.01	0.02	0.00	0.01	0.00
v64	0.00	0.00	0.00	0.00	0.00	0.00	0.01	0.00	0.01	0.00	0.00	0.00	0.00	0.00	0.00	0.00	0.00	0.00	0.00
v65	0.00	0.00	0.00	0.00	0.00	0.00	0.01	0.00	0.01	0.00	0.00	0.00	0.00	0.00	0.00	0.00	0.00	0.00	0.00
v66	0.00	0.00	0.00	0.00	0.00	0.00	0.01	0.00	0.01	0.00	0.00	0.00	0.00	0.00	0.00	0.00	0.00	0.00	0.00
v67	0.00	0.00	0.00	0.00	0.00	0.00	0.01	0.00	0.01	0.00	0.00	0.00	0.00	0.00	0.00	0.00	0.00	0.00	0.00
v68	0.00	0.00	0.00	0.00	0.00	0.02	0.03	0.00	0.03	0.01	0.00	0.01	0.00	0.00	0.01	0.01	0.00	0.01	0.00
v69	0.00	0.00	0.00	0.00	0.00	0.08	0.12	0.00	0.15	0.04	0.00	0.06	0.00	0.00	0.02	0.04	0.00	0.03	0.00
v70	0.00	0.00	0.00	0.00	0.00	0.05	0.08	0.00	0.10	0.03	0.00	0.04	0.00	0.00	0.01	0.03	0.00	0.02	0.00
v71	0.00	0.00	0.00	0.00	0.00	0.03	0.04	0.00	0.05	0.01	0.00	0.02	0.00	0.00	0.01	0.02	0.00	0.01	0.00
v72	0.00	0.00	0.00	0.00	0.00	0.01	0.01	0.00	0.01	0.00	0.00	0.01	0.00	0.00	0.00	0.00	0.00	0.00	0.00
v73	0.00	0.00	0.00	0.00	0.00	0.01	0.01	0.00	0.01	0.00	0.00	0.01	0.00	0.00	0.00	0.00	0.00	0.00	0.00
v74	0.00	0.00	0.00	0.00	0.00	0.01	0.02	0.00	0.03	0.01	0.00	0.01	0.00	0.00	0.00	0.01	0.00	0.00	0.00
v75	0.00	0.00	0.00	0.00	0.00	0.10	0.16	0.00	0.20	0.05	0.00	0.07	0.00	0.00	0.03	0.06	0.00	0.03	0.00
v76	0.00	0.00	0.00	0.00	0.00	3.33	5.30	0.00	6.71	1.83	0.00	2.52	0.00	0.00	1.01	1.87	0.00	1.09	0.00
v77	0.00	0.00	0.00	0.00	0.00	0.24	0.00	0.00	0.00	0.00	0.00	0.00	0.00	0.00	0.00	0.00	0.00	0.00	0.00
v78	0.00	0.00	0.00	0.00	0.00	0.00	0.00	0.00	0.00	0.00	0.00	0.00	0.00	0.00	0.00	0.00	0.00	0.00	0.00
v79	0.00	0.00	0.00	50.25	0.00	0.00	0.00	0.00	0.00	0.00	0.00	0.43	0.00	0.00	0.00	0.90	0.00	0.00	0.00
v80	0.00	0.00	0.00	50.25	0.00	0.00	0.00	0.00	0.00	0.00	0.00	0.00	0.00	0.00	0.00	0.00	0.00	0.00	0.00
v81	92.34	0.00	1.63	0.00	0.00	0.00	0.00	0.00	0.00	0.00	0.00	0.00	0.00	0.00	0.00	0.00	0.00	0.00	0.00
v82	92.34	0.00	0.00	0.00	0.00	0.00	0.00	0.00	0.00	0.00	0.00	0.00	0.00	0.00	0.00	0.00	0.00	0.00	0.00
v83	0.00	0.00	0.00	0.00	0.00	0.37	0.71	0.00	0.00	0.47	1.51	0.00	0.00	0.00	0.00	0.00	0.00	0.00	0.00
v84	0.00	0.00	0.00	0.00	0.00	0.16	0.63	0.00	0.32	0.14	0.00	0.12	0.00	0.00	0.24	0.36	0.12	0.05	0.00
v85	0.00	0.00	0.00	0.00	0.46	0.13	0.21	0.00	0.27	0.07	0.00	0.10	0.00	0.00	0.04	0.07	0.00	0.04	0.00
v86	0.00	0.26	1.63	0.00	0.00	0.83	0.34	0.00	0.65	0.12	1.51	0.24	0.40	0.00	0.07	0.12	0.00	0.15	0.17
v87	0.00	0.00	0.00	0.00	0.00	0.07	0.11	0.00	0.14	0.04	0.00	0.05	0.00	0.00	0.02	0.04	0.00	0.02	0.00
v88	0.00	0.00	0.00	0.00	0.00	0.16	0.26	0.00	1.08	1.06	0.00	0.12	0.00	0.00	0.05	0.09	0.00	0.05	0.00
v89	0.00	0.00	0.00	0.00	0.00	0.84	0.44	0.00	1.32	0.15	0.00	0.21	0.00	0.00	0.26	0.16	0.00	0.09	0.00
v90	0.00	0.00	0.00	0.00	0.00	0.22	0.60	0.00	0.38	0.10	0.00	0.80	0.00	0.00	0.05	0.60	0.00	0.35	0.00
v91	0.00	0.00	0.00	0.00	0.00	0.13	0.21	0.00	0.26	0.07	0.00	0.24	0.00	0.00	0.04	0.07	0.00	0.04	0.00
v92	0.00	0.00	0.00	0.00	0.00	0.22	0.35	0.00	0.44	0.12	0.00	0.16	0.00	0.00	0.07	0.12	0.00	0.07	0.00
v93	0.00	0.00	0.00	0.00	0.00	0.16	0.25	0.00	0.32	0.09	0.00	0.12	0.00	0.00	0.05	0.09	0.00	0.05	0.00
v94	0.00	0.00	0.00	0.00	0.00	0.18	0.29	0.00	0.87	0.10	0.00	0.14	0.00	0.00	0.05	0.10	0.00	0.06	0.00
v95	0.00	0.00	0.00	0.00	0.00	0.04	1.16	0.00	0.09	0.02	0.00	0.03	0.00	0.00	0.01	0.02	0.00	0.01	0.00
v96	0.00	0.00	0.00	0.00	0.00	0.20	0.32	0.19	0.41	0.11	0.00	0.15	0.00	0.00	0.06	0.11	0.00	0.07	0.00
v97	0.00	0.00	0.00	0.00	0.00	0.02	0.03	0.00	0.04	0.01	0.00	0.01	0.00	0.00	0.01	0.01	0.00	0.01	0.00
v98	0.00	0.00	0.00	0.00	0.00	0.06	0.09	0.00	0.11	0.03	0.00	0.04	0.00	0.00	0.02	0.03	0.00	0.02	0.00
v99	0.00	0.53	1.63	0.00	0.00	0.64	0.04	0.19	0.27	0.02	1.51	0.38	0.00	0.00	0.23	0.02	0.23	0.38	0.34
v100	369.35	0.95	0.00	0.00	0.00	1.69	5.99	0.49	1.21	1.17	3.02	2.09	0.40	0.21	0.57	2.16	0.38	0.96	0.44

Table C.2: EFMs for the Exponential Growth Phase (continuation).

	e1	e2	e3	e4	e5	e6	e7	e8	e9	e10	e11	e12	e13	e14	e15	e16	e17	e18
v1	0.00	0.00	0.00	0.00	0.00	0.03	0.00	0.00	0.03	0.00	0.00	0.00	0.00	0.00	0.00	0.00	0.00	0.00
v2	3.45	0.00	0.00	0.00	0.00	0.00	0.00	0.00	0.00	0.00	0.00	0.00	0.00	0.00	0.00	0.00	0.00	0.00
v3	1.15	0.42	0.73	0.00	8.81	0.01	1.25	0.88	0.00	1.13	2.26	1.13	1.09	1.50	3.43	1.04	1.33	1.36
v4	1.15	0.00	0.00	0.00	8.81	0.00	0.00	0.00	0.00	0.00	0.00	1.13	0.00	0.00	3.43	0.00	0.00	0.00
v5	1.15	0.00	0.00	0.00	8.81	0.00	0.00	0.00	0.00	0.00	0.00	1.13	0.00	0.00	3.43	0.00	0.00	0.00
v6	1.15	0.00	0.00	0.00	8.81	0.00	0.00	0.00	0.00	0.00	0.00	1.13	0.00	0.00	3.43	0.00	0.00	0.00
v7	3.45	0.00	0.00	0.00	26.43	0.00	0.00	0.00	0.00	0.00	0.00	3.39	0.00	0.00	10.28	0.00	0.00	0.00
v8	0.00	0.00	0.73	0.00	0.00	0.03	1.25	0.00	0.03	0.00	0.00	0.00	0.00	0.00	0.00	0.00	0.00	0.00
v9	2.30	0.00	7.34	0.00	0.00	0.00	1.25	0.00	0.03	4.52	6.78	0.00	1.09	1.50	1.71	3.12	1.33	2.72
v10	2.30	0.00	7.34	0.00	0.00	0.00	1.25	0.00	0.03	4.52	6.78	0.00	1.09	1.50	1.71	3.12	1.33	2.72
v11	2.30	0.42	7.34	0.00	0.00	0.01	1.25	0.00	0.03	4.52	6.78	1.13	2.18	1.50	1.71	3.12	1.33	2.72
v12	1.15	0.42	5.88	0.00	0.00	0.01	1.25	0.88	0.03	4.52	4.52	1.13	2.18	3.00	5.14	4.16	1.33	4.08
v13	2.30	0.42	8.08	0.00	0.00	0.01	1.25	0.88	0.03	5.65	6.78	1.13	2.18	3.00	5.14	4.16	1.33	4.08
v14	3.45	0.42	9.55	0.00	8.81	0.01	2.50	0.88	0.03	6.78	11.30	2.26	3.27	4.51	6.86	6.24	2.65	5.44
v15	0.00	0.42	9.55	0.00	8.81	0.01	2.50	0.88	0.03	6.78	11.30	2.26	3.27	4.51	6.86	6.24	2.65	5.44
v16	3.45	0.00	0.00	0.00	26.43	0.00	0.00	0.00	0.00	0.00	0.00	3.39	0.00	0.00	10.28	0.00	0.00	0.00
v17	1.15	0.00	0.00	0.00	8.81	0.00	0.00	0.00	0.00	0.00	0.00	1.13	0.00	0.00	3.43	0.00	0.00	0.00
v18	2.30	0.00	0.00	0.00	17.62	0.00	0.00	0.00	0.00	0.00	0.00	2.26	0.00	0.00	6.86	0.00	0.00	0.00
v19	1.15	0.00	0.00	0.00	8.81	0.00	0.00	0.00	0.00	0.00	0.00	1.13	0.00	0.00	3.43	0.00	0.00	0.00
v20	1.15	0.00	0.00	0.00	8.81	0.00	0.00	0.00	0.00	0.00	0.00	1.13	0.00	0.00	3.43	0.00	0.00	0.00
v21	3.45	0.00	0.00	0.00	0.00	0.00	0.00	0.00	0.00	0.00	0.00	0.00	0.00	0.00	0.00	0.00	0.00	0.00
v22	0.00	0.00	0.00	0.00	0.00	0.00	1.25	0.00	0.00	0.00	0.00	0.00	0.00	0.00	0.00	0.00	0.00	0.00
v23	1.15	0.00	0.00	0.00	0.00	0.00	0.00	0.00	0.00	0.00	0.00	0.00	0.00	0.00	0.00	0.00	0.00	0.00
v24	0.00	0.00	1.47	0.00	0.00	0.00	0.00	0.00	0.00	1.13	2.26	1.13	1.09	1.50	1.71	2.08	0.00	1.36
v25	0.00	0.42	0.00	0.00	0.00	0.00	0.00	0.00	0.00	0.00	0.00	1.13	0.00	0.00	0.00	0.00	0.00	0.00
v26	0.00	0.00	0.00	0.00	0.00	0.00	0.00	0.00	0.00	0.00	0.00	0.00	0.00	0.00	0.00	0.00	0.00	0.00
v27	0.00	0.42	0.00	0.81	0.00	0.00	1.25	0.88	0.00	1.13	2.26	0.00	1.09	1.50	0.00	1.04	1.33	1.36
v28	0.00	0.42	0.73	0.00	0.00	0.01	1.25	0.88	0.00	1.13	2.26	0.00	1.09	1.50	0.00	1.04	1.33	1.36
v29	0.00	0.42	0.00	0.00	0.00	0.00	1.25	0.00	0.00	1.13	2.26	0.00	1.09	1.50	0.00	1.04	1.33	1.36
v30	0.00	0.00	0.00	0.00	0.00	0.00	0.00	0.00	0.00	0.00	0.00	0.00	0.00	0.00	0.00	0.00	0.00	0.00
v31	0.00	0.00	0.00	0.00	0.00	0.00	0.00	0.00	0.00	0.00	0.00	0.00	0.00	0.00	1.71	1.04	0.00	0.00
v32	0.00	0.00	0.73	0.00	0.00	0.00	0.00	0.00	0.00	0.00	0.00	0.00	0.00	0.00	1.71	1.04	0.00	0.00
v33	0.00	0.00	0.73	0.00	0.00	0.00	0.00	0.88	0.00	1.13	0.00	0.00	0.00	1.50	3.43	1.04	0.00	1.36
v34	0.00	0.00	0.00	0.00	0.00	0.00	0.00	0.00	0.00	0.00	0.00	0.00	0.00	0.00	0.00	0.00	0.00	0.00
v35	0.00	0.00	0.00	0.00	0.00	0.00	0.00	0.00	0.00	0.00	1.13	0.00	0.55	0.75	0.00	1.56	0.66	0.68
v36	0.00	0.00	0.00	0.00	0.00	0.00	0.00	0.00	0.00	0.00	1.13	0.00	0.55	0.75	0.00	1.56	0.66	0.68
v37	1.15	0.00	2.20	0.00	0.00	0.00	0.00	0.00	0.00	1.13	3.39	0.00	0.55	0.75	0.00	1.56	0.66	0.68
v38	0.00	0.00	0.00	0.00	0.00	0.00	0.00	0.88	0.00	0.00	0.00	0.00	0.00	1.50	0.00	0.00	0.00	0.00
v39	0.00	0.00	0.00	0.00	0.00	0.00	0.00	0.00	0.00	1.13	0.00	0.00	0.00	0.00	1.71	0.00	0.00	1.36
v40	0.00	0.00	2.20	0.00	0.00	0.00	0.00	0.00	0.00	1.13	0.00	0.00	0.00	0.00	0.00	0.00	0.00	0.00
v41	1.15	0.00	2.20	0.00	0.00	0.00	0.00	0.00	0.00	1.13	2.26	0.00	0.00	0.00	0.00	0.00	0.00	0.00
v42	0.00	0.00	0.00	0.00	0.00	0.00	0.00	0.00	0.00	0.00	2.26	0.00	0.00	0.00	0.00	0.00	0.00	0.00
v43	1.15	0.00	0.00	0.00	0.00	0.00	0.00	0.00	0.00	0.00	2.26	0.00	0.00	0.00	0.00	0.00	0.00	0.00
v44	0.00	0.00	0.73	0.00	0.00	0.00	0.00	0.00	0.00	0.00	0.00	0.00	0.00	0.00	0.00	0.00	0.00	0.00
v45	0.00	0.00	0.73	0.00	0.00	0.00	0.00	0.00	0.00	0.00	0.00	0.00	0.00	0.00	0.00	0.00	0.00	0.00
v46	0.00	0.00	0.00	0.00	8.81	0.00	0.00	0.00	0.00	0.00	0.00	0.00	0.00	0.00	0.00	0.00	0.00	0.00
v47	0.00	0.00	1.47	0.00	8.81	0.00	1.25	0.00	0.00	1.13	2.26	1.13	1.09	1.50	1.71	2.08	1.33	1.36
v48	0.00	0.00	0.00	0.00	0.00	0.00	0.00	0.00	0.00	0.00	0.00	0.00	0.00	0.00	0.00	0.00	0.00	0.00
v49	0.00	0.00	0.00	0.00	0.00	0.00	0.00	0.00	0.00	0.00	0.00	0.00	0.00	0.00	0.00	0.00	0.00	0.00
v50	0.00	0.00	0.00	0.00	0.00	0.00	0.00	0.00	0.00	0.00	0.00	0.00	0.00	0.00	0.00	0.00	0.00	0.00

Table C.3: EFMs for the Transition Phase.

	e1	e2	e3	e4	e5	e6	e7	e8	e9	e10	e11	e12	e13	e14	e15	e16	e17	e18
v51	0.00	0.00	0.00	0.00	0.00	0.00	0.00	0.00	0.00	0.00	0.00	0.00	0.00	0.00	0.00	0.00	0.00	0.00
v52	0.00	0.00	1.47	0.00	8.81	0.00	1.25	0.00	0.00	1.13	2.26	1.13	1.09	1.50	1.71	2.08	1.33	1.36
v53	0.00	0.00	1.47	0.00	8.81	0.00	1.25	0.00	0.00	1.13	2.26	1.13	1.09	1.50	1.71	2.08	1.33	1.36
v54	0.00	0.00	1.47	0.00	8.81	0.00	1.25	0.00	0.00	1.13	2.26	1.13	1.09	1.50	1.71	2.08	1.33	1.36
v55	0.00	0.00	0.00	0.00	0.00	0.06	0.00	0.00	0.00	0.00	0.00	0.00	0.00	0.00	0.00	0.00	0.00	0.00
v56	0.00	0.00	0.00	0.00	0.00	0.00	0.00	0.00	0.00	0.00	0.00	0.00	0.00	0.00	0.00	0.00	0.00	0.00
v57	0.00	0.00	0.00	0.00	0.00	0.00	0.00	0.00	0.00	0.00	0.00	0.00	0.00	0.00	0.00	0.00	0.00	0.00
v58	0.00	0.00	0.00	0.00	0.00	0.00	0.00	0.00	0.00	0.00	0.00	0.00	0.00	0.00	0.00	0.00	0.00	0.00
v59	0.00	0.00	0.00	0.00	0.00	0.00	0.00	0.00	0.00	0.00	0.00	0.00	0.00	0.00	0.00	0.00	0.00	0.00
v60	0.00	0.00	0.00	0.00	0.00	0.00	0.00	0.00	0.00	0.00	0.00	0.00	0.00	0.00	0.00	0.00	0.00	0.00
v61	0.00	0.00	0.00	0.00	0.00	0.00	0.00	0.00	0.00	0.00	0.00	0.00	0.00	0.00	0.00	0.00	0.00	0.00
v62	0.00	0.00	0.00	0.00	0.00	0.00	0.00	0.00	0.00	0.00	0.00	0.00	0.00	0.00	0.00	0.00	0.00	0.00
v63	0.00	0.00	0.00	0.00	0.00	0.00	0.00	0.00	0.00	0.00	0.00	0.00	0.00	0.00	0.00	0.00	0.00	0.00
v64	0.00	0.00	0.00	0.00	0.00	0.00	0.00	0.00	0.00	0.00	0.00	0.00	0.00	0.00	0.00	0.00	0.00	0.00
v65	0.00	0.00	0.00	0.00	0.00	0.00	0.00	0.00	0.00	0.00	0.00	0.00	0.00	0.00	0.00	0.00	0.00	0.00
v66	0.00	0.00	0.00	0.00	0.00	0.00	0.00	0.00	0.00	0.00	0.00	0.00	0.00	0.00	0.00	0.00	0.00	0.00
v67	0.00	0.00	0.00	0.00	0.00	0.00	0.00	0.00	0.00	0.00	0.00	0.00	0.00	0.00	0.00	0.00	0.00	0.00
v68	0.00	0.00	0.00	0.00	0.00	0.00	0.00	0.00	0.00	0.00	0.00	0.00	0.00	0.00	0.00	0.00	0.00	0.00
v69	0.00	0.00	0.00	0.00	0.00	0.00	0.00	0.00	0.00	0.00	0.00	0.00	0.00	0.00	0.00	0.00	0.00	0.00
v70	0.00	0.00	0.00	0.00	0.00	0.00	0.00	0.00	0.00	0.00	0.00	0.00	0.00	0.00	0.00	0.00	0.00	0.00
v71	0.00	0.00	0.00	0.00	0.00	0.00	0.00	0.00	0.00	0.00	0.00	0.00	0.00	0.00	0.00	0.00	0.00	0.00
v72	0.00	0.00	0.00	0.00	0.00	0.00	0.00	0.00	0.00	0.00	0.00	0.00	0.00	0.00	0.00	0.00	0.00	0.00
v73	0.00	0.00	0.00	0.00	0.00	0.00	0.00	0.00	0.00	0.00	0.00	0.00	0.00	0.00	0.00	0.00	0.00	0.00
v74	0.00	0.00	0.00	0.00	0.00	0.00	0.00	0.00	0.00	0.00	0.00	0.00	0.00	0.00	0.00	0.00	0.00	0.00
v75	0.00	0.00	0.00	0.00	0.00	0.00	0.00	0.00	0.00	0.00	0.00	0.00	0.00	0.00	0.00	0.00	0.00	0.00
v76	0.00	0.00	0.00	0.00	0.00	0.06	0.00	0.00	0.00	0.00	0.00	0.00	0.00	0.00	0.00	0.00	0.00	0.00
v77	0.00	0.00	0.00	0.00	0.00	0.01	1.25	0.00	0.00	0.00	0.00	0.00	0.00	0.00	0.00	0.00	1.33	0.00
v78	0.00	0.00	0.00	0.00	0.00	0.00	0.00	0.00	0.00	0.00	0.00	0.00	0.00	0.00	0.00	0.00	0.00	0.00
v79	0.00	0.00	0.00	0.81	0.00	0.00	0.00	0.88	0.00	0.00	0.00	0.00	0.00	0.00	0.00	0.00	0.00	0.00
v80	0.00	0.00	0.00	0.81	0.00	0.00	0.00	0.00	0.00	0.00	0.00	0.00	0.00	0.00	0.00	0.00	0.00	0.00
v81	0.00	0.00	0.00	0.00	0.00	0.01	0.00	0.00	0.00	0.00	0.00	0.00	1.09	0.00	0.00	0.00	0.00	0.00
v82	1.15	0.00	0.00	0.00	0.00	0.00	0.00	0.00	0.00	0.00	0.00	0.00	0.00	0.00	0.00	0.00	0.00	0.00
v83	0.00	0.00	0.00	0.00	0.00	0.00	1.25	0.00	0.00	0.00	0.00	0.00	0.00	0.00	0.00	0.00	0.00	0.00
v84	0.00	0.00	0.00	0.00	0.00	0.00	0.00	0.00	0.00	0.00	0.00	0.00	0.00	0.00	0.00	0.00	0.00	0.00
v85	0.00	0.00	0.00	0.00	8.81	0.00	0.00	0.00	0.00	0.00	0.00	0.00	0.00	0.00	0.00	0.00	0.00	0.00
v86	0.00	0.42	0.00	0.00	0.00	0.01	0.00	0.00	0.00	0.00	0.00	1.13	0.00	0.00	0.00	0.00	0.00	0.00
v87	0.00	0.00	0.00	0.00	0.00	0.00	0.00	0.00	0.00	0.00	0.00	0.00	0.00	0.00	0.00	0.00	0.00	0.00
v88	0.00	0.00	0.00	0.00	0.00	0.00	0.00	0.00	0.00	1.13	0.00	0.00	0.00	0.00	1.71	0.00	0.00	1.36
v89	0.00	0.00	2.20	0.00	0.00	0.01	0.00	0.00	0.00	1.13	0.00	0.00	0.00	0.00	0.00	0.00	0.00	0.00
v90	0.00	0.00	0.00	0.00	0.00	0.00	0.00	0.00	0.00	0.00	1.13	0.00	0.55	0.75	0.00	1.56	0.66	0.68
v91	0.00	0.00	0.73	0.00	0.00	0.00	0.00	0.00	0.00	0.00	0.00	0.00	0.00	0.00	0.00	0.00	0.00	0.00
v92	0.00	0.00	0.00	0.00	0.00	0.00	0.00	0.00	0.00	0.00	2.26	0.00	0.00	0.00	0.00	0.00	0.00	0.00
v93	0.00	0.00	0.00	0.00	0.00	0.00	0.00	0.00	0.00	0.00	0.00	0.00	0.00	0.00	0.00	0.00	0.00	0.00
v94	0.00	0.00	0.00	0.00	0.00	0.00	0.00	0.00	0.00	0.00	0.00	0.00	0.00	0.00	1.71	1.04	0.00	0.00
v95	0.00	0.00	0.00	0.00	0.00	0.00	0.00	0.00	0.00	0.00	0.00	0.00	0.00	0.00	0.00	0.00	0.00	0.00
v96	0.00	0.00	0.00	0.00	0.00	0.00	0.00	0.88	0.00	0.00	0.00	0.00	0.00	1.50	0.00	0.00	0.00	0.00
v97	0.00	0.00	0.00	0.00	0.00	0.00	0.00	0.00	0.00	0.00	0.00	0.00	0.00	0.00	0.00	0.00	0.00	0.00
v98	0.00	0.00	0.00	0.00	0.00	0.00	0.00	0.00	0.00	0.00	0.00	0.00	0.00	0.00	0.00	0.00	0.00	0.00
v99	1.15	0.84	0.00	0.00	0.00	0.00	0.00	0.00	0.00	0.00	0.00	0.00	0.00	0.00	0.00	0.00	0.00	0.00
v100	10.35	1.25	14.69	0.00	26.43	0.06	4.99	1.75	0.10	10.17	20.34	4.51	5.45	7.51	15.42	9.37	5.31	8.16

Table C.4: EFMs for the Transition Phase (continuation).

	e1	e2	e3	e4	e5	e6	e7	e8	e9	e10	e11	e12	e13	e14	e15	e16	e17
v1	0.00	0.00	0.00	0.00	0.00	0.00	0.00	0.04	0.00	0.00	0.00	0.00	0.00	0.00	0.00	0.00	0.00
v2	0.63	0.00	0.00	0.00	0.00	0.00	0.00	0.00	0.00	0.00	0.00	0.00	0.00	0.00	0.00	0.00	0.00
v3	0.00	0.00	6.50	0.00	0.00	0.00	3.04	0.00	0.00	0.00	0.00	0.00	0.00	0.00	0.00	0.00	0.00
v4	0.00	0.00	0.00	0.00	0.00	0.72	0.00	0.04	0.28	10.83	8.82	8.12	28.06	0.56	0.73	0.62	0.34
v5	0.00	4.92	58.48	0.00	0.62	0.72	0.00	0.04	0.28	10.83	17.64	8.12	84.17	0.56	0.73	1.87	0.34
v6	0.00	4.92	58.48	0.00	0.62	0.72	0.00	0.04	0.28	10.83	17.64	8.12	84.17	0.56	0.73	1.87	0.34
v7	0.00	4.92	58.48	0.00	0.62	0.72	3.04	0.04	0.57	10.83	17.64	12.18	84.17	1.12	0.73	1.87	0.34
v8	0.00	4.92	38.99	0.00	0.62	0.72	3.04	0.04	0.57	21.66	26.46	12.18	56.12	1.12	0.73	1.24	0.34
v9	0.00	4.92	58.48	0.00	0.62	0.72	3.04	0.04	0.57	21.66	26.46	12.18	84.17	1.12	0.73	1.87	0.34
v10	0.00	9.84	64.98	0.00	0.62	0.96	3.04	0.04	0.57	27.07	30.86	16.24	126.26	1.12	1.09	2.49	0.34
v11	0.00	9.84	64.98	0.00	0.62	0.96	3.04	0.04	0.28	16.24	22.05	8.12	98.20	0.56	1.09	1.87	0.34
v12	0.00	0.00	0.00	0.00	0.00	0.00	0.00	0.00	0.28	10.83	8.82	8.12	28.06	0.56	0.00	0.62	0.00
v13	0.63	0.00	0.00	0.00	0.00	0.72	0.00	0.00	0.00	0.00	0.00	0.00	0.00	0.00	0.73	0.00	0.34
v14	0.00	0.00	6.50	0.00	0.00	0.24	0.00	0.00	0.28	5.41	4.41	4.06	14.03	0.56	0.36	0.62	0.34
v15	0.63	4.92	0.00	0.00	0.00	0.24	0.00	0.00	0.00	5.41	4.41	0.00	14.03	0.00	0.36	0.00	0.00
v16	0.00	0.00	0.00	0.00	0.00	0.00	0.00	0.00	0.28	0.00	0.00	0.00	0.00	0.00	0.00	0.00	0.00
v17	0.00	0.00	0.00	0.00	0.62	0.00	0.00	0.00	0.00	0.00	0.00	0.00	0.00	0.00	0.00	0.00	0.00
v18	0.00	0.00	0.00	0.00	0.00	0.00	0.00	0.00	0.00	0.00	0.00	0.00	0.00	0.00	0.00	0.00	0.00
v19	0.00	0.00	6.50	0.00	0.00	0.00	3.04	0.00	0.00	0.00	0.00	0.00	0.00	0.00	0.00	0.00	0.00
v20	0.63	4.92	0.00	0.57	0.62	0.00	0.00	0.00	0.00	0.00	0.00	0.00	0.00	0.00	0.00	0.00	0.00
v21	0.00	0.00	0.00	0.00	0.00	0.00	0.00	0.00	0.00	0.00	0.00	0.00	0.00	0.00	0.00	0.00	0.00
v22	0.00	0.00	0.00	0.00	0.00	0.00	0.00	0.00	0.00	0.00	0.00	0.00	0.00	0.00	0.00	0.00	0.00
v23	0.00	0.00	0.00	0.00	0.00	0.00	0.00	0.00	0.00	10.83	8.82	0.00	0.00	0.00	0.00	0.00	0.00
v24	0.00	0.00	0.00	0.00	0.00	0.00	0.00	0.00	0.00	0.00	0.00	0.00	0.00	0.00	0.00	0.00	0.00
v25	0.00	2.46	0.00	0.00	0.00	0.00	0.00	0.00	0.00	0.00	0.00	0.00	0.00	0.00	0.00	0.00	0.00
v26	0.00	2.46	0.00	0.00	0.00	0.00	0.00	0.00	0.00	0.00	0.00	0.00	0.00	0.00	0.00	0.00	0.00
v27	0.00	2.46	19.49	0.00	0.00	0.00	0.00	0.00	0.00	0.00	0.00	0.00	28.06	0.00	0.00	0.62	0.00
v28	0.00	0.00	0.00	0.00	0.00	0.00	0.00	0.00	0.00	10.83	0.00	0.00	0.00	0.00	0.00	0.00	0.00
v29	0.00	0.00	0.00	0.00	0.00	0.00	0.00	0.00	0.00	0.00	8.82	0.00	0.00	0.00	0.00	0.00	0.00
v30	0.00	0.00	19.49	0.00	0.00	0.00	0.00	0.00	0.00	0.00	0.00	0.00	0.00	0.00	0.00	0.00	0.00
v31	0.00	0.00	19.49	0.00	0.00	0.00	0.00	0.00	0.00	0.00	0.00	0.00	28.06	0.00	0.00	0.62	0.00
v32	0.00	0.00	0.00	0.00	0.00	0.00	0.00	0.00	0.00	0.00	0.00	0.00	28.06	0.00	0.00	0.00	0.00
v33	0.00	0.00	0.00	0.00	0.00	0.00	0.00	0.00	0.00	0.00	0.00	0.00	28.06	0.00	0.00	0.62	0.00
v34	0.00	0.00	0.00	0.00	0.00	0.00	0.00	0.00	0.00	0.00	0.00	0.00	0.00	0.00	0.00	0.00	0.00
v35	0.63	0.00	0.00	0.00	0.00	0.00	0.00	0.00	0.00	0.00	0.00	0.00	0.00	0.00	0.00	0.00	0.00
v36	0.00	0.00	0.00	0.00	0.00	0.00	0.00	0.00	0.00	0.00	0.00	0.00	0.00	0.00	0.00	0.00	0.00
v37	0.00	0.00	6.50	0.00	0.00	0.24	0.00	0.00	0.00	0.00	0.00	0.00	0.00	0.00	0.00	0.00	0.00
v38	0.00	0.00	0.00	0.00	0.00	0.00	0.00	0.00	0.00	0.00	0.00	0.00	0.00	0.00	0.00	0.00	0.00
v39	0.00	0.00	6.50	0.00	0.00	0.24	0.00	0.00	0.00	0.00	0.00	0.00	0.00	0.00	0.00	0.00	0.00
v40	0.00	4.92	6.50	0.00	0.00	0.24	0.00	0.00	0.00	5.41	4.41	4.06	14.03	0.00	0.36	0.00	0.00

Table C.5: EFMs for the Death Phase.

	e1	e2	e3	e4	e5	e6	e7	e8	e9	e10	e11	e12	e13	e14	e15	e16	e17
v41	0.00	4.92	6.50	0.00	0.00	0.24	0.00	0.00	0.00	5.41	4.41	4.06	14.03	0.00	0.36	0.00	0.00
v42	0.00	4.92	6.50	0.00	0.00	0.24	0.00	0.00	0.00	5.41	4.41	4.06	14.03	0.00	0.36	0.00	0.00
v43	0.00	4.92	0.00	0.00	0.00	0.00	0.00	0.00	0.00	5.41	4.41	4.06	14.03	0.00	0.36	0.00	0.00
v44	0.00	0.00	6.50	0.00	0.00	0.00	0.00	0.00	0.00	0.00	0.00	4.06	0.00	0.00	0.00	0.00	0.00
v45	0.00	0.00	0.00	0.00	0.00	0.00	0.00	0.00	0.00	0.00	0.00	0.00	0.00	0.00	0.00	0.00	0.00
v46	0.63	4.92	0.00	0.57	0.00	0.00	0.00	0.00	0.00	0.00	0.00	0.00	0.00	0.00	0.00	0.00	0.00
v47	0.00	0.00	6.50	0.00	0.00	0.00	3.04	0.00	0.00	0.00	0.00	0.00	0.00	0.00	0.00	0.00	0.00
v48	0.00	0.00	0.00	0.00	0.00	0.00	3.04	0.00	0.00	0.00	0.00	4.06	0.00	0.56	0.00	0.00	0.00
v49	0.00	0.00	0.00	0.00	0.00	0.00	0.00	0.00	0.00	0.00	0.00	0.00	0.00	0.00	0.00	0.62	0.00
v50	0.63	0.00	0.00	0.00	0.00	0.72	0.00	0.00	0.00	0.00	0.00	0.00	0.00	0.00	0.73	0.00	0.34
v51	0.00	0.00	6.50	0.00	0.00	0.24	0.00	0.00	0.00	0.00	0.00	0.00	0.00	0.00	0.00	0.00	0.00
v52	0.63	0.00	0.00	0.00	0.00	0.00	0.00	0.00	0.00	0.00	0.00	0.00	0.00	0.00	0.00	0.00	0.00
v53	0.00	0.00	0.00	0.00	0.00	0.00	0.00	0.00	0.28	0.00	0.00	0.00	0.00	0.00	0.00	0.00	0.00
v54	0.00	0.00	0.00	0.00	0.00	0.00	0.00	0.00	0.00	0.00	0.00	0.00	0.00	0.00	0.00	0.00	0.00
v55	0.00	0.00	0.00	0.00	0.00	0.00	0.00	0.00	0.00	0.00	8.82	0.00	0.00	0.00	0.00	0.00	0.00
v56	0.00	0.00	19.49	0.00	0.00	0.00	0.00	0.00	0.00	0.00	0.00	0.00	0.00	0.00	0.00	0.00	0.00
v57	0.00	2.46	0.00	0.00	0.00	0.00	0.00	0.00	0.00	0.00	0.00	0.00	0.00	0.00	0.00	0.00	0.00
v58	0.00	0.00	0.00	0.00	0.00	0.00	0.00	0.00	0.00	0.00	0.00	0.00	28.06	0.00	0.00	0.00	0.00
v59	0.00	0.00	6.50	0.00	0.00	0.24	0.00	0.00	0.00	0.00	0.00	0.00	0.00	0.00	0.00	0.00	0.00
v60	0.00	0.00	0.00	0.00	0.62	0.00	0.00	0.00	0.00	0.00	0.00	0.00	0.00	0.00	0.00	0.00	0.00
v61	0.00	0.00	0.00	0.00	0.00	0.00	0.00	0.00	0.00	0.00	0.00	0.00	0.00	0.00	0.00	0.00	0.00
v62	0.00	0.00	0.00	0.00	0.00	0.00	0.00	0.00	0.00	10.83	0.00	0.00	0.00	0.00	0.00	0.00	0.00
v63	0.00	0.00	0.00	0.57	0.62	0.00	0.00	0.00	0.57	0.00	0.00	0.00	0.00	0.56	0.00	0.62	0.34
v64	0.00	14.76	116.96	0.57	1.85	1.92	6.08	0.11	1.41	48.73	48.50	32.49	238.49	2.79	1.81	5.60	1.02

Table C.6: EFMs for the Death Phase (continuation).

Appendix D

Matlab Functions and Directories

D.1 MFA functions

First Step   Calculation of the specific growth rate and specific uptake/excretion rates.

- ``Exponential_regression``:
  Store of specific growth rate `mu` and the initial condition `X0` in the matlab MAT file ``rates_exponential_regression``.

- ``Linear_regression``:
  Store of specific uptake/excretion rates of substrates and products (`nu_s`, `nu_p`) in the matlab MAT file ``rates_linear_regression``.

Second Step   Construction of the stoichiometric matrices `N` and `Nm` and collecting of the specific uptake/excretion rates in vector `vm`. Stoichiometric matrix $\begin{pmatrix} \mathbf{N} & \mathbf{0} \\ \mathbf{N}_m & -\mathbf{v}_m \end{pmatrix}$ should be written directly as a matrix (either in Matlab, Excel, Open Office Calc, etc.) as it does not have a biological meaning to be written as a ``file.dat``.

Third Step   Computation of the flux distribution intervals.

- Download METATOOL from:
  http://pinguin.biologie.uni-jena.de/bioinformatik/networks/.
  Extract the script files into one directory and start Matlab into the directory where the files have been placed.

- Run METATOOL with matrix $\mathbf{A} = \begin{pmatrix} \mathbf{N} & \mathbf{0} \\ \mathbf{N}_m & -\mathbf{v}_m \end{pmatrix}$ as input. Execute the following commands:

```
ex= parse(íí);
ex.st= A;
ex.irrev react= ones(size(A,2));
ex= metatool(ex);

% To calculate the elementary modes call:
ex.ems= ex.subí * ex.rd ems;
```

- ``Calcul_S'':
  Verifies the presence of zero elements at the end of each column vector, so as to check whether the system is well posed or not. And normalizes all elementary vectors in matrix A so that the last element of each column is one. The output matrix is now called S.

- Intervals determination executing commands:

```
Mtrans=max(S');
M=Mtrans';
mtrans=min(S');
m=mtrans';
```

  Variables M and m contain the upper and lower bounds for all metabolic fluxes, respectively.

D.2 Model Reduction functions

First Step Calculation of the specific growth rate and specific uptake/excretion rates.

- ``Exponential_regression'':
  Store of specific growth rate mu and the initial condition X0 in the matlab MAT file ``rates_exponential_regression''.

- ``Linear_regression'':
  Store of specific uptake/excretion rates of substrates and products (nu_s, nu_p) in the matlab MAT file ``rates_linear_regression''.

Second Step Verification of the consistency between the underlying metabolic network and the calculated uptake and excretion rates.

- ``Verification_exponential_phase_rates''

- ``Verification_maintenance_phase_rates''

- `''Verification_death_phase_rates''`

These script files compare the sign of the entries in matrix `Nm` with the sign of the specific rates just calculated. The signs should be both, either positive or negative.

Third Step Calculation of the minimal set of EFM. R. Jungers algorithm can be downloaded from:
http://www.inma.ucl.ac.be/~jungers/contents/efm.zip.

You will need to install YALMIP, a solver for convex and non convex optimization problems. You will also need an optimization toolbox like the Matlab toolbox *optim* or *Sedumi*, a free Matlab toolbox for optimization.

- `''Model_reduction''`:
  Loads the stoichiometric matrices (`N`, `Nm` and `Nmcomplete`) and the specific uptake/excretion rates. It runs the algorithm for model reduction `''Find_E''` and calculates and saves matrices `NmE`, `w` and `NmEcomplete`, along with `VectPos` which contains the coordinates of the substrates in matrix `NmE_e`.

Fourth Step Construction of the model from matrix `NmE` and vectors `w` and `VectPos` obtained from `''Model_Reduction''`.

- `''Diff_Eq_Gen''`:
  The text generator uses the function `''num2Substrate''` to write the kinetic equations of the macroscopic reaction rates. (Currently, it uses the Monod kinetic law). The text generated is obtained as a Matlab m-file called `''Reaction_Rate''`.

- The dynamical model must be then written loading vector `w` containing the maximum reaction rates, including the text in `'Reaction_Rate''` which modulates these maximum rates with Monod factors, and write the differential equations in the form of `dx_dt = NmE*r` using matrix `NmE`.